

**Developing antibodies against *Plasmodium* lactate
dehydrogenase, glyceraldehyde-3-phosphate
dehydrogenase and phosphoethanolamine-N-
methyltransferase**

by

Robert Gerd Erich Krause

MSc. (*cum laude*) Biochemistry

Submitted in fulfilment of the academic requirements for the degree of Philosophy of Science
in the School of Biochemistry, Microbiology and Genetics

University of KwaZulu-Natal

Pietermaritzburg

As the candidate's supervisor I have approved this thesis for submission.

Signed: _____ Name: Prof. J.P.D. Goldring Date: _____

Abstract

Rapid diagnostic tests (RDTs) function in a diagnostic niche, linking point of care diagnosis with sophisticated lab-based methods tracking drug resistance. As ambitions move from malaria control to eradication, diagnosis is needed to identify the species causing disease, detect asymptomatic reservoirs and quantitate parasite loads. The latter is important to improve treatment dose and duration as well as preventing the spread of drug resistance. Multiple groups are developing alternate diagnostic methods; however improving RDTs would allow easier *in situ* implementation due to the popularity of these tests. This work aimed to identify alternate diagnostic targets and antibodies to those currently used in RDTs.

The current RDT target, lactate dehydrogenase (LDH), was included for comparative purposes. Two metabolic proteins were identified as potential diagnostic targets, namely glyceraldehyde-3-phosphate dehydrogenase (GAPDH) and phosphoethanolamine-N-methyltransferase (PMT). The latter, like the other RDT target histidine rich protein 2 (Hrp2), is a plasmodial protein that is not expressed in humans. GAPDH and PMT were chosen based on *in silico* data suggesting higher transcript and protein concentrations in infected red blood cells in comparison to LDH. Both proteins are expressed throughout the red blood cell and gametocyte stages of the parasite life cycle and are conserved in the three most malignant species, *Plasmodium falciparum*, *P. vivax* and *P. knowlesi*. The *P. falciparum* orthologue (among others) of each of the target proteins was recombinantly expressed, affinity purified and their quaternary structure assessed by molecular exclusion chromatography. LDH formed a 145 kilo Dalton (kD) tetramer in solution, which resolved as a 35 kD protein on reducing SDS-PAGE and was shown to be enzymatically active. Similarly GAPDH formed a tetramer in solution of 148 kD and was identified as a 38 kD monomer on SDS-PAGE. PMT remained as a monomer in solution of approximately 29 kD, similar to its reduced form on SDS-PAGE. These recombinant proteins had similar quaternary structures to their native counterparts and formed the basis of the tests characterising all the antibodies prepared and described here.

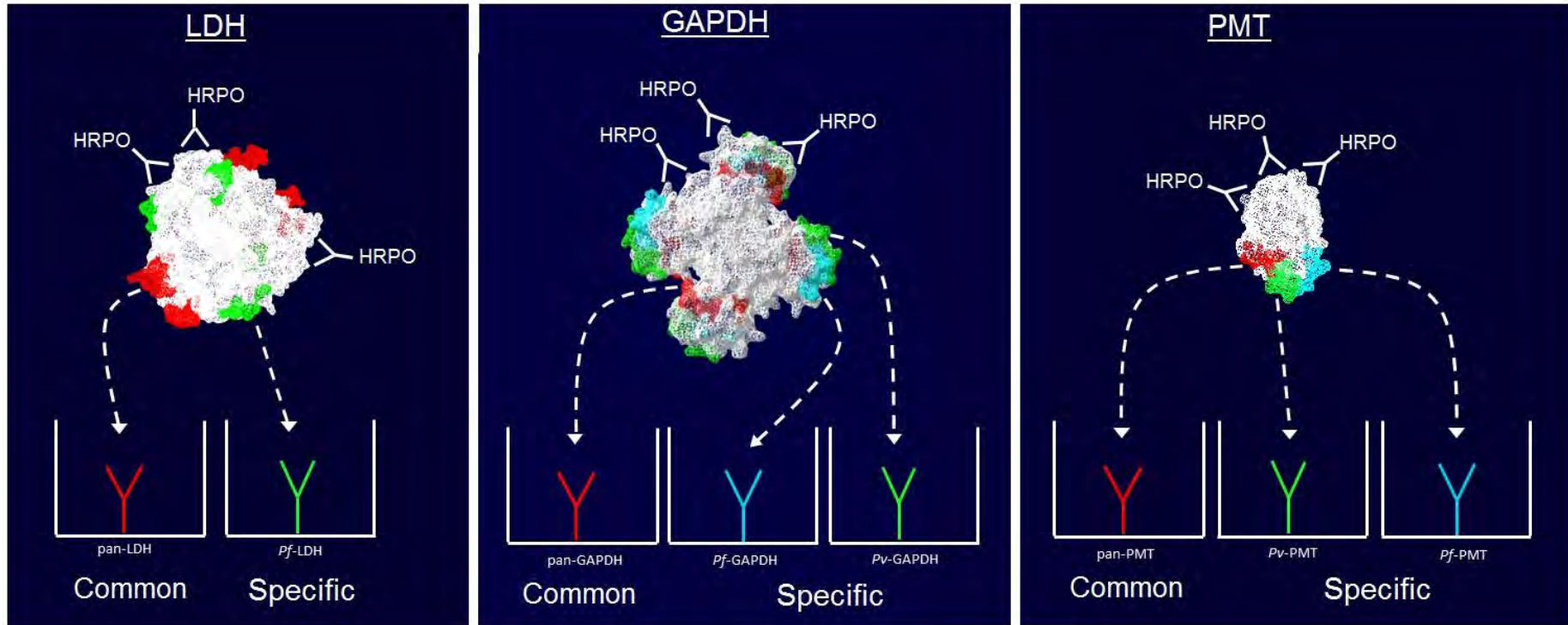
A peptide common to all *Plasmodium* PMT proteins (LENNQYTDEGVK) and peptides unique for *P. falciparum* GAPDH (ADGFLDIGEKKVSVFA), *P. falciparum* PMT (EVEHKYLHENKE), *P. vivax* PMT (VYSIKEYNSLKD) and *P. knowlesi* PMT (LYPTDEYNSLKD) were identified and synthesized. Chicken antibodies were raised against each peptide coupled to a rabbit albumin carrier protein and against purified recombinant PMT and GAPDH. Antibodies raised against the whole recombinant proteins were coupled to

HRPO and used as detection reagents in western blots and ELISAs. All antibodies detected only the *Plasmodium* parent proteins and did not cross react with human red blood cell, other malarial parasite or *E. coli* lysate proteins. Antibodies raised against the whole recombinant proteins and against unique and common peptides within these proteins detected all recombinant *Plasmodium* proteins tested. The species-specific anti-peptide antibodies detected only their specific *Plasmodium* protein orthologs. The antibodies detected each of the *P. falciparum* orthologs in parasite lysate samples by western blot. Detection of the respective recombinant proteins LDH and GAPDH in a double antibody sandwich ELISA assay, which mimics the RDT format, detected both proteins between 0.0004 to 1.5 µg.

Single chain fragment variable (scFv) antibody clones were isolated against all three target proteins using the *Nkuku*[®] chicken scFv library. Polyclonal chicken antibodies specific to the cmc peptide tag on the soluble scFvs were also produced and used to detect and purify soluble scFvs. The scFv clones detected their targets and did not cross react with human red cell or *E. coli* host cell proteins. Five distinct scFv clones were identified against rPfLDH, three against rPfGAPDH and one against the *P. vivax* PMT peptide epitope. These reagents represent unique antibody variable-gene regions which can be expressed for the detection of the specific target they detect. A human anti-malaria antibody pool obtained from malaria patients was assessed for the presence of specific antibodies against the three target proteins. Lower yields of specific human antibodies against *P. falciparum* GAPDH and PMT were attained from the pool in comparison to *P. falciparum* LDH. This suggests that there are low titres of host antibodies against these proteins which are therefore unlikely to interfere with antibody-based detection of *P. falciparum* GAPDH or PMT in the blood of patients in a malaria endemic area.

The chicken antibodies as well as the scFv clones need to be further characterised to determine their limits of detection. The concentration of each of the target proteins in parasite lysates needs to be determined in relation to LDH. The scFv expression and purification needs to be optimised further and all these reagents need to be tested in an ELISA and RDT format. The heat stability of these reagents should also be assessed. We propose the use of multiple test lines on RDTs to allow semi-quantitative detection of the parasite burden in patients. This could allow for discerning between mild and severe infections and aid with the dose and duration of anti-malarial drug treatment. These novel targets and immune-reagents present malaria diagnostic research with alternatives to the current targets and could allow for improved RDT based tests in the future.

Graphical Abstract



Preface

The experimental work described in this thesis was carried out in the Discipline of Biochemistry, School of Biochemistry, Microbiology and Genetics, University of KwaZulu-Natal, Pietermaritzburg from July 2012 to April 2016 under the supervision of Prof. J.P.D. Goldring.

These studies represent original work by the author and have not otherwise been submitted in any form to another University. Where use has been made of the work by other authors it has been duly acknowledged in the text.

Signed:

Date:

**Faculty of Science and Agriculture
Declaration of Plagiarism**

I, Robert Gerd Erich Krause declare that:

1. The research reported in this thesis, except where otherwise indicated, is my original research.
2. This thesis has not been submitted for any degree or examination at any other university.
3. This thesis does not contain other persons' data, pictures, graphs or other information, unless specifically acknowledged as being sourced from other persons.
4. This thesis does not contain other persons' writing, unless specifically acknowledged as being sourced from other researchers. Where other written sources have been quoted, then:
 - a. Their words have been re-written but the general information attributed to them has been referenced
 - b. Where their exact words have been used, then their writing has been placed in italics and inside quotation marks, and referenced.
5. This thesis does not contain text, graphics or tables copied and pasted from the Internet, unless specifically acknowledged, and the source being detailed in the thesis and in the References sections.

Signed:

Date:

Declaration Plagiarism 22/05/08 FHDR Approved

Acknowledgements

Science...

“Don’t get excited unless it’s in triplicate.”

“The experiment works...until I included all controls”

“The plan is to do A, B, C and end at D...we started with A, had to include 1, 2 and 3, revised B and C and ended at D, although future work should include...”

Science is exciting yet humbling at the same time. It tests your patience and teaches perseverance. If you don’t pay attention it will confuse and mislead you. If you do it right, there’s nothing else like it!

The list of people to thank for this thesis is too long to mention. I would like to thank Professor Goldring, my supervisor, for all his support, mentoring, patience and criticism, especially throughout my postgraduate studies. I would like to thank all the lecturers and administrative staff of the department as well as the support staff. Thank you to all my fellow lab-members and all the journal clubs, shut up and writes and fun runs along the way.

Thank you to the South African Malaria Initiative, the National Research Foundation of South Africa, the Medical Research Council and the University of KwaZulu-Natal for their financial assistance, without which my postgraduate studies would not have been possible.

I would like to thank my friends, family and loved ones, but above all I would like to dedicate this thesis to my parents and my brother. *“Ich hab euch lieb und danke für Alles!”*

“Aanhouer wen!”

Danket dem Herrn denn Er ist freundlich und Seine Güte währet ewiglich!

Amen.

Contents

Abstract	i
Graphical Abstract	iii
Preface	iv
Declaration of Plagiarism	v
Acknowledgements	vi
Contents	vii
List of Tables	xiv
List of Figures	xv
Abbreviations and symbols	xviii
Chapter 1	1
Introduction and literature review	1
1.1. An overview of malaria focused on diagnosis	1
1.1.1 Importance of diagnosis	1
1.1.2 Which species infect humans and differences in treatment?	1
1.1.3 Brief life cycle description.....	2
1.1.4 When do symptoms appear and what is the diagnostic window?.....	4
1.1.5 The importance of diagnosis to prevent spread of resistance	6
1.1.6 Complicated malaria infections	7
1.2. Malaria control to date and the setting of diagnosis.....	8
1.2.1 The importance of the malaria pool and the need for more sensitive diagnosis	12
1.2.2 Entomologic inoculation rate	12
1.2.3 Insecticide resistance	13
1.3. The stages of the malaria life cycle targeted for diagnosis	13
1.4. Methods to diagnose malaria.....	14
1.4.1 Clinical diagnosis of malaria	15
1.4.2 Serodiagnosis of malaria.....	15

1.4.3	Spectral analyses of malaria infections.....	16
1.4.4	Haemozoin based detection of malaria.....	17
1.4.5	Microscopic detection of malaria.....	19
1.4.6	Antigen detection methods.....	21
1.4.7	PCR based methods for malaria detection.....	21
1.5.	Molecular targets for malaria diagnosis and laboratory-based detection.....	22
1.5.1	Molecular targets for the diagnosis of malaria infection.....	22
1.5.2	Targets for transmission studies.....	25
1.6.	Methods and targets used to detect drug resistant strains.....	27
1.7.	The diagnostic niche of RDTs.....	27
1.8.	The aims and objectives of the current study.....	28
<hr/>		
Chapter 2	30
Materials and Methods	30
2.1	Introduction.....	30
2.2	Equipment.....	30
2.2	General molecular biology methods.....	31
2.2.1	Reagents.....	31
2.2.2	Bradford protein determinations.....	31
2.2.3	Sodium dodecyl sulphate polyacrylamide gel electrophoresis (SDS-PAGE) ...	32
2.2.4	Molecular exclusion chromatography (MEC) using the ÄKTA Prime Plus system.....	34
2.2.5	Colony Polymerase Chain Reaction (PCR).....	34
2.2.6	Plasmid isolation.....	35
2.2.7	Agarose gel electrophoresis.....	36
2.2.8	Sequencing.....	36
2.3	General immunochemical techniques.....	37

2.3.1	Reagents	37
2.3.2	Western blotting.....	37
2.3.3.	Direct ELISA method	38
2.4	Bioinformatics (Chapter 3).....	39
2.4.1	Identifying malaria protein targets for diagnosis	39
2.4.2	Sequence alignments.....	39
2.4.3	Predict7 TM	39
2.4.4	3D modelling.....	39
2.4.5	Sequencing (see section 2.2.8).....	40
2.5	Recombinant work with malarial proteins (Chapter 4).....	40
2.5.1	Reagents	40
2.5.2	Expression host <i>E. coli</i>	40
2.5.3	Expression vectors	40
2.5.4	Transformation of <i>E. coli</i> BL21(DE3) host	44
2.5.5	Expression of recombinant malarial proteins	44
2.5.6	Affinity purification	45
2.5.7	SDS-PAGE analysis, dialysis and storage of recombinant proteins.....	46
2.6	Raising antibodies (Chapter 5).....	46
2.6.1	Reagents.....	46
2.6.2	Peptide synthesis.....	47
2.6.3	Coupling peptides to rabbit albumin.....	47
2.6.4	Chicken immunisation.....	49
2.6.5	Isolation of crude IgY from chicken egg yolk	49
2.6.6	Preparation of affinity matrices	50
2.6.7	IgY affinity purification.....	52
2.6.8	Human IgG affinity purification	52
2.6.9	Conjugation of horse radish peroxidase to IgY antibodies.....	52

2.6.10	Enhanced chemiluminescence	53
2.6.11.	Double antibody sandwich ELISA method	53
2.7	ScFv work (Chapter 6)	54
2.7.1	Reagents	54
2.7.2	<i>E. coli</i> hosts	54
2.7.3	Helper phage	54
2.7.4	pHEN1 vector	55
2.7.5	Library preparation	55
2.7.6	Panning the <i>Nkuku</i> [®] library	59
2.7.7	Polyclonal ELISA to determine phagemid enrichment against target molecules	61
2.7.8	Picking single scFv clones	61
2.7.9	Preparation of scFv clone glycerol stocks	62
2.7.10	Transduction of <i>E. coli</i> expression host, Top10	62
2.7.11	Soluble expression of scFvs from Top10 <i>E. coli</i>	63
2.7.12	Periplasmic isolation of soluble scFv antibodies	63
2.7.13	Restriction digest	63
2.7.14	Nested PCR	64

Chapter 3 65

Search for possible new *Plasmodium* diagnostic target proteins and peptides for antibody production using a bioinformatics approach..... 65

3.1	Introduction	65
3.2	Results	68
3.2.1	Compilation of a list of proteins from which the diagnostic targets were selected.....	68
3.2.2	Peptide epitope selection.....	71

3.2.3	Verification of peptide epitopes in the recombinant proteins used in this study.....	82
3.3	Discussion	83
<hr/>		
Chapter 4	88
Recombinant expression, purification and characterisation of the potential <i>Plasmodium</i> diagnostic target proteins LDH, GAPDH and PMT		
4.1	Introduction	88
4.2	Results	91
4.2.1	Results from the <i>E. coli</i> expression host using the proposed expression and affinity purification strategies	91
4.2.2	Optimisation of expression and affinity purification strategies for the recombinant <i>Plasmodium</i> LDH proteins	93
4.2.3	Optimisation of expression and affinity purification strategies for the recombinant <i>Plasmodium</i> GAPDH proteins	97
4.2.4	Optimisation of expression and affinity purification strategies for the recombinant <i>Plasmodium</i> PMT proteins	100
4.2.5	Expression and affinity purification of the recombinant <i>Plasmodium</i> proteins.....	103
4.2.6	Assessing the recombinant <i>Plasmodium</i> proteins' native structures	108
4.3	Discussion.....	115
<hr/>		
Chapter 5	118
Assessment of polyclonal IgY raised against both the recombinant <i>Plasmodium</i> proteins and peptide targets of LDH, GAPDH and PMT		
5.1	Introduction	118
5.2	Results	121
5.2.1	Assessing the specificity of the IgY antibodies raised against rPfLDH and the selected LDH peptides	121

5.2.2	Assessing the specificity of the IgY antibodies raised against r <i>Pf</i> GAPDH and the selected GAPDH peptides.....	122
5.2.3	Assessing the specificity of the IgY antibodies raised against r <i>Pf</i> PMT, <i>Pv</i> PMT and the selected PMT peptides	124
5.2.4	Double antibody sandwich ELISAs for the detection of the recombinant <i>Pf</i> LDH and <i>Pf</i> GAPDH proteins in solution.....	131
5.2.5	Human IgG pool affinity purified over the respective recombinant <i>P. falciparum</i> protein AminoLink [®] columns	133
5.3	Discussion.....	134

Chapter 6	138
Selection of monoclonal recombinant scFv antibodies from the <i>Nkuku</i> [®] library against the potential <i>Plasmodium</i> target proteins and their respective peptide epitopes		
6.1	Introduction	138
6.2	Results	142
6.2.1	Raising and affinity purification of anti-cmyc IgY antibodies to detect soluble scFvs.....	142
6.2.2	Panning the <i>Nkuku</i> [®] library.....	143
6.2.3	Polyclonal phagemid ELISA results after rounds one to four of panning.....	144
6.2.4	Anti-LDH monoclonal phage selection	144
6.2.5	Anti-GAPDH monoclonal phage selection.....	149
6.2.6	Anti-PMT monoclonal phage selection	154
6.2.7	Detection of soluble scFv fragments using the anti-cmyc IgY	159
6.2.8	Sequencing results of the scFv clones	160
6.3	Discussion	167

Chapter 7	171
General discussion and future work.....		
		171

7.1	Brief overview	171
7.2	Identification of new malaria diagnostic candidates (chapter 3).....	172
7.3	Recombinant expression of the target proteins (chapter 4).....	172
7.4	Producing polyclonal IgY against the selected peptide and protein targets (chapter 5).....	173
7.5	Assessing the relative levels of human antibodies against each target from a human anti-malaria hyperimmune antibody pool (chapter 5).....	174
7.6	ScFv clones against all peptides, rPfLDH and rPfGAPDH from the <i>Nkuku</i> [®] library (chapter 6)	174
7.7	Future studies involving the scFv clones identified here	175
7.8	Comparative characterisation of the scFv and polyclonal IgY reagents	176
7.9	The possibility of capturing the native target proteins using IgY and scFv antibodies and exploiting their native enzymatic activity for detection	176
7.10	Retrospective analysis of the peptide targets with respect to post-translational modifications.....	177
7.11	Retrospective analysis of the peptide targets with respect to single point mutations.....	178
7.12	Comparing the half-lives of the target proteins	179
7.13	Essential field testing of the antibodies in an RDT format.....	179
7.14	A proposed semi-quantitative test for malaria.....	179
7.15	Conclusions.....	182

Bibliography.....	183
--------------------------	------------

List of Tables

Table #	Title	pg.
Table 1.1	Endemic malaria statistics for 2013 / 2014 from the WHO and malaria atlas project	11
Table 1.2	Summary of the source materials used for diagnosis	14
Table 1.3	A summary of methods based on the detection of the host response as well as <i>Plasmodium</i> specific metabolites	18
Table 1.4	A summary of methods based on the physical/visual detection of the <i>Plasmodium</i> parasite	18
Table 1.5	A summary of methods based on the detection of <i>Plasmodium</i> -specific molecular targets	20
Table 1.6	Molecular targets for diagnosis of malaria	26
Table 2.1	Running and stacking gel recipes to prepare a single gel for SDS-PAGE	33
Table 2.2	Primer sequences used in this study (sequencing and PCR)	35
Table 2.3	List of vectors used in the study for expression of the respective malarial proteins	41
Table 2.4	Expression media used per recombinant protein and additional supplements	45
Table 2.5	List of targets immunised into chickens for IgY production	47
Table 2.6	Media recipes for phage display work	55
Table 2.7	Malarial targets used to pan the <i>Nkuku</i> [®] library and the concentrations used per round	60
Table 3.1	Twenty highest expressed genes based on mRNA abundance (LeRoch <i>et al.</i> , 2003)	68
Table 3.2	Twenty most abundant proteins according to proteome data from Foth <i>et al.</i> , (2011)	69
Table 3.3	Compilation of the 35 most abundant proteins, highlighting potential diagnostic targets in green and proteins that were excluded in red	70
Table 3.4	Alignment and BLAST results of the selected <i>Plasmodium</i> LDH, GAPDH and PMT peptides	81
Table 3.5	Alignment and BLAST results for the sequenced vector DNA inserts and translated sequences	82
Table 4.1	The predicted monomeric and quaternary sizes of the native <i>Plasmodium</i> target proteins recombinantly expressed in this study	88
Table 4.2	Imidazole concentrations required for elution of bound BL21(DE3) proteins off the TALON [®] (Co ²⁺) resin	93
Table 4.3	Imidazole concentrations required for elution of bound recombinant <i>Plasmodium</i> LDH proteins off the TALON [®] (Co ²⁺) resin	97
Table 4.4	Imidazole concentrations required for elution of bound recombinant <i>Plasmodium</i> GAPDH proteins off the TALON [®] (Co ²⁺) resin	100
Table 4.5	Imidazole concentrations required for elution of bound recombinant <i>Plasmodium</i> PMT proteins off the TALON [®] (Co ²⁺) resin	103
Table 4.6	Optimized expression conditions for each recombinant proteins including affinity purified yields	103
Table 5.1	IgY yields per antigen used in this study	131
Table 6.1	Malarial recombinant protein or peptide targets used to pan the <i>Nkuku</i> [®] library and the concentrations used per round	143

List of Figures

Figure #	Title	pg.
Figure 1.1	Generic malaria life cycle diagram including estimated number of parasites released per stage	3
Figure 1.2	Dynamics of infection of each of the human infective malarias and the resulting diagnostic window for <i>P. falciparum</i> , <i>P. knowlesi</i> and <i>P. vivax</i>	5
Figure 1.3	Malaria control / eradication statistics and timeline	9
Figure 1.4	Basic outline of a simple rapid diagnostic test (RDT), both top and side view	28
Figure 2.1	Bradford standard curve	32
Figure 2.2	PCR cycle conditions	35
Figure 2.3	pKK223-3 expression plasmid vector map	41
Figure 2.4	pET-15b expression plasmid vector map	42
Figure 2.5	pET-28a expression plasmid vector map	43
Figure 2.6	pHEN1 vector map used in phage display	55
Figure 3.1	NAD ⁺ (H) linked glycolytic reactions involving GAPDH and LDH	66
Figure 3.2	Alignment of <i>Plasmodium</i> and mammalian LDH sequences indicating the peptides chosen for polyclonal chicken antibody and monoclonal scFv production, adapted from Hurdayal <i>et al.</i> (2010)	72
Figure 3.3	Predict7 TM analyses of three selected <i>Plasmodium</i> LDH peptides (data adapted from Hurdayal <i>et al.</i> (2010)	74
Figure 3.4	Alignment of <i>Plasmodium</i> and mammalian GAPDH sequences showing selected peptide epitopes chosen for polyclonal chicken antibody and monoclonal scFv production	75
Figure 3.5	Predict7 TM analyses of three selected <i>Plasmodium</i> GAPDH peptides	76
Figure 3.6	Alignment of <i>Plasmodium</i> PMT sequences showing selected peptide epitopes chosen for polyclonal chicken antibody and monoclonal scFv production	77
Figure 3.7	Predict7 TM analyses of four selected <i>Plasmodium</i> PMT peptides	78
Figure 3.8	Location of the <i>P. falciparum</i> specific and the pan- <i>Plasmodial</i> epitopes on the 3D crystal structure of <i>Pf/Pv</i> LDH (A), <i>Pf</i> GAPDH (B) and <i>Pf</i> PMT (C)	79
Figure 4.1	Untransformed BL21(DE3) host growth under different conditions and elution profiles off a TALON [®] (Co ²⁺) resin using a linear Imidazole gradient, analysed by silver staining on SDS-PAGE	92
Figure 4.2	Growth of r <i>Pf</i> LDH expressing cultures under varying conditions and elution profiles off a TALON [®] (Co ²⁺) resin analysed by SDS-PAGE	94
Figure 4.3	Growth of r <i>Pv</i> LDH expressing cultures under varying conditions and elution profiles off a TALON [®] (Co ²⁺) resin analysed by SDS-PAGE	95
Figure 4.4	Growth of r <i>Pv</i> LDH expressing cultures under varying conditions and elution profiles off a TALON [®] (Co ²⁺) resin analysed by SDS-PAGE	96
Figure 4.5	Growth of r <i>Pf</i> GAPDH expressing cultures under varying conditions and elution profiles off a TALON [®] (Co ²⁺) resin analysed by SDS-PAGE	98
Figure 4.6	Growth of r <i>Pv</i> GAPDH expressing cultures under varying conditions and elution profiles off a TALON [®] (Co ²⁺) resin analysed by SDS-PAGE	99
Figure 4.7	Growth of r <i>Pf</i> PMT expressing cultures under varying conditions and elution profiles off a TALON [®] (Co ²⁺) resin analysed by SDS-PAGE	101
Figure 4.8	Growth of r <i>Pv</i> PMT expressing cultures under varying conditions and elution profiles off a TALON [®] (Co ²⁺) resin analysed by SDS-PAGE	102
Figure 4.9	Recombinant expression and affinity purification of <i>Pf</i> , <i>Pv</i> and <i>Pv</i> LDH analysed by SDS-PAGE and Western blot	105

Figure 4.10	Recombinant expression and affinity purification of <i>Pf</i> and <i>Py</i> GAPDH analysed by SDS-PAGE and Western blot	106
Figure 4.11	Recombinant expression and affinity purification of <i>Pf</i> and <i>Pv</i> PMT analysed by SDS-PAGE and Western blot	107
Figure 4.12	Calibration of the Sephacryl S-200 molecular exclusion chromatography column	109
Figure 4.13	<i>rPf</i> LDH elution profile over a Sephacryl S-200 MEC column	110
Figure 4.14	<i>rPv</i> LDH elution profile over a Sephacryl S-200 MEC column	110
Figure 4.15	<i>rPy</i> LDH elution profile over a Sephacryl S-200 MEC column	111
Figure 4.16	Enzyme activity of both recombinant <i>Pf</i> LDH and <i>Pv</i> LDH assessed by measuring the increased formation of NADH due to the oxidation of L-lactate	111
Figure 4.17	<i>rPf</i> GAPDH elution profile over a Sephacryl S-200 MEC column	112
Figure 4.18	<i>rPy</i> GAPDH elution profile over a Sephacryl S-200 MEC column	113
Figure 4.19	<i>rPf</i> PMT elution profile over a Sephacryl S-200 MEC column	113
Figure 4.20	<i>rPv</i> PMT elution profile over a Sephacryl S-200 MEC column	114
Figure 5.1	An illustration of potential cross reactivity caused by linear and conformational epitopes recognised by a hypothetical antibody	119
Figure 5.2	Panel of western blots showing specificity of the respective anti-LDH IgY antibodies	121
Figure 5.3	Panel of western blots showing specificity of the respective anti-GAPDH IgY antibodies	122
Figure 5.4	Raising and affinity purification of IgY against the <i>Pf</i> GAPDH specific peptide (CAD)	123
Figure 5.5	Raising and affinity purification of IgY against the whole <i>rPf</i> PMT protein	125
Figure 5.6	Raising and affinity purification of IgY against the whole <i>rPv</i> PMT protein	126
Figure 5.7	Raising and affinity purification of IgY against the common PMT peptide (DEG)	127
Figure 5.8	Raising and affinity purification of IgY against the <i>P. falciparum</i> specific PMT peptide (CEV)	128
Figure 5.9	Raising and affinity purification of IgY against the <i>P. vivax</i> specific PMT peptide (VYS)	129
Figure 5.10	Raising and affinity purification of IgY against the <i>P. knowlesi</i> specific PMT peptide (LYP)	130
Figure 5.11	Double antibody-sandwich ELISAs to detect <i>rPf</i> LDH	132
Figure 5.12	Double antibody-sandwich ELISAs to detect <i>rPf</i> GAPDH	132
Figure 5.13	Affinity purified human IgG yields from an anti-malaria hyper immune serum pool against various recombinant <i>P. falciparum</i> proteins	133
Figure 6.1	Representation of the pHEN1 coding region including the scFv and protein III regions	139
Figure 6.2	Schematic representation of the panning procedure used to select for target antigen specific scFv-bearing phagemids from the <i>Nkuku</i> [®] library	140
Figure 6.3	Titres and affinity purification of anti-cmyc antibodies from chicken eggs	142
Figure 6.4	Polyclonal phagemid ELISA results for pans one to four of each of the respective target peptides and recombinant proteins	144
Figure 6.5	Monoclonal ELISA results for the anti- <i>rPf</i> LDH clones	145
Figure 6.6	Monoclonal ELISA results for the anti-APG (common LDH peptide) clones	146
Figure 6.7	Monoclonal ELISA results for the anti-FDC (<i>P. falciparum</i> LDH peptide) clones	147
Figure 6.8	Monoclonal ELISA results for the anti-KIT (<i>P. vivax</i> LDH peptide) clones	148

Figure 6.9	Monoclonal ELISA results for the anti-r <i>Pf</i> GAPDH clones	150
Figure 6.10	Monoclonal ELISA results for the anti-VMG (common GAPDH peptide) clones	151
Figure 6.11	Monoclonal ELISA results for the anti-WGK (<i>P. falciparum</i> GAPDH peptide) clones	152
Figure 6.12	Monoclonal ELISA results for the anti-ADG (<i>P. falciparum</i> GAPDH peptide) clones	153
Figure 6.13	Monoclonal ELISA results for the anti-DEG (common PMT peptide) clones	155
Figure 6.14	Monoclonal ELISA results for the anti-CEV (<i>P. falciparum</i> PMT peptide) clones	156
Figure 6.15	Monoclonal ELISA results for the anti-VYS (<i>P. vivax</i> PMT peptide) clones	157
Figure 6.16	Monoclonal ELISA results for the anti-LYP (<i>P. knowlesi</i> PMT peptide) clones	158
Figure 6.17	Expression of the top six anti-r <i>Pf</i> LDH scFvs analysed by SDS-PAGE and western blot	159
Figure 6.18	Expression and affinity purification of the anti-r <i>Pf</i> LDH scFv clone R4H1 analysed by SDS-PAGE and western blot	160
Figure 6.19	Colony PCR of the selected clones against r <i>Pf</i> LDH, r <i>Pf</i> GAPDH and the PMT peptides	161
Figure 6.20	Nested PCR of the selected clones against r <i>Pf</i> LDH, r <i>Pf</i> GAPDH and the common PMT peptide (VYS)	161
Figure 6.21	AluI digest of the selected clones against r <i>Pf</i> LDH, r <i>Pf</i> GAPDH and the common PMT peptide (VYS)	162
Figure 6.22	Alignment of the anti-r <i>Pf</i> LDH scFv clones' translated sequences with a chicken germline immunoglobulin and the Chiliza <i>et al.</i> , (2008) anti-LDH scFv sequences	163
Figure 6.23	Alignment of the anti-r <i>Pf</i> GAPDH scFv clones' translated sequences with a chicken germline immunoglobulin sequence	165
Figure 6.24	Alignment of the anti-common PMT peptide (VYS) scFv clones' translated sequences with a chicken germline immunoglobulin sequence	166
Figure 7.1	Proposed multi-test line semi-quantitative detection of malaria	180

Abbreviations and symbols

Abbreviation	Explanation	Abbreviation	Explanation	Abbreviation	Explanation
(H)-NMR	(Proton)-Nuclear magnetic resonance	dhps	Dihydropteroate synthase	HRPO	Horse radish peroxidase
18S rRNA	Small eukaryotic ribosomal subunit component	DMF	Dimethyl formazan	Ig	Immunoglobulin
ABTS	2,2'-azino-bis(3-ethylbenzothiazoline sulfonate	DMSO	Dimethyl sulfoxide	IPTG	isopropyl- β -D-1-thiogalactopyranoside
ACT	Artemisinin-based combination therapy	DNA	deoxyribonucleic acid	Kan	Kanamycin
AMA-1	Apical membrane antigen 1	dNTP	deoxyribonucleotide triphosphate	kD	kilo Daltons
AMP	Adenosine monophosphate	DTT	Dithiothreitol	kdr	Knock down resistance (pyrethroid)
Amp	Ampicillin	ECL	Enhanced chemiluminescence	LAMP	Loop mediated isothermal amplification
ATP	adenosine triphosphate	EDTA	Ethylenediaminetetraacetic acid	LB	Lysogeny Broth
BLAST	Basic local alignment search tool	ELISA	enzyme linked immunosorbent assay	LDH	lactate dehydrogenase
BSA	Bovine serum albumin	EMP1	Erythrocyte membrane protein 1	LFD	Lateral flow dipstick
cfu	Colony forming units	EtBr	Ethidium bromide	LF-RPA	Lateral flow recombinase polymerase amplification
COX-III	Cytochrome oxidase III gene	FAD	Flavin adenine dinucleotide	LOD	Limit of detection
crt	Chloroquine resistance transporter	Fc	Fragment crystallizable group	MAP	Malaria atlas project
CSP	Circumsporozoite protein	FCA	Freund's complete adjuvant	MBS	Maleimidobenzoyl-N-hydroxysuccinimide ester
cytb	Cytochrome b	FIA	Freund's incomplete adjuvant	mdr1	Multidrug resistance protein 1
DAS ELISA	Double antibody sandwich enzyme linked immunosorbent assay	GAPDH	glyceraldehyde-3-phosphate dehydrogenase	MEC	Molecular exclusion chromatography
DDT	Dichlorodiphenyltrichloroethane	HRP2	Histidine rich protein 2	MES	2-(N-Morpholino)ethanesulfonic acid
dhfr	Dihydrofolate reductase	HRP3	Histidine rich protein 3	mRNA	messenger ribonucleic acid

Abbreviation	Explanation	Abbreviation	Explanation	Abbreviation	Explanation
MWCO	Molecular weight cut off	pLDH	<i>Plasmodium</i> lactate dehydrogenase	TEMED	N',N',N',N',-tetramethylethylenediamine
NA	Not applicable / available	PMT	phosphoethanolamine-N-methyltransferase	USD	United States Dollar
NAD	nicotinamide adenine dinucleotide	POC	Point of care	varATS	var gene acidic terminal sequence
NALFIA	Nucleic acid lateral flow immunoassay	Pvr47	<i>P. vivax</i> species-specific repetitive sequence	VH	Variable heavy chain
NASBA	Nucleic acid sequence based amplification	qPCR	Quantitative real time polymerase chain reaction	VL	Variable light chain
NCBI	National Center for Biotechnology Information	RA	Rabbit albumin	WHO	World Health Organisation
ND	Not done / determined	RBC	Red blood cell		
O.D.	optical density (measured at 600 nm)	RDT	rapid diagnostic test		
PBS	Phosphate buffered saline	RFLP	Restriction fragment length polymorphism		
PCR	Polymerase chain reaction	RNA	Ribonucleic acid		
PEG	Polyethylene glycol	RT	Room temperature		
PfATPase6	P-type calcium ATPase gene	scFv	Single chain fragment variable		
pfnhe	<i>P. falciparum</i> Na ⁺ /H ⁺ exchanger	SDS	Sodium dodecyl sulphate		
Pfr364	<i>P. falciparum</i> species-specific repetitive sequence	SDS-PAGE	Sodium dodecyl sulphate polyacrylamide gel electrophoresis		
Pfs230p	Male gametocyte surface protein	SOC	Super optimal broth		
Pfs25	Female gametocyte surface protein	TAE	Tris, acetic acid, EDTA buffer		
pfu	Plaque forming units	TARE-2	Telomere-associated repetitive element 2		
Pfubp-1	Deubiquitinating enzyme	TB	Terrific broth		
pgmet	unique methionine tRNA gene	TBS	Tris buffered saline		

Chapter 1

Introduction and literature review

Epidemiology entails studying the cause, transmission, control and surveillance of disease. Diagnosis is key to the study of any disease and this review highlights the main diagnostic tools and targets used to study malaria.

1.1. An overview of malaria focused on diagnosis

1.1.1 Importance of diagnosis

Malaria is the leading global cause of human death due to a parasitic disease (Murray *et al.*, 2014). It affects approximately half the human population (3.2 billion people), where an estimated 1.2 billion people live in high-risk malaria endemic countries. Of the 124-283 million reported malaria cases, approximately 584000 deaths resulted, most of which (455000) were children under the age of five (Hay *et al.*, 2004; WHO 2015b world malaria report). This equates to a child dying of malaria and between 240-550 new malaria cases being diagnosed nearly every minute. The malaria cases may vary from mild (fever) to severe disease (prostration, impaired consciousness, difficulty breathing, jaundice, haemoglobinuria and severe anaemia (five-seven grams of haemoglobin per 100 ml of blood)) and cerebral malaria (Miller *et al.*, 1994). To date attempts to develop an effective vaccine have been unsuccessful and despite it being a curable disease malaria continues to claim human lives every day. Most deaths result from failure to diagnose and treat malaria before the onset of severe disease. Even with proper treatment severe malaria mortality rates exceed 20% (Antia *et al.*, 2008; Suh *et al.*, 2004). Until such time as a “silver bullet” is found, diagnosis and timely treatment are vital to curb the mortality due to malaria.

1.1.2 Which species infect humans and differences in treatment?

Malaria treatment varies depending on the species of parasite causing the disease. The eukaryotic protozoan parasites that cause malaria fall within the genus *Plasmodium* (Bannister *et al.*, 2000; Miller *et al.*, 1994) and include over 100 species infecting avian, reptilian, amphibian and simian hosts (Suh *et al.*, 2004). Of all the *Plasmodium* species known only five infect humans. These are *Plasmodium falciparum*, *P. vivax*, *P. knowlesi*, *P. malariae* and *P. ovale* (Daneshvar *et al.*, 2009; Sabbatani *et al.*, 2010).

Of these five species *P. falciparum* is the most aggressive pathogen causing cerebral malaria and death (Suh *et al.*, 2004; Welch, 1897). *P. knowlesi* has only recently been recognised as a human infecting species, although the first natural human infection was recorded in 1965 (Chin *et al.*, 1965; Cox-Singh *et al.*, 2008; Lee *et al.*, 2011; van Hellemond *et al.*, 2009; Yusof *et al.*, 2014). *P. knowlesi* has a shorter red blood cell cycle than *P. falciparum*, rapidly multiplies in the blood and also causes severe disease and death (Chin *et al.*, 1965; Daneshvar *et al.*, 2009; Ng *et al.*, 2008; Sabbatani *et al.*, 2010). *P. vivax* and *P. malariae* were first described and differentiated in 1890 by Grassi and Feletti (Collins and Jefferey, 2007; Grassi and Feletti, 1890), where *P. malariae* can cause severe malaria but is not fatal. *P. vivax* on the other hand has been reported to cause severe and fatal malaria in humans (Kochar *et al.*, 2005; Shaikh *et al.*, 2012) and its ability to remain dormant in the liver of infected patients even after drug clearance of the initial blood stage infection is shared by *P. ovale*. These dormant parasites can then cause relapsing blood infections more than two years later (Fujioka and Aikawa *et al.*, 2002; Perkins and Bell, 2008). Specific drugs targeting the liver stages of *P. vivax* and *P. ovale*, such as primaquine are required to clear dormant liver infections (Beeching *et al.*, 2007). *P. ovale*, the fifth of the human pathogens is the only species with humans as its sole host. It was first identified in 1922 and interestingly due to its benign nature; it was used to induce fever episodes as a treatment of neurosyphilis before the advent of penicillin (Collins and Jeffery, 2007). Each of the five species has different infection characteristics due to slight differences in their life cycles and requires species-specific diagnosis and treatment as a result.

1.1.3 Brief life cycle description

A generic malaria life cycle which summarises the number of parasites released at the end of each stage is shown in Figure 1.1. Since malaria is transmitted by a mosquito vector of the *Anopheles* genus (Ross R., 1897) the life cycle starts here. In order to produce eggs the female mosquitoes require a high protein source, blood, in their diets and they need to feed regularly. This makes them an ideal vector for parasite transmission. Whilst feeding, the female mosquito injects anticoagulants into the host blood. Approximately ten to 100 mature parasites (sporozoites), residing in the salivary glands of the mosquito, are injected at this point allowing them entry into their human host (Baldacci and Menard, 2004; Kappe *et al.*, 2010; Miller *et al.*, 1994).

Once inside the host the sporozoites actively move to the liver using gliding motility (Baldacci and Menard, 2004; Kebaier *et al.*, 2009; Shortt and Garnham, 1948). This process

may take up to an hour, depending on the route taken, either via the blood stream or the lymphatic system. The sporozoites invade the liver via specialised liver macrophages known as Kupffer cells (Cha et al., 2015). Inside a liver hepatocyte the sporozoites divide and change their morphology to blood infective forms known as merozoites. A single sporozoite may divide to form as many as 10000 to 30000 merozoites, which are released into the blood of the host after about one to two weeks once the infected liver cell bursts (Fujioka and Aikawa, 2002; Miller *et al.*, 1994).

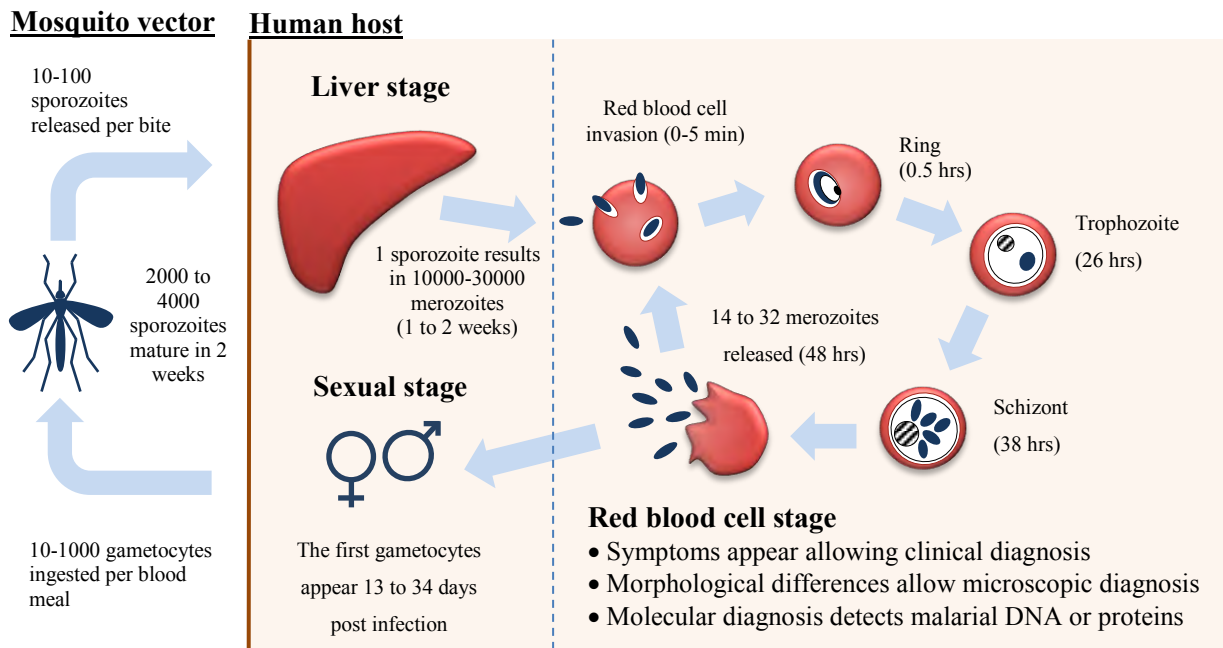


Figure 1.1 Generic malaria life cycle diagram including estimated number of parasites released per stage

The times for the red blood cell stages were based on the *P. falciparum* life cycle. The parasite numbers per stage were taken from Antia *et al.*, 2008; Baldacci and Menard, 2004; Fujioka and Aikawa, 2002; Kappe *et al.*, 2010; Miller *et al.*, 1994 and Smith and Craig, 2005.

The invasion of red blood cells occurs almost instantly (zero to five minutes) and was recorded by live cell imaging in a study by Gilson and Crabb (2009). The red blood cell cycle of the infection can take 24 (*P. knowlesi*), 48 (*P. falciparum*, *P. vivax*), 49 (*P. ovale*) or 72 (*P. malariae*) hours depending on the *Plasmodium* species causing the infection, where the *P. falciparum* blood stage times are shown in Figure 1.1 (Chin *et al.*, 1965; Daneshvar *et al.*, 2009; Fujioka and Aikawa, 2002; Lee *et al.*, 2011; Murray *et al.*, 2009). Once development in the red blood cells is complete, the cells rupture and the newly infective merozoites are released (between eight to 32 daughter merozoites) and infect naïve red blood cells (Antia *et al.*, 2008; Baldacci and Menard, 2004; Collins and Jeffery, 2005).

During the later stages of infection (usually after three to ten completed red blood cell cycles) a few of the merozoites mature into male or female gametocytes. Only once a female mosquito feeds on the infected host and ingests both gametocytes, does the sexual stage of the life cycle commence. The gametocytes fuse to form a zygote, which then forms a motile ookinete and migrates through the stomach wall to the midgut of the mosquito where it settles as an oocyst. Parasites divide and mature into sporozoites within the oocyst and are released to migrate to the salivary glands where they remain, until the mosquito seeks her next blood meal (Fujioka and Aikawa, 2002). Each of the *Plasmodium* species has different numbers of parasites and times for each developmental stage, which affects disease progression (see Figure 1.2).

1.1.4 *When do symptoms appear and what is the diagnostic window?*

During an infection the host remains asymptomatic until the parasite enters its red blood cell cycle. Due to the different *Plasmodium* species' infection characteristics, malaria symptoms present differently (Gwer *et al.*, 2007; Kidane and Morrow, 2000; Perkins and Bell, 2008; Sirima *et al.*, 2003). At the point where the infected red blood cells lyse, parasites as well as their metabolites are released into the host blood system. This allows the host's immune system direct contact with these factors and immune reactions follow, resulting in disease symptoms (Golgi, 1886; Miller *et al.*, 1994). At this stage patients may seek medical attention and diagnosis depending on the severity of the disease. The incubation time (period between the initial infective bite and appearance of symptoms) may vary depending on the number of infective sporozoites injected, the state of the host immune system and the effect of any treatment prior to diagnosis. Ideally diagnosis should occur before development of severe disease (Antia *et al.*, 2008; Barnes *et al.*, 2015; Suh *et al.*, 2004). The time taken for naïve and immune patients to develop severe infections can be estimated based on the numbers of parasites and time for each developmental stage from the life cycle (Figure 1.1) and accepting a simplified progression of disease. This is illustrated in Figure 1.2.

These simplified disease progress graphs illustrate the limited time during which diagnosis should ideally occur. It also highlights the window in which “normal” drug doses are effective for treatment of infections and at which point increased dose and duration of treatment are required. Hyperparasitemic infections (parasitemia greater than 100000 per microliter) require such treatment (Barnes *et al.*, 2015; White *et al.*, 2009).

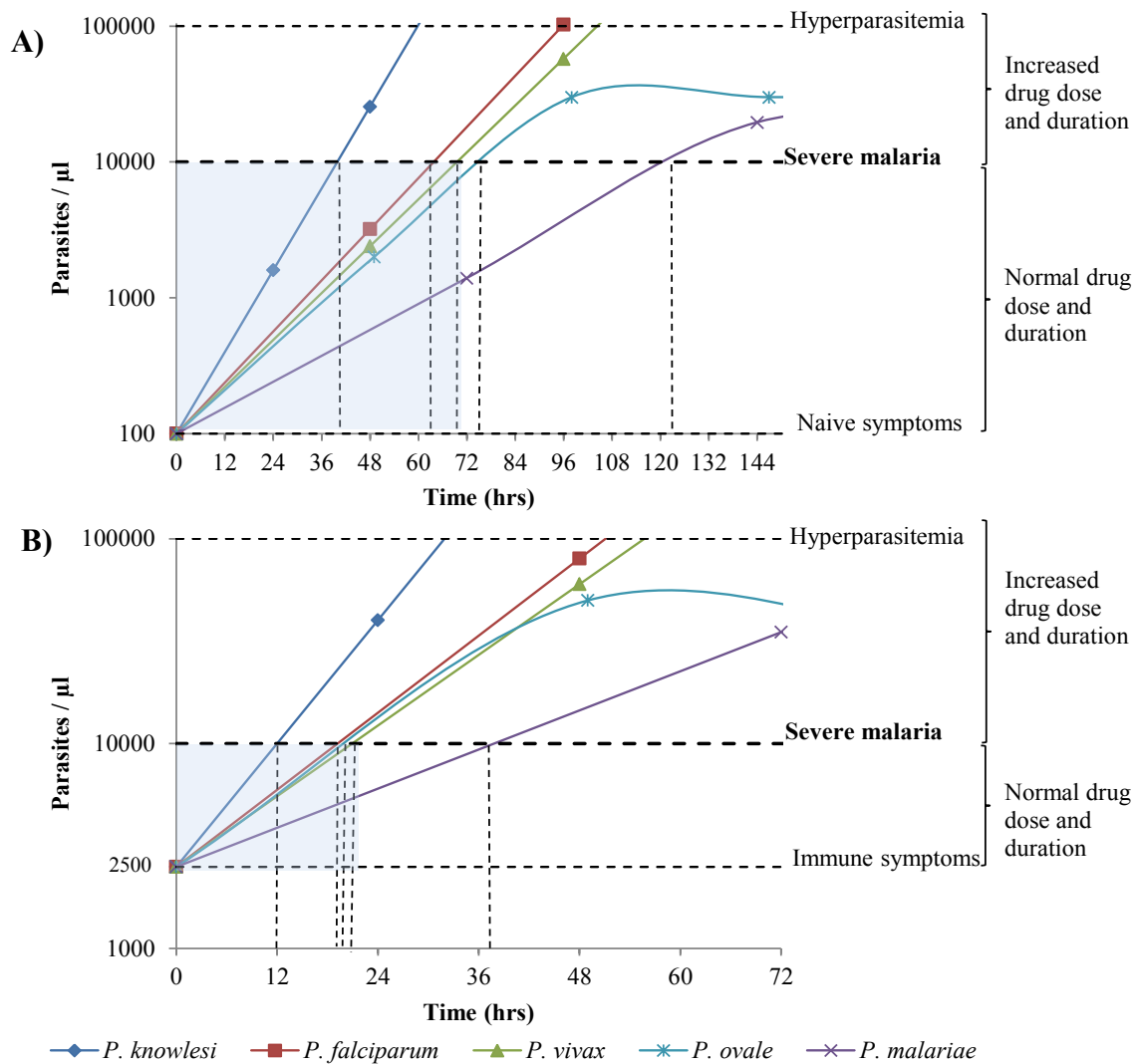


Figure 1.2 Dynamics of infection of each of the human infective malarials and the resulting diagnostic window for *P. falciparum*, *P. knowlesi* and *P. vivax*

The diagnostic window for *P. falciparum*, *P. knowlesi* and *P. vivax* is shaded in blue. This is the period within which malaria should ideally be diagnosed to optimally treat the infection with “normal” dose and duration of drugs. As parasitemia increases beyond 10000 parasites / microliter, increased dose and duration of drugs are recommended. The window falls between 36-72 hours for symptomatic naïve (A) and 12-21 hours for symptomatic immune patients (B) (Antia *et al.*, 2008; Baldacci and Menard, 2004; Barnes *et al.*, 2015; Chin *et al.*, 1965; Daneshvar *et al.*, 2009; Fujioka and Aikawa, 2002; Lee *et al.*, 2011; Miller *et al.*, 1994; Murray *et al.*, 2008 and 2009; White *et al.*, 2009).

Only three species of malaria have been reported to reach hyperparasitemic levels. These are *P. falciparum* (maximum parasitemia of 2500000 per microliter), *P. vivax* (maximum parasitemia of 100000 per microliter) and *P. knowlesi* (maximum parasitemia of 800000 per microliter) (Zimmerman and Howes, 2015). Human populations in endemic regions develop some form of non-sterilizing immunity against malaria, meaning that the dynamics of the disease are different between naïve and immune patients. In the case of naïve patients,

including children under five years old, malaria symptoms will start to appear once the parasitemia reaches 100 parasites per microliter, which is why the origin of Figure 1.2 (A) was set at this parasitemia (Hänscheid, 1999). In contrast, immune patients may remain asymptomatic with a parasitemia of 2500-10000 per microliter as shown in Figure 1.2 (B) (Hänscheid T., 1999). Severe malaria is usually diagnosed at greater than 10000 to 30000 parasites per microliter and prognoses deteriorate rapidly beyond this level of infection (Barnes *et al.*, 2015; White *et al.*, 2009).

Based on Figure 1.2 (A) malaria may cause severe disease within 36 to 72 hours in naïve hosts for most of the human infecting species. In the case of *P. malariae* this may take longer, causing severe disease around 120 hours after the first clinical symptoms appear in naïve patients. In immune hosts (Figure 1.2 (B)) symptomatic infections may escalate to hyperparasitemic infections within very short periods of time, between 12 to 36 hours, due to higher initial parasitemia. The WHO recommends treatment within 24 hours of the onset of fever and diagnosis within two hours of patients presenting for treatment (WHO guidelines for treatment of malaria, 3rd edition, 2015a). The window for diagnosis and timely treatment ideally lies between parasitemia causing symptoms and severe disease as shaded in blue in Figure 1.2. Importantly, any complications, such as drug-resistant infections, also need to be diagnosed to allow for timely changes in treatment if required.

The window for diagnosis narrows when considering that patients usually only present themselves to clinicians once they express symptoms and sometimes only after self-treatment has failed, resulting in an increased number of severe as opposed to mild malaria cases. This increases the time pressure on diagnosis and treatment. Diagnostic methods should ideally allow for rapid point of care diagnosis of the patient. Due to the high mortality, treatment may often be administered without confirmed diagnosis.

1.1.5 The importance of diagnosis to prevent spread of resistance

Treatment of malaria used to be based on the clinical diagnosis of disease and subsequent prescription of anti-malarial drugs. This was an effective strategy as little time was taken to treatment and antimalarial drugs such as chloroquine were readily available, cheap and effective. The unfortunate consequence of such “liberal” use of these drugs was that this practice selected for anti-malarial drug resistant parasite populations. The WHO no longer recommends fever as a sole diagnostic marker for malaria in the tropics and microscopic and/or molecular diagnosis as confirmation prior to treatment is now advised. Another factor

contributing to the spread of resistance is inadequate dosage and duration of anti-malarial drugs prescribed to patients with hyperparasitemic infections (Barnes *et al.*, 2015; White *et al.*, 2009). At hyperparasitemic levels, “normal” drug treatment regimens may still reduce the parasite load of the patient but are insufficient to clear the infection. This results in exposure of parasites to sub-optimal drug doses and the subsequent selection of resistant phenotypes. The ability to quantify the parasite load within the patient would allow clinicians to track disease progress and success of treatment. Diagnostic methods should ideally be able to quantify parasite load and be cheap enough to allow for repeat diagnoses to track treatment progress even in resource poor settings (Barnes *et al.*, 2015; White *et al.*, 2009).

1.1.6 *Complicated malaria infections*

Several additional challenges for diagnosis will be discussed to follow, including cerebral, placental and mixed infections. During a *P. falciparum* infection, the parasites produce proteins such as Histidine rich protein 2 (HRP2) and Erythrocyte membrane protein 1 (EMP1) which are located to knobs on the surface of the infected red blood cell (Bannister *et al.*, 2000). These proteins cause the infected red blood cells to stick to each other as well as to uninfected red blood cells. The infected cells also stick to endothelial cells of arterioles. These phenomena are referred to as rosetting and sequestration respectively (Leitgeb *et al.*, 2011). Resulting restricted blood flow causes cerebral malaria and organ failure in severe infections (David *et al.*, 1983; Leitgeb *et al.*, 2011). Malaria diagnosis during pregnancy is also complicated by this phenomenon, referred to as placental malaria. Sequestration and rosetting result in low levels of parasites in the peripheral blood, which makes microscopic detection of parasites difficult.

This makes it important to either complement or replace microscopic diagnosis with detection of soluble targets released by sequestered parasites, such as proteins, nucleic acids and carbohydrates, as detection of parasites in the blood becomes less reliable (Kattenberg *et al.*, 2011). There is also a need to detect liver dormant parasites in a similar way to detect potential relapse infections (Fujioka and Aikawa *et al.*, 2002).

Coinfection with different malaria species is also possible (Chuangchaiya *et al.*, 2010; Murray *et al.*, 2008). This affects treatment and highlights the need for species-specific diagnosis. Drug resistance to date is most prominent within strains of *P. falciparum* followed by *P. vivax* and, in many cases diagnosis of these species requires treatment with combination therapies as opposed to conventional drugs (WHO guidelines for treatment of malaria, 3rd

edition, 2015a). This complicates treatment strategies and makes them more expensive which has made diagnosis prior to treatment more “cost effective”. Fortunately the other three *Plasmodium* species have not yet developed any resistance to anti-malarial drugs, making them simpler and cheaper to treat. *P. knowlesi* remains susceptible to artemisinin with variable to moderate susceptibility to chloroquine, but should not be treated with mefloquine (Fatih *et al.*, 2012). Tracking the spread of drug resistance is critical in maintaining effective malaria control strategies and methods to diagnose resistance are essential (Carnevale *et al.*, 2007; Duraisingh *et al.*, 1998).

Several tropical diseases, including dengue, not only display similar symptoms to malaria, but also co-infect patients with malaria (Källander *et al.*, 2004; Rao *et al.*, 2015). This complicates clinical diagnosis and highlights the need for confirmed diagnosis using either microscopy or alternate molecular methods (Gwer *et al.*, 2007; Perkins and Bell, 2008). Regardless of the challenges, malaria control efforts have been successful at reducing the global distribution of malaria and the next section will highlight the successes achieved and the current setting of diagnosis in endemic regions that resulted.

1.2. Malaria control to date and the setting of diagnosis

Malaria used to be distributed globally, but has since been restricted to the tropics (Figure 1.3). Our understanding of malaria has been integral in its control and some of the major discoveries and implementation of control strategies were highlighted in Figure 1.3. Tropical fevers have long been treated using anti-malarial drugs including artemisinin and quinine (China since the 4th and South America since the 17th century respectively).

The cause of malaria, which was thought to be from bad air (“*mal-aria*” in Latin), was only discovered as late as 1880 by Laveran (Laveran, 1880). The subsequent detection of the *Plasmodium* parasite with a Giemsa stain for microscopy in 1891 is still used as the gold standard for malaria diagnosis today (Moody, 2002). Although this improved the diagnosis and treatment of malaria, only with the discovery of the mosquito vector by Ross in 1897 (Ross, 1897), was the life cycle of the parasite understood. Between the 1930s and 50s a whole range of anti-malarial drugs were developed and discovered as well as the pesticide DDT. Together these tools allowed the WHO to launch and oversee the first large scale control programme against malaria in 1955. Malaria was since eradicated from Japan, Europe and North America, soon followed by Russia and Australia.

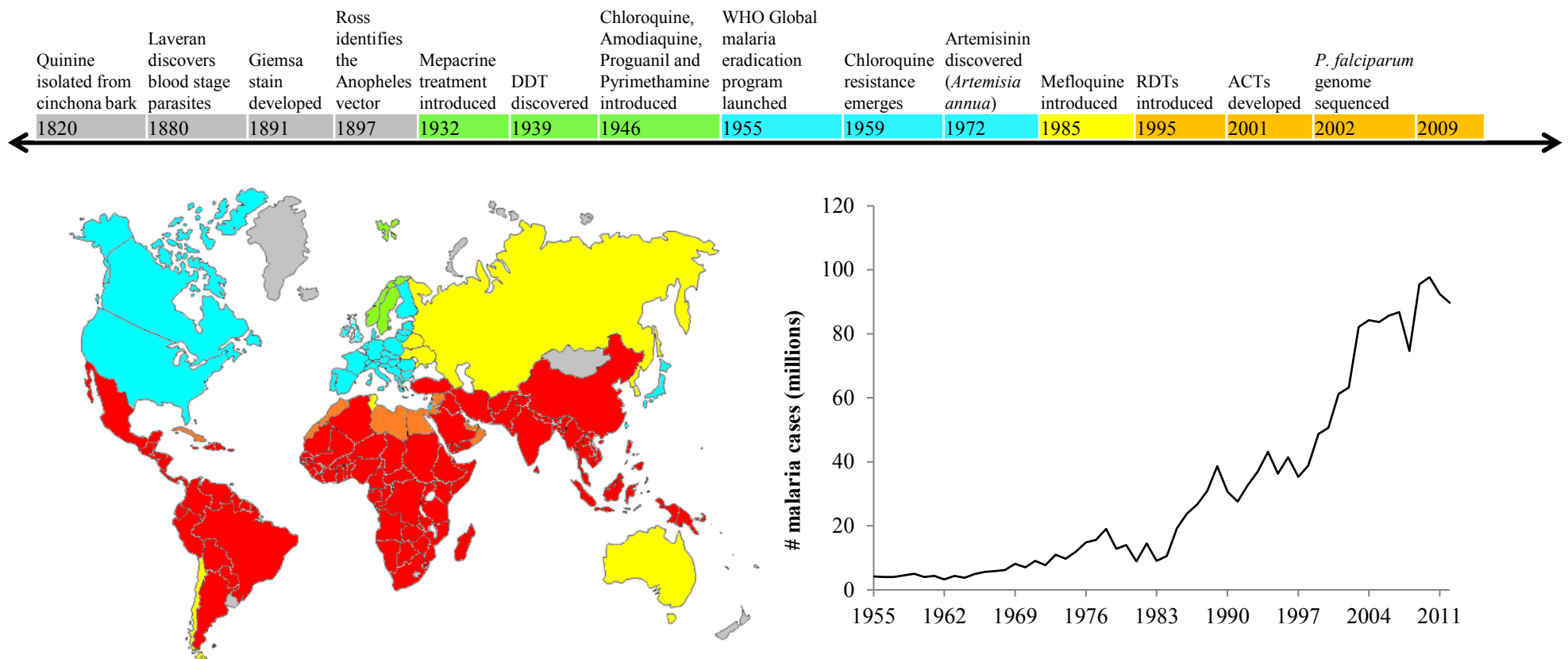






Figure 1.3 Malaria control / eradication statistics and timeline

The map defines the regions of the world in which malaria was found and from which it has either been eradicated or controlled. The shading represents regions in which control strategies were implemented according to the timeline colours, where grey areas represent regions in which endemic malaria was never reported and red areas indicate countries in which malaria is still found today. The graph alongside the map shows the number of malaria cases diagnosed per year from 1955 to 2012. Literature cited for these figures included Faechem *et al.*, 2010; Guerra *et al.*, 2007; Hay *et al.*, 2009 and the WHO 2015b.

As mentioned before, an unfortunate consequence of the “liberal” use of antimalarials and pesticides during this eradication strategy was the development and spread of resistant parasites and mosquito vectors. To counter this, greater emphasis has been placed on positive diagnosis prior to treatment, which led to the development and introduction of point-of-care diagnostic tests, such as rapid diagnostic tests (RDTs) in 1995. Although not as sensitive as more sophisticated and expensive molecular methods, these tests detect symptomatic infections within 15 minutes and are relatively simple to interpret (Moody, 2002).

In spite of these successes, malaria prevalence seems to have increased (graph in Figure 1.3). The emphasis on and availability of diagnosis has also increased together with control efforts. The resulting malaria mortalities have fallen from 839000 to 438000 from 2000 to 2015 (WHO guidelines for treatment of malaria 2015a). Better surveillance and record keeping are a spinoff of point-of-care diagnosis, enabling mapping of disease prevalence, transmission and drug resistance more accurately. The malaria atlas project (<http://www.map.ox.ac.uk/>) is a database which summarises and presents these data in regional to global formats with a user friendly interface. Such overviews are integral to organising control strategies, especially in light of malaria elimination ambitions. Statistics for current endemic regions were summarised in Table 1.1. Around 1.2 billion inhabitants live in high-risk malaria-endemic regions (WHO World Malaria Report 2015b). The cost associated with control as well as estimated and confirmed death tolls are also included. These numbers differ from the estimated global numbers as they only include confirmed “endemic cases” of malaria and not the number of “imported cases”. The total cost of control (in USD) in endemic regions was approximately 2.73 billion for the 2013 / 2014 period, of which 2.17 billion was for control in Africa alone. The greatest malaria burden remains in Africa and productivity losses amount to around 12 billion USD annually (Hay *et al.*, 2009; Suh *et al.*, 2004). The high cost of control on developing countries in endemic regions means that diagnosis needs to be cheap and simple. Point-of-care diagnosis is an ideal solution. Such diagnosis would allow rapid treatment of patients. In complicated infections, as described earlier, rapid provisional treatment may be life-saving, buying time for further diagnosis and more specific treatment for example. The addition of *P. knowlesi* to the human infecting species as well as the spread of artemisinin and multidrug resistance in the South-East Asia and Oceania regions is of great concern to control in these regions (Dondorp *et al.*, 2009; Moyes *et al.*, 2014). The absence of vectors transmitting *P. knowlesi* in Africa and the Americas has prevented it from spreading to these regions for the time being (Akler *et al.*, 2007; Koenderink *et al.*, 2010).

Table 1.1 Endemic malaria statistics for 2013 / 2014 from the WHO and malaria atlas project

Endemic region	Central & South America	Africa	Middle East & Asia	Oceania
				
Population at risk *	20,392,800 (389,575)	736,124,577 (75,191,566)	296,531,000 (1,814,993)	44,722,000 (561,763)
Control funding (USD)	155,300,000	2,173,400,000	283,900,000	121,000,000
Estimated deaths	260 - 1 180	235,856 - 570,230	502,881 - 1,065,380	12,720 - 40,230
Confirmed deaths	96	98,258	904	305
Plasmodium species	<i>P. falciparum</i> <i>P. ovale</i> <i>P. malariae</i> <i>P. vivax</i>	<i>P. falciparum</i> <i>P. ovale</i> <i>P. malariae</i> <i>P. vivax</i>	<i>P. falciparum</i> <i>P. ovale</i> <i>P. knowlesi</i> <i>P. vivax</i> <i>P. malariae</i>	<i>P. falciparum</i> <i>P. ovale</i> <i>P. knowlesi</i> <i>P. vivax</i> <i>P. malariae</i>
Drug resistance	Chloroquine / amodiaquine (<i>P.f</i>)	Chloroquine / amodiaquine (<i>P.f</i>) Primaquine (<i>P.v</i>)	Chloroquine / amodiaquine (<i>P.f</i>) Mefloquine / quinine (<i>P.f</i>) Primaquine (<i>P.v</i>) Artemisinin and ACT (<i>P.f</i>)	Chloroquine / amodiaquine (<i>P.f</i> ; <i>P.v</i>) Primaquine (<i>P.v</i>)
Anopheles species	<i>An. albimanus</i> <i>An. albitarsis</i> <i>An. aquasalis</i> <i>An. darlingi</i> <i>An. nuneztovari</i> <i>An. pseudopunctipennis</i>	<i>An. arabiensis</i> <i>An. culicifacies</i> <i>An. funestus</i> <i>An. gambiae</i> <i>An. melas</i> <i>An. merus</i> <i>An. moucheti</i> <i>An. nili</i> <i>An. sergentii</i>	<i>An. aconitus</i> <i>An. minimus</i> <i>An. barbirostris</i> <i>An. sacharovi</i> <i>An. culicifacies</i> <i>An. sergentii</i> <u><i>An. dirus</i></u> <i>An. fluviatilis</i> <u><i>An. stephensi</i></u> <u><i>An. latens</i></u> <i>An. lesteri</i> <i>An. subpictus</i> <u><i>An. leucosphyrus</i></u> <i>An. superpictus</i> <u><i>An. maculatus</i></u>	<i>An. aconitus</i> <u><i>An. leucosphyrus</i></u> <i>An. annularis</i> <u><i>An. maculatus</i></u> <u><i>An. balabacensis</i></u> <i>An. minimus</i> <i>An. barbirostris</i> <i>An. punctulatus</i> <u><i>An. cracens</i></u> <i>An. dirus</i> <i>An. sinensis</i> <i>An. farauti</i> <i>An. flavirostris</i> <i>An. koliensis</i>
Pesticide resistance	Carbamates Organochlorides Organophosphates Pyrethroids	Carbamates Organochlorides Organophosphates Pyrethroids	Carbamates Organochlorides Organophosphates Pyrethroids	Carbamates Organochlorides Pyrethroids

*The population at risk estimations include people living in high-risk malaria endemic regions only, with the total number of confirmed malaria cases in brackets. The *Anopheles* species underlined are known for transmitting *P. knowlesi* in endemic regions.

The step from control to elimination of malaria from a target area has several implications. Control entails reducing the risk of malaria-associated morbidity and mortality to a point where it is no longer considered a public health problem. Control does not aim to prevent all transmission. Elimination on the other hand requires identification and treatment of all infected individuals, whether symptomatic or asymptomatic to prevent transmission. Lower limits of detection are therefore required.

1.2.1 The importance of the malaria pool and the need for more sensitive diagnosis

Asymptomatic infections present perhaps the greatest challenge to malaria elimination and effectively act as reservoirs of malaria (Alves *et al.*, 2005; Hafalla *et al.*, 2011; Miller *et al.*, 1994). These individuals are unlikely to seek diagnosis. Moreover natural infection of great apes and monkeys with *P. falciparum* has been reported (Araujo *et al.*, 2013; Prugnolle *et al.*, 2010) and *P. knowlesi* naturally infects both humans and monkeys (Singh and Daneshvar, 2013). Natural human infection with the simian malarias *P. brazilianum* and *P. cynomolgi* has also been reported (Lalremruata *et al.*, 2015; Ta *et al.*, 2014). The natural reservoirs of human infecting *Plasmodium* species add to the asymptomatic pool and present a great challenge to the elimination agenda. As a result diagnostic research has focused on development of more sensitive diagnosis to enable population screening for asymptomatic infections. Detection of parasitic infections from alternate source material, such as faeces, has also allowed for identification of non-human primate carriers (Araujo *et al.*, 2013; Prugnolle *et al.*, 2010). Abkallo *et al.* (2014) argued that detection of DNA in faecal matter is not necessarily an indicator of a blood stage infection. Measuring the number of malaria carrying mosquitoes in an area (entomologic inoculation rate) is another method of assessing the malaria burden in an area (Bashar *et al.*, 2013; Durnez *et al.*, 2011; Koekemoer *et al.*, 2001; Mouatcho *et al.*, 2007).

1.2.2 Entomologic inoculation rate

Plasmodium's main *Anopheles* vectors generally inhabit the tropics (Kiszewski *et al.*, 2004; Table 1.1). The ability to identify parasite carrying vector species is important and monitoring parasite loads within these populations is another measure of the effect of control measures within a region. This will have more significance if transmission blocking drugs and vaccines are developed further (Stone *et al.*, 2015). "Prevention is better than cure" holds true for the control of malaria and preventing contact between the malaria vector and its host remains one of the most effective tools in the control of malaria, but the increased prevalence of insecticide resistance is concerning.

1.2.3 Insecticide resistance

The current insecticides used against *Anopheles* include 12 varieties from only four classes including organochlorides, organophosphates, carbamates and pyrethroids (Table 1.1). The latter is the only insecticide approved for use in treated bed nets (Betson *et al.*, 2009). Subsequent pyrethroid resistance has developed and was first recorded in the 1950s and has since spread against all four classes throughout endemic regions, predominantly due to the pyrethroid knock down resistance (*kdr*) mutation (Martinez-Torres *et al.*, 1998). Organophosphates are the only class without resistance in the Oceania region (Betson *et al.*, 2009; Blanford *et al.*, 2011; Malaria Atlas Project (<http://www.map.ox.ac.uk/>)). Alternate control measures are being developed including alternate pesticide formulations and biocontrol measures (Betson *et al.*, 2009; Blanford *et al.*, 2011). Since not all vectors are night feeders, controlling contact during the day becomes difficult and infection is inevitable in many circumstances. In addition the consequences of climate change and a change in the natural habitat of the vector may alter and affect countries currently without malaria (Siraj *et al.*, 2014; Tonnang *et al.*, 2010). Monitoring the entomological inoculation rates within control regions may become more important in the future. Diagnosis of human infection will be discussed further.

1.3. The stages of the malaria life cycle targeted for diagnosis

There are several approaches used for diagnosis and most focus on the blood stage of the infection since it is during that stage that the patient experiences the symptoms of malaria and has the highest parasite load of the life cycle (Antia *et al.*, 2008; Baldacci and Menard, 2004; Miller *et al.*, 1994; Figure 1.1). The source material, perhaps obviously, is patient blood. Several studies identified infections from alternate sources mentioned below, aiming to make diagnosis less invasive but also to improve surveillance of natural simian pools and vector populations (Abkallo *et al.*, 2014; Bass *et al.*, 2008; Jirku *et al.*, 2012; Moody, 2002; Najafabadi *et al.*, 2014; Stone *et al.*, 2015). Detection of parasite proteins or nucleic acids from faeces, urine and saliva is also possible. Development of less invasive methods is important as there are often beliefs associated with drawing patient's blood and for infants this may also be problematic. Abkallo *et al.* (2014) were able to detect liver stage infections in mice using PCR in both blood and faecal samples. The possibility of detecting alternate stages may have significance with regard to therapy as drugs preventing liver cell egress and gametocyte development may be applicable, thus limiting transmission. The different source materials used in these studies are summarised in Table 1.2.

Table 1.2 Summary of the source materials used for diagnosis

Life cycle stage	Source	Reference
Mosquito	Mouthparts	Bass <i>et al.</i> , 2008; Stone <i>et al.</i> , 2015
Liver	Blood	Abkallo <i>et al.</i> , 2014
	Faeces	Abkallo <i>et al.</i> , 2014
Red blood cell	Blood	Moody, 2002
	Serum	Moody, 2002
	Saliva	Najafabadi <i>et al.</i> , 2014
	Urine	Najafabadi <i>et al.</i> , 2014; Oguonu <i>et al.</i> , 2014
	Faeces	Jirku <i>et al.</i> , 2012
Gametocytes	Cerebrospinal fluid	Mikita <i>et al.</i> , 2014
	Blood	Schneider <i>et al.</i> , 2015

Importantly there has not been a lot of progress regarding the diagnosis of placental or cerebral malaria. For placental malaria, the most accurate diagnosis is still by histology of the placenta, when compared to diagnosis using PCR, RDT and blood microscopy (Kattenberg *et al.*, 2011). Due to sequestration of parasites in the placenta, parasitemia in the mother's blood is inherently low and the study by Kattenberg *et al.* (2011) recommends RDT or PCR as a reference test as opposed to conventional peripheral blood microscopy. An interesting approach by Mikita *et al.* (2014) was to diagnose cerebral malaria infections from cerebrospinal fluid of patients. Although diagnosis of infection was possible, there was no statistical link between normal and cerebral malaria infections. Diagnosis of cerebral malaria is still elusive, however, a study by Bachman *et al.* (2014) measured levels of increased carbonic anhydrase 3 and creatine kinase in cerebral malaria patient plasma. These may aid as markers in diagnosing the onset of cerebral malaria. Only with the development of alternate methods to microscopy, have other stages of the life cycle become viable for diagnosis. The next section will focus on the different methods for malaria diagnosis and the targets will be discussed thereafter.

1.4. Methods to diagnose malaria

Diagnostic methods are compared in terms of their sensitivity, specificity and limit of detection. Test sensitivity refers to the ability to correctly diagnose a set of known positive and negative samples. Specificity on the other hand measures the test's ability to correctly identify the infecting species causing malaria. Both are expressed as percentages of correctly diagnosed samples of a test pool. A test's limit of detection measures the lowest level of accurately detecting an infection. Any new test is traditionally compared to microscopy as a gold standard for diagnosis, although PCR is often used in addition to this (Moody, 2002; Murray *et al.*, 2008). This next section will describe methods used in malaria diagnosis and

compare them in terms of limits of detection alone. The reader is referred to the literature for additional information regarding sensitivity and specificity.

The first set of methods detects parasite induced reactions in the host including clinical symptoms (Miller *et al.*, 1994), host-immune-related proteins and parasite metabolites (Table 1.3). As a foreign particle in the human body, the parasite elicits an immune response against it and the metabolites it produces. This forms the basis for clinical diagnosis (fever patterns), serodiagnosis (parasite specific host antibodies) and spectral methods (increased levels of metabolites in sera) amongst others.

1.4.1 Clinical diagnosis of malaria

Clinical diagnosis is based on the symptoms expressed by the patient during an infection (Golgi, 1886; Miller *et al.*, 1994). Due to the differing lengths of the red blood cell stages of each of the human infecting *Plasmodium* species, different fever patterns result. *P. knowlesi* causes daily fever; *P. falciparum*, *P. vivax* and *P. ovale* cause tertian fever (every third day) and *P. malariae* causes quartan fever (every fourth day) episodes (Antia *et al.*, 2008; Collins and Jeffery, 2007; Daneshvar *et al.*, 2009; Sabbatani *et al.*, 2010). Due to the different levels of host immunity, the limit of detection for clinical diagnosis ranges from 100 to 10000 parasites per microlitre (Figure 1.2 and Table 1.3). The greatest advantage of clinical diagnosis is that it allows for point-of-care treatment. Fever is common to many tropical diseases however, including dengue and pneumonia (Källander *et al.*, 2004; Rao *et al.*, 2015) and the resulting accuracy of diagnosis for malaria falls to 20 to 30% (Gwer *et al.*, 2007; Perkins and Bell, 2008). The high mortality especially in children under the age of five has seen the implementation of integrated disease management strategies (Gove S., 1993), which has resulted in 40% reductions in mortality rates for this age group (Kidane and Morrow, 2000; Sirima *et al.*, 2003).

Snow *et al.* (2003) estimated 870 million fever cases in African children alone, which unfortunately highlight the “liberal” approach to using clinical diagnosis in the field. As mentioned previously the WHO now recommends either microscopy or a molecular based diagnosis for malaria prior to treatment. These will be discussed further.

1.4.2 Serodiagnosis of malaria

A more specific method diagnosing the immune reaction within the host is termed serodiagnosis. This method measures the antibodies in the patient raised specifically against the parasite (Olesen *et al.*, 2010; She *et al.*, 2007). An antibody response may result in as

little as one week after the onset of the red blood cell infection, which may be in as little as two to three weeks after an infective mosquito bite (Figure 1.1; She *et al.*, 2007). The ability of the test to determine the species causing disease is dependent on the antigen used in the ELISA. Quantitation of parasitemia is not possible and the ELISA format makes this a laboratory-based test. The biggest drawback of serodiagnosis is that antibodies persist for up to a year after parasite clearance, and in endemic regions “immune” individuals will have almost constant levels of parasite specific antibodies, making accurate diagnosis of current infections difficult, if not impossible (Makler *et al.*, 1998; She *et al.*, 2007).

1.4.3 Spectral analyses of malaria infections

Detecting abnormalities in patients’ blood as a direct result of parasitic infections forms the basis for the next set of tests, where most detect haemozoin. Catabolism of haemoglobin forms a major part of the parasite red blood cell stage (Bannister *et al.*, 2000; Olszewski *et al.*, 2011). As the resulting amino acids are metabolised, the central haeme group of the protein remains and is polymerised by the parasite into an insoluble crystalline form referred to as haemozoin. Both haeme and haemozoin are released into the blood of patients (Dostert *et al.*, 2009) as detected by Raman spectroscopy for example (Hobro *et al.*, 2013). The limit of detection of this method has improved dramatically from around 1000 parasites per microlitre to 2.5 – 50 parasites per microlitre using the surface enhanced method (Bilal *et al.*, 2015; Chen *et al.*, 2016). This enhancement does however require sample manipulation which was not previously necessary. The specialised equipment and interpretation of the spectra make this a laboratory based assay not suited to point-of-care diagnosis as yet. A different spectrum-based diagnostic method makes use of infra-red spectral analysis and is capable of detection within three minutes to a limit of one to 500 parasites per microlitre and samples only require methanol treatment in this case (Khoshmanesh *et al.*, 2014). Both surface enhanced Raman and infra-red spectrometry methods are capable of parasite quantification which would allow for monitoring patient treatment success (Khoshmanesh *et al.*, 2014). Alternatively parasite metabolites including NAD, FAD, porphyrin, tyrosine and tryptophan residue fluorescence is measured in comparison to uninfected blood. Differences in spectra are often disease specific, as with malaria, and were measured by NMR or spectrofluorometer, but require further assessment (Masilamani *et al.*, 2014; Teng *et al.*, 2014). The last set of methods in this group is based solely on haemozoin detection.

1.4.4 Haemozoin based detection of malaria

Targeting haemozoin for diagnosis has received a lot of attention to date. Following release of haemozoin into the blood, the particles are phagocytosed by white blood cells and can be detected using cell analysers or counters (Grimberg B.T., 2011; Hänscheid *et al.*, 1999; Rebelo *et al.*, 2013). Methods exploiting the birefringent and magnetic properties of haemozoin have since been developed and reduced the limit of detection from 500-1500 to 10-40 parasites per microlitre. With further testing these tests have the possibility of being used as point-of-care diagnostic tests (Butykai *et al.*, 2013; Delahunt *et al.*, 2014; Orban *et al.*, 2016; Pirnstill and Cote, 2015). Lower limits of detection have been achieved using mass spectrometry with sample analysis taking only a few minutes, however the sophisticated equipment required limits this to a laboratory setting (Demirev *et al.*, 2002; Scholl *et al.*, 2004). A transdermal diagnostic prototype capable of instant detection of haemozoin was developed by Lukianova-Hleb *et al.* (2015) with a very low limit of detection of ~1.7 parasites per microlitre.

Different optical detection methods have been developed, which make use of microscopy in some way. These are perhaps the more “traditional” methods as listed in Table 1.4 and discussed thereafter.

Table 1.3 A summary of methods based on the detection of the host response as well as *Plasmodium* specific metabolites

Method	Format	LOD (parasites / μ l)	Speciation	Quantitative	Monitoring treatment	Setting	Time	References
Clinical	Symptoms	100 (naïve) 2500-10000 (immune)	Yes	No	Yes	POC	Species dependent	Gwer <i>et al.</i> , 2007; Kidane and Morrow <i>et al.</i> , 2000; Perkins and Bell, 2008; Sirima <i>et al.</i> , 2003
Serodiagnosis	Parasite-specific antibodies	NA	Yes	No	No	Lab	2 to 4 hrs	Olesen <i>et al.</i> , 2010; She <i>et al.</i> , 2007
Raman spectra	Original method	1000	No	No	Yes	Lab	> 2 hrs	Bilal <i>et al.</i> , 2015; Hobro <i>et al.</i> , 2013
	Surface enhanced	2.5-50	No	Yes	Yes	Lab	> 1 hr	Chen <i>et al.</i> , 2016; Yuen and Liu, 2012
Infrared spectra	Attenuated total reflectance	< 1 (detection) -500 (quantification)	No	Yes	Yes	Lab	< 3 min	Khoshmanesh <i>et al.</i> , 2014
Haemozoin	Flow cytometry	500-1500	No	Yes	Yes	Lab	> 30 min	Grimberg, 2011; Hänscheid <i>et al.</i> , 1999; Rebelo <i>et al.</i> , 2013
	Dark-field / polarized microscopy	30	No	Yes	ND	POC	ND	Delahunt <i>et al.</i> , 2014; Pirnstill and Cote, 2015
	Magneto-optical	10-40	No	No	No	POC	> 30 min	Butykai <i>et al.</i> , 2013; Orban <i>et al.</i> , 2016
	Mass spectrometry	< 10	No	Yes	Yes	Lab	< 1 min	Demirev <i>et al.</i> , 2002; Scholl <i>et al.</i> , 2004
	Transdermal	1.7	No	No	No	POC	Instant	Lukianova-Hleb <i>et al.</i> , 2015

LOD limit of detection; NA data not available; ND not determined; POC point of care diagnosis

Table 1.4 A summary of methods based on the physical/visual detection of *Plasmodium* parasites

Method	Format	LOD (parasites / μ l)	Speciation	Quantitative	Monitoring treatment	Setting	Time	References
Microscopy	Giemsa	5-10 (expert) 100 (average)	Yes	Yes	Yes	POC	30 min-1 hr	Moody, 2002; Zimmerman and Howes, 2015
	Fluorescence	60	No	No	No	POC	10-15 min	Adeoye and Nga, 2007; Baird <i>et al.</i> , 1992
Optical tweezer		parasitemia dependent	No	Yes	Yes	Lab	40 rbc / min	Mohanty <i>et al.</i> , 2004

LOD limit of detection; NA data not available; ND not determined; POC point of care diagnosis; rbc red blood cell

1.4.5 Microscopic detection of malaria

Since the discovery of the blood stage of malaria and the development of the Giemsa stain, microscopy has remained the gold standard in malaria diagnosis (Moody, 2002). Visual identification of parasites under the microscope is still used for diagnosis today and exploits the terminally differentiated nature of red blood cells which lack DNA. The parasites do not lack DNA, thus detection of parasites within red blood cells based on DNA stains forms the basis of this method. Wright's, Field's and Leishman stains have also been developed (Moody, 2002; Sathpathi *et al.*, 2014; Suh *et al.*, 2004). Diagnosis to a species level is possible due to morphological differences between parasites (Anderios *et al.*, 2009; David *et al.*, 1983; Gkrania-Klotsas and Lever, 2007; Moody, 2002). The method also allows for quantification of the parasite burden by counting the number of infected red blood cells. This is either done in relation to a white blood cell count in a thick film preparation (number of infected red blood cells in comparison to 200 white blood cells) or red blood cells in a thin film preparation (a total of ~10000 red blood cells viewed ~ 40 fields of view at 100 X magnification). One microlitre of blood is assumed to contain ~ 5×10^6 red blood cells, therefore the following equation is used: 1% parasitemia = 5000 parasites per microliter of blood (Moody, 2002). The limit of detection for microscopy is subject to the expertise of the microscopist and can vary from five to ten, to 100 parasites per microliter (Moody, 2002; Zimmerman & Howes, 2015). To aid in this regard, Prescott *et al.* (2012) developed a microscopy image analysis slide reading device aiming to standardise microscopy by automation, but the method requires further optimisation. Fluorescence microscopy or the buffy coat method on the other hand has similar detection limits without the possibility of speciation; it does however take between half to a quarter of the time to diagnose a patient (Adeoye & Nga, 2007; Baird *et al.*, 1992). Three fluorescent dyes are currently available including acridine orange; benzothiocarboxypurine and rhodamine-123 (Moody, 2002). A portable format has also been developed (Sousa-Figueiredo *et al.*, 2010).

An interesting innovation is the use of optical tweezers in malaria diagnosis. This method measures the rotational ability of red blood cells once captured between optical tweezers. Due to the increased rigidity of the infected red blood cell membrane, these cells lose their inherent ability to rotate whereas normal cells do not. The basis is similar to a flow cytometric analysis, where currently 40 red blood cells can be analysed per minute (Mohanty *et al.*, 2004). The last set of methods is based on the detection of parasite-specific molecular targets listed in Table 1.5.

Table 1.5 A summary of methods based on the detection of *Plasmodium*-specific molecular targets

Method	Format	LOD (parasites / μ l)	Speciation	Quantitative	Monitoring treatment	Setting	Time	References
Antigen based	RDT	100	Yes	No	Yes	POC	15 min	Mouatcho and Goldring, 2013
	DAS ELISA	12	Yes	No	Yes	Lab	2-4 hrs	Noedl <i>et al.</i> , 2006; Sousa <i>et al.</i> , 2014
	pLDH	200	Yes	Yes	Yes	Lab	2-3 hrs	Makler <i>et al.</i> , 1993b; Piper <i>et al.</i> , 1999, 2011
	Immunomagnetic pLDH	21	Yes	Yes	Yes	Lab	45 min	Markwalter <i>et al.</i> , 2016
	Amperometric	^x (400)	Possible	Possible	Possible	POC	34-55 min	Sharma <i>et al.</i> , 2010
	Paper based	+ (0.7-12)	Possible	Possible	Possible	POC	ND	Grant <i>et al.</i> , 2016
	Electrochemical	*(< 3)	Possible	Possible	Possible	POC	1-2 hrs 15 min	Glavan <i>et al.</i> , 2014
PCR	Single	1-5	No	No	No	Lab	2 hrs	Demas <i>et al.</i> , 2011
	Multiplex	0.025-0.27	Yes	No	No	Lab	2 hrs	Chew <i>et al.</i> , 2012; Hofmann <i>et al.</i> , 2015
	Nested	0.1-10	Yes	No	No	Lab	4-4.5 hrs	Singh <i>et al.</i> , 1999
	Real time PCR (qPCR)	0.25-2.5	Yes	Yes	Yes	Lab	3 hrs	Kamau <i>et al.</i> , 2013; Rougemont <i>et al.</i> , 2004
	TARE-2	0.03-0.15	No	Yes	Yes	Lab	2-3 hrs	Hofmann <i>et al.</i> , 2015
	LF-RPA	4-20	No	No	No	POC	15-30 min	Kersting <i>et al.</i> , 2014
	NASBA	0.02	No	Yes	Yes	Lab	4 hrs	Schneider <i>et al.</i> , 2005
NALFIA	1-8	No	No	No	Lab	1 hr 15 min	Mens <i>et al.</i> , 2012	
LAMP	Turbidity	1-10	Yes	No	No	POC	30-40 min	Mohon <i>et al.</i> , 2014; Polley <i>et al.</i> , 2010
	LFD	ND	Yes	No	No	POC	1.5 hours	Yongkiettrakul <i>et al.</i> , 2014

LOD limit of detection; POC point of care diagnosis; LF lateral flow; LFD lateral flow dipstick

^x The amperometric method had a limit of detection of 60 ng/ml of HRP2, which is equivalent to ~ 400 parasites per microliter (Marquart *et al.*, 2012)

+ The paper based method was found to have a limit of detection equal to the CELISA test based on the detection of HRP2

* The electrochemical method was found to have a limit of detection 4 times lower than that of an HRP2 based DAS-ELISA (the CELISA was not used in this case)

1.4.6 Antigen detection methods

Molecular methods have the advantage of allowing diagnosis based on specific molecular target genes or proteins. Rapid diagnostic tests are perhaps the most user-friendly of these as they allow for point-of-care diagnosis within 15 minutes and are simple to perform and interpret. Current RDTs are based on the detection of three *Plasmodium* proteins namely Histidine rich protein 2 (HRP2), lactate dehydrogenase (LDH) and aldolase. Of these HRP2 is only found in *P. falciparum* where LDH and aldolase serve as pan malarial antigens. Hurdoyal *et al.*, (2010) identified species specific and pan malarial peptide epitopes on the surface of LDH for differentiation of the infecting species of malaria. RDTs will be discussed further at the end of this chapter as this forms part of the aims and objectives of the current study. A derivative of these assays is an antigen capture ELISA format which uses enzyme activity as part of the detection step. One of these assays employs the parasite LDH enzyme captured out of solution as part of the detection step with a resulting limit of detection of around 200 parasites per microlitre (Makler *et al.*, 1993a and b; Piper *et al.*, 1999). The most sensitive of these assays are the conventional double antibody sandwich ELISAs (DAS-ELISA) which detect as few as 12 parasites per microlitre (Noedl *et al.*, 2006; Sousa *et al.*, 2014). The detection methods for the latter methods rely on spectrophotometric analysis making both methods laboratory based. Novel innovations to circumvent this have been demonstrated by Glavan *et al.* (2014) and Grant *et al.* (2016) who developed paper based detection methods with similar detection sensitivities as the original DAS-ELISA method (Noedl *et al.*, 2006).

1.4.7 PCR based methods for malaria detection

Laboratory based diagnosis based on nucleic acid detection such as PCR reaches far lower limits of detection. These limits range from a low of 0.02 to a high of 20 parasites per microlitre of blood. This increase in sensitivity comes with increased complexity and several of the methods take hours to complete. PCR based assays may be divided into groups based on their methodology. Conventional methods include nested, single and multiplex PCR. Fluorescent dye based methods include real time and quantitative PCR and finally the simplified isothermal methods such as LAMP. There have been several groups focusing on simplification of these methods, most attempting to reduce the dependence on sample preparation, thermal cycling and visualisation protocols. A microwave based DNA extraction method for the LAMP assay was demonstrated by Port *et al.* (2014) by treating 10 µl samples at 800 W for two minutes and using the condensed droplets for LAMP assays. The presence

of PCR inhibitors in blood has been overcome with the development of mutant polymerases resistant to blood components and allows direct PCR in blood samples without additional sample preparation (Kermekchiev *et al.*, 2009; Mens *et al.*, 2012). Kersting *et al.* (2014) developed an isothermal method for DNA replication and subsequent detection using a lateral flow mechanism similar to RDTs. The resulting test had a limit of detection of four to 20 parasites per microlitre and took only 15 to 30 minutes to complete. The isothermal replication was performed between 30 to 45°C which is lower than the current LAMP methods (Mohon *et al.*, 2014; Polley *et al.*, 2010). Cyclic electrochemically controlled DNA helix denaturation and renaturation using intercalating agents that bind DNA in a redox dependent manner may also present novel approaches for PCR methods, reducing the need for thermal cycling (Syed *et al.*, 2012). Alternate detection methods such as multi-pathogen gold nanoprobe have also been developed, which can differentiate between single or mixed *Mycobacterium tuberculosis* and *P. falciparum* infections using a single gold nanoprobe (Veigas *et al.*, 2015). A simplification of the real time PCR format was demonstrated by Lucchi *et al.* (2013, 2014) using photo-induced electron transfer fluorogenic primers which avoid the need for internal probes or intercalating dyes. Multiplex assays are faster and more accurate than real time PCR at speciation (Lee *et al.*, 2015).

Interestingly several groups have adapted methods to make use of smart phone technology in diagnostic analyses. These have the advantage of providing global positioning as well as instant recording of diagnosis which may further aid record keeping (Gulka *et al.*, 2015; Pirnstill and Cote, 2015). The diagnostic ability of molecular tests is largely dependent on the target molecule that it detects and these are discussed next as listed in Table 1.6.

1.5. Molecular targets for malaria diagnosis and laboratory-based detection

The molecular targets can be separated into those used to diagnose infection, those used in transmission studies and those used to detect drug resistance.

1.5.1 Molecular targets for the diagnosis of malaria infection

Although microscopy is not a molecular method, it was included here as it is still recognised as the gold standard for comparison of tests (Aydin-Schmidt *et al.*, 2013; Moody, 2002). Microscopy allows for identification of all five human infecting species of *Plasmodium* as well as the detection of gametocytes. After drug clearance, the residual parasites are cleared from the blood of patients within two days (one to seven days) (Aydin-Schmidt *et al.*, 2013).

Due to sequestration of parasites, microscopy may underestimate parasitemia and molecular methods detecting parasite factors are preferred (Kattenberg *et al.*, 2011).

Haemozoin is released by all malaria parasites and during a symptomatic *P. falciparum* infection (one to 10% parasitemia) between 0.2-2 grams of haemozoin is released per completed red blood cell cycle (Frita *et al.*, 2012). During severe infections approximately 100 g of haemoglobin is digested per red blood cell cycle (Egan *et al.*, 2002; Frita *et al.*, 2012; Goldberg *et al.*, 1991). The released haemozoin crystals are rapidly phagocytosed by leucocytes (monocytes and neutrophils) (Grimberg, 2011; Hänscheid *et al.*, 1999; Rebelo *et al.*, 2013). In this form haemozoin remains in circulation between three to nine days, where haemozoin containing monocytes were detected up to 21 days after clearance of infection. Haemozoin also accumulates in tissues of the liver, spleen, brain and bone marrow where it can remain for up to 270 days after clearance of parasitemia (Day *et al.*, 1996). It should be noted, however, that although haemozoin detection does allow for quantitative measures of parasitemia, Rebelo *et al.* (2013) and Delahunt *et al.* (2014) demonstrated that haemozoin is only detectable in rings older than six to 18 hours. To add to this, the total parasite load may be underestimated due to sequestration of late trophozoite parasites especially in *P. falciparum* (Leitgeb *et al.*, 2011).

There are three recognised protein targets detected by current RDTs including HRP2, LDH and aldolase (Moody, 2002). HRP2 is the dominant target for most RDTs currently on the market including Paracheck Pf[®]; ParaHIT *f*[®] and ParaSight-F for example (Murray *et al.*, 2008). During its red blood cell development, the malaria parasite exports several proteins to the red cell surface, including HRP2, which aggregate and form knobs on the membrane surface (Bannister *et al.*, 2000). This protein is unique to *P. falciparum* (Murray *et al.*, 2008) and the histidine rich repeats present within this antigen make it an ideal target for antibody-based tests, as signal amplification results if antibodies bind these repeats. The histidine rich repeats have also been exploited similarly to His-tag technology, in that nickel-conjugant probes as opposed to antibodies can be used for detection (Gulka *et al.*, 2015). As a target for tracking therapeutic outcome in patients it is not preferred, however, due to its persistent nature. Marquart *et al.* (2012) demonstrated that the minimum period for clearance is seven days, however this may be prolonged based on the level of parasitemia reached during the infection, taking on average 28 days after successful drug cure of infections. HRP2 can also be detected in saliva and urine samples owing to its stable nature (Fung *et al.*, 2012; Oguonu *et al.*, 2014). Variable RDT results have been attributed to genetic variations of the HRP2

gene and HRP3 cross reactivity in some tests (Baker *et al.*, 2005). Verma *et al.* (2015) have since developed detection reagents specific for HRP2 alone. More alarmingly some strains in South America (Gamboa *et al.*, 2010; Houze *et al.*, 2011; Maltha *et al.*, 2012; Okoth *et al.*, 2015; Solano *et al.*, 2015), Senegal (Deme *et al.*, 2014; Wurtz *et al.*, 2013), India and the China-Myanmar Border (Kumar *et al.*, 2012, 2013; Li *et al.*, 2015b), do not express HRP2 and HRP3 or have several deletions compromising detection of the protein by RDTs.

For these reasons alternate targets have been sought, LDH and aldolase being amongst these. Both targets have comparably shorter half-lives in patient's blood with an average clearance of seven days, making them more suited for tracking infections (Ashley *et al.*, 2009; Iqbal *et al.*, 2004). Being conserved metabolic proteins these targets are common to all five species infective to humans and they are usually included as common malaria targets in diagnostic tests in combination with HRP2 (Brown *et al.*, 2004; Lee *et al.*, 2006; Shin *et al.*, 2013). Such tests include CARESTART™ (LDH) and BinaxNOW® (aldolase) (Ashley *et al.*, 2009; Murray *et al.*, 2008). LDH is a more popular target than aldolase due to lower sensitivity of aldolase based tests (Lee *et al.*, 2006). Isozymes of LDH for *P. falciparum* were first studied in the 1970s by Carter and Voller (Carter and Voller, 1973) and Vander Jagt *et al.* (1982) suggested the use of the specific activity of *Plasmodium* LDH as a measure of parasite purity. Since then an antibody based detection of *Plasmodium* LDH was used to detect parasites and measure drug sensitivity (Makler *et al.*, 1993a and b; Piper *et al.*, 2011). The first LDH based RDTs were developed in 1999 (Piper *et al.*, 1999) and tests targeting LDH alone include OptiMAL® and OptiMAL-IT®. LDH is present at lower levels than HRP2, and LDH based tests thus have higher limits of detection than those detecting HRP2 (Marquart *et al.*, 2012; Martin *et al.*, 2009).

Another parasite specific product released is DNA. The most common target used for diagnosis is the 18S rRNA gene (Dinko *et al.*, 2013; Snounou *et al.*, 1993). Different studies have assessed DNA clearance after drug cure of parasitemia and found there to be a two day lag on average (one to 28 days) (Aydin-Schmidt *et al.*, 2013; Jarra & Snounou, 1998) where Dakic *et al.* (2014) reported a six day lag in clearance. A drawback of the 18S rRNA gene target is its incompatibility with multiplex assays for detection of mixed infections. If species identification is required then a nested PCR approach is used which is more time consuming and technical to perform than multiplex PCR (Demas *et al.*, 2011). Targets with greater copy numbers than the traditional 18S rRNA gene target include TARE-2, varATS, Pvr47, Pfr364

and COX-III which at least in the case of TARE-2 and varATS were shown to result in lower limits of detection (Hofmann *et al.*, 2015, Table 1.5).

1.5.2 Targets for transmission studies

Some of the interesting markers listed include stage specific markers such as the male and female gametocyte markers Pfs230p and Pfs25 respectively detected by reverse transcriptase PCR (Schneider *et al.*, 2015). Monitoring male and female gametocyte ratios has implications in transmission blocking studies. Dissection of mosquitoes and measuring the number of sporozoites in the mouth parts is still seen as the gold standard in entomological studies (Durnez *et al.*, 2011). This method is labour intensive however and alternate methods that allow for higher throughput screening have been developed including ELISA and PCR based methods.

An ELISA targeting the circumsporozoite surface protein (CSP) of *Plasmodium* parasites has become the preferred method for detection of sporozoites found in mosquito mouth parts. In contrast, although PCR detects fewer parasites (ten versus 100 using ELISA), this method detects all forms of the parasite within the mosquito and not only the sporozoites, which is not ideal for transmission studies (Durnez *et al.*, 2011).

The CSP based ELISA has proven useful in multiple studies, although false positive results have been observed (Koekemoer *et al.*, 2001; Mouatcho *et al.*, 2007). Due to the heat labile nature of the CSP protein, Bashar *et al.* (2013) and Durnez *et al.* (2011) averted false positives by heating samples (100°C for ten minutes) prior to performing the ELISA. The last set of targets concern the detection of drug resistant parasite strains.

Table 1.6 Molecular targets for diagnosis and detection of malaria

Target	Species	Stage	Abundance / parasite	Clearance (days)	Comments	References
Whole parasites	All 5	RBC & gametocyte	NA	2 (1 to 7)	Gold standard for diagnosis	Aydin-Schmidt <i>et al.</i> , 2013
Hrp2	<i>P. f</i>	RBC	14 pg	28 (7 to 42)	Predominant target in RDTs	Aydin-Schmidt <i>et al.</i> , 2013; Marquart <i>et al.</i> , 2012; Mikita <i>et al.</i> , 2014
LDH	Unspecific; <i>P. f</i> ; <i>P. v</i>	RBC	2.3 pg	7 (2 to 14)	Common RDT target	Aydin-Schmidt <i>et al.</i> , 2013; Hurdayal <i>et al.</i> , 2010; Martin <i>et al.</i> , 2009
Aldolase	Unspecific	RBC	ND	7 (2 to 14)	Less common RDT target	Ashley <i>et al.</i> , 2009; Iqbal <i>et al.</i> , 2004
Haemozoin	Unspecific	RBC	8 pg	3 to 9 (up to 21)	Persists 196 to 270 days in tissue	Day <i>et al.</i> , 1996; Frita <i>et al.</i> , 2012
18S rRNA	All 5	RBC, gametocyte, mosquito	4 to 8 copies	2 (1 to 28)	Standard for molecular diagnosis in multiple studies	Snounou <i>et al.</i> , 1993; Aydin-Schmidt <i>et al.</i> , 2013
AMA-1	<i>P. k</i>	RBC	ND			Lau <i>et al.</i> , 2011
TARE-2	<i>P. f</i>	RBC	~ 250 copies			Hofmann <i>et al.</i> , 2015
varATS	<i>P. f</i>	RBC	59 copies			Hofmann <i>et al.</i> , 2015
Pvr47	<i>P. v</i>		14 to 41 copies			Demas <i>et al.</i> , 2011
Pfr364	<i>P. f</i>		14 to 41 copies			Demas <i>et al.</i> , 2011
COX-III	All 5	RBC	150 copies			Echeverry <i>et al.</i> , 2016
pgmet	All 5	RBC	1 copy			Beshir <i>et al.</i> , 2010
Pfs25	<i>P. f</i> ; <i>P. k</i> ; <i>P. v</i>	Female gametocyte	ND			Schneider <i>et al.</i> , 2015
Pfs230p	<i>P. f</i> ; <i>P. k</i> ; <i>P. v</i>	Male gametocyte	ND			Schneider <i>et al.</i> , 2015
CSP	<i>P. f</i> ; <i>P. v</i>	Mosquito sporozoites	ND		Heat treatment is essential to avoid false positives	Bashar <i>et al.</i> , 2013; Durnez <i>et al.</i> , 2011

NA not applicable; ND not determined; *P. falciparum* (*P. f*); *P. vivax* (*P. v*); *P. knowlesi* (*P. k*)

1.6. Methods and targets used to detect drug resistant strains

The drug resistance targets to date were summarised in a review by Sinha *et al.* (2014), including a total of nine genes that either have polymorphisms, single point mutations or altered copy numbers. The gene targets include: *pfhhe*; *crt*; *mdr1*; *dhfr*; *dhps*; *cytb*; *PfATPase6*; *Pfubp-1* and the K13 propeller. These impart resistance to: chloroquine; quinine; proguanil; sulfadoxine; pyrimethamine; mefloquine; halofantrine; atovaquone; artemisinin and artesunate. Methods to diagnose resistance are all PCR based and the most common is the restriction fragment length polymorphism (RFLP) assay and a nested PCR method (Duraisingh *et al.*, 1998). Since resistance has developed against such a wide variety of drugs, methods detecting multiple resistance phenotypes are essential.

Multiplex approaches have since been developed to detect several resistance phenotypes at once. If resistance markers are present, they are amplified and then detected with oligonucleotide-tagged-fluorescent probes using a DNA ligase. This results in specific fluorogenic read-outs depending on the type of marker present (Carnevale *et al.*, 2007). These tests have since been validated in the field (LeClair *et al.*, 2013; Nankoberanyi *et al.*, 2014). An alternate novel approach was to use H-NMR analyses of resistant and normal parasites. NMR profiles revealed differences in metabolites between these two forms of parasites, but the method needs further optimisation (Teng *et al.*, 2014).

1.7. The diagnostic niche of RDTs

Currently both microscopy and rapid diagnostic tests are used as point-of-care tests. The ability to use both test samples for further analysis using PCR based methods places them at a critical point in the patient treatment time line. Recent analysis revealed that dried blood spots were a better source material for subsequent PCR analysis (Wihokhoen *et al.*, 2016). Being paper based, RDTs thus have an added advantage over microscopy and subsequent PCR analyses could serve for quality control as well as surveillance of resistance markers (Bisoffi *et al.*, 2009; Ishengoma *et al.*, 2011; Veron and Carne, 2006). Although several more sensitive methods to RDTs are available, the setting of malaria still demands a simple test that diagnoses the disease. Misdiagnosis of the disease-causing pathogen in a mixed infection (malaria and an alternate disease) as a result of very low limits of detection, especially in immune adults, could result in inadequate treatment. Increased test sensitivity should ideally be accompanied by the ability to semi-quantitatively discriminate between severe and mild malaria cases. Inadequate dosing and duration of treatment during severe

malaria, especially hyperparasitemic infections, has been identified as a contributor to selection for drug resistance (Barnes *et al.*, 2015; White *et al.*, 2009). Based on the prevalence of resistance, especially in *P. falciparum*, speciation should also be prioritised.

To introduce the aims and objectives of this study a brief description and basic principle to RDTs is outlined in Figure 1.4.

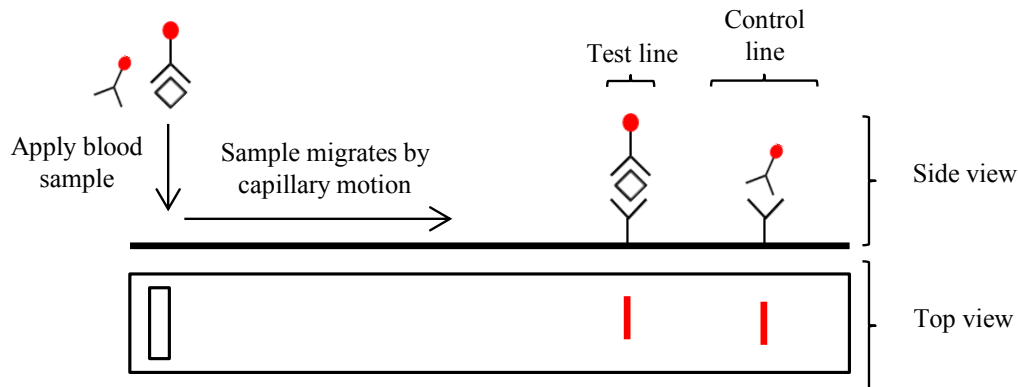


Figure 1.4 Basic outline of a simple rapid diagnostic test (RDT), both top and side view

Rapid diagnostic tests are immunochromatographic test strips that detect malaria antigens in infected blood samples using an antibody capture and detection step. The test sample (patient blood) is mixed with a lysis buffer solution containing a colloidal gold-labelled detection antibody. This antibody will bind its target malaria antigen if it is present in the blood sample. This solution is applied to the one end (left in Figure 1.4) of the test strip and migrates toward the other end (right in Figure 1.4) by capillary action. An antigen-specific antibody line fixed on the test strip then captures the detection antibody-antigen complex and due to the attached gold particle a visible test line forms. Any unbound detection antibody migrates further along the test strip and is captured by an antibody specific to the detection antibody, resulting in a control line that indicates the sample has migrated completely across the strip and that the test is working (Makler *et al.*, 1998; Murray *et al.*, 2008).

1.8. The aims and objectives of the current study.

Rapid diagnostic tests have several advantages, perhaps best summarised by their adherence to the ASSURED criteria for effective diagnostic methods (Peeling *et al.*, 2006). These stipulate that ideal diagnostic tests should be **A**ffordable, **S**ensitive, **S**pecific, **U**ser-friendly, **R**apid and robust, **E**quipment-free and **D**eliverable to end-users. There are several concerns regarding RDT performance however, which we wished to address in this study.

- 1) Firstly LDH was chosen as the model protein in this study, as it is a target that is currently being used in RDTs (Moody, 2002).
- 2) To achieve similar limits of detection to HRP2 based tests, we searched through transcript and proteomics data for alternative diagnostic targets. The HRP2 protein is present at approximately six times greater concentrations than LDH (Marquart *et al.*, 2012; Martin *et al.*, 2009). We identified two target proteins predicted to be present at higher concentration than LDH. These could potentially serve as alternatives to HRP2 rather than either of the current targets, LDH and aldolase. We adopted an approach outlined by Hurdayal *et al.* (2010) which entailed identifying *Plasmodium*-species-specific and *Plasmodium*-common peptide epitopes on the surface of the target proteins. These were used to raise polyclonal antibodies against our proposed targets. The resulting anti-peptide antibodies allowed species-specific detection of the target protein orthologs or detection of multiple *Plasmodium* target protein orthologs. This formed the aims of chapter 3.
- 3) RDTs detecting LDH or aldolase often detect multiple *Plasmodium* species. This has been attributed to the conserved nature of LDH and aldolase amongst *Plasmodium* species (Kawai *et al.*, 2009; Maltha *et al.*, 2010; McCutchan *et al.*, 2008). HRP2 based tests are unaffected as this antigen is only expressed in *P. falciparum* therefore making it a species specific antigen (Murray *et al.*, 2008). For this reason, multiple orthologs of the intended target proteins were recombinantly expressed, purified and their quaternary structures verified. This formed the aims and objectives of chapter 4.
- 4) Antibody specificities were assessed using these recombinant proteins in chapters 5 and 6. The aims in these two chapters were to produce antibodies and scFv clones with specificity to the target proteins and peptides and to demonstrate their use in an antigen capture and detection system.
- 5) Cross reactivity with Rheumatoid factor due to Fc portion of IgG molecules was averted by using chicken IgY and scFv antibodies which lack an Fc portion (Delves *et al.*, 2006; Iqbal *et al.*, 2000). This was an objective in chapters 5 and 6, although confirmative tests of antibody reactivity would be useful.

Finally additional concerns and future work are discussed in chapter 7 to end the thesis.

Chapter 2

Materials and Methods

2.1 Introduction

General materials and methods are described first here and the reader is referred back to these in later chapters where applicable. Hereafter the materials and methods section follows the flow of the thesis, where a list of materials was followed by a description of the methods used relative to each chapter. Unless specifically stated in text in the subsequent chapters, concentrations in the materials and methods section were used.

2.2 Equipment

General lab equipment included: Micro Tube Peristaltic pump MP-3 from EYELA Tokyo Rikakikai co. Ltd (Tokyo, Japan); Virsonic™ cell disruptor from VirTis (New York, USA); Edwards One Stage 5 A.C. pump from GEC. Machines Ltd. (Newcastle, UK); Avanti™ J-26 XPI and Allegra™ X-22R centrifuges from Beckman Coulter (California, USA); magnetic stirrers from Velp Scientifica (Europe); Orbital shaking incubator from New Brunswick Scientific (New Jersey, USA); UV-1800 Shimadzu spectrophotometer from Shimadzu corporation (Kyoto, Japan); water bath from GFL (Burgwedel, Germany); weigh balance from Denver Instruments (USA); pH meter from HANNA instruments; bench top orbital shaker and Spectrafuge bench top centrifuge from Labnet International Inc. (USA).

Specialised equipment used in molecular studies included: T100™ Thermal cycler, Basic PowerPac™, Miniprotean® 3 system with 1mm spacers, from Bio-Rad (California, USA); miniGES agarose gel system from Wealtec corporation (Taiwan). The ÄKTA Prime Plus System was from GE Healthcare (Buckinghamshire, England).

Equipment used in immunochemical studies included: TEZZ Mighty Small Transphor Unit from Hoefer Inc. (California, USA); Poly Prep® affinity columns from Bio-Rad (California, USA); VersaMax™ ELISA plate reader from Molecular Devices Corporation (California, USA).

Image capture systems included: MiniBis Pro DNR Bio-Imaging Systems (Israel) and the Syngene G:Box system (UK).

2.2 General molecular biology methods

This section describes general molecular biology methods used throughout the study.

2.2.1 Reagents

Bradford reagent, ethidium bromide (EtBr), β -mercaptoethanol, acrylamide, ethylenediaminetetraacetic acid (EDTA), N,N'-methylenebisacrylamide, bromophenol blue, Coomassie Brilliant Blue R-250 as well as G-250, glycine, sodium dodecyl sulphate (SDS), tris, tricine, ammonium persulphate, ovalbumin, Sephacryl S200 and N',N',N',N'-tetramethylethylenediamine (TEMED) were purchased from Sigma-Aldrich-Fluka (Steinheim, Germany). Di-potassium hydrogen orthophosphate, potassium dihydrogen orthophosphate, sodium carbonate, sodium dihydrogen orthophosphate, potassium chloride, sodium hydroxide, sodium chloride, disodium hydrogen orthophosphate anhydrous, magnesium chloride hexahydrate, silver nitrate, magnesium sulphate and sodium hydrogen carbonate were purchased from Merck (Damstadt, Germany). The following were purchased from Fermentas (Vilnius, Lithuania): Agarose, DNA MassRulerTM, 10mM dNTP mix, Alu1, EcoR1, Nde1, Pst1, Xho1, Buffer OTM, an unstained protein molecular weight marker ranging from 14.4 to 116 kD and a spectra multicolour broad range protein marker ranging from 10 to 260 kD. Molecular biology reagents purchased from Solis Biodyne (Tartu, Estonia) included the 10 \times PCR buffer (MgCl₂ and detergent-free), PCR MgCl₂ stock solution (25mM) and Taq polymerase. Snake skinTM dialysis membrane (10 kD MWCO) was purchased from Pierce Perbio Science (Erembodegem, Belgium). Bovine serum albumin (BSA) was purchased from Roche (Mannheim, Germany).

2.2.2 Bradford protein determinations

Protein sample concentrations were determined using the Bradford assay (Bradford, 1976). A standard curve was prepared using a 1 mg/ml BSA stock. The stock was diluted to give a range of concentration standards from (0-50 μ g) in triplicate. These were made up to 100 μ l with dH₂O, added to 900 μ l Bradford dye, vortexed and left to react with the dye for 15 minutes. Sample absorbance was read at 595 nm using a UV-1800 Shimadzu spectrophotometer and plotted against BSA concentration.

Unknown protein samples were prepared in the same way as the standards in that an appropriate dilution of the unknown was prepared which allowed the concentration to be extrapolated from the standard curve shown in Figure 2.1.

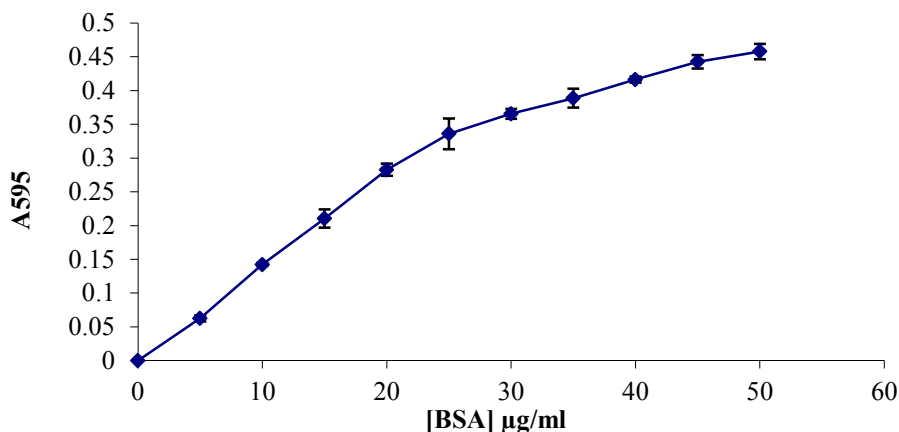


Figure 2.1 Bradford standard curve
All values are average values of triplicate readings with standard deviations shown.

2.2.3 Sodium dodecyl sulphate polyacrylamide gel electrophoresis (SDS-PAGE)

In order to assess the purity of protein samples and to determine their size, discontinuous SDS-PAGE was used as described by Laemmli (1970). Since the malarial recombinant proteins as well as the expressed single chain fragment variable (scFv) antibodies were all within 30 to 80 kD in size, a standard 12.5% running and 4% stacking gel was used throughout the study.

The gels were prepared according to Table 2.1, where the volumes stated are sufficient for a single gel, that is a 4.7 ml running and 1.25 ml stacking gel preparation. The buffers were named A through E for simplicity of the table and were as follows: A (4.1 M acrylamide and 52 mM N,N'-methylenebisacrylamide); B (1.5 M Tris buffer at pH 8.8); C (495 mM Tris buffer at pH 6.8); D (10% (w/v) SDS solution in dH₂O) and E (10% (w/v) ammonium persulfate solution in dH₂O). Gels were set using a Bio-Rad Miniprotein[®] 3 system with 1 mm spacers, with either 10 or 15-well combs, depending on the number of samples. The gel-casting unit was assembled according to manufacturer's instructions after cleaning plates with detergent and rinsing under dH₂O.

Once the TEMED was added, the running gel solution was swirled to mix and the entire 4.7 ml was gently poured into the gel casting cassette and overlaid with 200 μl dH₂O. This allows the gel to polymerise properly, as oxidation would otherwise inhibit gel polymerisation. Once polymerised, the water was decanted and the freshly prepared stacking gel solution was overlaid. A 10 or 15 well comb was then inserted immediately and the stacking gel was left to polymerise.

Table 2.1 Running and stacking gel recipes to prepare a single gel for SDS-PAGE

	12.5% Running gel (4.7 ml)	4% Stacking gel (1.25 ml)
A	1.97 ml	163 μ l
B	1.18 ml	0
C	0	313 μ l
D	47 μ l	12.5 μ l
E	47 μ l	6.25 μ l
dH₂O	1.45 ml	750 μ l
TEMED	2.4 μ l	2.5 μ l

Samples were prepared as follows: first diluted 1:1 in PBS and then 1:1 with 50% (v/v) sample buffer for non-reducing gels (2.5 ml solution C; 2 ml glycerol; 4 ml solution D; with few grains of bromophenol blue to colour the buffer). For reducing gels β -mercaptoethanol was added 1:10 to the sample buffer before mixing with the samples. The initial dilution with PBS often aided in reducing streaking of samples on the gel, especially with bacterial lysate samples and was therefore kept constant throughout the study.

After loading the samples the gels were electrophoresed at 20 mA per gel in tank buffer (25 mM tris; 192 mM glycine and 0.1% (w/v) SDS) until the dye front had migrated to within 1 to 0.5 cm from the bottom of the gel. The gels were then removed immediately and stained with Coomassie stain (45% (v/v) methanol; 10% (v/v) acetic acid; 0.25% (w/v) Coomassie brilliant blue R-250) for a minimum of 4 hours, followed by several changes of destaining solution (50% (v/v) methanol and 10% (v/v) acetic acid) and left in dH₂O until the gels had swollen back to their original size. The sizes of protein bands were determined by extrapolation from a graph of log molecular weight of molecular weight standards (either an unstained Fermentas marker or a prestained marker was used) run on the same gel, against their relative mobility (Rf values).

2.2.3.1 Silver staining

This method was performed according to (Chevallet *et al.*, 2006). Glassware used for staining was meticulously cleaned with detergent and then rinsed with fixing solution (50% (v/v) methanol; 12% (v/v) acetic acid and 0.5% (v/v) formaldehyde) and allowed to dry. SDS-PAGE gels were transferred to glass Petri dishes and fixed for 1 hour or overnight (16 hours) in fixing solution. All incubations and washes were performed on a rocker. The gels were washed three times with wash solution (50% (v/v) ethanol) after fixing, and then left in pre-treatment solution (4 mg/ml Na₂S₂O₃.5H₂O) for 1 minute and 15 seconds. Gels were then washed three times with dH₂O, 20 seconds per wash and then left in impregnation solution

(0.2% (v/v) AgNO₃; 0.3% (v/v) formaldehyde prepared just before use) for 20 minutes. Gels were washed three times with dH₂O, 20 seconds per wash and then incubated with developing solution (566 mM Na₂CO₃; 0.2% (v/v) formaldehyde; 2% (v/v) pre-treatment solution) until the first bands appeared. The developing solution was then replaced with dH₂O and bands were allowed to develop until the intensity was satisfactory, at which time the gels were incubated in stop solution (50% (v/v) methanol; 12% (v/v) acetic acid) for 10 minutes, and stored in 50% (v/v) methanol.

2.2.4 Molecular exclusion chromatography (MEC) using the ÄKTA Prime Plus system

Samples were dialysed into three changes (2 x two hours and one overnight incubation at 4°C) of MEC buffer (50 mM NaH₂PO₄; 150 mM NaCl at pH 8.0) each change was 100 times the sample volume. Prior to use all MEC buffers were degassed for 45 minutes at 4°C using an Edwards One Stage 5 A.C. pump.

The Sephacryl S-200 column was washed with 60 ml of 0.2 M NaOH, followed by 60 ml dH₂O and equilibrated with 240 ml MEC buffer (all done at 1 ml/min). For calibration of the column, the molecular weight standards were prepared to a final volume of 3 ml as follows: 6 mg blue dextran (2000 kD), and 15 mg each of sheep IgG (150 kD), bovine serum albumin (68 kD), ovalbumin (45 kD), and myoglobin (18.8 kD). The parameters for running the column were set to a flow rate of 0.5 ml/min and collection of 4 ml eluents. The absorbance at 280 nm (A_{280}) was constantly recorded once the samples were loaded to give a calibration curve of A_{280} plotted against elution volume (ml). After calibration, between four to 6 mg of each of the recombinant proteins (in 4 ml) was separated on the column at 0.5 ml/min for a total of 300 ml MEC buffer. All samples, including the standards, were ultra-centrifuged at 100000 x g, 20 minutes prior to loading the supernatant onto the column.

2.2.5 Colony Polymerase Chain Reaction (PCR)

Colony PCR was performed to verify the presence of plasmid inserts within the expression hosts. Single colonies were used to inoculate 5 ml LB media (with the respective antibiotic) and cultured overnight (16 hours) at 37°C. Following centrifugation (1210 x g, RT, five minutes) the supernatant media was discarded and the pellet suspended in 500 µl MiliQ dH₂O. Two microliters of this suspension was then diluted further in 50 µl MiliQ dH₂O. After boiling for 5 minutes, the samples were centrifuged (17530 x g, RT, 10 min), and 3 µl of the supernatant was transferred to a PCR tube and used as the template in the PCR reaction. The reaction mixture was completed by addition of the following: 1 µl each of the forward and

reverse primers (10 μ M); 0.25 μ l Taq polymerase (5 units / μ l); 2 μ l MgCl₂ (25 mM); 0.8 μ l dNTPs (10 mM); 2 μ l 10 x PCR buffer (MgCl₂ free) and made up to 20 μ l with MiliQ dH₂O. The reaction conditions were represented in Figure 2.2 below and a total of 30 cycles were run per reaction.

The specific annealing temperature of the primers used differed per reaction, and were optimised using gradient PCR if required.

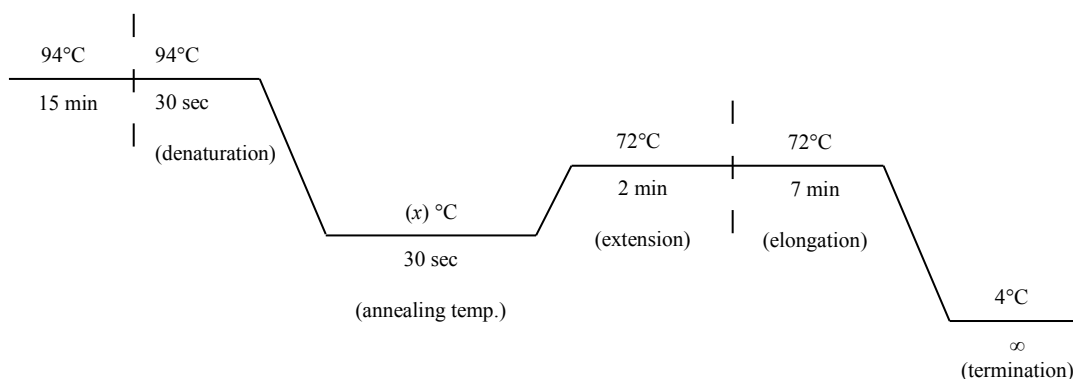


Figure 2.2 PCR cycle conditions

The conditions were standard for all PCR performed, except in the case of the annealing temperature “x” of the specific primers used, which were optimised if required.

The primers were listed in Table 2.2, with the respective annealing temperatures used.

Table 2.2 Primer sequences used in this study (sequencing and PCR)

Primer	Sequence	Annealing temp. (°C)
T7 promoter primer #69348-3	TAA TAC GAC TCA CTA TAG GG	55
T7 reverse primer #69337-3	GCT AGT TAT TGC TCA GCG G	55
pLDH forward primer	GGA TCT GGT ATG ATT GGA GGT GTT ATG GCC	65
pLDH reverse primer	TTC GAT TAC TTG TTC TAC ACC ATT ACC ACC	65
OP52	CCC TCA TAG TTA GCG TAA CG	55
M13 reverse	CAG GAA ACA GCT ATG AC	55
ScFv nested PCR primer	TCA GGT GGA GGT GGC TCT GG	55

2.2.6 Plasmid isolation

Plasmid isolation was performed (Sambrook *et al.*, 1989) for both the malarial protein and scFv expression vectors. This served as the DNA template for PCR, restriction digests and sequencing analyses described later.

In general a 10 ml overnight (16 hour) culture of a single colony was grown at 37 °C, centrifuged (1210 x g, 4 °C, 5 min) and the supernatant discarded. The cell pellet was

suspended in 200 μ l GTE solution (25 mM Tris; 1 mM EDTA; 50 mM glucose at pH 8.0), left at room temperature (RT) for 5 minutes and then transferred to a microfuge tube, containing 2 μ l RNase A (10 mg/ml in 10 mM Tris; 1 mM EDTA at pH 8.0). All subsequent sample incubations were done on ice. Four hundred microlitres NaOH/SDS solution (200 mM NaOH; 35 mM SDS) was added and the sample was incubated for 5 minutes to allow cell lysis. Hereafter, 300 μ l potassium acetate (3 M potassium acetate at pH 4.8 titrated with glacial acetic acid) was added, mixed thoroughly and incubated for 5 minutes. Following the formation of a coarse white precipitate (cell debris and chromosomal DNA), the sample was centrifuged (17530 x g, RT, five minutes) and 800 μ l of the supernatant was transferred to a fresh tube. Six hundred microliters isopropanol was added, mixed thoroughly and incubated for 30 minutes, after which the sample was centrifuged (17530 x g, RT, 5 minutes) to pellet the plasmid DNA. The pellet was then washed with ice cold 70% (v/v) ethanol and centrifuged (17530 x g, RT, 5 minutes), with the final plasmid pellet suspended in 50 μ l TE buffer (10 mM Tris; 1 mM EDTA at pH 8.0) and resolved on a 1% agarose gel to check its purity.

2.2.7 Agarose gel electrophoresis

Agarose gels were used to assess the purity of the isolated plasmid vectors (isolated as described in section 2.2.5), or to analyse their restriction digestion or PCR amplification products.

The miniGES agarose gel system was assembled to give gels with 7 x 6.5 cm dimension. 30 ml of TAE buffer (2 M Tris; 50 mM EDTA; 0.95 M glacial acetic acid, pH 8.0) was used to prepare 1 or 3% (w/v) agarose gels (0.3 or 0.9 g agarose respectively). This solution was heated in a microwave until the agarose had melted completely. Once cooled to \sim 47 $^{\circ}$ C, EtBr (1% (w/v) stock in TAE buffer) was added to a final concentration of 0.00006 % (w/v) and the solution was poured into the gel cassette and allowed to set after the comb had been placed into the gel. Samples were prepared by diluting 5:1 in Fermentas sample loading buffer (0.25% (w/v) bromophenol blue and 40% (w/v) sucrose in TAE buffer). The gels were run at 80 V for 40 minutes, visualised under UV light and images captured using a MiniBis Pro DNR gel imaging system. The sizes of bands in base pairs (bp) were extrapolated from a graph of relative distance travelled from the sample loading well to log of the band size in bp of DNA standards (DNA MassRulerTM) run on the same gel.

2.2.8 Sequencing

Sequencing was used as confirmation of both the recombinant malarial protein and scFv coding sequences and was performed at the Central Analytical Facility at Stellenbosch University. The plasmid DNA isolated as described in section 2.2.6 served as the template for the sequencing reactions, with a list of primers given in the Table 2.2. The rP₁LDH and P_vLDH samples were sequenced with the pLDH primers, where all other pET vector samples were sequenced with the T7 forward and reverse primers. The scFv samples were sequenced using the OP52 and M13 reverse primers. The resulting consensus sequences were analysed by Clustal Omega alignment to assess their identity with the corresponding coding sequences and the IgY light and heavy chain germline sequences in the case of the scFv sequences.

2.3 General immunochemical techniques

The general immunochemical techniques used during this study are described next.

2.3.1 Reagents

Nunc MaxiSorp™ 96-well ELISA plates were from Nunc products (Roskilde, Denmark). 4-chloro-1-naphthol, Biomax® X-ray film, p-iodophenol, luminol, Ponceau S and Tween-20 were purchased from Sigma-Aldrich-Fluka (Steinheim, Germany). Citrate and hydrogen peroxide were purchased from Merck (Darmstadt, Germany). 2,2'-azino-bis(3-ethoxybenzothiazolinesulfonate) (ABTS) was purchased from Boehringer (Mannheim, Germany). Hybond-C™ Extra nitrocellulose membrane was purchased from GE Healthcare (Buckinghamshire, England). Peroxidase-conjugated rabbit anti-IgY and peroxidase conjugated goat anti-mouse IgG antibodies were from Jackson Immunochemicals (Pennsylvania, USA).

2.3.2 Western blotting

This method (Towbin *et al.*, 1979) follows on from the SDS-PAGE method described in 2.2.3. After resolving protein samples on an SDS-PAGE gel, the proteins were transferred onto a nitrocellulose membrane. This was done by sandwiching the gel and nitrocellulose between two pairs of blotting paper and one set of sponges in a blotting cassette. The gels and nitrocellulose were soaked in blotting buffer (50 mM Tris; 192 mM glycine; 20% (v/v) methanol) for 10 minutes prior to preparing the sandwich, and the nitrocellulose was carefully rolled onto the gel to avoid trapping air bubbles. The cassettes were inserted into the cassette holder and placed in the blotting tank, after which they were immersed in blotting

buffer. Electrophoretic transfer was carried out overnight at 20 mA. The nitrocellulose pieces were then carefully removed and blocked with 10 ml of a 5% (w/v) low fat milk powder in TBS (20 mM Tris; 200 mM NaCl at pH 7.4) solution for one hour. The nitrocellulose strips were then washed three times in 10 ml TBS for 5 minutes per wash. Primary antibody solutions were prepared in 0.5% (w/v) BSA-TBS as specified and nitrocellulose strips were incubated for 2 hours with these solutions, followed by three washes in TBS as described before. The nitrocellulose strips were then incubated for 1 hour with secondary antibody solution 1/12000 (unless stated otherwise) in 0.5% (w/v) BSA-TBS, followed by three washes in TBS as described before. Finally the nitrocellulose strips were developed for ten to 30 minutes using 2 ml of a substrate stock solution (0.3% (w/v) 4-chloro-1-naphthol in methanol) diluted in 8 ml TBS containing 4 μ l H₂O₂. After developing the nitrocellulose strips were washed with dH₂O and left to dry.

2.3.3. Direct ELISA method

Antigens were diluted to 1 μ g / ml in PBS (137 mM NaCl; 3 mM KCl; 7 mM Na₂HPO₄; 1.5 mM KH₂PO₄ at pH 7.2) and 150 μ l was pipetted to each well. The plates were incubated overnight at 4°C to allow coating of the wells. All wash steps were done with PBS containing 0.1% (v/v) Tween 20 and repeated three times and all incubations subsequent to coating were done at 37°C, except with substrate, which was left at room temperature. After coating, the plates were washed and then blocked with 200 μ l 0.5% (w/v) BSA-PBS per well and incubated for 1 hour. After a wash step the plates were incubated for 2 hours with 100 μ l of the antigen-specific primary antibody and washed again. They were then incubated with 120 μ l of the rabbit-anti-chicken HRPO antibody diluted 1/15000 for 1 hour and washed. All antibody solutions were prepared in 0.5% (w/v) BSA-PBS. Finally the plates were incubated with 150 μ l substrate (0.05% (w/v) ABTS; 0.0015% (v/v) H₂O₂ prepared in a 0.15 M citrate phosphate buffer at pH 5.0) per well and left to develop in the dark at room temperature for 30 minutes. The plates were then read immediately in an ELISA-plate reader at 405 nm. Background controls included: no antigen (or no coat), no primary antibody and no detection antibody in separate wells during each of the respective ELISA incubation steps. All results were corrected for background. Positive controls included a no blocking control. Additional controls were stated in text where applicable.

2.4 Bioinformatics (Chapter 3)

The *in silico* work done to identify the malaria protein targets: LDH, GAPDH and PMT, as well as deciding on the respective peptide epitopes to target is described below. All results from this work were compiled into chapter 3.

2.4.1 Identifying malaria protein targets for diagnosis

The initial identification of possible protein targets for diagnosing malaria were based on mining of literature which focused on transcriptional and translational studies of *Plasmodium falciparum*. Most of this data could also be found on the malaria site PlasmoDB (www.plasmodb.org/). A potential target's suitability was then assessed using the following set of programmes.

2.4.2 Sequence alignments

In order to assess a protein target's homology with its related malaria and human orthologs, alignments were performed. The primary protein amino acid sequences were aligned using Clustal Omega (<http://www.ebi.ac.uk/Tools/msa/clustalo/>). The sequences were obtained either from NCBI (www.ncbi.org/) or PlasmoDB (www.plasmodb.org/) as indicated in text. Sanger sequencing results obtained in later chapters were aligned with their respective DNA coding sequences, or the IgY heavy and light chain germline sequences for scFvs, also obtained from NCBI or PlasmoDB as indicated (chapters 3 and 6).

2.4.3 Predict7TM

Using the protein alignment data obtained above, specific peptide sequences of ten to 16 amino acids in length were selected. These were either species-specific peptides, in which case they had sequences unique to their respective *Plasmodium* species, or alternatively they were common conserved peptides, common to all human-infecting *Plasmodium* species but differing from the corresponding human peptides. Predict 7TM was used to assess the physical properties of the candidate peptides in terms of hydrophilicity, surface probability, antigenicity and flexibility. Most important was to ensure that the peptides were soluble (hydrophilic) and found on the surface of the parent protein (surface probable).

2.4.4 3D modelling

To verify the location of the candidate peptides, they were located on the surface of their respective parent 3D protein models. The 3D crystal structures were downloaded from the Swiss model repository (<http://swissmodel.expasy.org/repository/>) and manipulated with Deep view Swiss pdb viewer downloaded from <http://www.expasy.org/spdbv/>.

2.4.5 Sequencing (see section 2.2.8)

The sequencing results for each of the recombinant proteins were included in chapter 3 as part of the bioinformatics approach to verify the location of the selected peptide sequences within the recombinant proteins used further.

2.5 Recombinant work with malarial proteins (Chapter 4)

The three chosen malaria proteins were recombinantly expressed, purified and partially characterised. Together these results formed chapter 4.

2.5.1 Reagents

Isopropyl thioglucoopyranoside (IPTG), ampicillin and kanamycin were purchased from Sigma-Aldrich-Fluka (Steinheim, Germany). Molecular biology grade DTT was purchased from Fermentas (Vilnius, Lithuania). TALON[®] cobalt metal affinity resin was from Clontech Laboratories Inc. (California, USA). Imidazole, polyethylene glycol 20000 (PEG 20000), MES hydrate, tryptone, agar bacteriological, D(+) glucose anhydrous, sucrose, glycerol and yeast extract were purchased from Merck (Damstadt, Germany). A DNA purification kit was purchased from PEQLAB Biotechnologie (Erlangen, Germany). 0.22 and 0.45 µm syringe filters were from PALL Life Sciences (Ann Arbor, MI, USA).

2.5.2 Expression host *E. coli*

The *E. coli* BL21(DE3) strain (Novagen, Damstadt, Germany) was used as the host for expression of all malarial proteins throughout this study. The strain's genotype is as follows: (F⁻ ompT gal dcm lon hsdSB(rB- mB-) λ(DE3 [lacI lacUV5-T7 gene 1 ind1 sam7 nin5])). The choice of *E. coli* strain was primarily based on the protease deficiency of this strain.

2.5.3 Expression vectors

The malarial target proteins had previously been cloned into their respective vectors as listed in the Table 2.3. All three PMT proteins were kindly provided by Prof. B. Mamoun (Harvard University). The coding genes for *Pf*LDH (*Pf*(K1) strain) and *Pv*LDH were cloned into pKK223-3 and were kindly provided by Professor R.L. Brady (University of Bristol, UK). *Pf*GAPDH (from the *Pf*(3D7) strain) was cloned into the pET-15b vector and kindly provided by Professor L. Tilley (Satchell *et al.*, 2005). Finally the two *P. yoelii* proteins, *Py*LDH and *Py*GAPDH had previously been cloned into pET-28a vector (Novagen, Darmstadt, Germany) in our laboratory.

Table 2.3 List of vectors used in the study for expression of the respective malarial proteins

Vector name	Resistance marker	Vector size (bp)	Protein target	Promoter	Tag
pET-15b	Ampicillin	5708	<i>Pf</i> GAPDH <i>Pf</i> PMT	T7 / lac	N-terminal His (6)
pET-28a(+)	Kanamycin	5369	<i>Py</i> LDH <i>Py</i> GAPDH <i>Pv</i> PMT	T7	N-terminal His (6)
pKK223-3	Ampicillin	4600	<i>Pf</i> LDH <i>Pv</i> LDH	Tac	None

Recombinant protein expression from all vectors was inducible with IPTG due to the presence of T7, lac or Tac promoters. The resulting recombinant proteins were all tagged with at least one set of six recurring histidine residues, which allowed for affinity purification.

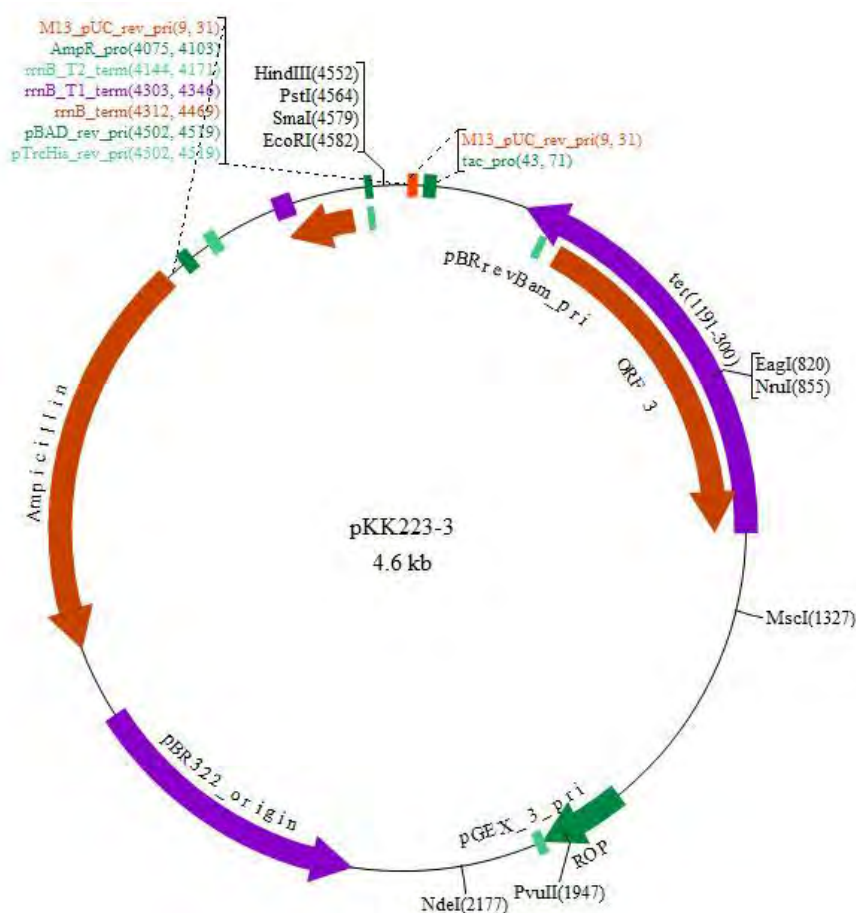


Figure 2.3 pKK223-3 expression plasmid vector map

The vector map depicts the restriction sites available for inserting the desired coding sequence. The *Pf*LDH sequence was inserted between the *Pst*I and *Eco*RI restriction sites. The vector codes for ampicillin resistance, which is used as the selective maker for transformed cells. The size of the plasmid without insert is 4.6 kb as shown in the centre of the map. The map was obtained from <http://www.biovisualtech.com/bvplasmid/pKK223-3.htm>.

In the case of the pKK223-3 vector, the histidine tags were attached to the respective LDH inserts via PCR amplification (Turgut-Balik *et al.*, 2004). Detailed maps of the vectors used in this study are shown in Figures 2.3 to 2.5.

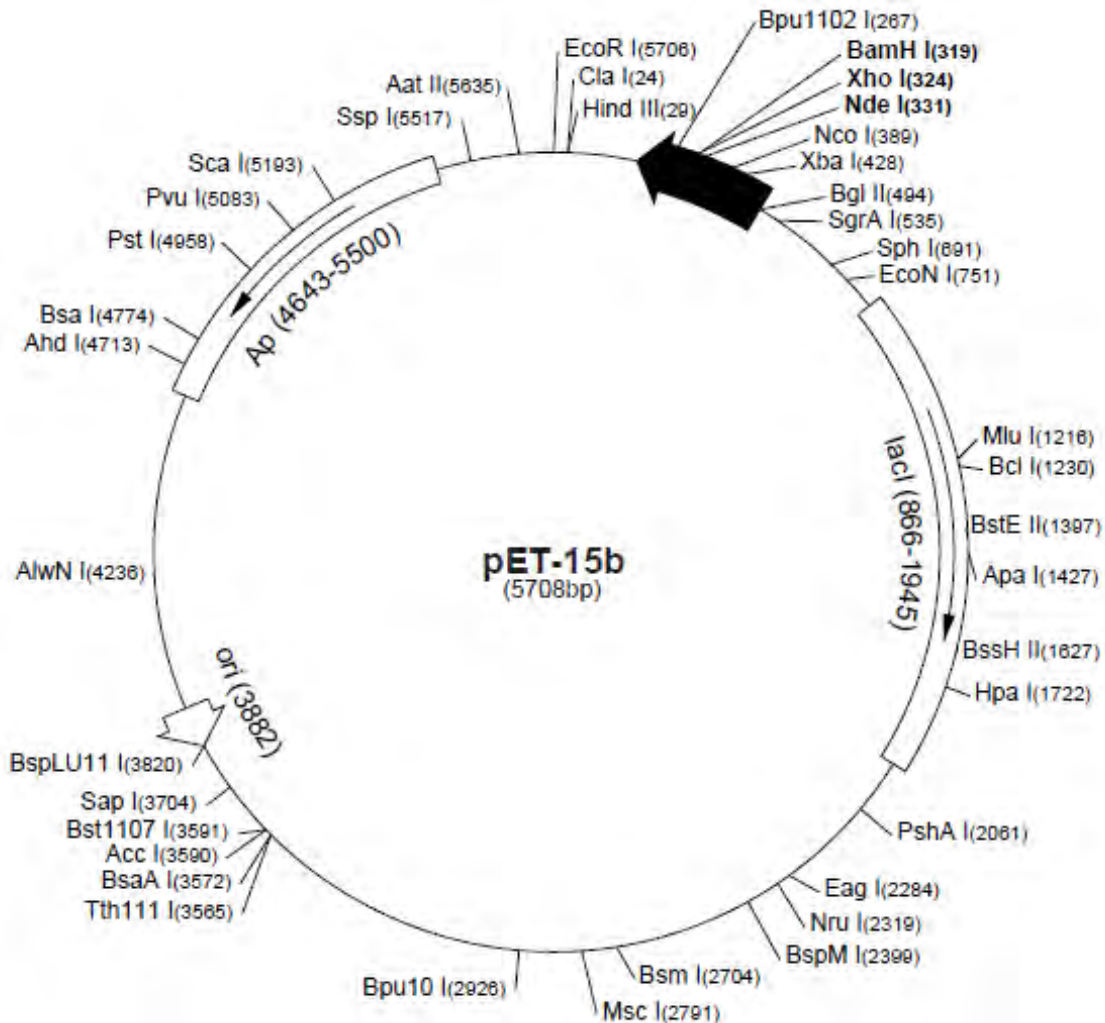


Figure 2.4 pET-15b expression plasmid vector map

The vector map depicts the restriction sites available for inserting the desired coding sequence. The *Pf*GAPDH and *Pf*PMT sequences were inserted between the *Xho*I and *Nde*I restriction sites. The vector codes for ampicillin resistance (Ap), which is used as the selective maker for transformed cells. The size of the plasmid without an insert is 5.7 kb as shown in the centre of the map. The map was obtained from https://www.embl.de/pepcore/pepcore_services/strains_vectors/vectors/pdf/pET-15b_map.pdf.

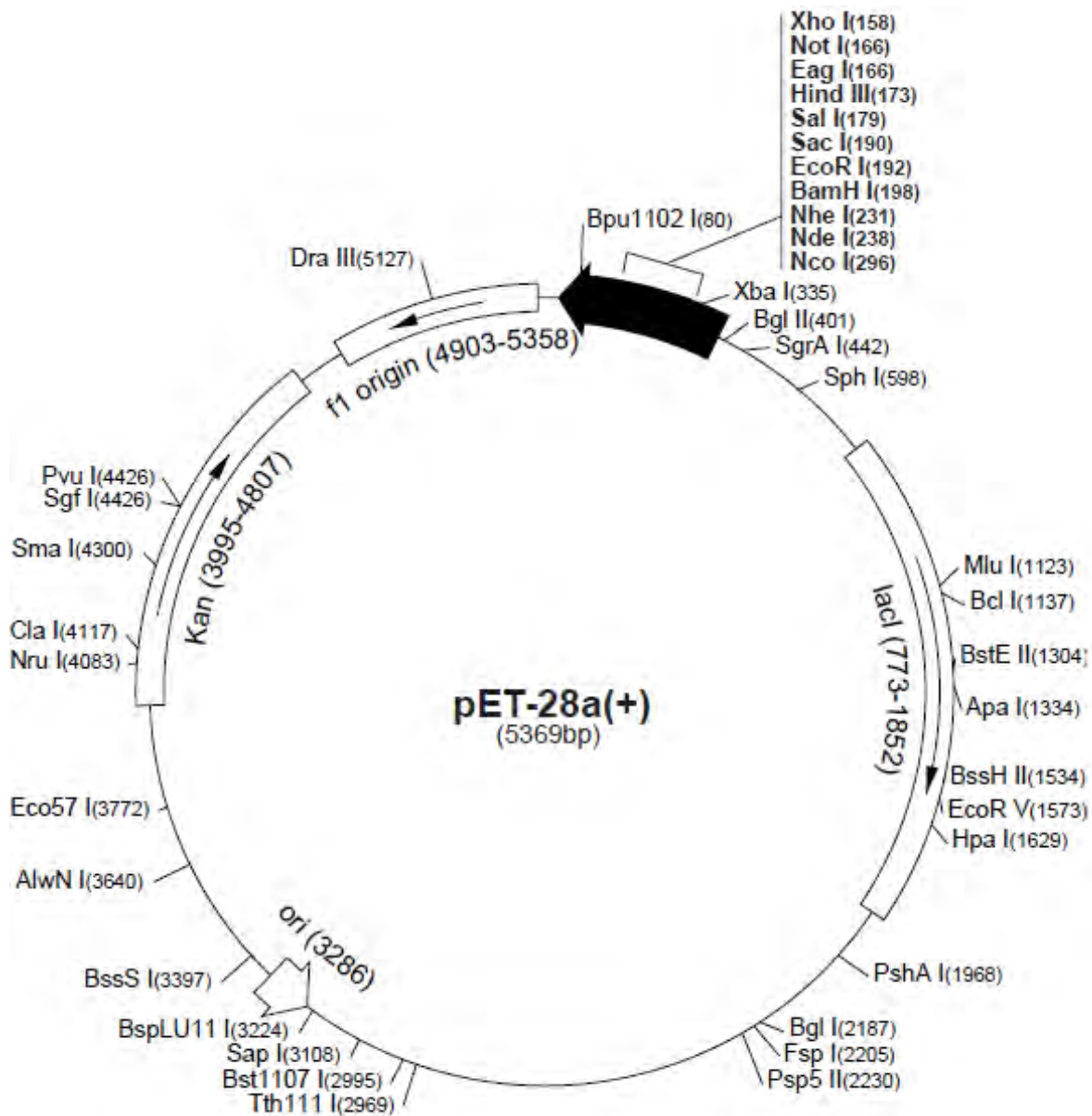


Figure 2.5 pET-28a expression plasmid vector map

The vector map depicts the restriction sites available for inserting the desired coding sequence. The *PyLDH* and *PyGAPDH* sequences were inserted between the *EcoRI* and *NotI* or *NdeI* and *XhoI* restriction sites respectively. The vector codes for Kanamycin resistance (Kan), which is used as the selective marker for transformed cells. The size of the plasmid without an insert is 5.4 kb as shown in the centre of the map. The map was obtained from https://www.embl.de/pepcore/pepcore_services/strains_vectors/vectors/pdf/pET-28a-c_map.pdf.

Several methods were used for confirmation of the vector inserts prior to sequencing. These methods included restriction digestion and PCR amplification of the inserts, both giving size confirmation. This was ultimately followed by sequencing, where only the sequencing data was included in this study.

2.5.4 Transformation of *E. coli* BL21(DE3) host

Approximately 50 to 100 ng of plasmid DNA was added to 50 µl competent *E. coli* BL21(DE3) and mixed gently. The samples were incubated on ice for 30 minutes and then heat shocked at 42°C for 45 seconds and returned to the ice for a further 2 minutes. Four hundred and fifty microliters SOC media (2% (w/v) Tryptone; 0.5% (w/v) Yeast extract; 10 mM NaCl; 2.5 mM MgCl₂; 10 mM MgSO₄ and 20 mM Glucose) was added per sample and incubated at 37°C, 200 rpm for an hour. The entire volume was plated onto two LB plates (pre-warmed to 37°C for 30 min) containing either Ampicillin (50 µg/ml) or Kanamycin (25 µg/ml) and incubated overnight (16 hours) at 37°C. Individual colonies were inoculated into 5 ml LB media containing the appropriate antibiotic (Ampicillin at 50 µg/ml or Kanamycin at 25 µg/ml) and incubated overnight (16 hours) at 37°C, 200 rpm. Glycerol stocks of transformed cells were prepared from overnight cultures (850 µl) combined with 150 µl glycerol (50% (v/v)) and stored at -70°C.

For further work single colonies of transformed *E. coli* were picked off LB agar (1% (w/v) tryptone; 0.5% (w/v) yeast extract; 85 mM NaCl; 11 mM glucose; 1.5% (w/v) bacto-agar prepared in dH₂O and autoclaved) plates (containing the specific antibiotic), which were three way streaked from glycerol stocks and incubated overnight (16 hours) at 37°C.

Colony PCR (section 2.2.5) was performed to verify the presence of inserts within the expression hosts. As a final verification, the malarial protein vector inserts were sequenced as described in section 2.2.8. The consensus sequences were aligned with sequences obtained from PlasmoDB.

2.5.5 Expression of recombinant malarial proteins

As a general rule, no bacterial culture volumes exceeded 20% of the culture flask volume in which they were grown. Volumes mentioned in text therefore refer to culture volumes, keeping this rule in mind. Single colonies were picked off agar plates and inoculated into 10 ml LB broth (as for LB agar, without the addition of agar) prepared in dH₂O and autoclaved) and incubated overnight (16 hours) at 37°C. These cultures were then used to inoculate larger broth volumes, which were induced for expression of the respective recombinant proteins. Different broth formulations were used, either for induction with IPTG or auto-induction (without IPTG). To simplify interpretation of the expression conditions used per protein, Table 2.4 was included.

Table 2.4 Expression media used per recombinant protein and additional supplements

Recombinant protein	Expression media / broth	Antibiotic ($\mu\text{g} / \text{ml}$)	IPTG (mM)	Temp. ($^{\circ}\text{C}$)	Time. (hrs)
<i>Pf</i> LDH	TB	Amp. (50)	auto	37	16
<i>Pv</i> LDH	TB	Amp. (50)	auto	37	16
<i>Py</i> LDH	TB	Kan. (25)	auto	37	16
<i>Pf</i> GAPDH	TB	Amp. (50)	auto	37	16
<i>Py</i> GAPDH	TB	Kan. (25)	auto	37	16
<i>Pf</i> PMT	LB	Amp. (100)	1	37	16
<i>Pv</i> PMT	TB	Kan. (25)	auto	37	16
<i>Py</i> PMT	TB	Kan. (25)	1	37	16

TB: Terrific broth; LB: Lysogeny broth; Amp.: Ampicillin; Kan.: Kanamycin; auto: auto-induction (without IPTG)

The Terrific broth (TB) formulation, prepared in dH_2O and autoclaved, was as follows: 1.2% (w/v) tryptone, 2.4% (w/v) yeast extract, 0.4% (w/v) glycerol, 0.231% (w/v) KH_2PO_4 , 1.254% (w/v) K_2HPO_4 . All additional media supplements were prepared in dH_2O and filter sterilised through 0.22 μm syringe filters and stored in 1 to 2 ml aliquots at -20°C . All cultures were supplemented once with their respective antibiotics, and IPTG was also only added once. For the cultures requiring IPTG, they were grown to an optical density measured at 600 nm ($\text{O.D.}_{600\text{nm}}$) of between 0.5-0.6 before supplementing. In preparation for affinity purification all expression cultures were grown overnight, the cells were pelleted by centrifugation at 4000 x g for 30 min at 4°C and the supernatant media removed.

2.5.6 Affinity purification

Following expression, each recombinant His₆-tagged protein was extracted from prepared expression culture pellets (described above 2.5.5) and passed over a separate TALON (Co^{2+}) affinity matrix for purification as described below.

The pelleted culture samples were suspended to 5% of their original culture volume in wash buffer (50 mM NaH_2PO_4 ; 300 mM NaCl; 10 mM imidazole; 0.02% (w/v) NaN_3 at pH 8.0) and lysed using 4 x 30 second sonication steps (0.6-0.8 Watts). Samples were then centrifuged (12000 x g, 4°C , 20 minutes) and 10 ml at a time, the clear supernatant lysate samples were incubated for 20 minutes with 1 ml of a packed TALON (Co^{2+}) affinity resin (i.e. 2 ml of 50% slurry). The resin had been equilibrated prior to this step with two 10 ml changes of wash buffer, with a 5 minute centrifugation step at 1210 x g after each wash and removal of the supernatant buffer. After the sample incubation, the resin was washed twice with wash buffer as described above and transferred to a column. The bound recombinant

protein was eluted using 5 ml elution buffer (the wash buffer with 250 mM imidazole instead) and profiles were recorded using absorbance at 280 nm (A_{280}). The protein concentration of specific eluents was determined by the Bradford method as described in 2.2.2.

The resin was regenerated by washing with 10 ml MES buffer (20 mM MES at pH 5.0) for 20 minutes, followed by a 10 ml wash with dH₂O and stored at 4°C in storage buffer (20% (v/v) ethanol; 0.1% (w/v) NaN₃ prepared in dH₂O). The resin was reused for further purifications, but each recombinant protein was assigned its own batch of resin to avoid contamination.

2.5.7 SDS-PAGE analysis, dialysis and storage of recombinant proteins

To assess the purity of the affinity purified recombinant proteins, samples were purified and resolved by reducing 12.5% SDS-PAGE as described in section 2.2.3. For long term storage recombinant protein samples were dialysed (see section 2.2.4) into PBS, 10% (v/v) glycerol, 5 mM EDTA, 10 mM DTT at pH 8.0 and snap frozen in liquid nitrogen and stored at -70°C.

2.6 Raising antibodies (Chapter 5)

In order to raise chicken antibodies, the immunogenic proteins and peptides had to be prepared as described here.

2.6.1 Reagents

Ellman's reagent, formamide, Freund's complete adjuvant (FCA), Freund's incomplete adjuvant (FIA), maleimidobenzoyl-N-hydroxysuccinimide ester (MBS), rabbit albumin (RA), L-cysteine, sodium azide, Sephadex G-25 and Sephadex G-10 were purchased from Sigma-Aldrich-Fluka (Steinheim, Germany). Polyethylene glycol 6000 (PEG 6000) was purchased from Merck (Darmstadt, Germany). SulfoLink™ and AminoLink™ coupling gels were purchased from Pierce Perbio Science (Erembodegem, Belgium). Synthetic peptides were synthesized by GL Biochem (Shanghai, China).

This included preparation of the purified whole malaria recombinant proteins (section 2.5) as well as specifically selected peptide targets (sections 2.4 and 2.6.2). All antibodies raised and used in this study were listed in Table 2.5. Only the PMT, cmc and the second *P. falciparum* GAPDH specific peptide (C-ADGFLDIGEKKVSVFA) IgY were raised during this study. The rest had all been raised and purified previously in our laboratory. In total, 46 chickens were

immunised, with most giving high yields of final specific IgY. The sequence identity between the chicken and target proteins / peptides was also listed.

Table 2.5 List of targets immunised into chickens for IgY production

Target	Target species	Target description	Type	Percent identity with chicken sequence	Chickens	
LDH	<i>P. falciparum</i>	rPfLDH	protein	31	6	
		LISDAELEAIFD-C	peptide	0	2	
	<i>P. vivax</i>	rPvLDH	protein	29	2	
		KITDEEVEGIFD-C	peptide	8	2	
	common	<i>P. yoelii</i>	rPyLDH	protein	28	2
			APGKSDKEWNRDDL-C	peptide	14	2
GAPDH	<i>P. falciparum</i>	rPfGAPDH	protein	66	6	
		C-ADGFLDIGEKKVSVFA	peptide	25	2	
		C-AEKDPSQIPWGKCQV	peptide	40	2	
	common	<i>P. yoelii</i>	rPyGAPDH	protein	64	2
			C-KDDTPIYVMGINH	peptide	54	2
PMT	<i>P. falciparum</i>	rPfPMT	protein	0	2	
		C-EVEHKYLHENKE	peptide	0	2	
	<i>P. vivax</i>	rPvPMT	protein	0	2	
		VYSIKEYNSLKD-C	peptide	0	2	
	<i>P. knowlesi</i>	rPkPMT	protein	0	2	
		LYPTDEYNSLKD-C	peptide	0	2	
	common		LENNQYTDEGVK-C	peptide	0	2
scFv		C-EQKLISEEDLN	peptide	0	2	

2.6.2 Peptide synthesis

The peptides for this study were all from GL Biochem (Shanghai) Ltd. Terminal cysteine residues were added to the original sequences to allow for coupling to carrier proteins (section 2.6.3) or resins (section 2.6.6).

2.6.3 Coupling peptides to rabbit albumin

Due to the general low immunogenicity of peptides, they were coupled to rabbit albumin as a carrier protein (Harlow and Lane, 1988). The coupling was performed with the heterobifunctional coupling agent, maleimidobenzoyl-N-hydroxysuccinimide ester (MBS), using the terminal cysteine sulfhydryl groups of the peptides and free amine groups on the carrier protein. The reaction to couple 4 mg of peptide to rabbit albumin involved two steps:

1) Activation of the rabbit albumin carrier protein with MBS, and 2) reduction of the target peptide's terminal cysteine sulfhydryl groups. These were outlined below.

1) Activation of the rabbit albumin carrier protein with MBS:

The ratio of peptide to carrier is 40:1, therefore the mass of rabbit albumin (RA) required for coupling was calculated as follows, where the molar mass of rabbit albumin is 68.2 kD:

$$68200 \times \frac{1}{40} \times \frac{4 \times 10^{-3} \text{ g (peptide)}}{Mr \text{ peptide}} \times 1000 = \text{carrier (mg)}$$

The ratio of carrier to MBS is 1:40, therefore the mass of MBS required for coupling was calculated as follows, where the molar mass of MBS is 314.26 g / mol.

$$314.26 \times 40 \times \frac{\text{carrier (mg)}}{68200} \times 1000 = \text{MBS (mg)}$$

The calculated amounts of RA were dissolved in 500 μ l PBS and the MBS was dissolved in 200 μ l Dimethyl formamide (DMF) and 300 μ l PBS. Once dissolved, the two solutions were combined and left to stand at room temperature for 30 minutes. This incubation was timed to start 30 minutes into the peptide incubation with DTT.

2) Reduction of the target peptide's terminal cysteine sulfhydryl groups.

Four milligrams of the target peptide was dissolved in 50 μ l DMSO and made up to 500 μ l in reducing buffer (100 mM Tris; 1 mM EDTA; 0.02% (w/v) NaN_3 at pH 8.0), after which 500 μ l 10 mM DTT solution (10 mM DTT in reducing buffer) was added and the solution was mixed and incubated at 37°C in a water bath for 90 minutes.

Two molecular exclusion chromatography columns (Sephadex G-10 and G-25) were washed with at least two column volumes of 0.2 M NaOH and then equilibrated with MEC buffer (100 mM NaH_2PO_4 ; 0.02% (w/v) NaN_3 at pH 7.0). A Sephadex G-10 column (column volume 20 ml) was used to separate the reduced peptide from DTT. The eluted 500 μ l fractions were assessed for reduced peptide by adding 10 μ l eluent to 10 μ l Ellman's reagent (4 mg/ml) prepared freshly in Ellman's buffer (100 mM Tris; 1 mM EDTA; 0.1% (w/v) SDS

at pH 8.0). Yellow reactions indicated reduced peptide eluents. These were pooled and used for coupling to the MBS activated RA carrier.

The activated RA carrier was prepared by separating it on a Sephadex G-25 column (column volume 120 ml) following the 30 minute incubation at room temperature with MBS as explained above. Fractions (1 ml) were collected and fractions with A_{280} values greater than 0.3 were pooled and combined with the reduced peptide fractions eluted off the Sephadex G-10 column. This mixture was then left to stand at room temperature for 3 hours with gentle stirring. The resulting peptide-carrier conjugate solution was then split into four aliquots and stored at -20°C until required for immunisation.

Only one of the peptides was insoluble in the DMSO and reducing buffer solution, and had to be solubilised in DMSO alone. An alternative method was used for coupling of this peptide as described by Lateef *et al.* (2007).

2.6.4 Chicken immunisation

Ethical clearance for the use of experimental animals in this study was granted by the animal ethics committee of UKZN (Ethics number 004/15//Animal).

A total of 200 μg of pure recombinant protein was used to immunise each chicken. Alternatively 4 mg of a prepared peptide conjugate sample was used to immunise each chicken. The protein or peptide preparations were split into four aliquots allowing for one priming and three booster immunisations. These samples were prepared in PBS and were mixed 1:1 with either Freund's complete adjuvant (FCA) or Freund's incomplete adjuvant (FIA). The FCA formulation contains heat killed *Mycobacterium* and was used for primary immunisations, whereas the incomplete adjuvant (FIA) without *Mycobacterium* was used for booster immunisations (weeks two, four and six). All samples were prepared by trituration with a syringe until thick water in oil emulsions formed. The immunisations were administered intramuscularly into each chest muscle, where the skin was wiped locally with 70% (v/v) ethanol prior to immunisation.

2.6.5 Isolation of crude IgY from chicken egg yolk

The immunised chickens were kept in laying batteries to allow for easy collection of eggs. These were dated and kept at 4°C until required. Importantly IgY from single eggs collected prior to immunisation (non-immune) and at the end of each week following immunisation were isolated first. This allowed for monitoring of antibody production (by ELISA method,

see section 2.7.3) throughout the immunisation schedule and up to weeks 12 or 14 after the first immunisation. In turn this allowed for selective isolation of IgY from weeks with high antibody responses only. IgY was thus generally isolated from weeks three to 12 or 14 as described by Polson *et al.* (1985).

The egg yolk was separated from egg white and then drained from the yolk sac and its volume determined. The yolk volume was increased three fold with isolation buffer (100 mM NaH₂PO₄; 0.02% (w/v) NaN₃ at pH 7.6) and PEG (Mr 6000) was added to a final concentration of 3.5% (w/v). The solution was stirred gently to dissolve the PEG, followed by centrifugation (4420 x g, 4°C, 30 minutes), and removal of the precipitated vitellin pellet. The supernatant was filtered through cotton wool and its volume recorded. The PEG concentration was increased to 12% (w/v) and stirred gently until dissolved. In this case the sample was centrifuged (12000 x g, 4°C, 10 minutes) and the precipitate was retained and dissolved in a volume of isolation buffer equal to that of the filtrate. The PEG concentration was brought to 12% (w/v) again and allowed to dissolve completely with gentle stirring. The sample was then centrifuged (12000 x g, 4°C, 10 minutes) and the final pellet dissolved in 1/6 of the initial yolk volume with storage buffer (100 mM NaH₂PO₄; 0.1% (w/v) NaN₃ at pH 7.6) and stored at 4°C.

In order to purify specific antibodies from the stored batches of crude IgY, the respective malarial target proteins or peptides were coupled to AminoLink™ or SulfoLink™ resins respectively. Both methods are described in the following section.

2.6.6 Preparation of affinity matrices

AminoLink™ and SulfoLink™ resins were used to couple the whole recombinant *Plasmodium* proteins or the specifically selected peptides respectively as described to follow.

2.6.6.1 Recombinant malarial proteins coupled to AminoLink™ resins

AminoLink™ coupling exploits the free primary amines on the surface of proteins. Due to the hydrophilic or charged nature of these groups, they are often found on the surface of proteins and include the N-terminal and lysine side chain amines. Therefore the purified recombinant proteins were coupled to AminoLink™ resins as outlined here.

Five milligrams of the purified recombinant protein was dialysed (10 kD MWCO) against coupling buffer (100 mM NaH₂PO₄; 300 mM NaCl; 0.05% (w/v) NaN₃ at pH 7.2). The coupling buffer was modified from the manufacturer's instruction by the addition of 300 mM

NaCl to aid protein solubility. Two millilitres of the AminoLink™ resin (resulting in a 1 ml packed resin) was poured into a mini-column and the storage buffer drained after the resin had settled. The resin was then equilibrated with 6 ml coupling buffer and drained. The dialysed protein solution was then added (2-4 ml) and 0.1 ml was retained to determine the coupling efficiency of the protein to the column. Forty microliters cyanoborohydride solution (5 M NaCNBH₃; 1 M NaOH) was added, and the column was mixed end-over-end for 6 hours at room temperature. The column was then drained of buffer and an eluent sample retained to determine the coupling efficiency of the protein to the column. The column was then washed with 4 ml coupling buffer after which 2 ml quenching buffer (1M Tris-HCl at pH 7.4) was added with 40 µl cyanoborohydride and mixed on an end-over-end mixer for 30 minutes. The column was then drained again and washed with 10 ml wash solution (100 mM NaH₂PO₄; 0.2% (w/v) NaN₃ at pH 6.5) and stored at 4°C until required. Coupling efficiency was assessed by measuring protein concentration after coupling using the Bradford assay (section 2.2.2).

2.6.6.2 Peptides coupled to SulfoLink™ resin

SulfoLink™ resin was used for producing peptide-linked affinity columns, linking the peptides via terminal cysteine sulfhydryl residues.

Five milligrams of the peptide to be coupled was dissolved in 100 µl DMSO and 400 µl general buffer (50 mM Tris-HCl; 50 mM EDTA at pH 8.5), to which 500 µl DTT was added and the sample was then incubated for 1.5 hours at 37°C (water bath). A Sephadex G-10 column (column volume 75 ml), washed with at least two column volumes of 0.2 M NaOH and then equilibrated with general buffer, was used to separate the reduced peptide from the DTT. This was done by collecting 500 µl eluents off the column and combining 10 µl of each eluent separately with 10 µl Ellman's reagent as described in 2.6.3. The reduced peptides reacted with the Ellman's reagent to give a yellow solution. The eluents containing the reduced peptide were pooled and added immediately to 1 ml (packed resin volume) of SulfoLink™ resin equilibrated in general buffer and mixed for 15 minutes after which it was left to stand for 30 minutes. After three washes with general buffer (1 column volume each) 1 ml of a 50 mM L-Cysteine solution was added to the resin, mixed for 15 minutes on an end over end mixer and left to stand for 30 minutes. The column was drained and washed with 16 column volumes washing buffer followed by two column volumes of a 0.1 M phosphate buffer at pH 7.6 and stored at 4°C until use.

2.6.7 IgY affinity purification

Crude IgY isolated from weeks showing high antibody responses were pooled and used for affinity purification. The crude IgY was circulated over the column overnight at room temperature. The column was then washed with PBS until the A_{280} of eluting samples dropped down to between 0.01-0.02. Eppendorfs were prepared for collection of eluents by adding 100 μ l neutralisation buffer (1 M NaH_2PO_4 ; 0.02% (w/v) NaN_3 at pH 8.5) to each tube. The specific antibodies bound to the antigen on the affinity column were then eluted with a change in pH by adding 8 ml elution buffer (100 mM glycine; 0.02% (w/v) NaN_3 at pH 2.8) to the column and collecting 1 ml eluents. Affinity purified samples with A_{280} values greater than 0.2 were pooled and the final IgY concentration was calculated using the sample A_{280} value and the extinction coefficient of IgY ($\epsilon = 1.25$) (Goldring and Coetzer, 2003). The pooled samples were kept at 4°C until required and the remainder was discarded.

2.6.8 Human IgG affinity purification

Three hundred milligrams of a human anti-malaria hyperimmune serum pool was used to affinity purify human IgG antibodies against five recombinant *P. falciparum* proteins. These include rPfLDH, rPfGAPDH, rPfPMT, rPfHsp70 and rPfCox17. The latter two proteins were included for comparison. The purification of the human IgG antibodies was essentially as described above in section 2.6.7. The final IgG concentration was calculated using a human IgG extinction coefficient ($\epsilon = 1.35$) (Semenova *et al.*, 2004).

2.6.9 Conjugation of horse radish peroxidase to IgY antibodies

Conjugation of HRPO to antibodies was performed as per Kumar *et al.* (2014). Eight milligrams of horse radish peroxidase (HRPO) (1360 Units) was dissolved in dH_2O . Two hundred microliters 0.1 M sodium periodate was added and the solution turned from brown to a greenish brown and was stirred gently for 20 minutes at room temperature. The solution was then dialysed overnight (16 hours) at 4°C against sodium acetate buffer (0.1 M sodium acetate; 0.22% (v/v) acetic acid at pH 4.4), after which 20 μ l sodium carbonate buffer (13 ml of a 0.2 M sodium carbonate solution and 37 ml of a 0.2 M sodium hydrogen carbonate solution were made up to 200 ml at pH 9.5) was added to raise the pH of the solution to between 9-9.5. One millilitre (8 mg) of the IgY sample to be conjugated was added immediately. The antibody-HRPO mixture was inverted every 15 minutes and left at room temperature for a total of 2 hours. Finally 100 μ l sodium borohydride solution (4 mg/ml) was added to reduce any unbound HRPO and the solution was left to stand for 2 hours at 4°C. The IgY-HRPO solution was then dialysed against a 0.1 M borate buffer at pH 7.4 after which an

equal volume of 60% (v/v) glycerol (prepared in borate buffer) was added and the samples were stored at 4°C.

The IgY antibodies were characterised further using western blotting (section 2.3.2), ELISA (section 2.3.3) and ECL described below.

2.6.10 Enhanced chemiluminescence

The procedure (Mruk *et al.*, 2011) follows that of western blotting (section 2.3.2), except that TTBS (0.1% (v/v) Tween 20 added to the TBS buffer as described in 2.5.1) was used and the blocking was performed with 8% (w/v) low fat milk powder in TTBS, and wash steps were increased to 8 minutes per wash. After blocking for 1 hour and washing three times 8 minutes with TTBS, the blots were incubated with primary antibody overnight (16 hours) at 4°C with rocking. The primary and secondary antibodies were prepared in 0.5% (w/v) BSA-TTBS to the desired concentrations, which were both optimised. Detection of the chemiluminescent signal was done using the Syngene G:Box system (UK). The chemiluminescent reagent was then prepared by mixing 50 µl of a luminol stock solution (40 mg/ml luminol in 1% (v/v) DMSO), 25 µl of a p-iodophenol stock (0.1 M p-iodophenol in 1 ml DMSO) and 10 ml 0.1 M Tris-HCl pH 8.5 buffer directly onto the blots and exposure was optimised per sample.

2.6.11. Double antibody sandwich ELISA method

Plates were coated with 150 µl of an antigen-specific capture antibody at a concentration of 1 µg / ml prepared in PBS and incubated overnight at 4°C. All other antibody solutions were prepared in 0.5% (w/v) BSA-PBS As in the direct ELISA method, all subsequent incubation steps were done at 37°C and all wash steps were repeated three times with PBS containing 0.1% (v/v) Tween 20. After coating plates were washed and incubated with 0.5% (w/v) BSA-PBS for 1 hour and washed. The antigen-containing sample (150 µl) was then loaded per well at the desired concentration which had to be optimised to avoid the prozone effect. Recombinant protein solutions were prepared in 0.5% (w/v) BSA-PBS and used to prepare antigen standard curves. Plates were incubated for 2 hours, washed and then incubated with 150 µl of a detection antigen-specific antibody linked to HRPO diluted 1/200 for 2 hours and washed again. Substrate solution (150 µl) was added per well and the plates were incubated in the dark for 30 minutes at room temperature, after which they were immediately read in an ELISA-plate reader at 405 nm. Background controls included separate wells in which: antigen, capture antibody or detection antibody were excluded during the respective

incubations. All results were corrected for background readings. Positive controls included a no blocking control. Additional controls were stated in text where applicable.

2.7 ScFv work (Chapter 6)

The next section describes the scFv work done to identify monoclonal recombinant antibodies against the target proteins and peptides. These results are shown in chapter 6.

2.7.1 Reagents

TG1 *E. coli*, M13KO7 helper phage and the *Nkuku*[®] phagemid library were kindly provided by the Onderstepoort Veterinary Institute, South Africa (van Wyngaardt *et al.*, 2004). Ninety six well culture plates and immunotubes were from NUNC (Roskilde, Denmark). The anti-M13 monoclonal antibody was from Thermo Scientific (Waltham, MA, USA) and the Goat anti-mouse-HRPO secondary antibody was from Jackson Immunochemicals (Pennsylvania, USA).

2.7.2 *E. coli* hosts

The following *E. coli* host strains were used for the panning and expression of the scFv library. The *E. coli* TG1 strain was used as the host for panning experiments since it has a *supE* mutation, which allows for the expression of scFv fusion proteins with the minor coat protein III and subsequent display of the scFv on the phage surface. The *E. coli* Top10 strain lacks the *supE* mutation and is therefore used solely as an expression host for the recombinant expression of soluble scFv particles.

E. coli TG1 with genotype: (F' [traD36 proAB⁺ lacI^q lacZΔM15]supE thi-1 Δ(lac-proAB) Δ(mcrB-hsdSM)5, (r_K⁻m_K⁻)) (Lucigen).

E. coli Top10 with genotype: (F'[lacIq Tn10(tetR)] mcrA Δ(mrr-hsdRMS-mcrBC) φ80lacZΔM15 ΔlacX74 deoR nupG recA1 araD139 Δ(ara-leu)7697 galU galK rpsL(StrR) endA1 λ-) (Invitrogen).

2.7.3 Helper phage

The M13 phage used here has a single stranded DNA genome and forms part of the Ff filamentous phage group that infects male *E. coli* cells (Hoogenboom *et al.*, 1991).

2.7.4 pHEN1 vector

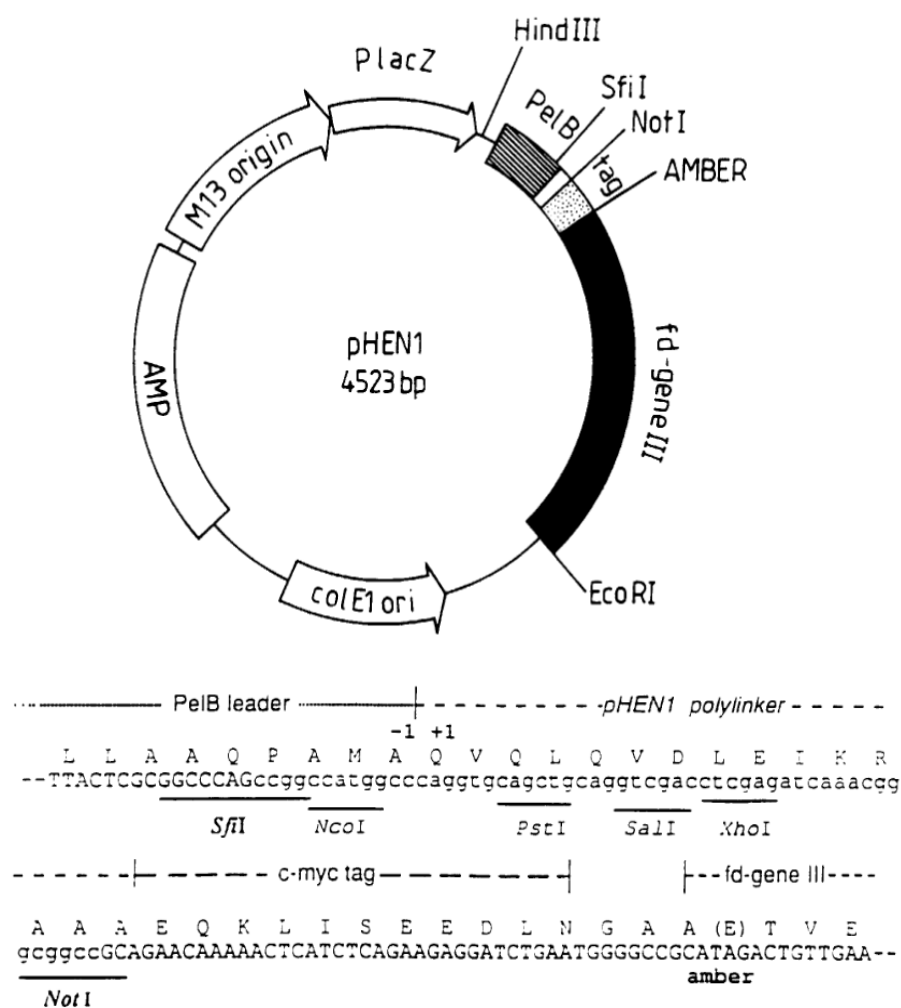


Figure 2.6 pHEN1 vector map used in phage display

The vector map depicts the *SfiI* and *NotI* restriction sites used to inserting the scFv coding sequences. The vector codes for Ampicillin resistance. The size of the plasmid without an insert is 4.5 kb as shown in the centre of the map. The vector map was adapted from Hoogenboom *et al.* 1991.

2.7.5 Library preparation

Before panning the library, several stocks and media had to be prepared. These will be mentioned first and used as reference throughout this section.

Table 2.6 Media recipes for phage display work

Media name	Recipe	Antibiotic
2xYT	1.6% (w/v) tryptone, 1% (w/v) yeast extract, 0.5% (w/v) NaCl	
2xYT (A/G)	as above, with 2% (w/v) glucose	100 µg /ml Amp.
TYE	1% (w/v) tryptone, 0.5% (w/v) yeast extract, 0.8% (w/v) NaCl	
TYE (A/G)	as above, with 2% (w/v) glucose	100 µg /ml Amp.

The above media may have been adapted with the addition of 1.5% (w/v) agar to allow for agar plate preparation, or with the addition of kanamycin at 50 µg/ml. These changes were mentioned in the methods section where applicable. As a general rule, all bacterial culture volumes never exceeded 20% of the culture flask volume in which they were grown. Volumes mentioned in text therefore refer to culture volumes, keeping this rule in mind.

2.7.5.1 Preparation of *E. coli* TG1 cells (panning host)

The host *E. coli* for the panning protocol were TG1 cells. Since this strain has a *supE* mutation, it is able to read through the amber codon in the pHEN1 vector and thus translate an scFv fusion protein with the minor phage coat protein 3. This allows the rescued phage to display the scFv on its surface.

We were provided with an initial uninfected *E. coli* TG1 glycerol stock, which was streaked onto TYE agar plates (Table 2.6) and incubated overnight at 37°C. A single colony was then picked and inoculated into 10 ml 2xYT (Table 2.6) and grown overnight (16 hours) at 37°C at 200 rpm. Fresh glycerol stocks were prepared with a final concentration of 15% (v/v) glycerol and stored at -70°C until required. Importantly these stocks were always streaked onto TYE (A/G) plates (Table 2.6) prior to preparing working cultures to ensure they were not accidentally infected with phage.

As *E. coli* strains with an F' genotype replicate, they form pili which the M13 phage uses in its mode of infection. Pili production occurs during the log or exponential growth phase of these *E. coli* and as such, log cultures were used throughout the panning procedures. These were prepared by inoculating 25 to 50 ml 2xYT broth 1/100 with overnight TG1 cultures and allowing them to grow to an O.D. at 600 nm of 0.5 to 0.6. Both cultures were then kept at 4°C and were used within one week of preparation.

2.7.5.2 Preparation of M13KO7 helper phage stocks

Due to the presence of the scFv fusion on the viral coat protein 3, the phagemids are not as infective as the wild type phage (M13KO7). The M13KO7 phage is therefore used to “rescue” the phagemids out of infected *E. coli* cells, resulting in a mosaic of wild-type and scFv-fusion coat protein 3 on the surface of rescued phages. This improves the infectivity of the phagemid particles whilst the phagemids still display the specific scFv on their surface, which can be selected for by affinity interactions or panning as described later.

Prior to panning, the wild type M13KO7 phage is grown and stocks at specific concentrations are prepared. Phage concentration is measured as infectivity or the number of plaque forming units per millilitre (pfu/ml). An initial M13KO7 glycerol stock was diluted in 2xYT (Table 2.6) to approximately 1×10^{-10} , with the last three doubling dilutions ($1 \times 10^{-8,9,10}$) prepared in 200 μ l 2xYT. One hundred microliters of each of these dilutions was added to 100 μ l of a TG1 log culture and left at room temperature (RT) for 5 minutes. Thereafter, the dilutions were added to 3 ml of molten (kept at 47°C) 0.7% (w/v) 2xYT agar and poured onto 2xYT agar plates which were pre-warmed to 37°C. The plates were then allowed to set and were incubated at 37°C overnight (16 hours).

The M13KO7 phage caused plaques of approximately 1 mm diameter on the TG1 *E. coli* lawn. A single plaque was punched out with the reverse end of a pipette tip and inoculated into 4 ml 2xYT, to which 40 μ l of an overnight TG1 culture had been added simultaneously. The culture was then incubated for 2 hours at 37°C, shaking at 100 rpm. This served as the inoculum for two 400 ml 2xYT cultures, which were incubated for another hour at 37°C, shaking at 100 rpm. Thereafter kanamycin was added to a final concentration of 50 μ g/ml and the cultures were grown overnight under the same conditions. The *E. coli* were then pelleted by centrifugation (10800 x g for 15 minutes at 4°C) and the supernatant medium was retained.

2.7.5.2.1 Phage and phagemid precipitation protocol

Phages and phagemids were all precipitated from supernatant media using the following protocol: The supernatant volume was increased by $\frac{1}{4}$ of its initial volume with the addition of a precipitation solution (20% (w/v) PEG 6000 and 2.5 M NaCl in distilled water and autoclaved). After a 30 minute incubation (1 hour for phagemids) on ice, the solution was centrifuged (10800 x g for 15 minutes at 4°C) and the pelleted phages retained. A second centrifugation (2000 x g for 2 minutes at 4°C) served to further condense the phage pellet as well as allowing removal of any remaining supernatant. This pellet was suspended in 6 ml PBS (1 ml for phagemids) and filter sterilised through a 0.45 μ m syringe filter.

The filtered sample was titred by preparing a range of dilutions in 2xYT as described earlier. The last three dilutions, $1 \times 10^{-8,9,10}$ were plated and titres were determined by counting the number of plaques formed on the *E. coli* lawn the next day.

$$\text{Pfu/ml} = [(\# \text{ plaques on plate}) \times \text{dilution factor}] / (0.5 \times 0.1 \text{ ml})$$

The filtered stock was diluted to 1×10^{12} pfu/ml in 15% (v/v) glycerol and stored as 1 ml aliquots at -70°C for long term, or 4°C for up to 6 months.

2.7.5.3 Culturing the *Nkuku*[®] phagemid library

The *Nkuku*[®] library was provided as an *E. coli* TG1 glycerol stock. Before the first panning rounds were performed, the library was cultured to prepare fresh glycerol stocks. A large culture (500 ml 2xYT (Amp.)) was inoculated with 250 μl of the initial glycerol stock, ensuring an initial O.D. of approximately 0.05. This was incubated at 37°C shaken at 240 rpm until log phase was reached, with an O.D. of approximately 0.5. A hundred millilitres of this culture was used to prepare phagemid stocks which will be explained to follow. The remaining culture was grown for an additional 3 hours under the same conditions and then centrifuged (3300 x g for 15 minutes) to pellet the TG1 cells. These were suspended in 1/100 of the initial culture volume of 2xYT and aliquots containing 15% (v/v) glycerol were stored at -70°C .

The 100 ml sample removed from the initial culture above was used to prepare phagemid stocks of the library. In other words, these were rescued from the TG1 *E. coli* cells using the wild type M13KO7 helper phage. The helper phage was added in a ratio of 20 helper phages to one bacterial cell. The bacterial population density was estimated based on its O.D., where an O.D. of one was representative of 8×10^8 bacteria / ml. The culture was incubated at 37°C for 30 minutes standing and 30 minutes shaking at 100 rpm to allow the helper phages to infect the TG1 cells. After a centrifugation (3300 x g for 15 minutes) the pelleted cells were suspended in 1 liter 2xYT (ampicillin and kanamycin) and incubated overnight at 30°C shaking at 240 rpm to allow for rescuing of the phagemids from the TG1 cells. The TG1 cells were pelleted by centrifugation (3300 x g for 20 minutes) the following day and the phagemids in the supernatant media were precipitated as described (section 2.7.5.2.1). The phagemid pellets were suspended in 20 ml PBS in this case, centrifuged (11000 x g for 2 minutes) to remove any precipitant material and the supernatant sterilised through a $0.45 \mu\text{m}$ syringe filter. This served as the starting stock used for panning the library and was stored at 4°C .

Finally the phagemid library stock solution was titred before panning, which is important as using too little of the stock during panning rounds would underrepresent the library which may result in poor panning yields. The phagemid stock was thus titred by preparing a series of dilutions up to 1×10^{-6} in 2xYT. Again the last three dilutions were made up to 200 μl in

2xYT and 100 µl of each was combined with an equal volume of log phase TG1 cells and left at RT for 5 minutes. The entire volume was plated onto TYE A/G agar plates and incubated overnight at 30°C. Titres were determined in terms of the number of colonies counted per plate and expressed as colony forming units (cfu) per 1 ml. For accurate estimations, plates with between 30 to 300 colonies were counted.

$$\text{Cfu/ml} = [(\# \text{ colonies on plate}) \times \text{dilution factor}] / (0.5 \times 0.1 \text{ ml})$$

2.7.6 Panning the *Nkuku*[®] library

The process of selecting scFv clones from the library which had affinity for the target molecule, in this case the malarial proteins and peptides, was termed panning. Once the various stocks had been prepared as described in section 2.7.5, panning of the library could begin. There were two types of targets which the library was panned for, similar to those used to immunise chickens (section 2.6) and these were listed in Table 2.7.

Immunotubes were coated overnight at 4°C with the target molecules in 3.5 ml PBS. Each successive panning round was coated with decreasing concentrations of the target molecules, for a total of four rounds. In the case of the recombinant proteins a range of 100, 50, 25 and 10 µg/ml was used, where the peptides were coated at 50, 25, 10 and 1 µg/ml (Table 2.7).

The coated tubes were washed three times with PBS and then blocked with 5 ml of a 2% (w/v) milk powder PBS solution for an hour. The tubes were washed twice with PBS containing 0.1% (v/v) Tween 20 (PBST) followed by two washes of PBS. The phagemid stock prepared previously (section 2.7.5.3) was diluted to between 1×10^{12} to 10^{13} cfu/ml in 3.5 ml of a 2% (w/v) milk powder PBST solution and incubated for 30 minutes at RT prior to adding it to the immunotubes. This was done to block the milk powder binders from binding to the blocked immunotubes.

Table 2.7 Malarial targets used to pan the *Nkuku*[®] library and the concentrations used per round

Target	Target species	Target description	Type	Panning rounds 1 to 4 concentrations used (µg/ml)
LDH	<i>P. falciparum</i>	rPfLDH	protein	100, 50, 25, 10
		LISDAELEAIFD-C	peptide	50, 25, 10, 1
	<i>P. vivax</i>	rPvLDH	protein	100, 50, 25, 10
		KITDEEVEGIFD-C	peptide	50, 25, 10, 1
	<i>P. yoelii</i> common	rPyLDH	protein	Not done
		APGKSDKEWNRDDL-C	peptide	50, 25, 10, 1
GAPDH	<i>P. falciparum</i>	rPfGAPDH	protein	100, 50, 25, 10
		C-ADGFLDIGEKKVSVFA	peptide	50, 25, 10, 1
		C-AEKDPSQIPWGKCQV	peptide	50, 25, 10, 1
	<i>P. yoelii</i> common	rPyGAPDH	protein	Not done
		C-KDDTPIYVMGINH		50, 25, 10, 1
PMT	<i>P. falciparum</i>	rPfPMT	protein	Not done
		C-EVEHKYLHENKE	peptide	50, 25, 10, 1
	<i>P. vivax</i>	rPvPMT	protein	Not done
		VYSIKEYNSLKD-C	peptide	50, 25, 10, 1
	<i>P. knowlesi</i> common	rPkPMT	protein	Not done
		LYPTDEYNSLKD-C	peptide	50, 25, 10, 1
		LENNQYTDEGVK-C	peptide	50, 25, 10, 1

The immunotubes were then incubated with the 3.5 ml phagemid preparation at RT for 30 minutes on an end-over-end rotator, followed by standing for 90 minutes. Following 20 washes with PBST and 20 with PBS, the tubes were incubated with 3.5 ml of a log phase TG1 culture and incubated for no longer than 30 minutes at 37°C. This step served both as the elution step and infection of TG1 cells, since the bound phagemids were released from the column by infecting the TG1 cells. This was used as it is a much gentler elution method than pH dependent elution methods and potentially allows for selection of much rarer phagemid binders from the library (Noppe *et al.*, 2009). After the 30 minute incubation the infected TG1 cells were pelleted by centrifugation (3,300 x g for 10 minutes). The pellet was suspended in 1 ml 2xYT and the entire volume was plated onto three TYE (A/G) plates and incubated overnight at 30°C. All colonies were then suspended in 5 ml 2xYT and between 200 to 500 µl of this suspension was used to inoculate 50 ml 2xYT (A/G) media, ensuring that the initial O.D. was as close to 0.05 as possible. The remainder of the suspended colonies were used to prepare glycerol stocks (15% (v/v) glycerol) and were stored as stocks of the

specific panning round performed. These could then be used to repeat a panning round, starting with inoculation of the 50 ml 2xYT (A/G) broth as described above. This culture was grown to log phase (O.D. ~0.5) and 5 ml of this was then removed and rescued with M13KO7. The infected cells were pelleted by two centrifugation steps (3300 x g for 10 minutes) and removal of the supernatant each time. The pellet was then suspended in 25 ml 2xYT (Amp. and Kan.) and incubated overnight at 30°C shaking at 240 rpm. The cells were pelleted again by centrifugation (3300 x g for 20 minutes) and the rescued phagemids in the supernatant were precipitated as described previously in section 2.7.5.2.1. Half a millilitre was used for the next panning round and 0.5 ml was stored at 4°C for use in the polyclonal ELISA described to follow. These panning rounds were repeated a total of four times with the target molecule concentrations decreasing after each round as described in Table 2.7.

2.7.7 Polyclonal ELISA to determine phagemid enrichment against target molecules

In order to assess whether enrichment was achieved after each selection round, the phagemid solutions prepared at the end of each round (section 2.7.6) were assessed using an ELISA format. This was done by coating ELISA plates overnight with 100 µl of the respective target molecules prepared in PBS, either 5 µg/ml for peptides, or 100 µg/ml for rPfLDH and rPfGAPDH. Three washes with PBS were performed between each of the ELISA plate incubation steps where mentioned and all incubations were performed at 37°C. The plates were blocked by incubating with 2% (w/v) milk powder in PBS for one hour, whilst the prepared phagemid solutions were diluted 1/20 in the same final concentration of milk powder PBS with 0.1% (v/v) Tween 20 for at least 30 minutes at RT. Once the plates were blocked and washed, the phagemid solutions were added (50 µl / well) and incubated for 1 hour. After washing, the plates were incubated for another hour with 50 µl / well of a 1/10000 dilution of an anti-M13 mouse monoclonal antibody prepared in 0.5% (w/v) BSA-PBS. A secondary goat anti-mouse antibody, coupled to HRPO, at a 1/1000 dilution in 0.5% (w/v) BSA-PBS was added (50 µl / well) and the plates were incubated for 1 hour. Finally 100 µl / well substrate (0.05% (w/v) ABTS; 0.0015% (v/v) H₂O₂) prepared in a 0.15 M citrate phosphate buffer at pH 5.0, was added per well and incubated in the dark for 1 hour before measuring product development at 405 nm.

2.7.8 Picking single scFv clones

If enrichment was achieved, then the next step was to isolate single colonies from the panned library and assess their specificity for the target molecules. This entailed diluting the TG1

glycerol stocks prepared at the end of each selection round and growing these on TYE (A/G) plates overnight. The stocks were diluted in 2xYT to get single colonies for selection.

Forty eight colonies were selected from each selection round per target molecule, giving a total of 196 single colonies per target molecule ranging from panning rounds one to four. These were used to inoculate individual wells of 96-well culture plates (master plates) containing 100 μ l / well 2xYT (A/G). The plates were grown overnight at 30°C with shaking at 220 rpm. A small inoculum (5 μ l) of each clone was transferred to a duplicate plate (clone plate) containing 150 μ l 2xYT (A/G) per well. Fifty microlitres of a 60% (v/v) sterile glycerol solution was then added to each well of the master plate which was then stored at -70°C.

The clone plates were then grown at 37°C for 2.5 hours with shaking at 220 rpm. Hereafter phagemids were rescued from the TG1 host *E. coli* with the addition of 50 μ l / well of a 2×10^9 pfu/ml M13KO7 stock prepared in 2xYT (A/G). The plates were incubated at 37°C for 30 minutes and then centrifuged (600 x g for 10 minutes). The supernatant was discarded and the pellets suspended in 150 μ l 2xYT containing ampicillin (100 μ g/ml) and kanamycin (25 μ g/ml) and grown at 30°C overnight, 220 rpm and then centrifuged (600 x g for 10 minutes). The culture supernatants containing the rescued phagemid particles were then used in an ELISA, which was performed as described for the polyclonal ELISA procedure (2.7.7). The only change was the use of a 1/10 dilution of the supernatant culture prepared here as the phagemid sample. The ELISA controls for the individual selected scFv clones included no coat / antigen, no phagemid / scFv, no anti-M13 or anti-cmyc antibody and no goat anti-mouse-HRPO or rabbit anti-chicken-HRPO antibody. A no blocking control was used as a positive control.

2.7.9 Preparation of scFv clone glycerol stocks

Six clones showing highest A_{405} values in the monoclonal ELISA assay were selected for each target molecule. Five microlitres of inoculum per sample was used to prepare 10 ml overnight cultures in 2xYT (A/G), grown at 37°C with 200 rpm shaking. Aliquots were prepared, containing 15% (v/v) glycerol and stored at -70°C.

2.7.10 Transduction of *E. coli* expression host, Top10

An *E. coli* strain with an F' positive genotype but lacking the *supE* mutation was selected as the host for soluble expression of scFv clones. The lack of the *supE* mutation results in termination of the translated scFv proteins at the amber stop codon present in the pHEN1

phagemid vector. This allows for soluble expression of the scFv's without attachment to the phage coat protein 3 as was the case in the TG1 host. The F' genotype was necessary to allow for infection or transduction of the *E. coli* strains with the rescued phagemids.

The selected clones were streaked onto TYE (A/G) plates (incubated overnight at 37°C) and single colonies were used to inoculate 5 ml 2xYT (A/G) media and grown overnight at 37°C shaking at 200 rpm. The cultures were pelleted by centrifugation (3300 x g for 10 minutes) and the supernatant was used to prepare phagemid stocks (section 2.7.5.2.1).

The expression host *E. coli* Top10 were prepared by inoculating 5 ml 2xYT media with single colonies grown on 2xYT agar plates (overnight at 37°C) and incubating these cultures overnight at 37°C while shaking at 200 rpm. Log phase (O.D. ~0.5) cultures were grown from 1/100 inoculations of 50 ml 2xYT media with the respective overnight cultures, grown at 37°C at 200 rpm shaking.

Half a millilitre of the respective phagemid preparations were incubated with 0.5 ml of the log phase Top10 *E. coli* for 30 minutes at 37°C and then plated onto 2xYT (A/G) media (incubated overnight at 37°C). Single colonies were then inoculated into 5 ml 2xYT (A/G) media and grown overnight at 37°C of which 1 ml aliquots were prepared in a final glycerol concentration of 15% (v/v) and stored at -70°C.

2.7.11 Soluble expression of scFvs from Top10 *E. coli*

Overnight cultures of the respective transduced scFv clones were used to inoculate 100 ml 2xYT (A/G) media and grown to O.D. ~0.5 at 37°C. Once at O.D. the cultures were split into 50 ml volumes and pelleted by centrifugation (4000 x g for 10 minutes). The pellets were suspended in either 50 ml TB or 2xYT (ampicillin with 1 mM IPTG) and incubated overnight at 37°C, shaking at 220 rpm.

2.7.12 Periplasmic isolation of soluble scFv antibodies

The overnight expression cultures were pelleted by centrifugation (4000 x g for 10 minutes at 4°C). All subsequent steps were done on ice and using ice cold buffers (chilled on ice for at least 30 minutes before use). The pellets were suspended in 12.5 ml sucrose buffer (50 mM Tris, 1 mM EDTA, 20% (w/v) sucrose at pH 7.4) in 50 ml sterile Falcon tubes and stirred gently using a small magnetic stirrer for 10 minutes. The cells were pelleted again (4000 x g for 10 minutes at 4°C) and the supernatant was removed. The pellets were suspended in 5 ml MgCl₂ buffer (5 mM MgCl₂ with 0.1% (w/v) NaN₃) and stirred gently again for 10 minutes

to lyse the *E. coli* periplasm by osmotic shock. A final centrifugation (4000 x g for 10 minutes at 4°C) pelleted the cytoplasmic fraction and the supernatant containing the *E. coli* periplasmic fraction was retained and the centrifugation repeated to remove any residual precipitants. The periplasmic supernatant was stored at 4°C until use. Samples were run on SDS-PAGE as outlined in section 2.2.3 to assess their purity.

2.7.13 Restriction digest

Restriction digests were performed on colony PCR products of each of the clones as mentioned in 2.2.5. To obtain a DNA fingerprint of each of the selected clones, each purified plasmid sample was digested with AluI, which is a high frequency endonuclease that recognises the sequence AG[^]CT. The PCR amplicons (10 µl) were digested overnight at 37°C with 5 units of AluI (1 µl), 2 µl 10 x digestion buffer and 18 µl MilliQ dH₂O. The samples were then resolved on 3% agarose gels for analysis (section 2.2.7).

2.7.14 Nested PCR

To confirm the presence of the (GGGGS)₃ linker region common to all scFv's in the present library, we designed a nested PCR primer targeting this region. All scFv clones were subjected to this and if positive they were sent for sequencing to the Central Analytical Facility, Stellenbosch University (section 2.2.8 and Primer Table 2.5).

Chapter 3

Search for possible new *Plasmodium* diagnostic target proteins and peptides for antibody production using a bioinformatics approach

3.1 Introduction

Relative expression and proteomics data derived from the malaria parasite's red blood cell cycle provide valuable data which could be used to identify potential new diagnostic target proteins (Foth *et al.*, 2011; LeRoch *et al.*, 2003; www.PlasmoDB.org). Ideally an immunodiagnostic target should be present throughout the *Plasmodium* red cell cycle as this is when disease symptoms appear and patients seek medical help (Antia *et al.*, 2008; Golgi, 1886; Miller *et al.*, 1994). The target proteins should also be present at relatively high concentrations, therefore using these data sets parasite proteins, of which there are 5554 (Foth *et al.*, 2011), can be ranked according to their relative abundance which dramatically narrows the search. The targets should also be unique, or have a unique structural component to the parasite homologue, which could be exploited for diagnosis. Using the bioinformatics approach outlined here, two possible diagnostic target proteins were identified and are briefly introduced. The first potential target was glyceraldehyde-3-phosphate dehydrogenase (GAPDH), which is involved in glycolysis and the second was phosphoethanolamine-N-methyltransferase (PMT), which is involved in phospholipid metabolism.

During a malaria infection a single merozoite divides into 14-36 new parasites within 24-72 hours in a human *Plasmodium* infection (Antia *et al.*, 2008; Baldacci and Menard, 2004; Collins and Jeffery, 2007). This process has a high energy demand resulting in up to 100-fold greater glycolytic rates in infected compared to uninfected red blood cells (Daubenberger *et al.*, 2000; Mehta *et al.*, 2006). Since two current RDT target proteins, aldolase and LDH are both involved in glycolysis, targeting proteins which functions within the same pathway and are suggested to be present at higher concentrations than LDH and aldolase (Foth *et al.*, 2011; LeRoch *et al.*, 2003) would be attractive. Another important metabolic pathway is phospholipid metabolism. The parasite needs to produce sufficient phospholipid membranes to envelope each newly developing daughter merozoite. The phospholipid content of *P. falciparum* therefore increases between five to six fold after infecting a red blood cell for example (Dechamps *et al.*, 2010). Current RDTs targeting a metabolic enzyme also have the

advantage, of monitoring treatment outcome. This was shown with RDTs using LDH as the target antigen, which was no longer detected in patient blood two to seven days after the clearance of an infection (Iqbal *et al.*, 2004, Murray *et al.*, 2008).

Anaerobic glycolysis yields two ATP molecules from the breakdown of glucose to pyruvate and L-lactate. In the absence of oxygen, the pathway has ten reactions of which the fifth and last reactions are coupled by a dinucleotide cofactor $\text{NAD}^+(\text{H})$ and involve two dehydrogenases: GAPDH and LDH respectively (Voet and Voet, 2004).

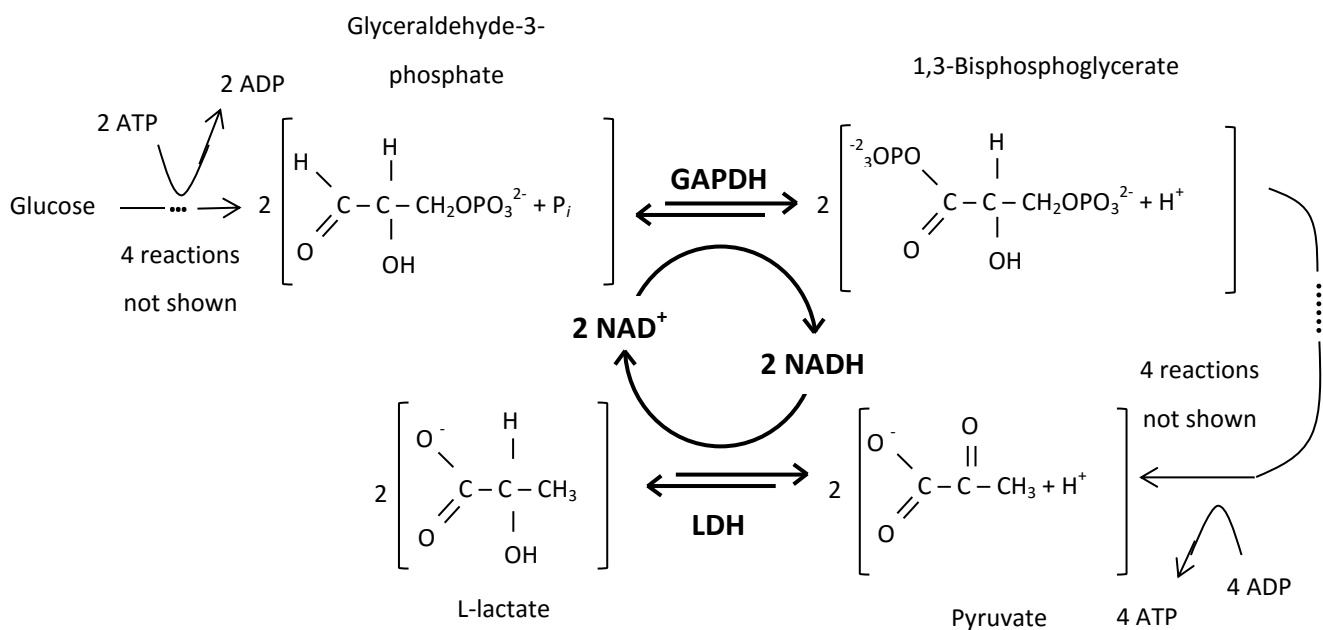


Figure 3.1 $\text{NAD}^+(\text{H})$ linked glycolytic reactions involving GAPDH and LDH
The respective reduction and oxidation of $\text{NAD}^+(\text{H})$ by GAPDH and LDH highlighted in bold (Voet and Voet, 2004).

From a glycolysis perspective, an excess of either GAPDH or LDH would be redundant due to limiting $\text{NAD}^+(\text{H})$ levels. *In vitro*, however, *P. falciparum* GAPDH mRNA levels exceed LDH levels by three to four fold (LeRoch *et al.* 2003) and semi-quantitative proteome data also suggest greater GAPDH to LDH levels (Foth *et al.*, 2011; Lasonder *et al.*, 2002; Nirmalan *et al.*, 2004; Smit *et al.*, 2010). This suggests a greater demand for GAPDH in relation to LDH and that *Plasmodium* GAPDH may have additional functions to glycolysis. These non-glycolytic functions, often termed “moonlighting” functions have been identified in seven of the ten glycolytic enzymes (Alam *et al.*, 2014; Gómez-Arreaza *et al.*, 2014). These moonlighting functions of GAPDH as well as the possible post-translational modifications

involved will be discussed later as possible explanations for comparatively higher levels of GAPDH to LDH.

The second new target, PMT, is involved in phospholipid synthesis. Interestingly, no homologs of higher or lower eukaryote phosphatidylethanolamine methyltransferases were identified in the *P. falciparum* genome. Instead, Pessi *et al.* (2004 and 2005) identified a plant-like phosphoethanolamine methyltransferase gene homolog (*PfPMT*) in *P. falciparum* and hypothesised that the protein was involved in an alternate serine decarboxylase-phosphoethanolamine methyltransferase pathway. Several plant-like *P. falciparum* proteins are targeted to the apicoplast (Foth *et al.*, 2003), however *PfPMT* lacks any signal or transit peptides (Pessi *et al.*, 2004) and localises as a soluble protein within the Golgi (Witola *et al.*, 2006). In culture *PfPMT* expression increased by three-fold as the parasite progressed from its initial ring to trophozoite stages (Pessi *et al.*, 2004; LeRoch *et al.*, 2003) and was expressed during the gametocyte and sporozoite stages of the life cycle (www.PlasmoDB.org). Analysis of the *P. falciparum* proteome also confirmed the presence of *PfPMT* throughout the red blood cell cycle ranking it within the top 20 most abundant soluble proteins (Foth *et al.*, 2011; Nirmalan *et al.*, 2004). PMT homologs were identified in *Burkholderia pseudomallei*, *B. oklahomensis*, *Xenopus laevis*, *X. tropicalis*, *Caenorhabditis briggsae*, *Danio rerio*, *Branchiostoma floridae*, *Caenorhabditis elegans* and *Anopheles gambiae*, but critically no human homologs exist (Pessi *et al.*, 2004; Bobenchik *et al.*, 2011, 2013). In theory antibodies raised against such a target are unlikely to cross-react with human proteins, therefore reducing misdiagnosis.

Differences in the PMT and GAPDH primary amino acid sequences could potentially be exploited to develop immune-reagents for species identification, as demonstrated by Hurdayal *et al.* (2010), targeting unique LDH peptide epitopes. This strategy was adopted in this work and the aim was to identify and exploit unique and conserved amino acid sequences on both GAPDH and PMT. The LDH sequences identified by Hurdayal *et al.* (2010) were also included in this study. This is therefore outlined in chapter 3 in which the bioinformatics approach taken to identify the two novel protein targets and their respective surface epitopes is described.

3.2 Results

3.2.1 Compilation of a list of proteins from which the diagnostic targets were selected

Based on the *Plasmodium* transcriptional data compiled by LeRoch *et al.*, in 2003, a list of the 20 highest expressed genes was generated as shown in Table 3.1. These data present the average expression values of the listed genes throughout the whole red blood cell cycle of the *P. falciparum* parasite.

Table 3.1 Twenty highest expressed genes based on mRNA abundance (LeRoch *et al.*, 2003)

#	Gene ID	Average expression*	Protein name / function
1	PF11_0040	12186.5	Early transcribed membrane protein 11.2
2	PFB0120w	11956.4	Early transcribed membrane protein, putative
3	PF14_0598	7940.3	Glyceraldehyde-3-phosphate dehydrogenase
4	PF08_0054	6703.5	Heat shock 70 kDa protein
5	PF11_0224	6221.5	Circumsporozoite-related antigen
6	PF11_0508	5995.7	Hypothetical protein
7	PF10_0019	5451.5	Early transcribed membrane protein
8	PF10_0159	5364.3	Glycophorin-binding protein 130 precursor
9	PF10_0372	5347.6	Hypothetical protein
10	PF14_0486	5253.6	Elongation factor 2
11	PF11_0043	4279.6	60S acidic ribosomal protein p1, putative
12	PFA0420w	4273.9	Hypothetical protein
13	PFL2515c	3797	Hypothetical protein
14	MAL6P1.91	3783.1	Ornithine aminotransferase
15	PF13_0346	3771.4	Ubiquitin/ribosomal fusion protein uba52 homologue, putative
16	PFI1090w	3741.4	S-adenosylmethionine synthetase, putative
17	PFE0070w	3723.9	Interspersed repeat antigen, putative
18	PF11_0039	3708.1	Early transcribed membrane protein 11.1
19	PF14_0678	3666.8	Exported protein 2
20	PF14_0425	3564.5	Fructose-bisphosphate aldolase

*Average transcription values for the ring to trophozoite stages of the red blood cell life cycle.

The second data set was from a proteomics study of the *P. falciparum* red blood cell cycle (Foth *et al.*, 2011). In this study proteins were ranked according to their relative abundance, with ten being the highest and one being the lowest ranking. Table 3.2 was compiled by selecting the top 20 proteins from the data, where their respective transcriptional rankings from the LeRoch *et al.*, (2003) study were also included.

Table 3.2 Twenty most abundant proteins according to proteome data from Foth *et al.*, (2011)

#	PlasmoDB / NCBI ID	Protein name	Transcription ranking *	Ring ▲	Trophozoite ▲	Schizont ▲
1	PF14_0598	Glyceraldehyde-3-phosphate dehydrogenase (GAPDH)	3	10	10	10
2	PF08_0054	Heat shock protein 70-1	4	10	10	10
3	PFI1090w	S-adenosylmethionine synthetase	16	10	10	10
4	PFI0875w	Heat shock protein 70-2 (BiP)	24	10	10	10
5	PF08_0019	Receptor for activated C kinase (PfRACK) = Guanine nucleotide-BP	28	10	10	10
6	PF10_0155	Enolase	65	10	10	10
7	PF07_0029	Heat shock protein 86	121	10	10	10
8	PFI1105w	Phosphoglycerate kinase	205	10	10	10
9	MAL13P1.214	Phosphoethanolamine N-methyltransferase, putative	812	10	10	10
10	PFL1070c	HSP90 (Endoplasmic homolog precursor, putative)	1078	10	10	10
11	PFI1475w	Merozoite surface protein 1 (MSP1)	454	10	9	10
12	PFL2215w	Actin I	138	10	9	9
13	PFF1300w	Pyruvate kinase, putative	788	9	9	10
14	PF14_0655	RNA helicase 45 (H45, eIF4A)	1041	9	10	9
15	MAL13P1.56	M1-family aminopeptidase	2916	9	10	9
16	PFF0435w	Ornithine aminotransferase	14	9	9	9
17	PF14_0425	Fructose-bisphosphate aldolase	20	9	9	9
18	PF13_0141	L-lactate dehydrogenase (LDH)	35	9	9	9
19	MAL8P1.17	Protein disulfide isomerase (PDI-8)	47	9	9	9
20	PF11_0208	Phosphoglycerate mutase	64	9	8	8

* Note the transcription ranking according to the LeRoch *et al.* (2003) data was included here and not the average expression values shown in Table 3.1.

▲ These columns include the Foth *et al.* (2011) data

Finally Tables 3.1 and 3.2 were combined, resulting in the 35 most abundant proteins throughout the parasite intra-erythrocytic cycle as shown in Table 3.3.

The list of 35 proteins was narrowed down to seven proteins of interest for use as diagnostic targets and those of interest were highlighted in green, where excluded proteins were highlighted in red. The criteria used are explained briefly to follow.

Table 3.3 Compilation of the 35 most abundant proteins, highlighting potential diagnostic targets in green and proteins that were excluded in red

#	Gene ID	Protein name	Known function	Conserved amongst human malaria species	Human orthologue	Pan- <i>Plasmodium</i> peptides	Species-specific peptides	Crystal structure available
1	PF11_0040	Early transcribed membrane protein 11.2	yes	only <i>P.f.</i>	no	no	no	
2	PFB0120w	Early transcribed membrane protein 2, putative	yes	only <i>P.f.</i>	no	no	no	
3	PF14_0598	Glyceraldehyde-3-phosphate dehydrogenase (GAPDH)	yes	all 5	yes	yes	yes	yes
4	PF08_0054	Heat shock 70 kDa protein	yes	<i>P.f., P.v., P.k.</i>	yes	yes	no	
5	PF11_0224	Circumsporozoite-related antigen	yes	only <i>P.f.</i>	no	no	no	
6	PF11_0508	Hypothetical protein	no					
7	PF10_0019	Early transcribed membrane protein	yes	only <i>P.f.</i>	no	no	no	
8	PF10_0159	Glycophorin-binding protein 130 precursor	yes	only <i>P.f.</i>	no	no	no	
9	PF10_0372	Hypothetical protein	no					
10	PF14_0486	Elongation factor 2	yes	<i>P.f., P.v., P.k.</i>	yes	yes	no	
11	PF11_0043	60S acidic ribosomal protein p1, putative	yes	<i>P.f., P.v., P.k.</i>	no	yes	no	
12	PFA0420w	Hypothetical protein	no					
13	PFL2515c	Hypothetical protein	no					
14	MAL6P1.91	Ornithine aminotransferase	yes	<i>P.f., P.v., P.k.</i>	yes	yes	no	
15	PF13_0346	Ubiquitin-60S ribosomal protein L40	yes	<i>P.f., P.v.</i>	yes	no	no	
16	PFI1090w	S-adenosylmethionine synthetase, putative	yes	<i>P.f., P.v., P.k.</i>	yes	yes	no	
17	PFE0070w	Interspersed repeat antigen, putative	yes	only <i>P.f.</i>	no	no	no	
18	PF11_0039	Early transcribed membrane protein 11.1	yes	only <i>P.f.</i>	no	no	no	
19	PF14_0678	Exported protein 2	yes	only <i>P.f.</i>	no	no	no	
20	PF14_0425	Fructose-bisphosphate aldolase	yes	<i>P.f., P.k.</i>	yes	no	yes	
21	PFI0875w	Heat shock protein 70-2 (BiP)	yes	only <i>P.f.</i>	yes	no	no	
22	PF08_0019	Receptor for activated C kinase (PfRACK) = Guanine nucleotide-BP	yes	<i>P.f., P.v., P.k.</i>	yes	yes	no	
23	PF10_0155	Enolase	yes	<i>P.f., P.v., P.k.</i>	yes	yes	no	
24	PF07_0029	Heat shock protein 86	yes	<i>P.f., P.v., P.k.</i>	yes	yes	yes	Only the N-terminus
25	PFI1105w	Phosphoglycerate kinase	yes	<i>P.f., P.v., P.k.</i>	yes	yes	no	
26	MAL13P1.214	Phosphoethanolamine N-methyltransferase, putative (PMT)	yes	<i>P.f., P.v., P.k.</i>	no	yes	yes	yes
27	PFL1070c	Heat shock protein 90 (Endoplasmic homolog precursor, putative)	yes	<i>P.f., P.v., P.k.</i>	yes	yes	yes	Only the N-terminus
28	PFI1475w	Merozoite surface protein 1 (MSP1)	yes*	all 5	no	yes	yes	
29	PFL2215w	Actin I	yes*	<i>P.f., P.v., P.k.</i>	no	yes	yes	
30	PFF1300w	Pyruvate kinase, putative	yes	<i>P.f., P.v., P.k.</i>	yes	yes	yes	yes
31	PF14_0655	RNA helicase 45 (H45, eIF4A)	yes	<i>P.f., P.v., P.k.</i>	yes	yes	yes	no
32	MAL13P1.56	M1-family aminopeptidase	yes	<i>P.f., P.v., P.k.</i>	no	yes	yes	yes
33	PF13_0141	L-lactate dehydrogenase (LDH)	yes	all 5	yes	yes	yes	yes
34	MAL8P1.17	Protein disulfide isomerase (PDI-8)	yes	<i>P.f., P.v., P.k.</i>	yes	yes	yes	yes
35	PF11_0208	Phosphoglycerate mutase	yes	<i>P.f., P.v., P.k.</i>	yes	yes	yes	yes

* denotes proteins that are either membrane bound or associated with the insoluble cytoskeleton.

Pan-*Plasmodium* and species-specific peptides were chosen based on ClustalΩ alignments and BLASTp searches.

Available *P. falciparum* crystal structures were searched for on the RCSB PDB database.

All proteins with unknown functions were excluded since only proteins involved in metabolic processes were of interest. Any membrane-bound or cytoskeletal proteins were also excluded from further analysis as indicated in Table 3.3 with an asterisk. This was decided based on the inherent difficulties of expression of membrane bound proteins and the additional requirements to solubilise these if used in an RDT or ELISA test format. Only proteins of known function, which were conserved in *P. falciparum*, *P. vivax* and *P. knowlesi* species, were further pursued, as this would potentially allow tests to specifically detect all three infections. Ideally a protein unique to the parasite and not present in the human genome would be targeted, but this was not used as an exclusion criterion. The primary amino acid sequences of the proteins with human orthologs were evaluated and those with close to 100% identity were excluded since antibodies against the *P. falciparum* proteins would detect the human proteins and not be of use for diagnosis. Finally proteins without crystal structures were excluded since a criterion for the selection of peptide epitopes was to verify their presence on the surface of the proteins, where they are more likely to be detected by antibodies.

GAPDH was chosen as the first diagnostic target since it was the highest expressed of the seven remaining proteins in Table 3.3. PMT was chosen as the second target as it was the highest expressed protein of those without human orthologs. LDH was included as the model control protein in this study as a current diagnostic protein. The available amino acid sequences of each protein were aligned and potential species-specific and common malaria peptide epitopes were identified as described in section 3.2.2.

3.2.2 Peptide epitope selection

The choice of peptide epitopes was outlined in Figures 3.2 to 3.8. All peptides were a minimum of 12 to 16 amino acids long with a cysteine (C) added to either the N- or C-terminals to facilitate coupling reactions. Coupling via amino groups was avoided due to the presence of lysine residues in most of the selected peptides. To select specific *Plasmodium* peptide epitopes, multiple protein sequence alignments of the *Plasmodium* orthologs were used. Epitopes were selected from regions of low similarity to the mammalian (human and mouse) and chicken proteins in the cases of LDH and GAPDH. In order to raise antibodies in chickens or in mice (monoclonal antibodies), sequence identity between mouse, chicken and *Plasmodium* proteins was assessed. This was not necessary for PMT as the protein is not found in mammals or avian species which we confirmed.

```

PfLDH -----MAPKAKIVLVGSGM 14
PvLDH -----MTPKPKIVLVGSGM 14
PkLDH -----MAPKPKIVLVGSGM 14
PyLDH -----MAPKAKIVLVGSGM 14
P. spp ID          *: * * * * *
HuLDHh -----MATLKEKLIAPVAEEEA TPNNKITVVGVGQ 31
GallusLDH -----MSLKDHLIHNVKHEEHAHANIKISVVGVA 30
HuLDHm -----MATLKDQLIYNLLKEEQ-TPQNKITVVGVA 30
MouseLDH MSKSSGGYTYTETSVLFFHFKVSKDSKSMATLKDQLIVNLLKEEQ-APQNKITVVGVA 59
Overall ID          . * * : * * *

PfLDH IGGVMATLIVQKNLGD-VVLFDIVKNMPHGKALDTSHTNVMAYSNCKVSGSNTYDDLGA 73
PvLDH IGGVMATLIVQKNLGD-VVMPFDVKNMPQGKALDTSHTSNVMAYSNCKVSGSNTYDDLKGA 73
PkLDH IGGVMATLIVQKNLGD-VVMPFDVKNMPQGKALDTSHTSNVMAYSNCKVSGSNTYDDLKGA 73
PyLDH IGGVMATLIVQKNLGD-VVLFDIVKNMPHGKALDTSHTNVMAYSNCKVSGSNTYDDLKDA 73
P. spp ID          * * * * * : * * * * * : * * * * * : * * * * * : * * * * *
HuLDHh VGMACAISILGKSLADELALVDVLEDKLKGEMMDLQHGSLFLQ-TPKIVADKDYSVTANS 90
GallusLDH VGMACAISILMKDLADELALVDVVEDKDKGEMMDLQHGSLFLK-TPKIIISGKDYSVTAHS 89
HuLDHm VGMACAISILMKDLADELALVDVIEDKDKGEMMDLQHGSLFLR-TPKIVSGKDYNVVTANS 89
MouseLDH VGMACAISILMKDLADELALVDVMEKDKLKGEMMDLQHGSLFLK-TPKIVSSKDYCVTANS 118
Overall ID      : * . * * : * . * * : . : * * : : * : . * : . : * :

PfLDH DVVIVTAGFTKAPGKSDKEWNRDDLPLNNKIMIEIGGHIKKNCNPAFIIVVTNPVDVMV 133
PvLDH DVVIVTAGFTKAPGKSDKEWNRDDLPLNNKIMIEIGGHIKNLCNPAFIIVVTNPVDVMV 133
PkLDH DVVIVTAGFTKAPGKSDKEWNRDDLPLNNKIMIEIGGHIKKLCNPAFIIVVTNPVDVMV 133
PyLDH DVVIVTAGFTKAPGKSDKEWNRDDLPLNNKIMIEIGGHIKNNCNPAFIIVVTNPVDVMV 133
P. spp ID          * * * * * : * * * * * : * * * * * : * * * * * : * * * * *
HuLDHh KIVVVTAGVRQEGESRLN-----LVQRNVNVFKFIIPQIVKYSPODCIIIVSNPVDILT 145
GallusLDH KLVIVTAGARQEGESRLN-----LVQRNVNIFKFIIPNVVKYSPOCKLLIVSNPVDILT 144
HuLDHm KLVIIITAGARQEGESRLN-----LVQRNVNIFKFIIPNVVKYSPOCKLLIVSNPVDILT 144
MouseLDH KLVIIITAGARQEGESRLN-----LVQRNVNIFKFIIPNVVKYSPOCKLLIVSNPVDILT 173
Overall ID      . : * * : * * : * : * : * : * : * : * : * : * : * : * : * : * :

PfLDH QLLHQHSGVVPKMKIIGLGGVLDTSRLKYYISQKLNVCPRDVNAHIVGAHGNKMMVLLKRYI 193
PvLDH QLLFEHSGVVPKMKIIGLGGVLDTSRLKYYISQKLNVCPRDVNALIVGAHGNKMMVLLKRYI 193
PkLDH QLLFEHSGVVPKMKIIGLGGVLDTSRLKYYISQKLNVCPRDVNALIVGAHGNKMMVLLKRYI 193
PyLDH QLLHQHSGVVPKMKIIGLGGVLDTSRLKYYISQKLNVCPRDVNAHIVGAHGNKMMVLLKRYI 193
P. spp ID          * * * : * * * * * : * * * * * : * * * * * : * * * * *
HuLDHh YVTWKLISGLPKHRVIGSGCNLDSARFRYLMGKLGHPSSCHGWILGEHGDSSVAVWVSGV 205
GallusLDH YVAWKISGFPKHRVIGSGCNLDSARFRHLMGERLGIHPLSCHGWIVGEHGDSSVPVWVSGV 204
HuLDHm YVAWKISGFPKHRVIGSGCNLDSARFRYLMGERLGVHPLSCHGWVGEHGDSSVPVWVSGM 204
MouseLDH YVAWKISGFPKHRVIGSGCNLDSARFRYLMGERLGVHALSCHGWVGEHGDSSVPVWVSGV 233
Overall ID      : : * * . * . : * * * * : * : : * : : . . : * * : . * : :

```

```

PfLDH TVGGIPLQEFINNKLI--SDAELEAIFDRVTNTALEIVNLHASPYVAPAAAI IEMAESYL 251
PvLDH TVGGIPLQEFINNKLI--TDEEVEGIFDRVTNTALEIVNLLASPYVAPAAAI IEMAESYL 251
PkLDH TVGGIPLQEFINNKLI--TDEEVEAIFDRVTNTALEIVNLLASPYVAPAAAI IEMAESYL 251
PyLDH TVGGIPLQEFINNKLI--TDQELDAIFDRVTNTALEIVNLHASPYVAPAAAI IEMAESYL 251
P. spp ID          * * * * * : * * * * * : * * * * * : * * * * * : * * * * *
HuLDHh NVAGVSLQELNPEMGTNDNSENWKEVHKMVVESAYEVIKLKYTNWAIIGLSVADLIESML 265
GallusLDH NVAGVSLKALHPDMGTADKEHWEVHKQVVD SAYEVIKLKYTSWAIGLSVADLAETIM 264
HuLDHm NVAGVSLKTLHPDLGTDKKEQWKEVHKQVVD SAYEVIKLKYTSWAIGLSVADLAESIM 264
MouseLDH NVAGVSLKSLNPELGTADKEQWKEVHKQVVD SAYEVIKLKYTSWAIGLSVADLAESIM 293
Overall ID      . * . * : * : : . . . . . * : * * : * * . * . : : * : :

PfLDH KDLKKVLCISTLLEGQYGH-SDFGGT PVLGANGVEQVIELQLNSEKAKFDEAIAETK 310
PvLDH KDIKKVLCISTLLEGQYGH-SDFGGT PVLVIGGTGVEQVIELQLNAEETKDFDEAVAETK 310
PkLDH KDIKKVLCISTLLEGQYGH-SDFGGT PVLVIGGTGVEQVIELQLTAEKAKFDEAVAETK 310
PyLDH RDLRKLVCISTLLEGQYGH-SDFAGT PVLVIGGNGVEQVIELQLNADEKAKFDEAVAETS 310
P. spp ID          : * : * * : * * * * * : * * * * * : * * * * * : * * * * * : * * * * *
HuLDHh KNLSRIHPVSTMVKGMYGIENEVFLSLPCILNARGLTSVINQKLKDEVAQLKKSADTLW 325
GallusLDH KNLRRVHPISTAVKGMHGKDDVFLSVPCVLGSSGITDVKMILKPDDEEKIKKSADTLW 324
HuLDHm KNLRRVHPVSTMIGKLYGKDDVFLSVPCILGQNGISDLVKVTLTSEEEARLKKSADTLW 324
MouseLDH KNLRRVHPISTMIKGLYGINEDVFLSVPCILGQNGISDVVKVTLTPEEEARLKKSADTLW 353
Overall ID      : : : : * * : * : * . : * . * : : * : : : * . : * : : : :

PfLDH RMKALA--- 316
PvLDH RMKALI--- 316
PkLDH RMKALI--- 316
PyLDH RMKALI--- 316
P. spp ID          * * * * *
HuLDHh DIQKDLKDL 334
GallusLDH GIQKELQF- 332
HuLDHm GIQKELQF- 332
MouseLDH GIQKELQF- 361
Overall ID      : :

```

Figure 3.2 Alignment of *Plasmodium* and mammalian LDH sequences indicating the peptides chosen for polyclonal chicken antibody and monoclonal scFv production, adapted from Hurdal et al. (2010)

A multiple sequence alignment of the *P. falciparum* (PfLDH); *P. vivax* (PvLDH); *P. knowlesi* (PkLDH), *P. yoelii* (PyLDH), human heart (HuLDHh), human muscle (HuLDHm), chicken (GallusLDH) and mouse (MouseLDH) LDH amino acid sequences was done in ClustalΩ. The first criterion for peptide selection was % identity (ID) and residues were annotated as follows: “*” identical residues; “:” conserved residues; “.” semi-conserved residues and blank spaces represented no identity between the sequences. Percentage identity was assessed between the 4 *Plasmodium* sequences (P. spp ID) and between all 8 LDH sequences (Overall ID). Specific peptides were selected based on lowest percentage identity and common peptides on 100 % identity between the *Plasmodium* sequences. The three peptide sequences of interest were underlined in green and blue for the specific peptides and red for the common peptide. Sequence accession numbers from PlasmoDB are PfLDH: PF3D7_1324900; PvLDH: PVX_116630; PkLDH: PKH_122820 and PyLDH: PY03885. NCBI ID's for HuLDHh: P07195.2 and HuLDHm: P00338.2; GallusLDH: P00340.3 and MouseLDH: NP_001129541.2 (accessed 14.9.15).

For common epitopes (underlined in red in the figures) 100% identity between the malaria sequences was ideal, where low sequence identity was required for the species specific epitopes (underlined in green / blue in the figures). Further analysis of all the peptide targets was done by using an epitope prediction program Predict7TM (Carmenes *et al.*, 1989), followed by location of the targets on the protein crystal structures of the *P. falciparum* proteins and finally by BLASTp analysis. The results were therefore presented and discussed in this order for all three proteins, starting with LDH.

The common LDH peptide “APGKSDKEWNRDDL” (red; residues 85 to 98) in the *P. falciparum* sequence (Figure 3.2) was chosen within a region that contained five amino acids “WNRDD” absent from the mammalian and chicken proteins scoring only 20% identity compared to 100% identity between the *Plasmodium* orthologs. In contrast the *P. falciparum* specific “LISDAELEAIFD” (green; residues 208 to 219) and the *P. vivax* specific “KITDEEVEGIFD” peptides (blue; residues 208 to 219, Figure 3.2) lacked a two amino acid insert present within the mammalian and chicken proteins of which one was a conserved “D”.

After Predict7TM analysis (Figure 3.3 (A)), a cysteine required for coupling was added to the C-terminus of the common peptide (designated C). This exposed the more immunogenic N-terminus, with residues “KSDK” scoring close to and above one for hydrophilicity and surface probability. Similarly for the *P. falciparum* and the *P. vivax* specific peptides the cysteine was also added to the C-terminus. The residues “AE” for the *P. falciparum* peptide (Figure 3.2 (B)) scored close to one for hydrophilicity and close to 0.5 for surface probability. The *P. vivax* peptide scored similarly for residues “KITDEEV” (Figure 3.2 (C)). All three peptides had similar flexibility at either terminus therefore hydrophilicity and surface probability was more important for the coupling orientation.

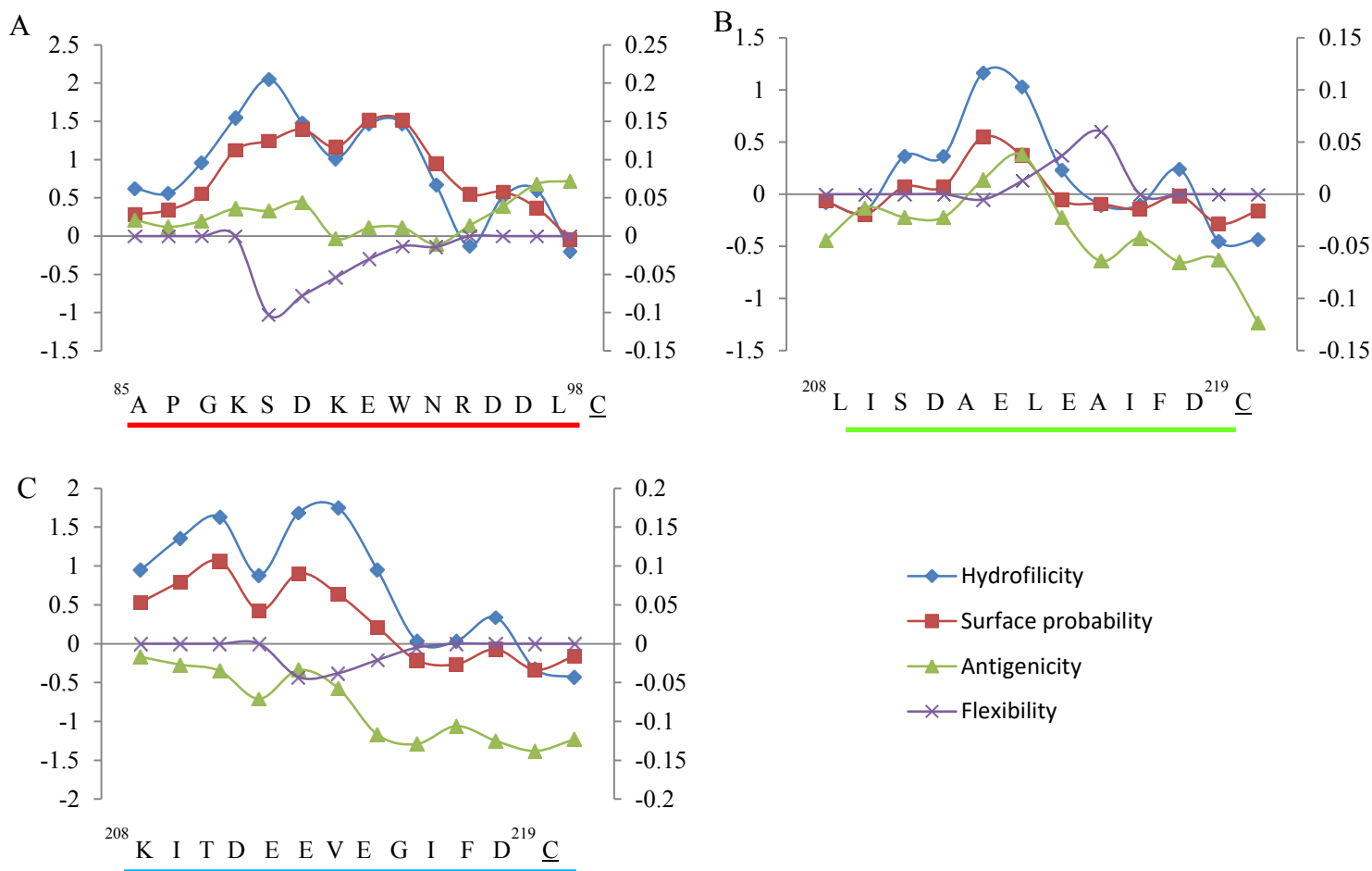


Figure 3.3 Predict7TM analyses of three selected *Plasmodium* LDH peptides (data adapted from Hurdayal *et al.* (2010))

Predict7TM plots of the three LDH peptides illustrating hydrophilicity, surface probability, flexibility and antigenicity (key in the bottom right). The common peptide was plotted in (A), the *P. falciparum* specific peptide in (B) and the *P. vivax* specific peptide in (C). Flexibility and antigenicity were plotted on the secondary axes in each graph. The amino acid sequences were shown along the bottom of the graphs, with the numbering of the first and last amino acid residues shown in superscript corresponding to the residue number in the *P. falciparum* primary sequence. The addition of a C-terminal cysteine was indicated with a “C” in each case.

The GAPDH sequences were aligned as shown in Figure 3.4. The common peptide “KDDTPIYVMGINH” (red; residues 126 to 138), where the “K” residue was a single amino acid insert which was absent from the chicken and mammalian sequences. This peptide sequence was 100% conserved amongst the *Plasmodium* sequences and shared only 54% identity with the mammalian and chicken sequences. The two *P. falciparum* specific peptides “ADGFLDIGEKKVSVFA” (green; residues 63 to 78) and “AEKDPSQIPWGKCQV” (blue; residues 78 to 92) scored 6 and 30% identity with their mammalian and chicken orthologs. The *Plasmodium* sequence aligning with the “KG” insert was avoided and will be discussed later.

PfGAPDH	MAVTKLGINGFGRIGRLVFRAAFGRKDIEVVAINDPFMDLNHLCYLLKYDSVHGQFPCEV	60
PvGAPDH	MAVTKLGINGFGRIGRLVFRAAAYERSDIEVVAVNDPFMDIKHLCYLLKYDSIHGVFPAEV	60
PkGAPDH	MAATKLGINGFGRIGRLVFRSAYERNDEVVAVNDPFMDIKHLCYLLKYDSVHGVFPAEV	60
PyGAPDH	MAITKVGINGFGRIGRLVFRSAQERSDIEVVAINDPFMDINHLIYLLKHDSVHGKFPCEV	60
P. spp ID	** *:*****:*****:** *:****:*****:*** ***:** * ** *	
GallusGAPDH	--MVKVGVNGFGRIGRLVTRAAVLSGKVQVVAINDPFIDLNYMVYMFKYDSTHGHFQGTV	58
HuGAPDH	MGKVKVGVNGFGRIGRLVTRAAFNSGKVDVAINDPFIDLNYMVYMFQYDSTHGKHFQGTV	60
MouseGAPDH	--MVKVGVNGFGRIGRLVTRAAICSGKVEIVAINDPFIDLNYMVYMFQYDSTHGKFNQGTV	58
Overall ID	.*:***** ** * .:****:*****:***: .:****:*** ** *	
PfGAPDH	<u>THADGFL</u> <u>LIGEKKVSVFAEKDPSQIPWGK</u> <u>QVDV</u> VCES	120
PvGAPDH	TPGDGCF ^T TVGNKKIFVHSEKDPAQIPWGKYEDV	120
PkGAPDH	TPGDGFF ^T IGNKKIFVHHEKDPANI ^T PWGKYGIDV	120
PyGAPDH	TPTEGGIMVGSKKVVYNERDPAQIPWGKHAIDV	120
P. spp ID	* :* :*.**:*. **:****:***** :*****:****:***:*****	
GallusGAPDH	KAENGLVINGHAITIFQERDPSNIKWADAGAEEYV	118
HuGAPDH	KAENGLVINGNPITIFQERDPSKIKWGDAGAEEYV	120
MouseGAPDH	KAENGLVINGKPIITIFQERDPTNIKWGEAGAEEY	118
Overall ID	. :* : : . :. *:****:*** *.. : * ***** * * : :****:***:***	
PfGAPDH	MSAPPKDDTPIYVMGINHHDQYDTKQLIVSNASCT	180
PvGAPDH	MSAPPKDDTPIYVMGINHDKYDPKQLIVSNASCT	180
PkGAPDH	MSAPPKDDTPIYVMGINHDKYDPKQITVSNASCT	180
PyGAPDH	MSAPPKDDTPIYVMGINHEKYNSSQITVSNASCT	180
P. spp ID	*****:*****:****:***:*****:****:***:*****	
GallusGAPDH	ISAPS-ADAPMFVMGVNHEKYDKSLKIVSNASCT	177
HuGAPDH	ISAPS-ADAPMFVMGVNHEKYD ^N SLKIISNASCT	179
MouseGAPDH	ISAPS-ADAPMFVMGVNHEKYD ^N SLKIVSNASCT	177
Overall ID	:*** *:****:***:****:***: . *:*****:****:***:****:****:*****	
PfGAPDH	ASTANQLVVDGSPKGGKDWGRAGCALSNIIIPAST	240
PvGAPDH	ASTANQLVVDGSPKGGKDWGRAGCALSNIIIPAST	240
PkGAPDH	ASTANQLVVDGSPKGGKDWGRAGCAL ^T NIIPAST	240
PyGAPDH	ASTANQLVVDGSPKGGKDWGRAGSALLNIIIPAST	240
P. spp ID	*****:*****:****:***:*****:****:***:*****	
GallusGAPDH	AITATQKTVDGPS--GKLWRDGRGAAQNIIPAST	235
HuGAPDH	AITATQKTVDGPS--GKLWRDGRGALQNIIPAST	237
MouseGAPDH	AITATQKTVDGPS--GKLWRDGRGAAQNIIPAST	235
Overall ID	* **.* ***** ** * ** * * *****:*****:****:***	
PfGAPDH	GTVSVDLVCRLEKPAKYEIVALEIKKAAEGPLKGI	300
PvGAPDH	GTVSVDLVCRLEKPAKYEIEIAAQMKAAEGPLKGI	300
PkGAPDH	GTVSVDLVCRLEKPAKYEIEIAAHMKAAEGPLKGI	300
PyGAPDH	GTVSVDLVCRLEKPAKYEIVAKKIKEASEGPLKGI	300
P. spp ID	*****:*****:****:***:*****:****:***:*****	
GallusGAPDH	PNVSVDLTCRLEKPAKYDDIKRVVKAADGPLKGI	295
HuGAPDH	ANVSVDLTCRLEKPAKYDDIKVVVKQASEGPLKGI	297
MouseGAPDH	PNVSVDLTCRLEKPAKYDDIKVVVKQASEGPLKGI	295
Overall ID	.*****:****:***:****:***: . * :****:*****:****:*** ** :****	
PfGAPDH	KAGLALNDNFFKLVSWYDNEWGYSNRVLDLAVHITNN-	337
PvGAPDH	KAGLALNDNFFKIVSWYDNEWGYSNRVLDLAVHITKH-	337
PkGAPDH	KAGLALNDNFFKIVSWYDNEWGYSNRVLDLAIHITKH-	337
PyGAPDH	KAGLALNDNFFKIVSWYDNEWGYSNRLLDLAIHITKH-	337
P. spp ID	*****:*****:****:***:*****:****:***:*****	
GallusGAPDH	GAGIALNDHFV ^K LVSWYDNEFGYSNRVVDLMAHMASKE	333
HuGAPDH	GAGIALNDHFV ^K LISWYDNEFGYSNRVVDLMAHMASKE	335
MouseGAPDH	GAGIALNDN ^F V ^K LISWYDNEYGYSNRVVDLMAHMASKE	333
Overall ID	**:* **.* *:****:*****:****:*** :****	

Figure 3.4 Alignment of *Plasmodium* and mammalian GAPDH sequences showing selected peptide epitopes chosen for polyclonal chicken antibody and monoclonal scFv production

A multiple sequence alignment of the *P. falciparum* (PfGAPDH); *P. vivax* (PvGAPDH); *P. knowlesi* (PkGAPDH); *P. yoelii* (PyGAPDH); human (HuGAPDH); chicken (*GallusGAPDH*) and mouse (*MouseGAPDH*) GAPDH amino acid sequences was done using ClustalΩ. Percentage identity (ID) was the first criterion for selection and residues were annotated as follows: “*” identical residues; “.” conserved residues; “.” semi-conserved residues and blank spaces represented no identity between the sequences. Percentage identity was assessed between the 4 *Plasmodium* sequences (P. spp ID) and between all 7 GAPDH sequences (Overall ID). Specific peptides were selected based on lowest percentage identity and common peptides on 100% identity between the *Plasmodium* sequences. The three peptide sequences of interest were underlined in green and blue for the specific peptides and red for the common peptide. Sequence accession numbers from PlasmDB are PfGAPDH: PF3D7_1462800; PvGAPDH: PVX_117322; PkGAPDH: PKH_124290; PyGAPDH: PY17X_1330200. NCBI ID's for Human GAPDH: P04406.3; Chicken (*Gallus gallus*) GAPDH: NP_989636.1; Mouse GAPDH: AAH83149.1 (accessed 16.9.15).

In contrast to the LDH peptides, the cysteine was added N-terminally to all three GAPDH peptides as shown by the C in Figure 3.5 to follow. Flexibility was prioritised for coupling of the common and the second *P. falciparum* specific peptides (Figure 3.5 (A and C) respectively). The coupling orientation for the first *P. falciparum* peptide (green) in Figure 3.5 (B) followed the same logic as the LDH peptides described earlier. In this case flexibility scores were similar at either end of the peptide.

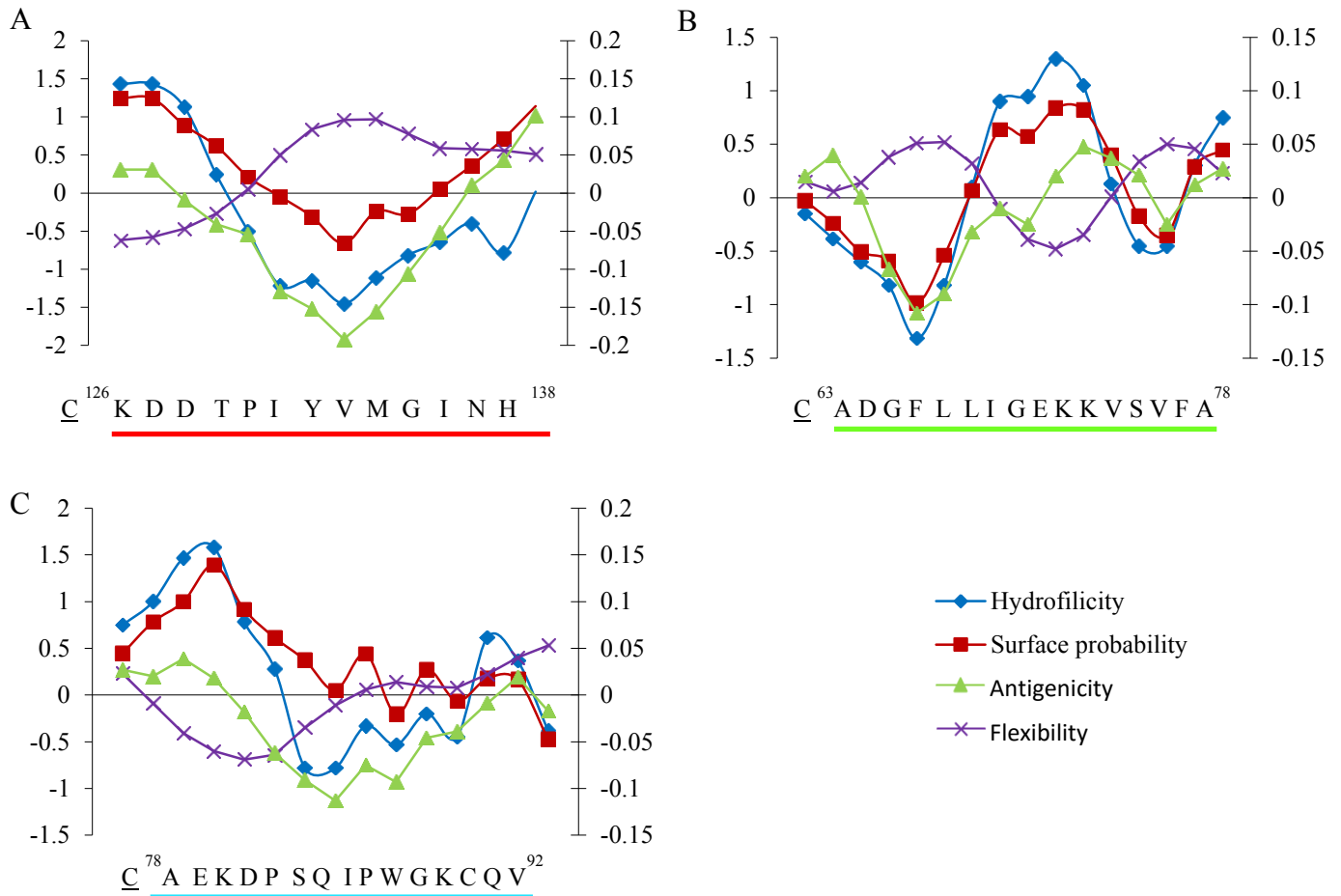


Figure 3.5 Predict7™ analyses of three selected *Plasmodium* GAPDH peptides

Predict7™ plots of the three GAPDH peptides illustrating hydrophilicity, surface probability, flexibility and antigenicity (key in the bottom right). The common peptide plotted in (A) and the two *P. falciparum* specific peptides were plotted in (B) and (C). Flexibility and antigenicity were plotted on the secondary axes in each graph. The amino acid sequences were shown along the bottom of the graphs, with the numbering of the first and last amino acid residues shown in superscript corresponding to the residue number in the *P. falciparum* primary sequence. The addition of a C-terminal cysteine was indicated with a “C” in each case.

Finally the PMT peptides were selected (Figure 3.6) and since PMT is not found in humans or chickens and is absent from mouse-infecting malarias, the alignment was a lot simpler than that of LDH and GAPDH. The common *Plasmodium* peptide “LENNQYTDEGVK” (red) included amino acids 14 to 25 of *P. falciparum* PMT and scored 83% identity with the

P. vivax and *P. knowlesi* proteins. There were two substitutions in both the *P. vivax* and *P. knowlesi* sequences, namely a “T” for “S” and a “V” for “I”. The *P. falciparum* specific peptide “EVEHKYLHENKE” (blue) shared only 33% identity with its *P. vivax* and *P. knowlesi* counterparts including amino acids “E, L, E and K” in that order.

```

PfpMT  MTLIENLNSDKTFLENNQYTDEGVKVYEFIFGENYISSGGLEATKKILSDIELNENSKVL 60
PvpMT  ---MISEPVDIKYLENNQYSDEGIKAYEFIFGEDIYSSGGI IATTKILSDIQLDANSKVL 57
PkpMT  ---MVSEVDIEYLENNQYSDEGIKAYEFIFGEDIYSSGGIVATTKILSDIYLEPNSKVL 57
      : . * :*****:*:* * *****:*****: **.****** *: *****
PfpMT  DIGSGLGGGCMYINEKYGAHTHGIDICSNIVNMANERVSGNNKIIFEANDILTKEFPENN 120
PvpMT  DIGSGLGGGCKYINEKYGAHVHGVVDICEKMVTIAKLRNQDKAKIEFEAKDILKKDFPEST 117
PkpMT  DIGSGLGGGCKYINEKYDAHVYGVDICEKMIAIAKLRNKDKSKVEFEAMDILKKDFPECT 117
      ***** * *****.*:*:*:*:*: :*: * ..: *: *** **.*:*:* *
PfpMT  FDLIYSRDAIHLHLSLENKNKLFQKCYKWLKPTGTLITDYCATEKENWDDEFKEYVKQRK 180
PvpMT  FDMIYSRDSILHLSYADKKMLFEKCYKWLKPNGILLITDYCADKIENWDDEEFKAYIKRK 177
PkpMT  FDMIYSRDAIHLHPYADKKLFEKCYKWLKPNGILLITDYCADKIENWDDEEFKAYINKRK 177
      **:*****:*:* *:*: ***** * ***** : *****:* *::**
PfpMT  YTLITVEEYADILTACNFKNVVSKDLSDYWNQLLEVEHKYLHENKEEFLKLFSEKKFISL 240
PvpMT  YTLMPIQEYGLIKSCKFQNVEAKDISDYWLELLQLLELSKLEEKKEEFLKVYSIKEYNSL 237
PkpMT  YTLIPIQDYGLIKSCNFQNVQAKDISDYWLELLQMELNKLLEKKDEFLKLYPTDEYNSL 237
      ***: .: :* *::: *:*:* *:*:***** :*:*:* * . *.*:*:*:*:*:.. :*: **
PfpMT  DDGWSRRIKIDSKRKMQRWGYFKATKN- 266
PvpMT  KDGWTRKIKDKTRDLQKWGYFKAQKMI 264
PkpMT  KDGWTRKIKDKTRHLQKWGYFKAQKMV 264
      .***:*****:*:*:*:***** *

```

Figure 3.6 Alignment of *Plasmodium* PMT sequences showing selected peptide epitopes chosen for polyclonal chicken antibody and monoclonal scFv production

A multiple sequence alignment of the *P. falciparum* (PfpMT); *P. vivax* (PvpMT); *P. knowlesi* (PkpMT) PMT amino acid sequences was done using ClustalΩ. Percentage identity (ID) was the first criterion for selection and residues were annotated as follows: “*” identical residues; “:” conserved residues; “.” semi-conserved residues and blank spaces represented no identity between the sequences. Percentage identity was assessed between the three malaria sequences. Specific peptides were selected based on lowest percentage identity and common peptides on 100% identity between the malaria sequences. The three peptide sequences of interest were underlined in blue and green for the specific peptides and red for the common peptide. Sequence accession numbers are PfpMT: PlasmoDB ID: PF3D7_134300; PvpMT: PlasmoDB ID: XP_001614208.1; PkpMT: PlasmoDB ID: XP_002259925.1.

Choosing the *P. vivax* and *P. knowlesi* epitopes proved more challenging as they shared greater identity with each other (88%) than with the *P. falciparum* sequence (64 and 62% respectively). The epitopes highlighted in green, residues 228 to 239, were chosen as the species specific peptides for *P. vivax* “VYSIKEYNSLKD” and *P. knowlesi* “LYPTDEYNSLKD” detection respectively. The sequences differed by four of the twelve amino acids, namely “V, S, I and K” all situated toward the N-termini of the peptides.

The coupling orientation of the peptides was determined next (Figure 3.7). The orientation of the common peptide was based on exposing the greater surface probable amino acids and hydrophilic N-terminus, since flexibility was similar at either end. Although the flexibility in the case of the *P. falciparum* peptide was greatest toward the N-terminus, the coupling cysteine “C” was added to the same terminus due to the very high surface probability and

hydrophilicity scores at the C-terminus. Finally the *P. vivax* and *P. knowlesi* peptides were coupled via their C-termini, therefore exposing the greater surface probable and hydrophilic N-termini, but more importantly the N-terminal ends contained the four variable amino acids mentioned above.

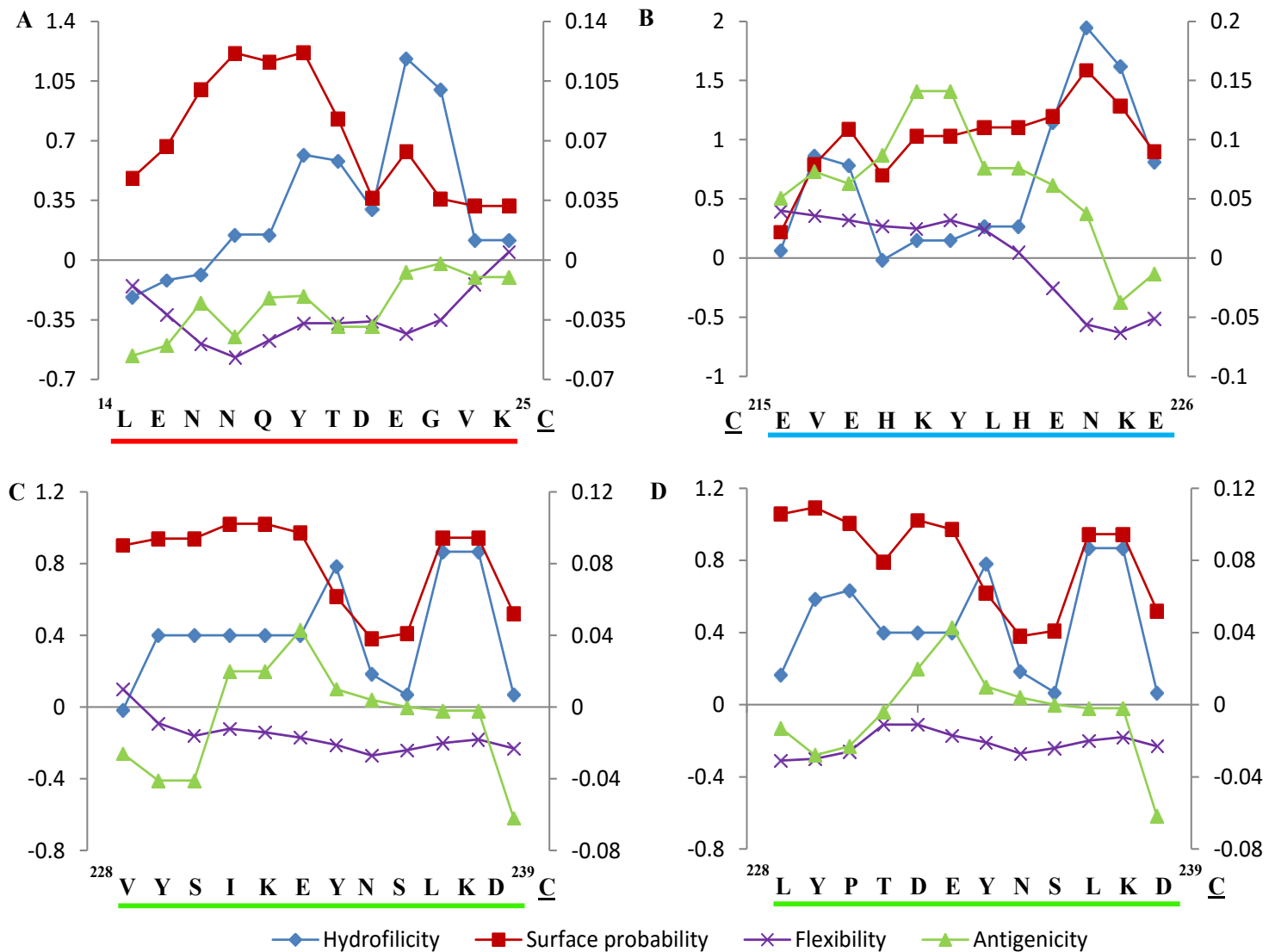


Figure 3.7 Predict7™ analyses of four selected *Plasmodium* PMT peptides

Predict7™ plots of the three PMT peptides illustrating hydrophilicity, surface probability, flexibility and antigenicity (key in the bottom right). The common peptide was plotted in (A) with the species specific peptides for *P. falciparum*, *P. vivax* and *P. knowlesi* plotted in (B to D) respectively. Flexibility and antigenicity were plotted on the secondary axes in each graph. The amino acid sequences were shown along the bottom of the graphs, with the numbering of the first and last amino acid residues shown in superscript corresponding to the residue number in the *P. falciparum* primary sequence. The addition of a C-terminal cysteine was indicated with a “C” in each case.

The selected peptides were shown to be surface located on the respective crystal structures of each of the proteins as highlighted in Figure 3.8, complementing the Predict7™ results.

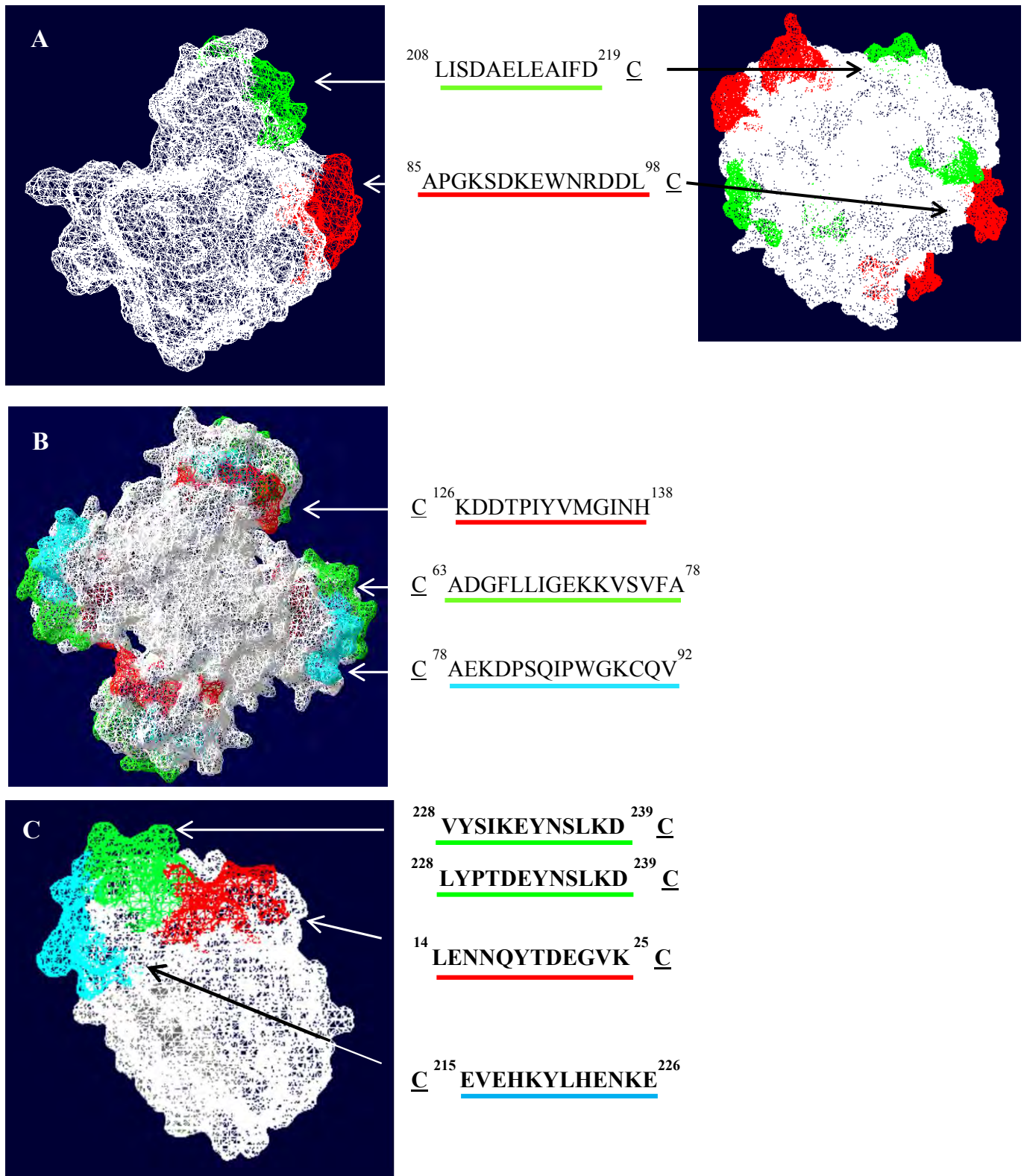


Figure 3.8 Location of the *P. falciparum* specific and the pan-*Plasmodial* epitopes on the 3D crystal structure of *Pf/PvLDH* (A), *PfGAPDH* (B) and *PfPMT* (C)

The selected peptide sequences were located on the surface of the 3D structure of *PfLDH* (shown as a monomer) on the left in (A) with the *PvLDH* tetramer shown on the right, *PfGAPDH* (shown as a tetramer) in (B) and *PfPMT* (shown as a monomer) in (C) and highlighted in their corresponding colours on the structure using Swiss-Pdb viewer 4.0.1 (<http://www.expasy.org/spdbv/>). The amino acid sequences were shown alongside of the structure, with the first and last amino acid residues shown in superscript and the addition of an N- or C-terminal cysteine indicated with a “C” in each case. Structural data for *PfLDH* (1t2d), *PvLDH* (2aa3) *PfGAPDH* (1ywg) and *PfPMT* (3uj6) obtained from Swiss-Pdb.

It should be noted that a tetrameric crystal structure of *P. falciparum* LDH was not available and the monomer was shown instead (Figure 3.8 (A)), with the tetrameric *P. vivax* LDH alongside. Only one of the four specific peptides (green) was not visible as it was hidden behind the molecule.

Table 3.4 summarises the selected peptides, where the chosen peptides were underlined. The common LDH peptide was identical in all but *P. malariae* where it scored 93% identity due to a semi-conserved valine for alanine substitution in its sequence. The common peptide for GAPDH was identical throughout all five human infecting malarias. Finally, for PMT the common peptide had 83% identity in both *P. vivax* and *P. knowlesi*. This was due to conserved substitutions of threonine to serine and valine to isoleucine in both cases for all the *Plasmodium* species sequences available. As expected the species specific peptides all scored below 75% identity with their respective orthologs, with the *Pf*LDH specific peptide scoring the highest identity of 75% with both *P. malariae* and *P. ovale*. The only peptide not highlighted was the *P. knowlesi* PMT peptide, as it spans the same region as the *P. vivax* peptide and its BLAST result identified only *P. knowlesi* PMT (indicated with “#” in the *Pv*PMT column).

Each selected peptide was subjected to NCBI BLASTp analysis and the results that had 100% sequence coverage and 100% sequence identity were listed in Table 3.4. As expected the common peptides in each case had the greatest number of BLAST hits as they were located in highly conserved regions. Only *Plasmodium* hits were identified for all peptides, supporting the specificity of the peptides for malaria diagnosis. In contrast to the common peptides, the species specific peptides BLAST analysis identified some similar simian malaria species. In the case of both the LDH common and *P. falciparum* peptides, hits from as yet unclassified gorilla and chimpanzee *Plasmodium* clades were also identified. The *P. vivax* PMT peptide identified a methanogen (*Methanobrevibacter wolinii*) isolated from sheep faeces. Importantly in all cases, no alternative human pathogen sequences were returned which suggests that the peptides were specific to malaria proteins and should therefore not result in cross reactivity with alternate human pathogen proteins sequenced and identified to date. In addition to this, no alternate human, mouse, chicken or rabbit proteins were identified. This would rule out cross reactivity with linear epitopes in human proteins and also validates the potential use of the animal species for anti-peptide-antibody production.

Table 3.4 Alignment and BLAST results of the selected *Plasmodium* LDH, GAPDH and PMT peptides

<i>Plasmodium</i> species	<u>PfLDH</u>	<u>LDH common</u>	<u>PfGAPDH 1</u>	<u>PfGAPDH 2</u>	<u>GAPDH common</u>	<u>PfPMT</u>	<u>PvPMT</u>	<u>PMT common</u>
<i>falciparum</i>	<u>LISDAELEAIFD</u> (100)	<u>APGKSDKEWNRDDL</u> (100)	<u>ADGFLLLIGEKKVSVFA</u> (100)	<u>AEKDPSQIPWGKQCV</u> (100)	<u>KDDTPIYVMGINH</u> (100)	<u>EVEHKYLHENKE</u> (100)	<u>LFSEKKFISL</u> (40)	<u>LENNQYTDEGVK</u> (100)
<i>vivax</i>	<u>KITDEEVEGIFD</u> (58)	<u>APGKSDKEWNRDDL</u> (100)	<u>GDGCFTVGNNKIFVHS</u> (38)	<u>SEKDPAQIPWGKYEI</u> (67)	<u>KDDTPIYVMGINH</u> (100)	<u>QLELSKLEEKKE</u> (42)	<u>VYSIKEYNSL</u> (100)	<u>LENNQYSDEGIK</u> (83)
<i>malariae</i>	<u>KITDAELDAIFD</u> (75)	<u>VPGKSDKEWNRDDL</u> (93)	<u>GDGKIIVGNKTINIHN</u> (25)	<u>NEKEPSQIPWGKYGI</u> (67)	<u>KDDTPIYVMGINH</u> (100)	-	-	-
<i>ovale</i>	<u>KITDAELDAIFD</u> (75)	<u>APGKSDKEWNRDDL</u> (100)	<u>GEGMFTVGDKKIYVHS</u> (31)	<u>SEKDPAQIPWGKYAI</u> (67)	<u>KDDTPIYVMGINH</u> (100)	-	-	-
<i>knowlesi</i>	<u>KITDEEVEAIFD</u> (67)	<u>APGKSDKEWNRDDL</u> (100)	<u>GDGFFTIGNKKIFVHH</u> (50)	<u>HEKDPANIPWGKYGI</u> (60)	<u>KDDTPIYVMGINH</u> (100)	<u>QMELNKLEEKD</u> (33)	<u>LYPTDEYNSL</u> (60)	<u>LENNQYSDEGIK</u> (83)
Overall Identity	*:* *:..***	.*****	..* : :*:*. : .:	**.*:***** :	*****	::* . *.*::	::. .: **	*****:***.*
BLAST	<i>falciparum</i> , gorilla clade G1 to G3, chimpanzee clade C2 and C3	<i>falciparum</i> , <i>vivax</i> , <i>knowlesi</i> , <i>ovale</i> , <i>yoelii</i> , <i>nigeriensis</i> , <i>semiovale</i> , <i>fragile</i> , <i>cynomolgi</i> , gorilla clade G1 to G3, chimpanzee clade C2 and C3, <i>chabaudi chabaudi</i> , <i>berghei</i> , <i>yoelii</i> , <i>yoelii</i> , <i>vinkei</i> , <i>petteri</i>	<i>falciparum</i>	<i>falciparum</i> , <i>reichenowi</i>	<i>falciparum</i> , <i>vivax</i> , <i>ovale</i> , <i>curtisi</i> , <i>chabaudi</i> , <i>chabaudi</i> , <i>malariae</i> , <i>knowlesi</i> , <i>coatneyi</i> , <i>reichenowi</i> , <i>fragile</i> , <i>brasilianum</i> , <i>cynomolgi</i> , <i>berghei</i> , <i>vinkei</i> , <i>vinkei</i> , <i>yoelii</i> , <i>yoelii</i> , <i>inui</i> , <i>gallinaceum</i>	<i>falciparum</i>	<i>vivax</i> , <i>Methanobrevibacter wolinii</i> , # <i>knowlesi</i>	<i>falciparum</i> , <i>reichenowi</i>

Percentage sequence identity of the chosen peptide sequence (underlined) are given in brackets. Overall identity between the peptide sequences was annotated as follows: “*” identical residues; “.” conserved residues; “:” semi-conserved residues and blank spaces represented no identity between the sequences. The *malariae* and *ovale* sequences were from partial sequences attained from NCBI (accessed 21.9.15). Accession numbers were as follows: *P. malariae* LDH AAS77572.1, *P. ovale* LDH AIU41758.1, *P. malariae* GAPDH ABU50375.1 and *P. ovale* GAPDH AJG43655.1. The BLAST results list species with 100% sequence coverage and identity with the underlined peptide sequences. The *P. knowlesi* BLAST result was included under the *PvPMT* column and identified only *P. knowlesi* PMT as indicated with “#”.

3.2.3 Verification of peptide epitopes in the recombinant proteins used in this study.

The recombinant proteins expressed in this study included *P. falciparum* LDH, GAPDH and PMT; *P. vivax* LDH and PMT; *P. knowlesi* PMT and *P. yoelii* LDH and GAPDH. Plasmid DNA coding for each of the proteins was isolated from the *E. coli* BL21(DE3) expression hosts and sequenced. The consensus sequences were then aligned with the respective coding sequences to verify the identity of the insert DNA. The consensus sequences were also translated and aligned with their respective protein sequences as some of the sequences were codon optimised for expression in *E. coli*. The summarised sequence identity results of the coding sequence and translated protein sequences were shown in Table 3.5.

Table 3.5 Alignment and BLAST results for the sequenced vector DNA inserts and translated sequences

Protein	<i>Plasmodium</i> species	strain	DNA sequence identity (%)	Translated protein identity (%)
LDH	<i>falciparum</i>	K1	98	98
	<i>vivax</i>	Sal-1	99.7	100
	<i>yoelii</i>	17XNL	98	98
GAPDH	<i>falciparum</i>	3D7	96	99
	<i>yoelii</i>	17XNL	91	96
PMT	<i>falciparum</i>	3D7	99	100
	<i>vivax</i>	Sal-1	78	95

All sequences aligned with greater than 90% identity to their corresponding DNA coding sequences except for *P. vivax* PMT showing 78% identity. The resulting translated protein sequences either aligned just as well (*Pf*LDH and *Py*LDH) or better than their respective DNA sequences. Most notably was the codon optimised *Pv*PMT sequence which had only 78% identity with its corresponding DNA coding sequence, but when translated showed 95% identity to its protein amino acid sequence.

3.3 Discussion

Ideally an immuno-diagnostic target molecule should be present throughout the malaria red blood cell cycle and expressed at relatively high levels to allow for detection of the target during early stages of infection while parasitemia is still low. The target molecule should also be parasite specific and not expressed in the host, or if protein in nature, have parasite specific peptides within its sequence, which could be exploited for diagnosis. The bioinformatics approach used in this study to identify such potential targets was outlined in this chapter.

The aim to identify highly abundant proteins was addressed using transcriptome and proteomic data (LeRoch *et al.*, 2003; Foth *et al.*, 2011; www.PlasmoDB.org). LeRoch *et al.* (2003), Bozdech *et al.* (2003) and others hypothesised that the malaria parasite may have a “just in time” strategy for gene expression. Simply put the genes of the proteins required during a specific growth stage are transcribed and translated as the parasite requires them. Foth *et al.* (2011) studied the proteome of the parasite and found other possibilities. The “just in time” hypothesis was supported for some genes, but others exhibited delayed translation while they still mirrored their respective mRNA fluctuations. Finally a third group of genes clearly experienced alternate control of its proteome most likely involving post-translational modifications, meaning that their protein levels did not necessarily correlate with mRNA levels. The list of 35 potential proteins compiled here included proteins described by all three criteria.

Post translational modifications have been identified in LDH, GAPDH and PMT. Post translational modifications include acetylation, nitrosylation, phosphorylation, methylation and ubiquitination amongst others (Alam *et al.*, 2014; Chung *et al.*, 2009). In humans, post translational modifications result in approximately 1.8 million protein variants from only ~30000 open reading frames (Alam *et al.*, 2014). Acetylation of lysine residues was long known to be essential in histone function (Chung *et al.*, 2009), but has only been recognised as a regulatory modification in other malaria proteins in the last three to five years with Miao *et al.* publishing the malaria “acetylome” in 2013, which interestingly included LDH, GAPDH and PMT. Acetylation is thought to play a role in the regulation of glycolysis (Guarente, 2011), where alternate modifications such as phosphorylation seem to “switch on” non-glycolytic moonlighting functions (Sirover 1999, 2005, 2012). Importantly post translational modifications such as acetylation and phosphorylation may affect antibody

affinities due the change in charge of the amino acid side chains and these possibilities are discussed in the general discussion (chapter 7).

Buehner *et al.* first described the common N-terminal nucleotide (NAD⁺(H)) binding motifs between mammalian LDH and GAPDH (Rossmann fold) in 1973. This nucleotide binding ability has since implicated both mammalian enzymes in transcriptional regulation (Kim and Dang., 2005). Although this has not been empirically shown for *Plasmodium* LDH or GAPDH, both orthologs also share a common Rossmann fold (Adams *et al.*, 1973; Akinyi *et al.*, 2008; Daubenberger *et al.*, 2000; Granchi *et al.*, 2010), suggesting they may also share this moonlighting function. Several additional moonlighting functions found with mammalian GAPDH, as a result of post translational modifications, have also been described (Alam *et al.*, 2014). These may explain the apparent increased abundance of GAPDH in relation to LDH in *Plasmodium*. Some of these functions include: DNA repair, RNA binding, telomere binding, cell cycle regulation, histone expression, membrane fusion, phosphorylation, phosphatidyl serine binding, nitric oxide interaction, cytoskeletal binding and apoptosis (Demarse *et al.*, 2009; Kaneda *et al.*, 1997; Kim and Dang, 2005; Sirover M.A., 1999, 2012; Tristan *et al.*, 2011). Mammalian GAPDH has been shown to interact with Band 3 on the erythrocyte surface in an NADH and ATP dependent manner (Heard *et al.*, 1998). Structurally *P. falciparum* GAPDH shares 63.5% amino acid sequence identity with its human counterpart (Daubenberger *et al.*, 2003), and forms a tetramer in solution (337 aa; 36651 Da; pI 7.59) (Berwal *et al.*, 2008; Daubenberger *et al.*, 2000; PlasmoDB; Satchell *et al.*, 2005). *P. falciparum* GAPDH shares several post translational modification sites with its human counterpart, in addition to a few unique sites (Alam *et al.*, 2014). In *P. falciparum* studies thus far, GAPDH has been detected in parasite membrane fractions in a GTPase (Rab2) dependent manner and the authors suggested roles in apicoplast formation and vesicle transport (Daubenberger *et al.*, 2003), although sequence analysis suggests GAPDH to be cytosolic and not plastid targeted (Akinyi *et al.*, 2008; Alam *et al.*, 2014). These findings suggest there may be multiple additional functions for both “housekeeping” genes which may explain their different abundances within the parasite in spite of their linked role in cycling cellular NAD⁺(H).

The choice of peptides in this study was based on the approach taken by Hurdayal *et al.* (2010). The current diagnostic target LDH was the subject of that study and was therefore included as a model for this study. The peptide selection strategy from the Hurdayal *et al.* (2010) study was to choose specific and common peptide epitopes that were unique to the

Plasmodium proteins using multiple sequence alignment and epitope prediction programs. Polyclonal antibodies raised against these peptides then allowed for the specific detection of *Plasmodium* LDH even to a species level. The GAPDH and PMT peptides were identified using a similar strategy and would serve as the target antigens for raising polyclonal chicken antibodies as well as chicken scFv antibodies as described in the later chapters. The chosen peptides were between ten and 16 amino acids in length, which is sufficient to allow specific detection of the parent protein (Hurdayal *et al.*, 2010; Tomar *et al.*, 2006). Multiple sequence alignments were used to identify the common and species specific targets. Predict7TM analysis was then used to analyse the potential peptides. Since each amino acid side chain has unique properties, this program uses algorithms to compare primary amino acid sequences and is able to predict secondary structure (Chou and Fasman, 1979); surface probability (Emini *et al.*, 1985; Kyte and Doolittle, 1982); hydrophilicity (Hopp and Woods, 1981) and antigenicity (Jameson and Wolf, 1988). Since the recognition of proteins in an RDT or ELISA format uses antibodies, the peptides had to be located on the surface of their respective proteins, to facilitate antibody recognition (Saravanan *et al.*, 2009) making the hydrophilicity plots very important. To complement these plots, target peptides were also located and shown to be on the surface of their respective parent protein crystal structures. The greater the hydrophilicity also meant that the peptides were likely to be easily solubilised and stable in solution which is essential for use in an ELISA format. Due to the small size of peptides, they are not able to stimulate an immune response by themselves and require coupling to larger carrier proteins such as rabbit albumin used in this study (Hurdayal *et al.*, 2010; Tomar *et al.*, 2006). For this purpose and to allow coupling to an affinity resin, terminal cysteine residues were added to the selected peptides during synthesis. The Predict7TM plots were important in deciding whether the cysteines were added N- or C-terminally as it was preferred to expose the side with the greatest hydrophilicity, surface probability and flexibility.

Both sets of peptides selected from LDH were within regions that had insertions either in the *Plasmodium* proteins or the mammalian counterparts. The common peptide had a five amino acid insertion and formed part of the cofactor binding loop (Alam *et al.*, 2014; Gomez *et al.*, 1997). The specific peptides lacked a two amino acid insertion present in the mammalian proteins. The GAPDH peptides were selected from the regions of greatest variation, which is within the Rossman fold with 68% variance amongst the *Plasmodium* (Akinyi *et al.*, 2008; Fast *et al.*, 2001). One of the major differences between human and *Plasmodium* GAPDH is

the presence of a two amino acid (K194; G195) insert within a structural region called the S-loop (residue 188 to 203) in the *Plasmodium* protein (Daubenberger *et al.*, 2000; Satchell *et al.*, 2005). The S-loop separates the Rossman folds of the adjacent subunits in the tetrameric form of the enzyme (Akinyi *et al.*, 2008). Another difference is a substitution of two amino acids (L187; V188 for K187; T188) in the same region of the *Plasmodium* protein (Daubenberger *et al.*, 2000). These changes are thought to be responsible for the ferriprotoporphyrin susceptibility of the *Plasmodium* protein in comparison to its human counterpart (Akinyi *et al.*, 2008; Satchell *et al.*, 2005).

PfPMT is not expressed in humans and its closest homolog is a histamine methyltransferase which is also a small-molecule S-adenocyl-L-methionine dependent methyl transferase with 7-16% sequence identity and approximately 31% sequence similarity around the substrate binding site (Horton *et al.*, 2001). Amongst the different *Plasmodium* species PMT has only been confirmed in *P. falciparum*, *P. vivax* and *P. knowlesi*, with over 62% sequence identity between these species. Following genome sequencing PMT may also be expressed in *P. reichenowi* and *P. gallinaceum*, but appears to be absent from all rodent malaria species (Dechamps *et al.*, 2010). PMT homologs were identified in *Burkholderia pseudomallei*, *B. oklahomensis*, *Xenopus laevis*, *Xenopus tropicalis*, *Caenorhabditis briggsae*, *Danio rerio*, *Branchiostoma floridae*, *Caenorhabditis elegans* and *Anopheles gambiae*, but critically, no human homologs exist (Pessi *et al.*, 2004; Bobenchik *et al.*, 2013). In theory, antibodies raised against such a target should have no cross-reactivity with the human proteome. The closest homolog to *PfPMT* in humans is a histamine methyltransferase which is also a small-molecule SAM-dependent methyl transferase with 7-16% sequence identity and approximately 31% sequence similarity around the substrate binding site (Horton *et al.*, 2001).

Selection of *P. falciparum* specific peptide sequences was less challenging than selecting the *P. vivax* and *P. knowlesi* peptides. This was because the *P. falciparum* proteins had lower identity with their *Plasmodium* counterparts. As a result, the chosen *P. vivax* and *P. knowlesi* LDH species specific peptides aligned with 91% identity, the GAPDH sequences had around 80% identity and the PMT sequences 60%. It would be important to test the specificity of the antibodies produced against these targets using *P. vivax* and *P. knowlesi* proteins and parasite lysates. In this study, the *P. falciparum* and *P. vivax* LDH and PMT, *P. falciparum* GAPDH, as well as the *P. yoelii* LDH and GAPDH proteins were expressed and purified. The coding DNA for each recombinant protein was verified by sequencing. According to Hill *et al.*,

(2000); Kristensen *et al.*, (1992) and Lamperti *et al.*, (1992) Genbank entries may carry between 3.1 to 3.6% error rates. The sequences in this study were all within 4% identity of their respective database entries, where only the *P. yoelii* GAPDH sequence scored 91% and the *P. vivax* PMT sequenced scored 78 %. The *P. vivax* PMT sequence was codon optimised for expression in *E. coli* however, which explained its lower identity (Garg *et al.*, 2015). When translated, it scored 95% identity with the primary protein amino acid sequence and the *P. yoelii* GAPDH amino acid sequence scored 96%. Overall the sequencing results were satisfactory and validated the presence of the peptide targets on the recombinant proteins expressed and used in this study as described in the next chapter.

Chapter 4

Recombinant expression, purification and characterisation of the potential *Plasmodium* diagnostic target proteins LDH, GAPDH and PMT

4.1 Introduction

Each of the *Plasmodium* target proteins sequenced in chapter 3 was recombinantly expressed and characterised as described here. This included three orthologs of LDH from *Plasmodium falciparum*, *P. vivax* and *P. yoelii*; two of GAPDH from *P. falciparum* and *P. yoelii* and two of PMT from *P. falciparum* and *P. vivax*. The DNA of the genes encoding the recombinant proteins was sequenced and translated, confirming the presence of the peptide epitopes selected in chapter 3. It was important to assess if these translated proteins folded into similar quaternary structures as their native counterparts. If they did then the predicted surface location of the peptide epitopes was likely and would reinforce their use for raising antibodies as described in chapters 5 and 6. The objectives described in this chapter were therefore to express, purify and evaluate the sizes of the recombinant proteins both as reduced monomers and in their native forms in solution. The predicted sizes of each of the expressed proteins and their quaternary structures are summarised in Table 4.1 (www.plasmodb.org).

Table 4.1 The predicted monomeric and quaternary sizes of the native *Plasmodium* target proteins recombinantly expressed in this study

Protein name	Expected Mw (kD)	Quaternary structure (kD)
<i>Pf</i> LDH	34	tetramer (136)
<i>Pv</i> LDH	34	tetramer (136)
<i>Py</i> LDH	34	tetramer (136)
<i>Pf</i> GAPDH	37	tetramer (148)
<i>Py</i> GAPDH	37	tetramer (148)
<i>Pf</i> PMT	31	monomer (31)
<i>Pv</i> PMT	31	monomer (31)

All sizes were from PlasmoDB (www.plsmodb.org).

The BL21(DE3) *E. coli* strain was used as the expression host in work described in this chapter. Since the plasmid vectors used here were all dependent on the *T7/lac* promoter (pET-15b and pET-28a(+)) or the *tac* promoter (pKK223-3), an *E. coli* strain containing a T7 RNA polymerase (hence the (DE3) nomenclature) capable of binding these promoter regions

was required (de Boer *et al.*, 1983). The BL21 nomenclature refers to the strain's protease deficiency which avoids the need for additional protease inhibitor cocktails in the isolation procedure and circumvents protease degradation of the expressed proteins. The BL21 strains all lack the ompT and lon proteases (Casali, 2003; Sorensen and Mortensen, 2005). This was also important since high density cultures that reach stationary growth phase, like those used here (~ 16 hour, overnight cultures) often induce protease expression resulting from a depletion of nutrients in the media (Sivashanmugam *et al.*, 2009).

The abovementioned promoter regions or the *lac/tac* operator inhibit transcription of the target gene of the plasmid vector if bound by a LacI repressor. In the presence of allolactose or IPTG (allolactose is a metabolite of lactose and IPTG is a non-hydrolysable analogue) LacI loses its affinity for and releases the operator as it binds allolactose or IPTG in solution. This in turn allows the transcription and subsequent expression of the target gene (Schumann and Ferreira, 2004; Sorensen and Mortensen, 2005). *E. coli* cells metabolise the simpler monosaccharide glucose prior to switching to more complex disaccharides such as lactose. Importantly only *E. coli* strains that harbour the *lacZ* (β -galactosidase) or *lacY* (lactose permease) genes are known to import and convert lactose to allolactose such as the BL21(DE3) strain used here (Casali, 2003; Studier, 2005). The addition of glucose in culture media therefore not only prevents target gene expression, but also promotes rapid growth of the culture (Sorensen and Mortensen, 2005). Once an increased biomass is achieved and the culture is growing rapidly (exponential growth phase at an O.D. of around 0.5) the *E. coli* culture can be induced manually with the addition of lactose or IPTG to the culture allowing targeted gene expression.

To avoid the manual induction of expression, cultures may also be grown in more complex auto-inducing media such as terrific broth (TB) used in this study (Studier W.F., 2005). In this case the *E. coli* cultures are grown in glucose and glycerol containing media allowing their rapid growth, where glycerol does not interfere with induction (Blommel *et al.*, 2007; Studier, 2005). Instead of manually adding lactose or IPTG, the culture is left to grow for an extended period (~ 16 hours) and expression of the target gene occurs when the *E. coli* cells transition from glucose to lactose metabolism as the glucose is depleted. A low glucose concentration within the cells induces cyclic AMP production which is necessary to completely activate the *lac/tac* operon (Rosano and Ceccarelli, 2014). Once the cells start metabolising lactose to allolactose, the LacI repressor releases the *lac/tac* operator resulting in target gene expression as described earlier. Longer culturing periods of up to 40 hours

were described by Sivashanmugam *et al.*, (2009). Over such a long period, protein degradation and plasmid loss or instability may occur however. This is primarily due to media acidification which means that the pH needs to be monitored in such cultures. This is critical with Amp^r plasmids as ampicillin degrades rapidly in low pH thus reducing its selective pressure (Sivashanmugam *et al.*, 2009).

Protein expression in *E. coli* has some guidelines but most conditions may be optimised. Importantly media and culture growth should be monitored and optimised as they are usually protein dependent (Sivashanmugam *et al.*, 2009). This was observed for the expression of *PfGAPDH* and *PfPMT* from the same plasmid vector discussed later. Adequate culture growth is important as high cell densities usually translate in greater expression yields, which is why rich media (such as LB or TB) promoting such growth are used (Studier W.F., 2005). High cell densities are important if plasmids with low to moderate copy numbers are used. In this case the pET and pKK plasmids both have moderate copy numbers of 15 to 20 per cell (Rosano and Ceccarelli, 2014). Importantly with such expression conditions, the use of multiple small cultures as opposed to single large cultures is recommended, as well as a final culture volume no greater than 20% of the flask volume to allow better O₂ saturation (Rosano and Ceccarelli, 2014; Sivashanmugam *et al.*, 2009; Studier, 2005).

This chapter therefore describes the expression of the potential *Plasmodium* diagnostic target proteins identified in chapter 3. These were purified and characterised in order to verify their use for raising antibodies in the chapters 5 and 6 to follow.

4.2 Results

All the recombinant proteins used in this study were expressed from a common, protease deficient *E. coli* BL21(DE3) host strain. Each of the proteins was expressed as a His-tag conjugate, although they were not all expressed from the same plasmid vector. This allowed for affinity purification using a TALON[®] Cobalt (Co²⁺) affinity resin with imidazole as the eluent. The results described here are the optimisation of expression and affinity purification strategies used and further characterisation of each of the recombinant proteins.

4.2.1 Results from the *E. coli* expression host using the proposed expression and affinity purification strategies

Since the *E. coli* host and affinity resin were common to all the purified proteins, the first objective was to assess the growth of the untransformed host under the proposed culture temperatures and media used. Figure 4.1 (A) shows a growth time of around 2 hours for each of the LB cultures to reach an O.D. of ~ 0.5, where the TB cultures at either 30 or 37°C took between 2.5 to 3 hours. The addition of IPTG to the LB cultures at this time did not appear to have a detrimental effect on the growth of the *E. coli* host cells when compared to the LB cultures without IPTG addition. In all cases the logarithmic growth phase lasted for about 2 hours, where after a reduction in growth rate occurred, known as the stationary phase.

The second control was to assess if any *E. coli* host proteins would co-purify with the target recombinant proteins on the TALON[®] Co²⁺ resin and whether the different culture conditions resulted in increased co-purified proteins. To do this each of the untransformed cultures were prepared by sonication and the cleared lysate supernatants were “purified” using the TALON[®] Co²⁺ resin. Washes were performed until the absorbance at 280 nm was below 0.02, which is why in some instances the number of washes varied in the subsequent elution profiles (Figures 4.2 to 4.8). In order to elute the bound proteins a 0 to 500 mM imidazole gradient over 20 ml was used. Figure 4.1 (B) shows that *E. coli* host proteins were bound to the resin even after the wash steps. When the samples were run on SDS-PAGE, bands were only detected once silver stained (Figure 4.1 (C)), with the greatest number of contaminants eluting within the first four to five fractions, correlating to ~80 to 100 mM imidazole required for the removal of these proteins from the resin. Based on these results later purifications were adapted to include 10 mM imidazole in the lysate and wash buffers to reduce the number of *E. coli* host proteins co-purifying with the target proteins (Figures 4.10 to 4.12).

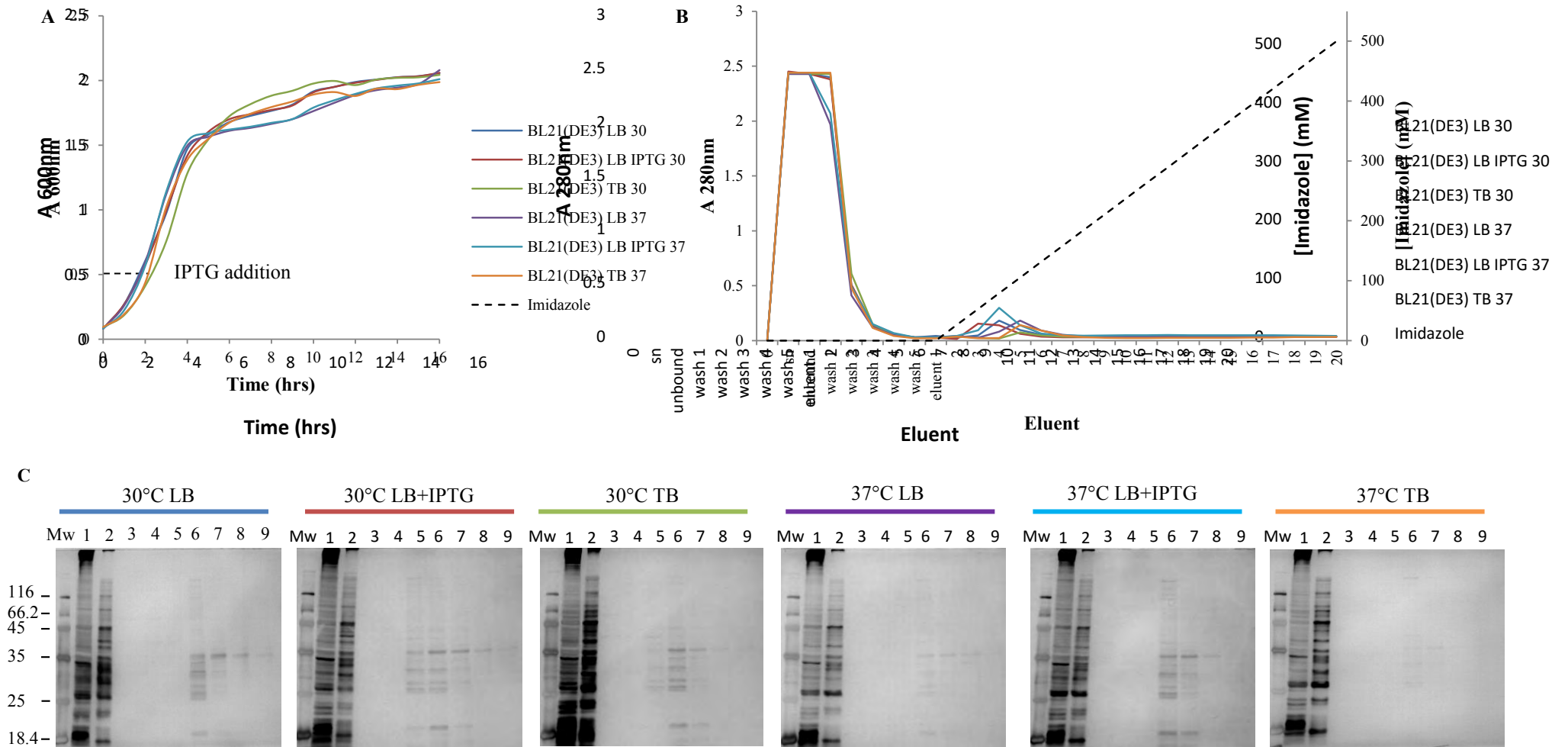


Figure 4.1 Untransformed BL21(DE3) host growth under different conditions and elution profiles off a TALON[®] (Co²⁺) resin using a linear imidazole gradient, analysed by silver staining on SDS-PAGE

Growth curves of the expression host *E. coli* strain BL21(DE3) in different culture media at 30 and 37°C were plotted, with the addition of IPTG for induced cultures at O.D. ~ 0.5 indicated on the y-axis in (A). Each of the cultures were lysed by sonication and incubated on 1 ml packed TALON[®] (Co²⁺) resin and the bound *E. coli* proteins were eluted with a linear imidazole gradient from 0 to 500 mM as shown on the secondary axis in (B), eluting protein measured at 280 nm on the primary axis. The key to both (A) and (B) was shown between the graphs. Lysates and eluents of the corresponding cultures plotted in (A and B) were run on 12.5% reducing SDS-PAGE gels (C) and silver stained. The samples run in each lane were as follows: molecular weight marker (Mw); original sample lysate loaded onto the TALON[®] resin (lane 1); unbound sample (lane 2); final wash (lane 3); eluents 1 to 6 (lanes 4 to 9).

The imidazole concentrations required to elute the BL21(DE3) proteins off the TALON[®] (Co²⁺) resin were between 80 to 100 mM as summarised in Table 4.2.

Table 4.2 Imidazole concentrations required for elution of bound BL21(DE3) proteins off the TALON[®] (Co²⁺) resin

Culture	Growth conditions	Eluent peak #	Imidazole (mM)
BL21(DE3)	LB 30°C	4	80
	LB 30°C + IPTG	3	50
	TB 30°C	5	100
	LB 37°C	5	100
	LB 37°C + IPTG	4	80
	TB 37°C	5	100

4.2.2 Optimisation of expression and affinity purification strategies for the recombinant *Plasmodium* LDH proteins

The *rPf*LDH and *rPv*LDH proteins were expressed from a pKK223-3 vector, with a His tag introduced during the cloning procedure, allowing for the TALON[®] Co²⁺ purification, where *rPy*LDH was expressed from a pET-28a(+) plasmid. All growth curves had similar trends, where the TB cultures for all three proteins had the fastest growth rates to O.D. ~0.5 as shown in Figures 4.2 to 4.4 (A). The *rPy*LDH TB cultures had an initial O.D. that was higher than the LB cultures and maintained this difference in O.D. even during the stationary growth phase till around the tenth hour after inoculation. The *rPf*LDH cultures were the only cultures with a noticeable lag phase after inoculation.

For *rPf*LDH the highest 280 nm absorbance values were observed for the TALON[®] (Co²⁺) resin elution profiles of the induced LB cultures grown at 37°C and both the 30 and 37°C TB cultures. With regard to *rPv*LDH the best elution profiles were attained for the TB cultures and the induced 37°C LB culture (Figure 4.3 (B)). The TB cultures expressing *rPy*LDH gave the highest absorbance readings in this case (Figure 4.2 to 4.4 (B)).

Analysis of the eluents on SDS-PAGE showed that some cultures had more co-purifying proteins, but these were also limited to the first two to three eluents in each case, which correlated to the elution of the *E. coli* host proteins seen in Figure 4.1 (C). It should be noted that the purifications performed here did not include imidazole in the wash steps. Some leaky expression was observed for all three proteins with cultures grown in LB media without IPTG induction.

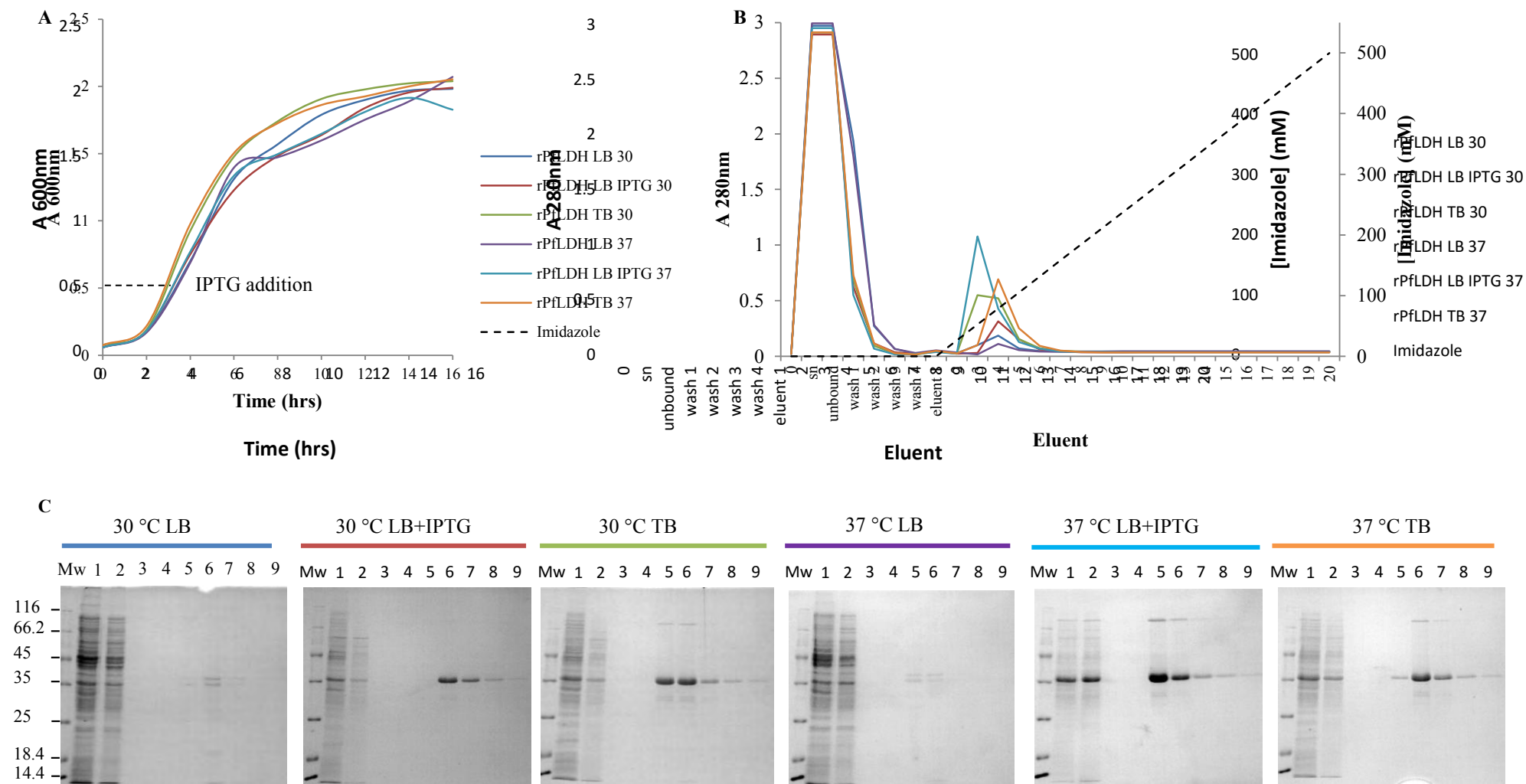


Figure 4.2 Growth of *rPfLDH* expressing cultures under varying conditions and elution profiles off a TALON[®] (Co²⁺) resin analysed by SDS-PAGE
 Growth curves of the expression host *E. coli* strain BL21(DE3) expressing *rPfLDH* (pKK223-3 vector) in different culture media at 30 and 37°C were plotted, with the addition of IPTG for induced cultures at O.D. ~ 0.5 indicated on the y-axis in (A). Each of the cultures were lysed by sonication and incubated on 1 ml packed TALON[®] (Co²⁺) resin and the bound *rPfLDH* was eluted with a linear imidazole gradient from 0 to 500 mM as shown on the secondary axis in (B), eluting protein measured at 280 nm on the primary axis. The key to both (A) and (B) was shown between the graphs. Lysates and eluents of the corresponding cultures plotted in (A and B) were run on 12.5% reducing SDS-PAGE gels and Coomassie stained (C). The samples run in each lane were as follows: molecular weight marker (Mw); original sample lysate loaded onto the TALON[®] resin (lane 1); unbound sample (lane 2); final wash (lanes 3); eluents 1 to 6 (lanes 4 to 9).

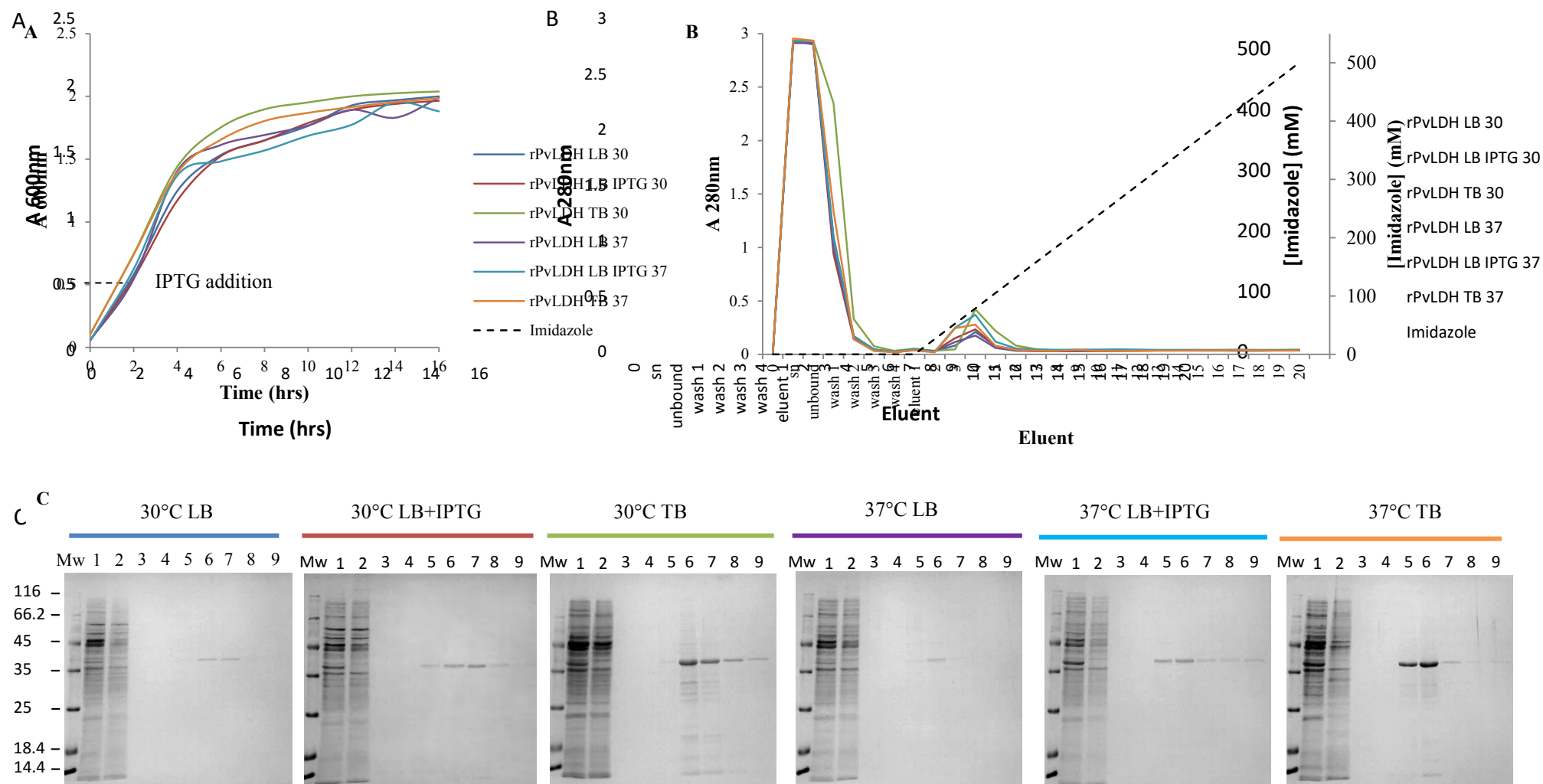


Figure 4.3 Growth of rPvLDH expressing cultures under varying conditions and elution profiles off a TALON[®] (Co²⁺) resin analysed by SDS-PAGE

Growth curves of the expression host *E. coli* strain BL21(DE3) expressing rPvLDH (pKK223-3 vector) in different culture media at 30 and 37°C were plotted, with the addition of IPTG for induced cultures at O.D. ~ 0.5 indicated on the y-axis in (A). Each of the cultures were lysed by sonication and incubated on 1 ml packed TALON[®] (Co²⁺) resin and the bound rPvLDH was eluted with a linear imidazole gradient from 0 to 500 mM as shown on the secondary axis in (B), eluting protein measured at 280 nm on the primary axis. The key to both (A) and (B) was shown between the graphs. Lysates and eluents of the corresponding cultures plotted in (A and B) were run on 12.5% reducing SDS-PAGE gels and Coomassie stained (C). The samples run in each lane were as follows: molecular weight marker (Mw); original sample lysate loaded onto the TALON[®] resin (lane 1); unbound sample (lane 2); final wash (lane 3); eluents 1 to 6 (lanes 4 to 9).

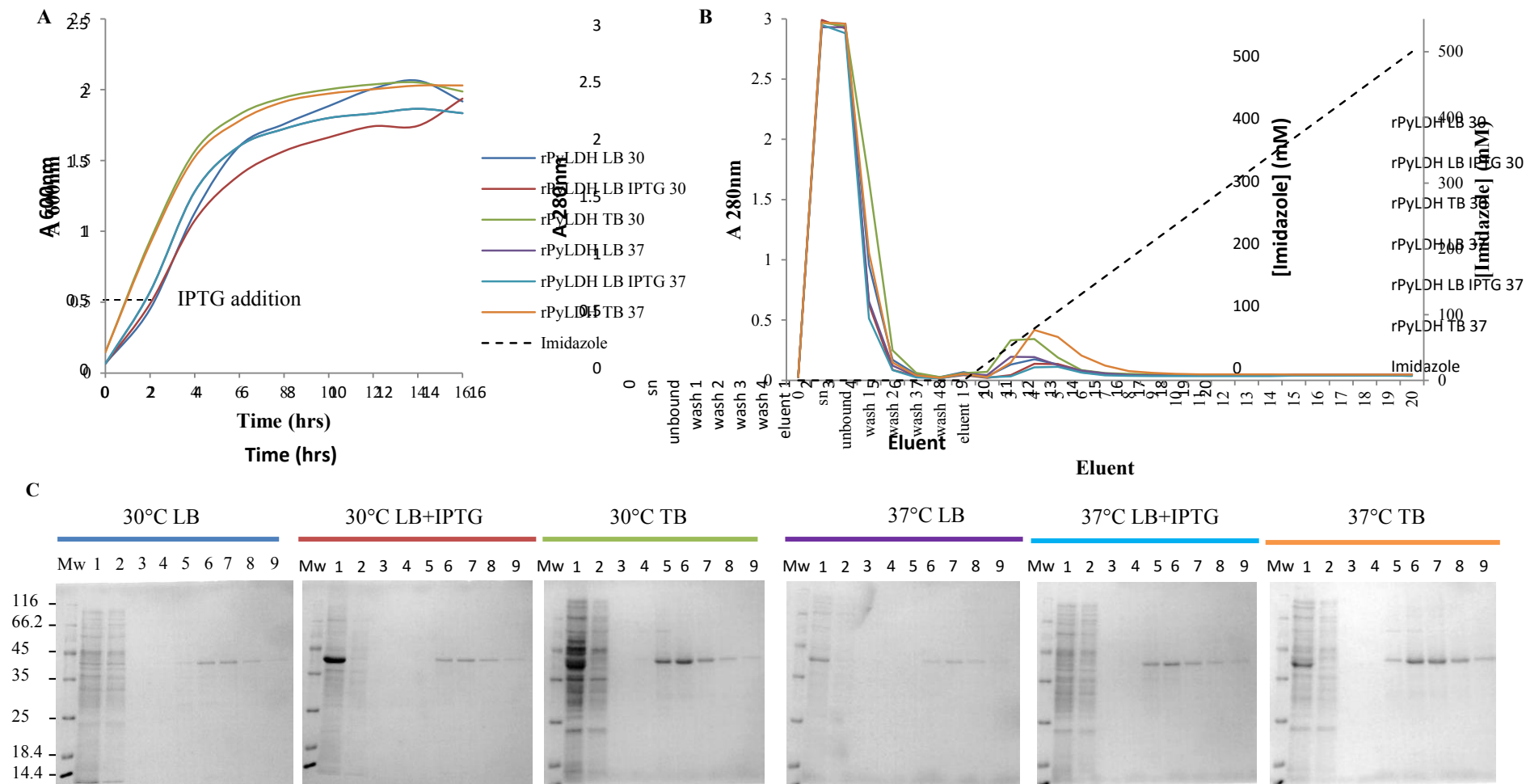


Figure 4.4 Growth of rPyLDH expressing cultures under varying conditions and elution profiles off a TALON[®] (Co²⁺) resin analysed by SDS-PAGE
 Growth curves of the expression host *E. coli* strain BL21(DE3) expressing rPyLDH (pET-28a(+)) vector) in different culture media at 30 and 37°C were plotted, with the addition of IPTG for induced cultures at O.D. ~ 0.5 indicated on the y-axis in (A). Each of the cultures were lysed by sonication and incubated on 1 ml packed TALON[®] (Co²⁺) resin and the bound rPyLDH was eluted with a linear imidazole gradient from 0 to 500 mM as shown on the secondary axis in (B), eluting protein measured at 280 nm on the primary axis. The key to both (A) and (B) was shown between the graphs. Lysates and eluents of the corresponding cultures plotted in (A and B) were run on 12.5% reducing SDS-PAGE gels and Coomassie stained (C). The samples run in each lane were as follows: molecular weight marker (Mw); original sample lysate loaded onto the TALON[®] resin (lane 1); unbound sample (lane 2); final wash (lane 3); eluents 1 to 6 (lanes 4 to 9).

The imidazole concentrations required to elute the respective *Plasmodium* LDH proteins expressed here off the TALON[®] (Co²⁺) resin are summarised in Table 4.3 below.

Table 4.3 Imidazole concentrations required for elution of bound recombinant *Plasmodium* LDH proteins off the TALON[®] (Co²⁺) resin

Growth conditions	rPfLDH [Imidazole] (mM)	rPvLDH [Imidazole] (mM)	rPyLDH [Imidazole] (mM)
LB 30°C	80	80	80
LB 30°C + IPTG	80	80	80
TB 30°C	50	80	80
LB 37°C	80	80	50
LB 37°C + IPTG	50	80	100
TB 37°C	80	80	80

Recombinant *P. falciparum* LDH eluted off the TALON[®] (Co²⁺) resin at imidazole concentrations between 50 to 80 mM; rPvLDH at 80 mM and rPyLDH between 50 to 100 mM, dependant on the conditions used for expression.

4.2.3 Optimisation of expression and affinity purification strategies for the recombinant *Plasmodium* GAPDH proteins

The growth curves of the GAPDH expressing cultures all reached an O.D. value of ~ 0.5 within 2 to 3 hours after inoculation. However, unlike the LDH cultures, the TB cultures did not show faster growth times in comparison to the LB cultures (Figure 4.5 and 4.6 (A)). A pET-15b plasmid was used for rPfGAPDH expression and a pET-28a(+) plasmid vector for rPyGAPDH. Unlike the rPyLDH cultures that grew better in TB media, the GAPDH cultures grew similarly in LB or TB media, even though the same plasmid vector was used.

Both of the recombinant GAPDH proteins eluted between fractions two and ten in this instance, which correlated to an imidazole concentration range of ~30 to 260 mM (Figure 4.5 and 4.6 (B)). The TB cultures in both cases showed about double the amount of protein eluted (absorbance at 280 nm) in comparison to the LB induced cultures, and the SDS-PAGE analysis supported these results, although smaller molecular weight products were more abundant in the TB cultures (Figure 4.5 and 4.6 (C)).

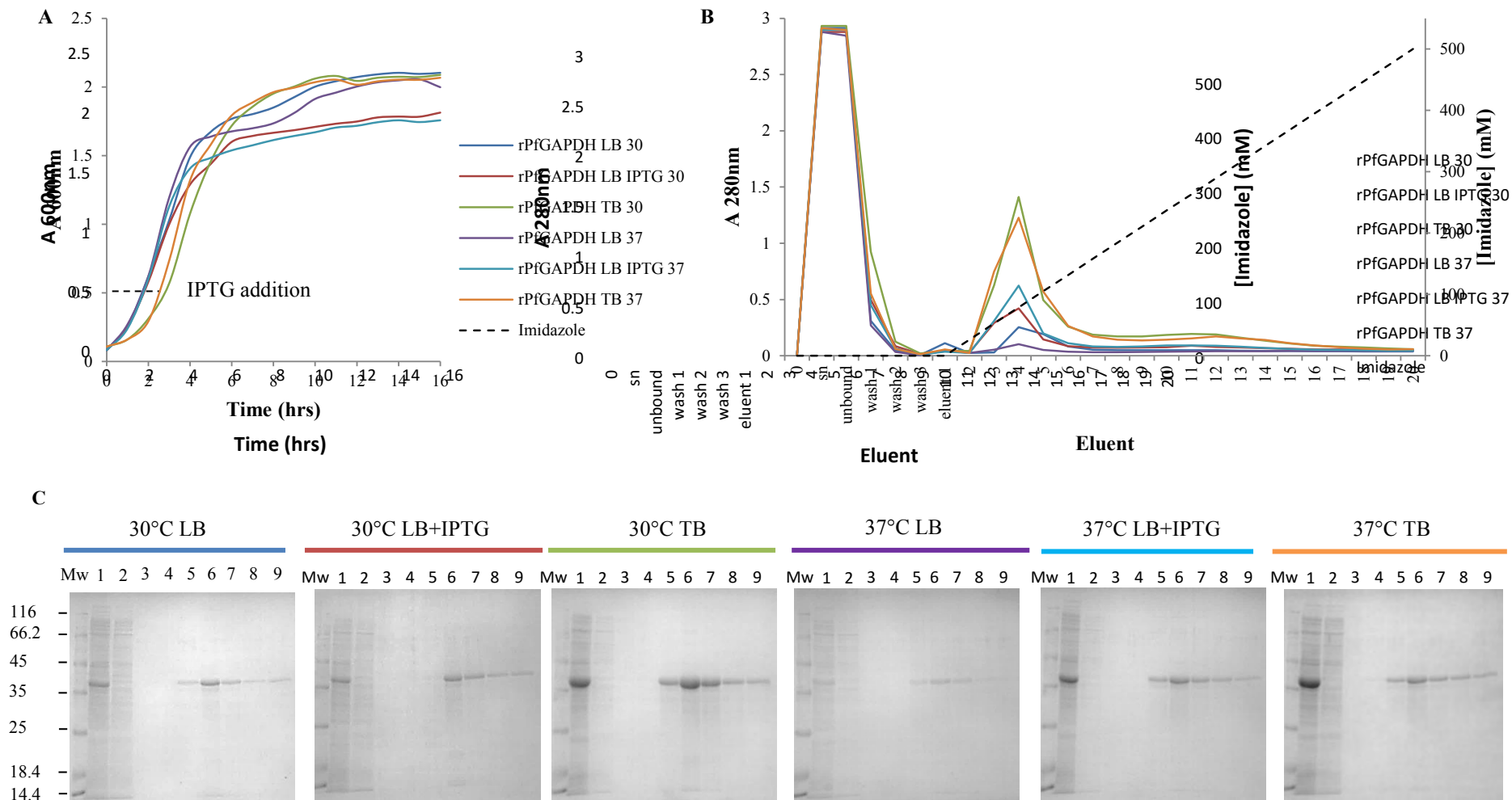


Figure 4.5 Growth of *rPfGAPDH* expressing cultures under varying conditions and elution profiles off a TALON[®] (Co²⁺) resin analysed by SDS-PAGE
 Growth curves of the expression host *E. coli* strain BL21(DE3) expressing *rPfGAPDH* (pET-15b vector) in different culture media at 30 and 37°C were plotted, with the addition of IPTG for induced cultures at O.D. ~ 0.5 indicated on the y-axis in (A). Each of the cultures were lysed by sonication and incubated on 1 ml packed TALON[®] (Co²⁺) resin and the bound *rPfGAPDH* was eluted with a linear imidazole gradient from 0 to 500 mM as shown on the secondary axis in (B), eluting protein measured at 280 nm on the primary axis. The key to both (A) and (B) was shown between the graphs. Lysates and eluents of the corresponding cultures plotted in (A and B) were run on 12.5% reducing SDS-PAGE gels and Coomassie stained (C). The samples run in each lane were as follows: molecular weight marker (Mw); original sample lysate loaded onto the TALON[®] resin (lane 1); unbound sample (lane 2); final wash (lane 3); eluents 1 to 6 (lanes 4 to 9).

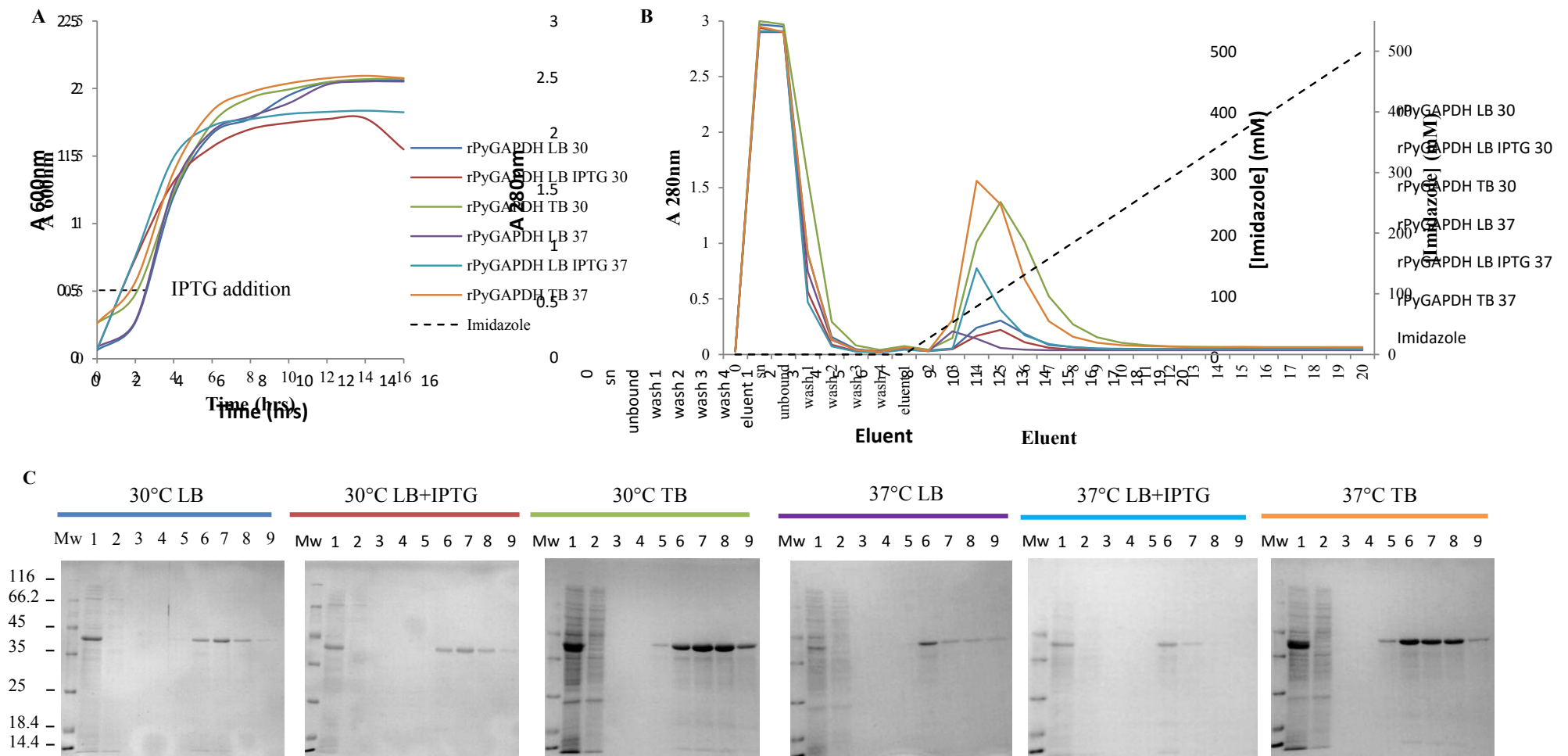


Figure 4.6 Growth of rPyGAPDH expressing cultures under varying conditions and elution profiles off a TALON[®] (Co²⁺) resin analysed by SDS-PAGE
 Growth curves of the expression host *E. coli* strain BL21(DE3) expressing rPyGAPDH (pET-28a(+)) vector) in different culture media at 30 and 37°C were plotted, with the addition of IPTG for induced cultures at O.D. ~ 0.5 indicated on the y-axis in (A). Each of the cultures were lysed by sonication and incubated on 1 ml packed TALON[®] (Co²⁺) resin and the bound rPyGAPDH was eluted with a linear imidazole gradient from 0 to 500 mM as shown on the secondary axis in (B), eluting protein measured at 280 nm on the primary axis. The key to both (A) and (B) was shown between the graphs. Lysates and eluents of the corresponding cultures plotted in (A and B) were run on 12.5% reducing SDS-PAGE gels and Coomassie stained (C). The samples run in each lane were as follows: molecular weight marker (Mw); original sample lysate loaded onto the TALON[®] resin (lane 1); unbound sample (lane 2); final wash (lane 3); eluents 1 to 6 (lanes 4 to 9).

The imidazole concentrations required to elute the respective *Plasmodium* GAPDH proteins expressed here off the TALON[®] (Co²⁺) resin were summarised in Table 4.4 below.

Table 4.4 Imidazole concentrations required for elution of bound recombinant *Plasmodium* GAPDH proteins off the TALON[®] (Co²⁺) resin

Growth conditions	rPfGAPDH [Imidazole] (mM)	rPyGAPDH [Imidazole] (mM)
LB 30°C	80	100
LB 30°C + IPTG	80	100
TB 30°C	80	100
LB 37°C	80	80
LB 37°C + IPTG	80	80
TB 37°C	80	80

Recombinant *P. falciparum* GAPDH eluted off the TALON[®] (Co²⁺) resin at around 80 mM imidazole, where rPyGAPDH eluted between 80 to 100 mM imidazole dependant on the conditions used for expression.

4.2.4 Optimisation of expression and affinity purification strategies for the recombinant *Plasmodium* PMT proteins

For both recombinant PMT proteins the culture growth curves followed a similar pattern with the exception of the TB cultures of rPvPMT, which had the best growth times to O.D. of ~ 0.5 in comparison to the other cultures (Figure 4.7 and 4.8 (A)). As was observed with LDH and GAPDH cultures an O.D. of ~ 0.5 was reached within 2 to 3 hours after inoculation.

Interestingly rPfPMT was the only protein studied here that did not express well in the TB culture system (Figure 4.7 (B)), even though the same pET-15b plasmid was used as for rPfGAPDH. The SDS-PAGE analysis showed a similar banding pattern for the non-induced LB cultures and the TB cultures (Figure 4.7 (C)). The rPfGAPDH cultures on the other hand yielded absorbance values approximately double that of the induced LB cultures. Expression of rPfPMT was best with IPTG induction in LB media at either 30 or 37°C.

In contrast to this, the expression of rPvPMT was best when cultures were grown in TB at 30°C, which exceeded the corresponding induced LB culture yield (absorbance 280 nm) by approximately two-fold (Figure 4.8 (B)). In this case the pET-28a(+) vector was used and the result correlated with that observed for rPyGAPDH and rPyLDH.

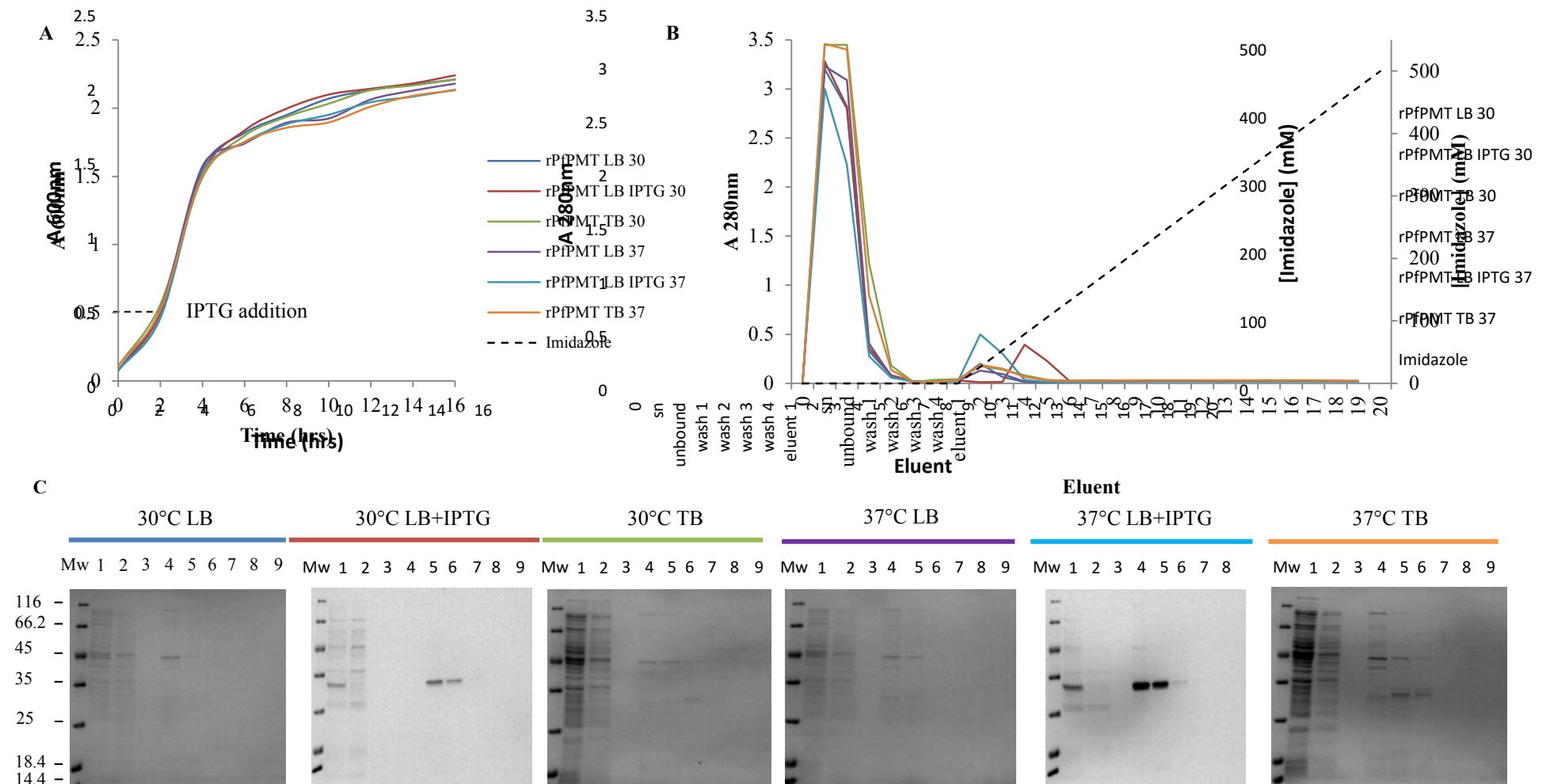


Figure 4.7 Growth of *rPfPMT* expressing cultures under varying conditions and elution profiles off a TALON[®] (Co²⁺) resin analysed by SDS-PAGE
 Growth curves of the expression host *E. coli* strain BL21(DE3) expressing *rPfPMT* (pET-15b vector) in different culture media at 30 and 37°C were plotted, with the addition of IPTG for induced cultures at O.D. ~ 0.5 indicated on the y-axis in (A). Each of the cultures were lysed by sonication and incubated on 1 ml packed TALON[®] (Co²⁺) resin and the bound *rPfPMT* was eluted with a linear imidazole gradient from 0 to 500 mM as shown on the secondary axis in (B), eluting protein measured at 280 nm on the primary axis. The key to both (A) and (B) was shown between the graphs. Lysates and eluents of the corresponding cultures plotted in (A and B) were run on 12.5% reducing SDS-PAGE gels and Coomassie stained (C). The samples run in each lane were as follows: molecular weight marker (Mw); original sample lysate loaded onto the TALON[®] resin (lane 1); unbound sample (lane 2); final wash (lane 3); eluents 1 to 6 (lanes 4 to 9).

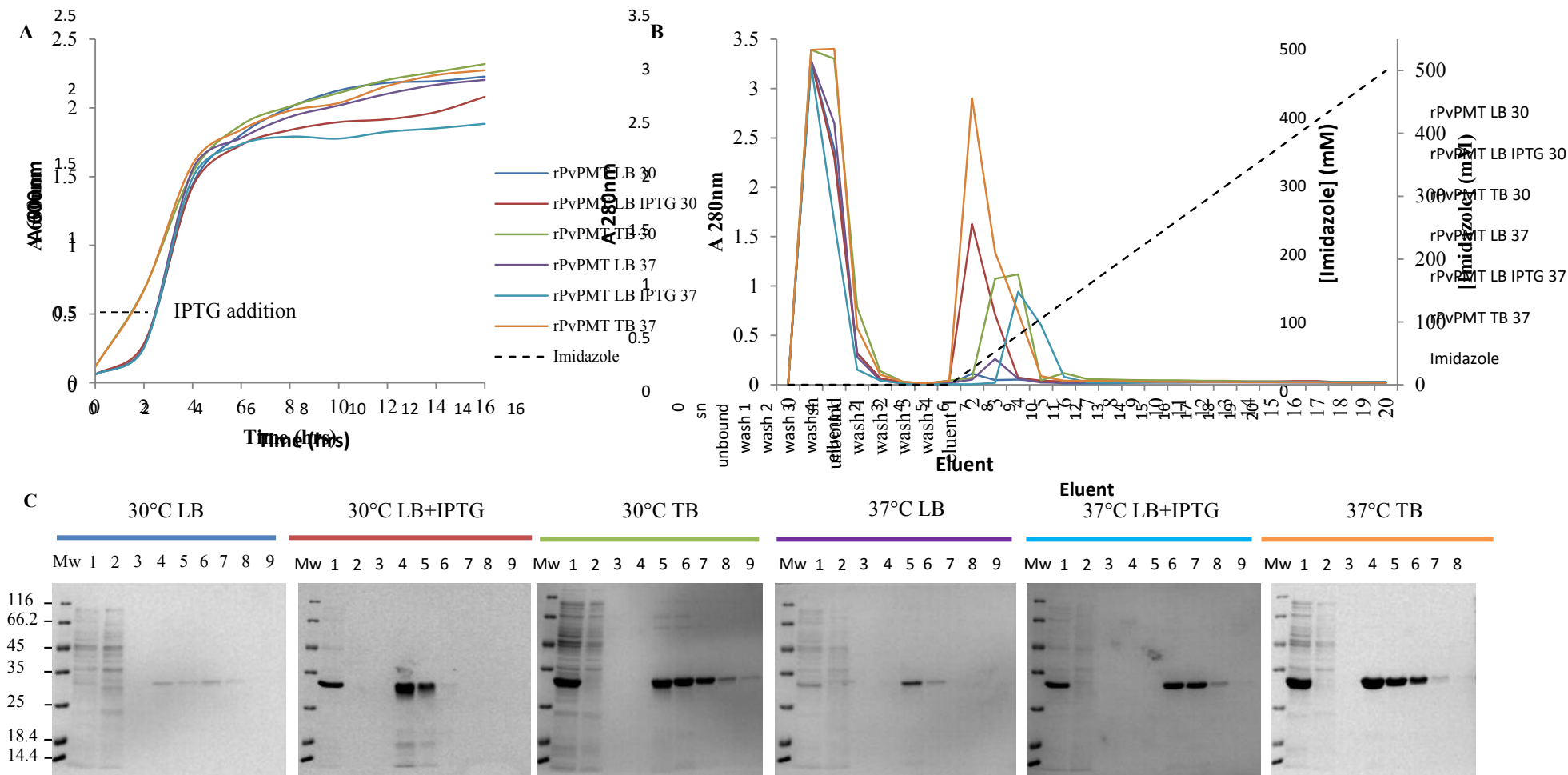


Figure 4.8 Growth of rPvPMT expressing cultures under varying conditions and elution profiles off a TALON[®] (Co²⁺) resin analysed by SDS-PAGE
 Growth curves of the expression host *E. coli* strain BL21(DE3) expressing rPvPMT (pET-28a(+)) vector) in different culture media at 30 and 37°C were plotted, with the addition of IPTG for induced cultures at O.D. ~ 0.5 indicated on the y-axis in (A). Each of the cultures were lysed by sonication and incubated on 1 ml packed TALON[®] (Co²⁺) resin and the bound rPvPMT was eluted with a linear imidazole gradient from 0 to 500 mM as shown on the secondary axis in (B), eluting protein measured at 280 nm on the primary axis. The key to both (A) and (B) was shown between the graphs. Lysates and eluents of the corresponding cultures plotted in (A) and (B) were run on 12.5% reducing SDS-PAGE gels and Coomassie stained (C). The samples run in each lane were as follows: molecular weight marker (Mw); original sample lysate loaded onto the TALON[®] resin (lane 1); unbound sample (lane 2); final wash (lane 3); eluents 1 to 6 (lanes 4 to 9).

The imidazole concentrations required to elute the respective *Plasmodium* PMT proteins expressed here off the TALON[®] (Co²⁺) resin were summarised in Table 4.5 below.

Table 4.5 Imidazole concentrations required for elution of bound recombinant *Plasmodium* PMT proteins off the TALON[®] (Co²⁺) resin

Growth conditions	r <i>Pf</i> PMT [Imidazole] (mM)	r <i>Pv</i> PMT [Imidazole] (mM)
LB 30°C	25	25
LB 30°C + IPTG	80	25
TB 30°C	25	80
LB 37°C	25	50
LB 37°C + IPTG	25	80
TB 37°C	25	25

Both of the recombinant *Plasmodium* PMT proteins eluted off the TALON[®] (Co²⁺) resin between 25 to 80 mM imidazole, dependant on the conditions used for expression.

4.2.5 Expression and affinity purification of the recombinant *Plasmodium* proteins

From the initial optimisation experiments, each of the recombinant proteins was expressed and purified, with the final yields of purified protein obtained from 50 ml cultures shown in Table 4.6.

Table 4.6 Optimized expression conditions for each recombinant proteins including affinity purified yields

Protein	Plasmid vector	Antibiotic (µg/ml)	Media	Induction	Temp. (°C)	Yield (mg / 50 ml culture)
<i>Pf</i> LDH	pKK223-3	Ampicillin (50)	TB	auto	37	9.5
<i>Pv</i> LDH	pKK223-3	Ampicillin (50)	TB	auto	30	2.96
<i>Py</i> LDH	pET-28a(+)	Kanamycin (25)	TB	auto	37	6.05
<i>Pf</i> GAPDH	pET-15b	Ampicillin (50)	TB	auto	30	6.55
<i>Py</i> GAPDH	pET-28a(+)	Kanamycin (25)	TB	auto	37	8.95
<i>Pf</i> PMT	pET-15b	Ampicillin (100)	LB	1 mM IPTG	37	5.57
<i>Pv</i> PMT	pET-28a(+)	Kanamycin (25)	TB	auto	37	5.87

The media used in each case was abbreviated as TB for Terrific broth and LB for Lysogeny broth.

The only notable changes from the optimisation results were that *rPf*LDH was expressed in TB at 37°C in further experiments, since yields from a 50 ml culture were around 9.5 mg, which was more than adequate. The *rPf*LDH yields may have been improved further by using

the LB with IPTG induction method. The second change was that *rPjPMT* was expressed overnight using the LB with IPTG induction method. All proteins were expressed at greater than 5 mg from 50 ml cultures, except for *rPvLDH* which yielded approximately 3 mg per 50 ml culture. Another change to the methodology used in the optimisation studies was that 10 mM imidazole was included in the lysis and wash buffers, with 250 mM imidazole used in the elution buffer.

Examples of the resulting purifications were shown in Figures 4.9 to 4.11 to follow. Purity of the eluted proteins was assessed on 12.5% reducing SDS-PAGE and the recombinant proteins were detected in each case with an anti-His tag mouse monoclonal antibody in western blots shown alongside the respective gels.

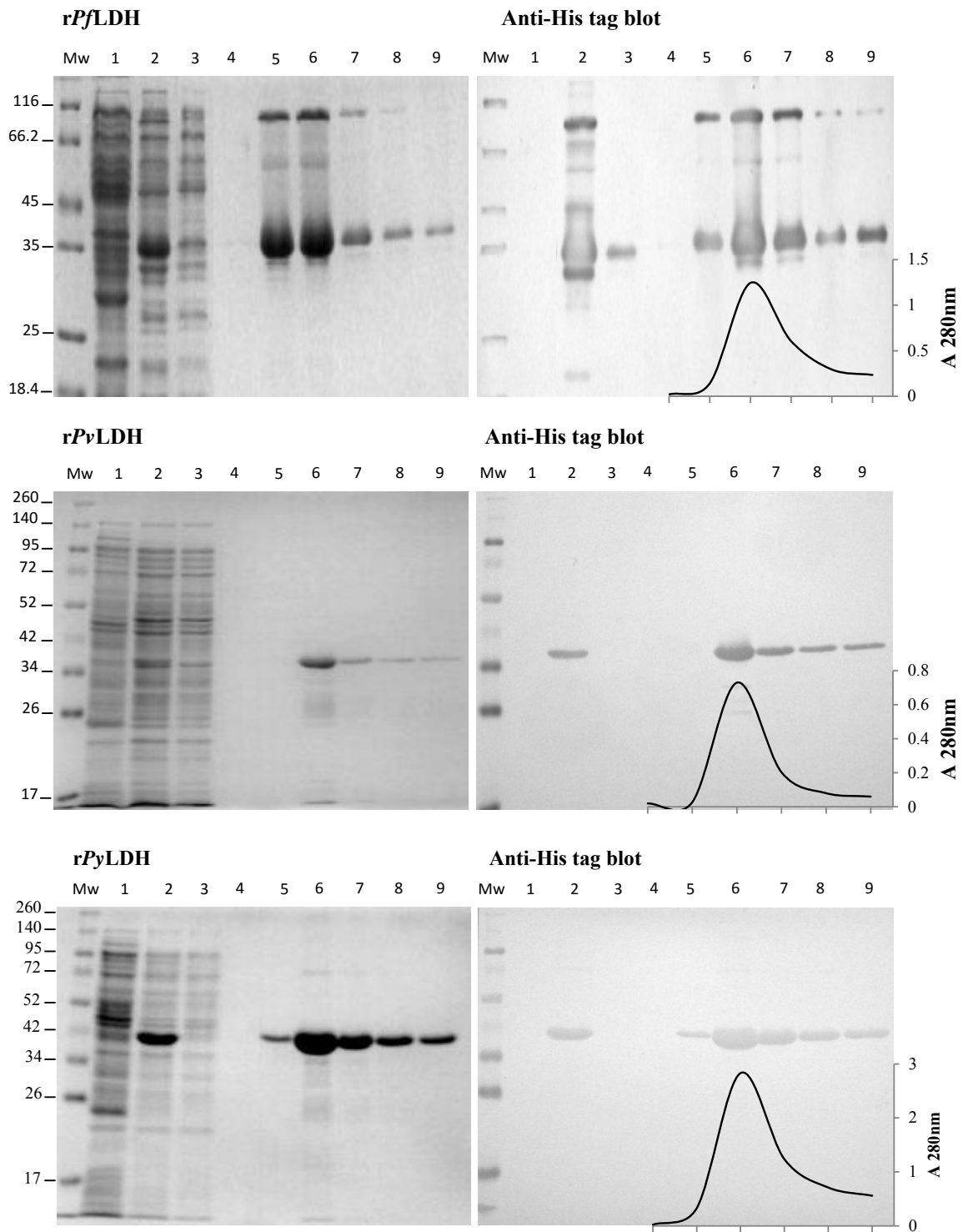


Figure 4.9 Recombinant expression and affinity purification of *Pf*, *Pv* and *Py*LDH analysed by SDS-PAGE and western blot

All three recombinant proteins were expressed in *E. coli* BL21(DE3) cells. The His-tagged proteins were affinity purified using a TALON[®] (Co²⁺) resin and the purification steps were analysed on 12.5% reducing SDS-PAGE gels (left panel) and probed with an anti-His tag mouse monoclonal antibody at 1/10000 dilution and a secondary goat anti-mouse-HRPO antibody at 1/6000 dilution (right panel). The elution profiles measuring absorbance at 280 nm were shown as inserts in the respective western blots. The lanes were loaded with molecular weight marker (Mw); BL21(DE3) untransformed cell lysate (lane 1); supernatant sample loaded onto the TALON[®] (Co²⁺) resin (lane 2); unbound lysate (lane 3); 10 mM imidazole wash sample (lane 4); eluents 1 to 5 using 250 mM imidazole (lanes 5 to 9).

The recombinant *Pf*LDH had an estimated molecular weight of ~ 37 kD in the anti-His blot, with an additional protein band at ~ 84 kD, suggesting the presence of a dimeric form of the protein. Two additional minor bands of ~ 35 kD and ~ 63 kD were also detected (Figure 4.9). None of the untransformed *E. coli* BL21(DE3) lysate proteins (lane 2, Figures 4.9) were detected in any of the western blots probed with anti-His tag antibodies. Recombinant *Pv*LDH was detected as a single band of approximately 39 kD, where *rPy*LDH was similarly detected at ~ 40 kD, with low concentrations of a dimer at around 90 kD. The overall yield of the *rPf*LDH may have been improved further since the protein was still detected in the unbound fraction, suggesting the TALON[®] (Co²⁺) resin may have been saturated.

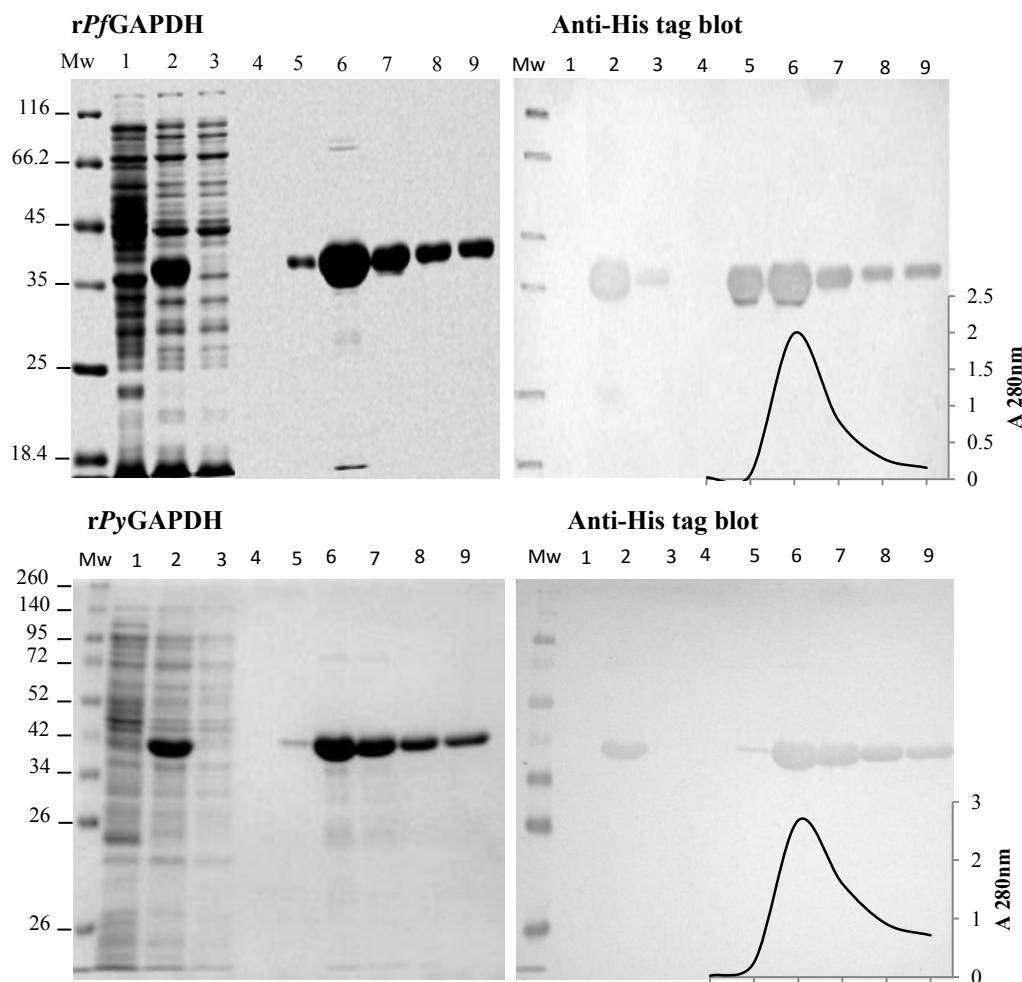


Figure 4.10 Recombinant expression and affinity purification of *Pf* and *Py*GAPDH analysed by SDS-PAGE and western blot

Both recombinant proteins were expressed in *E. coli* BL21(DE3) cells. The His-tagged proteins were affinity purified using a TALON[®] (Co²⁺) resin and the purification steps were analysed on 12.5% reducing SDS-PAGE gels (left panel) and probed with an anti-His tag mouse monoclonal antibody at 1/10000 dilution and a secondary goat anti-mouse-HRPO antibody at 1/6000 dilution (right panel). The elution profiles measuring absorbance at 280 nm were shown as inserts in the respective western blots. The lanes were loaded with molecular weight marker (Mw); BL21(DE3) untransformed cell lysate (lane 1); supernatant sample loaded onto the TALON[®] (Co²⁺) resin (lane 2); unbound lysate (lane 3); 10 mM imidazole wash sample (lane 4); eluents 1 to 5 using 250 mM imidazole (lanes 5 to 9).

The recombinant *Pf*GAPDH protein had an estimated molecular mass of 38 kD, where *rPy*GAPDH was detected at ~ 40 kD. Similarly to the *rPf*LDH result, some *rPf*GAPDH was detected in the unbound sample run in lane three (Figure 4.10), suggesting some of the protein was unable to bind the TALON[®] (Co²⁺) resin. This was also the case for both *rPf*PMT and *rPv*PMT as shown in Figure 4.11. The *rPf*PMT was detected at ~ 29 kD and the *rPv*PMT at ~30 kD in their respective blots.

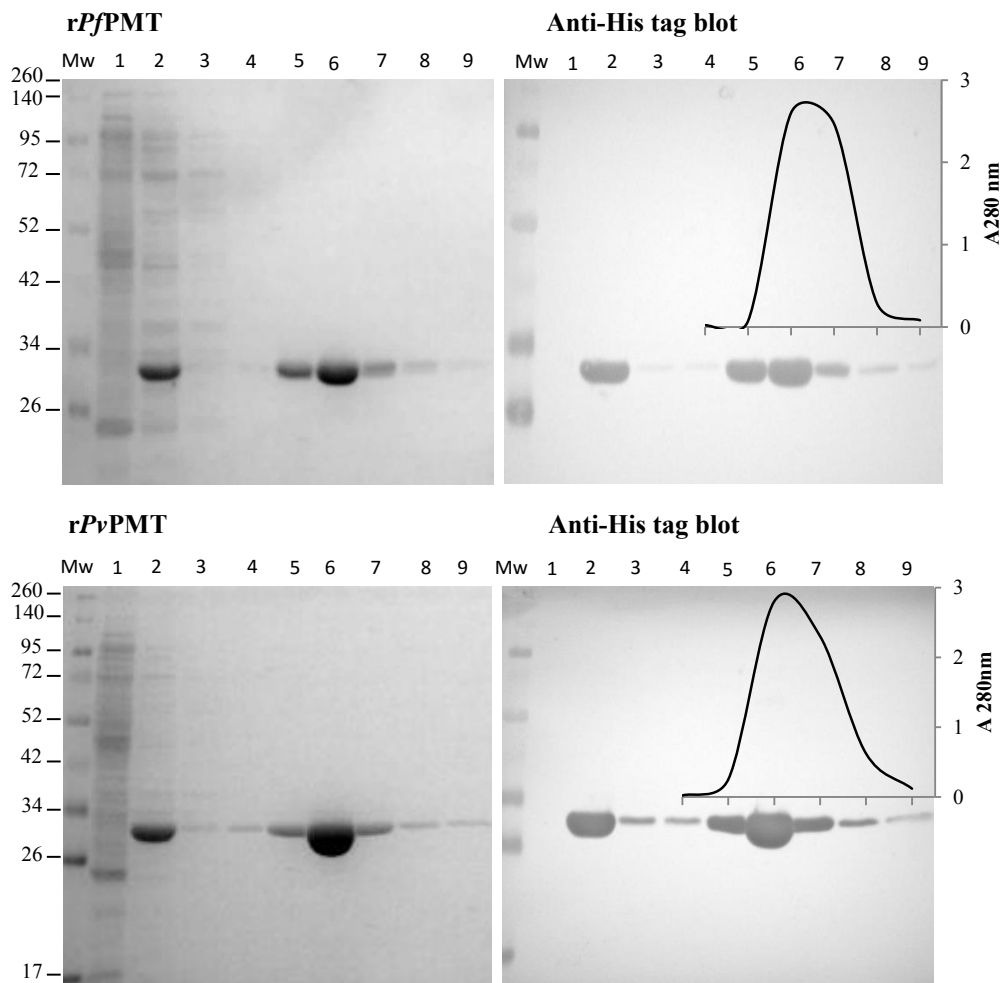


Figure 4.11 Recombinant expression and affinity purification of *Pf* and *Pv*PMT analysed by SDS-PAGE and western blot

Both recombinant proteins were expressed in *E. coli* BL21(DE3) cells. The His-tagged proteins were affinity purified using a TALON[®] (Co²⁺) resin and the purification steps were analysed on 12.5% reducing SDS-PAGE gels (left panel) and probed with an anti-His tag mouse monoclonal antibody at 1/10000 dilution and a secondary goat anti-mouse-HRPO antibody at 1/6000 dilution (right panel). The elution profiles measuring absorbance at 280 nm were shown as inserts in the respective western blots. The lanes were loaded with molecular weight marker (Mw); BL21(DE3) untransformed cell lysate (lane 1); supernatant sample loaded onto the TALON[®] (Co²⁺) resin (lane 2); unbound lysate (lane 3); 10 mM imidazole wash sample (lane 4); eluents 1 to 5 using 250 mM imidazole (lanes 5 to 9).

4.2.6 Assessing the recombinant *Plasmodium* proteins' native structures

The next experiments were performed to assess the size of the recombinant proteins' structures to determine whether they had similar sizes in solution as they are predicted to have within the parasites themselves (compare to Table 4.1). LDH and GAPDH are both known to form tetramers in solution for example, where PMT is a monomer. Figures 4.12 to 4.19 therefore show results of molecular exclusion chromatography (MEC) for each of the proteins as well as an activity assay performed with both *rPfLDH* and *rPvLDH*.

For the MEC experiments a Sephacryl S-200 column was used as it has a separation range of 5000 to 250000 Da. The column was calibrated with the elution profile shown in Figure 4.12 (A). The resulting standard curve used to estimate the sizes of the recombinant protein eluents was shown in (B).

The first of the recombinant proteins assessed was *rPfLDH*, which ran at ~ 37 kD on the reducing SDS-PAGE gel shown previously (Figure 4.9). The recombinant protein eluted with an estimated molecular mass of 145 kD (Figure 4.13 (A)). This was close to the calculated tetrameric size of 148 kD (4 x 37 kD). In comparison *rPvLDH* eluted with an estimated molecular mass of 95 kD (Figure 4.14). It ran as a 39 kD band on reducing SDS-PAGE previously (Figure 4.9) which suggests it eluted as a dimeric protein close to an estimated molecular mass of 78 kD (2 x 39 kD). Finally *rPyLDH* eluted with an estimated molecular mass of 112 kD (Figure 4.15). This was close to a trimeric form estimated from its molecular mass determined by SDS-PAGE of 41 kD (Figure 4.9).

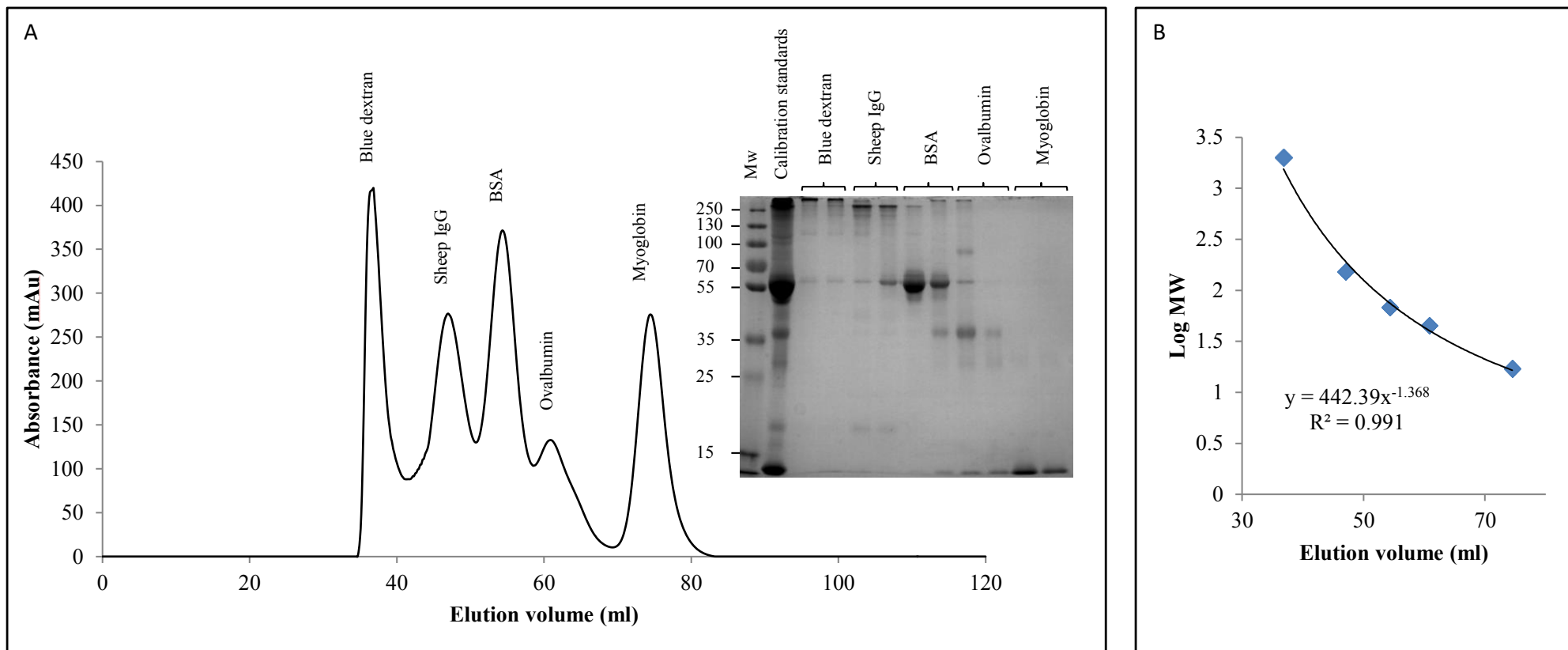


Figure 4.12 Calibration of the Sephacryl S-200 molecular exclusion chromatography column

The HiPrep 16/60 pre-packed Sephacryl S-200 High Resolution column (column volume of 120 ml) was calibrated using the following standards: 3 mg Blue Dextran (2000 kD); 5 mg Sheep IgG (150 kD); 5 mg BSA (68 kD); 5 mg Ovalbumin (45 kD); 5 mg Myoglobin (17 kD), and the profile was recorded on the ÄKTAprime plus system (A), with the standards and their respective peaks analysed on a 12.5% reducing SDS-PAGE gel (insert in A). The column was run at 0.5 ml/min and 2 ml fractions were collected, with a total of 120 ml run over the column per run using a 50 mM NaH₂PO₄, 300 mM NaCl pH 8.0 buffer. Standard curve of molecular weights in (B).

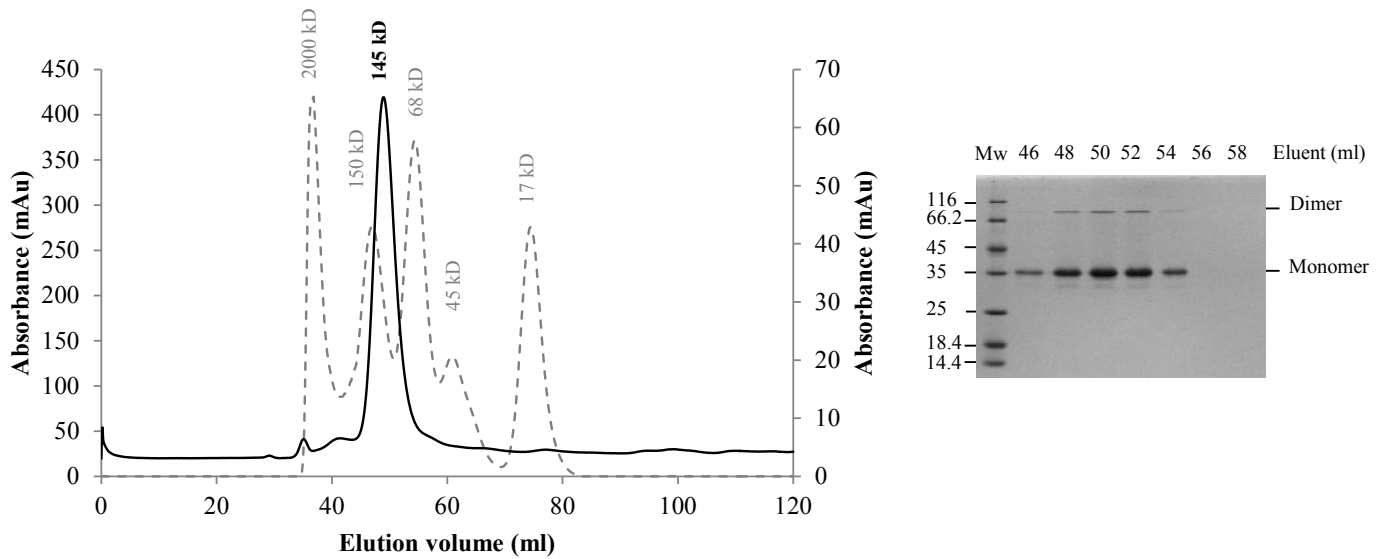


Figure 4.13 *rPfLDH* elution profile over a Sephacryl S-200 MEC column

Four milligrams of affinity purified *rPfLDH* was passed over a HiPrep 16/60 pre-packed Sephacryl S-200 high resolution column with a column volume of 120 ml, using a 50 mM NaH₂PO₄; 300 mM NaCl pH 8.0 running buffer. The profile was recorded on the ÄKTAprime plus system using milli Absorbance units (mAu) labelled on the primary and secondary axes (A). The solid line depicts the *rPfLDH* elution profile (plotted on the secondary axis), with the calibration standards included as the dashed line (plotted on the primary axis). The eluted fractions comprising the ~145 kDa peak were evaluated on a 12.5% reducing SDS-PAGE gel stained with Coomassie blue (B). The lanes were labelled as follows: molecular weight marker (Mw), followed by the respective 2 ml eluents 46 to 58, with the dimeric and monomeric forms labelled alongside the gel.

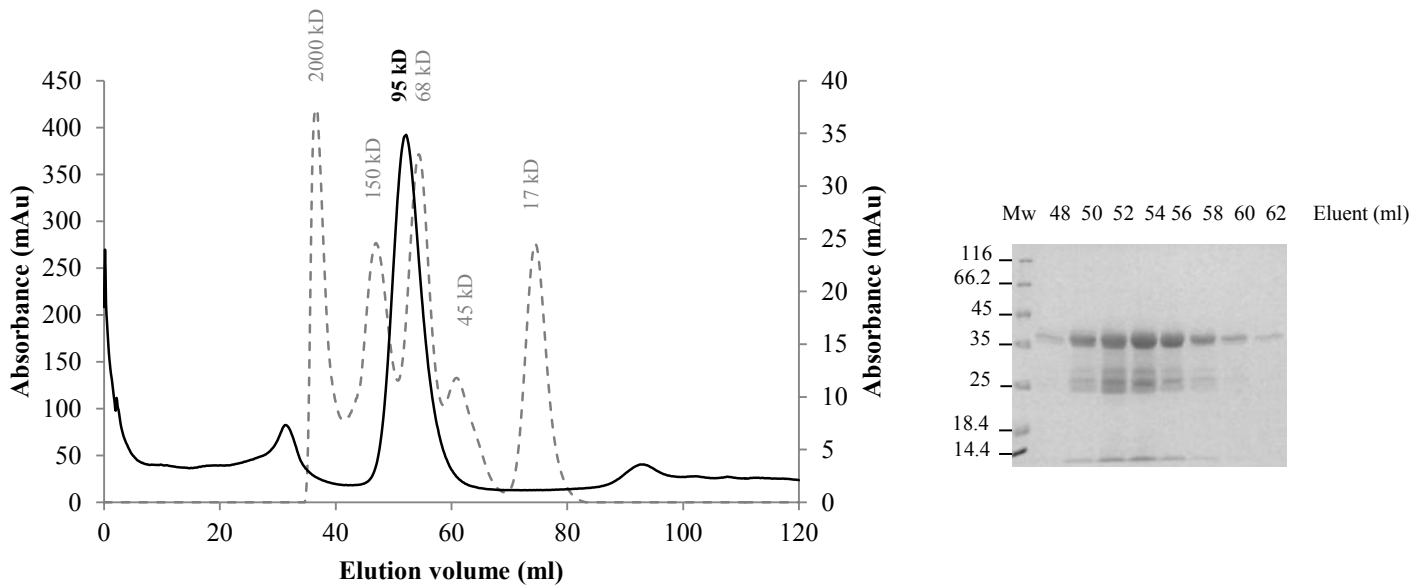


Figure 4.14 *rPvLDH* elution profile over a Sephacryl S-200 MEC column

Four milligrams of affinity purified *rPvLDH* was passed over a HiPrep 16/60 pre-packed Sephacryl S-200 high resolution column with a column volume of 120 ml, using a 50 mM NaH₂PO₄; 300 mM NaCl pH 8.0 running buffer. The profile was recorded on the ÄKTAprime plus system using milli Absorbance units (mAu) labelled on the primary and secondary axes (A). The solid line depicts the *rPvLDH* elution profile (plotted on the secondary axis), with the calibration standards included as the dashed line (plotted on the primary axis). The eluted fractions comprising the ~95 kDa peak were run on a 12.5% reducing SDS-PAGE gel and Coomassie stained (B). The lanes were labelled as follows: molecular weight marker (Mw), followed by the respective 2 ml eluents 48 to 62.

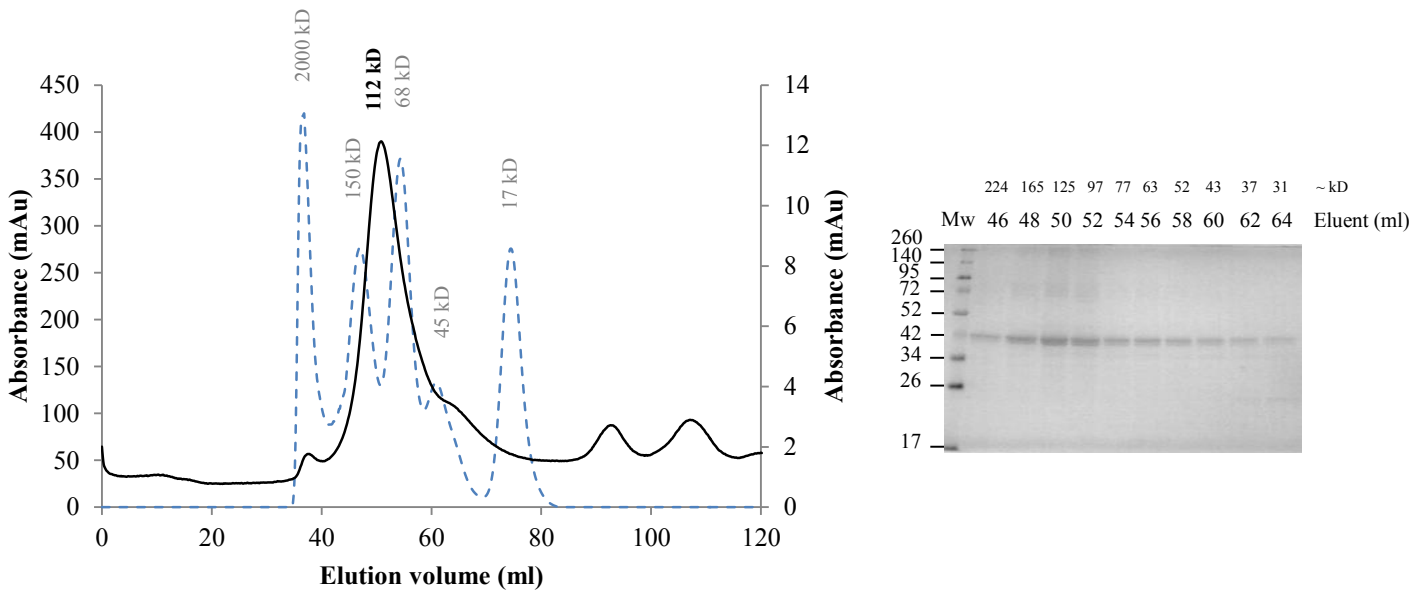


Figure 4.15 rPyLDH elution profile over a Sephacryl S-200 MEC column

Four milligrams of affinity purified rPyLDH was passed over a HiPrep 16/60 pre-packed Sephacryl S-200 high resolution column with a column volume of 120 ml, using a 50 mM NaH_2PO_4 ; 300 mM NaCl pH 8.0 running buffer. The profile was recorded on the ÄKTAprime plus system using milli Absorbance units (mAu) labelled on the primary and secondary axes (A). The solid line depicts the rPyLDH elution profile (plotted on the secondary axis), with the calibration standards included as the dashed line (plotted on the primary axis). The eluted fractions comprising the ~112 kDa peak were run on a 12.5% reducing SDS-PAGE gel and Coomassie stained (B). The lanes were labelled as follows: molecular weight marker (Mw), followed by the respective 2 ml eluents 46 to 64.

As further confirmation of the native conformation of the rPjLDH and rPvLDH, dehydrogenase activity of both proteins was demonstrated as shown in Figure 4.16. The oxidation of L-lactate by LDH producing NADH was measured at 340 nm, showing an increase of NADH over time.

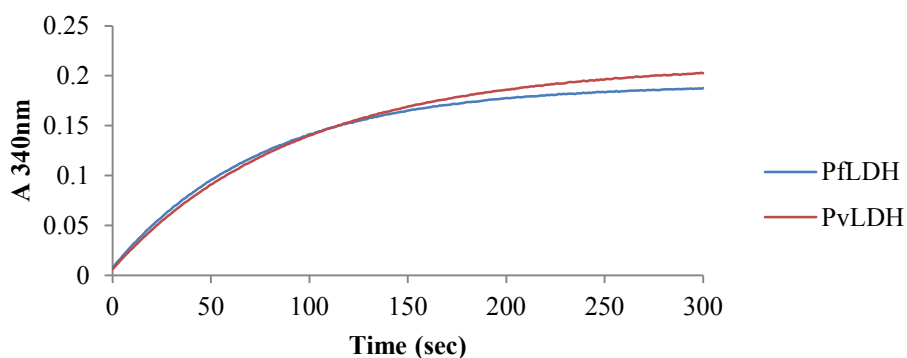


Figure 4.16 Enzyme activity of both recombinant PjLDH and PvLDH assessed by measuring the increased formation of NADH due to the oxidation of L-lactate

Recombinant PjLDH and PvLDH both displayed dehydrogenase activity with the oxidation of L-lactate (1mM) resulting in the concomitant reduction of NAD (200 μM) to NADH. The increased NADH was measured as an increase in absorbance at 340 nm over a 5 min period. 35 μM of each of the recombinant proteins was used and the reactions were performed in a 100 mM Tris pH 9.0 buffer at 25°C. The control reaction without recombinant LDH or with 35 μM BSA instead remained at 0 even after 20 min.

Under native conditions the purified *rPf*GAPDH eluted in two peaks estimated at 148 kD and 36 kD from the Sephacryl column. Comparing this to the SDS-PAGE result in Figure 4.10 where *rPf*GAPDH was detected at ~ 38 kD, the eluted peak of 148 kD was close to the expected tetrameric form and that of 35 kD was close to the monomeric form. Interestingly the monomer in the SDS-PAGE gel (B) ran slightly lower at ~ 35 kD than it did in Figure 4.10, although a different molecular weight marker was also used in this case.

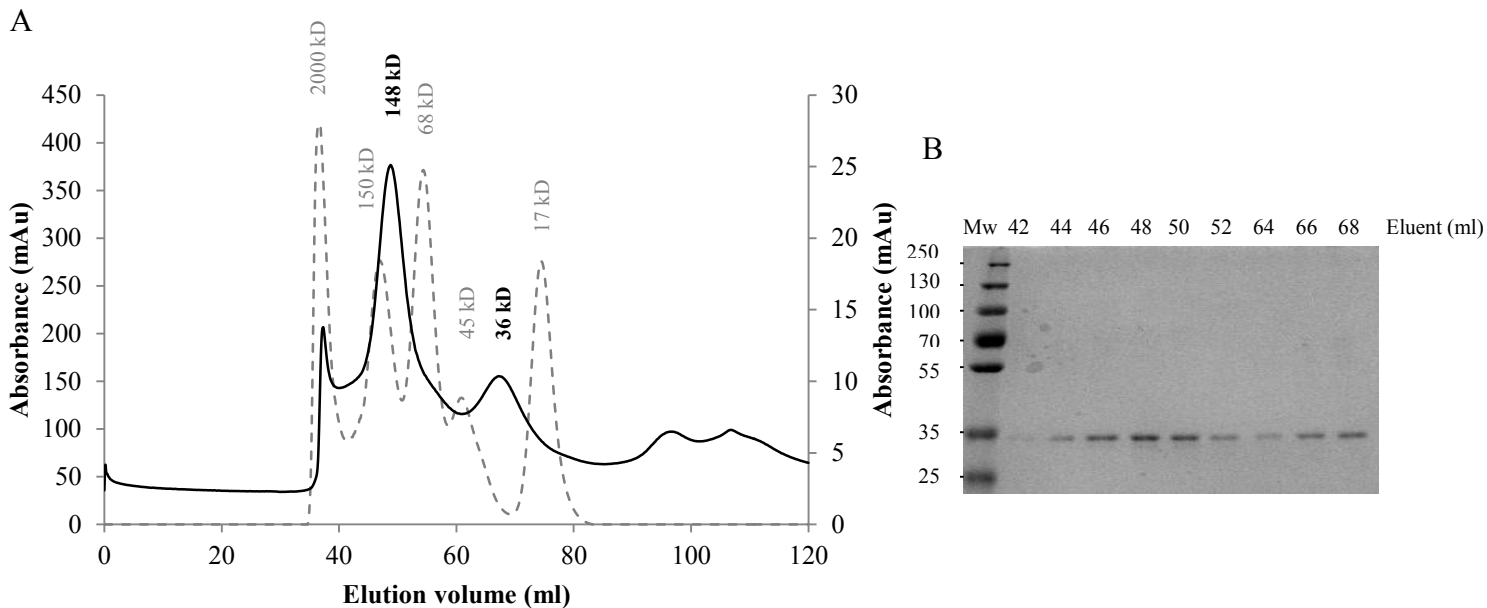


Figure 4.17 *rPf*GAPDH elution profile over a Sephacryl S-200 MEC column

Four milligrams of affinity purified *rPf*GAPDH was passed over a HiPrep 16/60 pre-packed Sephacryl S-200 high resolution column with a column volume of 120 ml, using a 50 mM NaH₂PO₄; 300 mM NaCl pH 8.0 running buffer. The profile was recorded on the ÄKTAprime plus system using milli Absorbance units (mAu) labelled on the primary and secondary axes (A). The solid line depicts the *rPf*GAPDH elution profile (plotted on the secondary axis), with the calibration standards included as the dashed line (plotted on the primary axis). The eluted fractions comprising the ~148 and ~ 36 kDa peaks were run on a 12.5% reducing SDS-PAGE gel and Coomassie stained (B). The lanes were labelled as follows: molecular weight marker (Mw), followed by the respective 2 ml eluents 42 to 52 and 64 to 68.

In comparison *rPy*GAPDH was estimated to be around 41 kD on the SDS-PAGE gel (Figure 4.10), and eluted as an estimated 110 kD protein from the Sephacryl column (Figure 4.17), which suggested trimer formation.

Finally analysis of the PMT proteins revealed that both proteins formed monomers in solution, with *rPf*PMT eluting as an estimated 29 kD protein and *rPv*PMT as a ~ 27 kD protein.

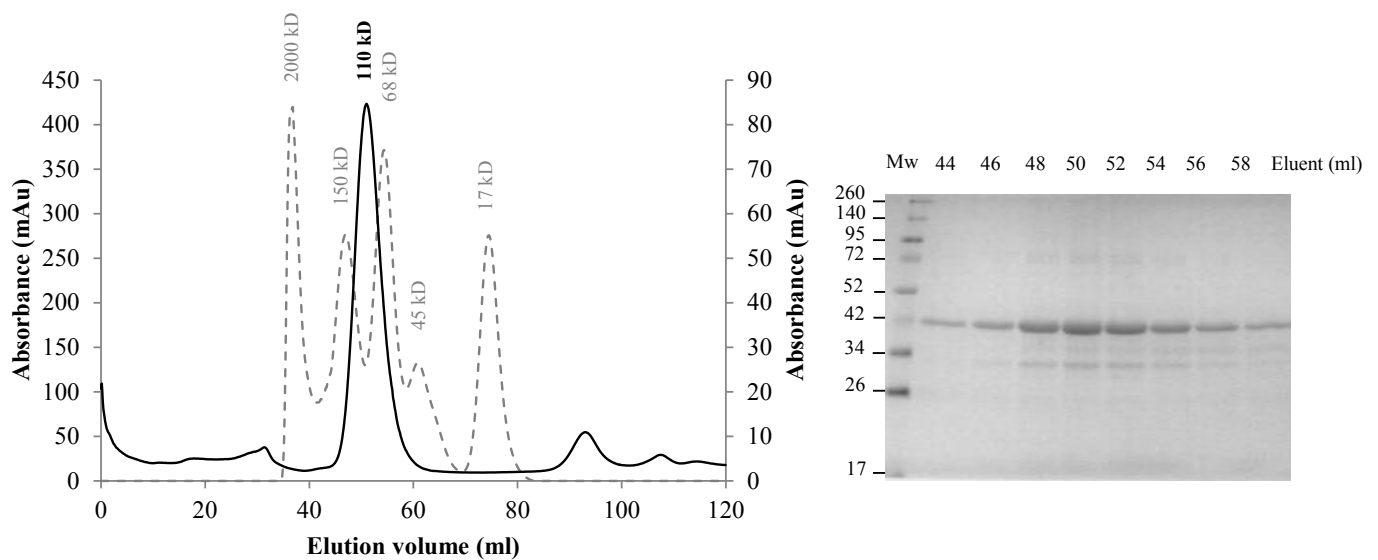


Figure 4.18 *rPyGAPDH* elution profile over a Sephacryl S-200 MEC column

Four milligrams of affinity purified *rPyGAPDH* was passed over a HiPrep 16/60 pre-packed Sephacryl S-200 high resolution column with a column volume of 120 ml, using a 50 mM NaH_2PO_4 ; 300 mM NaCl pH 8.0 running buffer. The profile was recorded on the ÄKTAprime plus system using milli Absorbance units (mAu) labelled on the primary and secondary axes (A). The solid line depicts the *rPyGAPDH* elution profile (plotted on the secondary axis), with the calibration standards included as the dashed line (plotted on the primary axis). The eluted fractions comprising the ~110 kDa peak were run on a 12.5% reducing SDS-PAGE gel and Coomassie stained (B). The lanes were labelled as follows: molecular weight marker (Mw), followed by the respective 2 ml eluents 44 to 58.

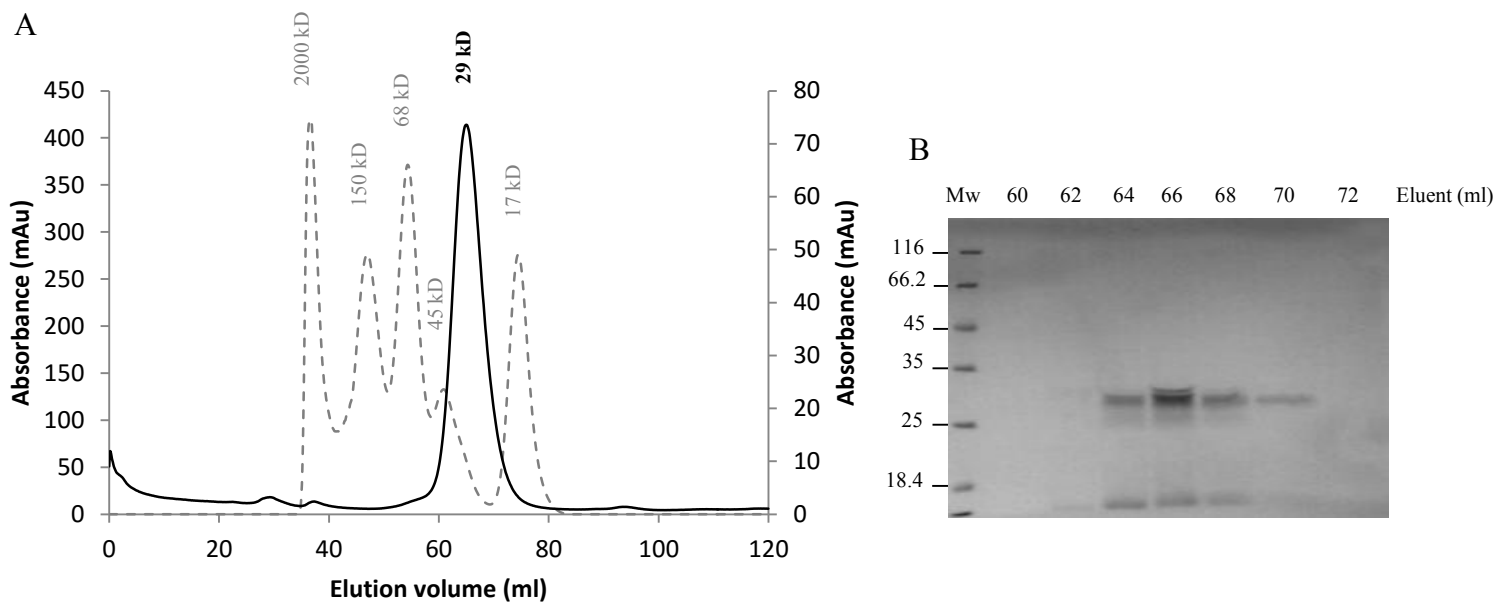


Figure 4.19 *rPfPMT* elution profile over a Sephacryl S-200 MEC column

Four milligrams of affinity purified *rPfPMT* was passed over a HiPrep 16/60 pre-packed Sephacryl S-200 high resolution column with a column volume of 120 ml, using a 50 mM NaH_2PO_4 ; 300 mM NaCl pH 8.0 running buffer. The profile was recorded on the ÄKTAprime plus system using milli Absorbance units (mAu) labelled on the primary and secondary axes (A). The solid line depicts the *rPfPMT* elution profile (plotted on the secondary axis), with the calibration standards included as the dashed line (plotted on the primary axis). The eluted fractions comprising the ~29 kDa peak were run on a 12.5% reducing SDS-PAGE gel and Coomassie stained (B). The lanes were labelled as follows: molecular weight marker (Mw), followed by the respective 2 ml eluents 60 to 72.

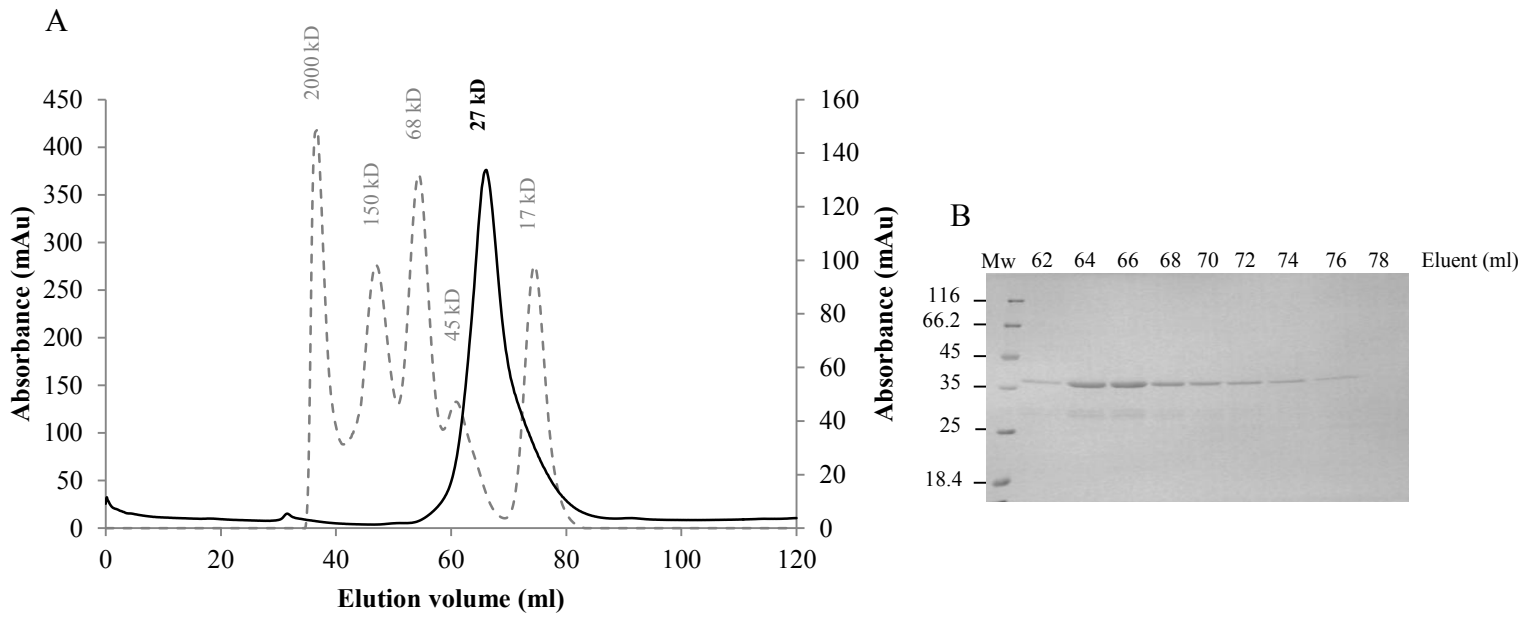


Figure 4.20 *rPvPMT* elution profile over a Sephacryl S-200 MEC column

Four milligrams of affinity purified *rPvPMT* was passed over a HiPrep 16/60 pre-packed Sephacryl S-200 high resolution column with a column volume of 120 ml, using a 50 mM NaH_2PO_4 ; 300 mM NaCl pH 8.0 running buffer. The profile was recorded on the ÄKTAprime plus system using milli Absorbance units (mAu) labelled on the primary and secondary axes (A). The solid line depicts the *rPvPMT* elution profile (plotted on the secondary axis), with the calibration standards included as the dashed line (plotted on the primary axis). The eluted fractions comprising the ~27 kDa peak were run on a 12.5% reducing SDS-PAGE gel and Coomassie stained (B). The lanes were labelled as follows: molecular weight marker (Mw), followed by the respective 2 ml eluents 62 to 78, with their respective estimated molecular weights indicated above the lanes.

4.3 Discussion

E. coli expression host results under the proposed expression and affinity purification conditions

Prior to expression of the recombinant *Plasmodium* proteins as described in this chapter, the effect of the proposed temperatures and media on the untransformed expression host *E. coli* BL21(DE3) cells was assessed. The growth between cultures was very similar, regardless of temperature or media taking approximately 2 hours to reach an O.D. of ~ 0.5 and reaching the stationary phase at around 4 hours. This was comparable to results by Larentis *et al.*, (2014) for their un-induced cultures, although they used *E. coli* BL21 (DE3) Star™/p E cells. The addition of 1 mM IPTG did not seem to have a detrimental effect on the host *E. coli* growth either. Overall none of the transformed cultures were drastically affected by induction of expression since most cultures grew comparably to their uninduced counterparts. This was important since there is usually a positive correlation between expression host growth and final protein yields (Larentis *et al.*, 2014). Reduced growth rates may be expected after expression is induced due to competition for the translation machinery and depletion of biomolecules within the host *E. coli* (Choveaux *et al.*, 2012; Larentis *et al.*, 2014). To maintain selective pressure for transformed host *E. coli*, antibiotics were used here. Unlike ampicillin, kanamycin is not hydrolysed during culture, making it an ideal antibiotic for long term cultures (16 hours). In the initial 16 hour expression experiments *E. coli* cultures transformed with Amp^r plasmids were supplemented with ampicillin every 2 hours to avoid the loss of selection due to hydrolysis of the antibiotic. Busso *et al.* (2008) suggested the joint use of carbenicillin and ampicillin for such long term cultures containing Amp^r plasmids. In doing so, ampicillin imparts an early, strong selective pressure against *E. coli* before it becomes hydrolysed and carbenicillin then maintains the selective pressure over a longer period, thus avoiding periodic supplementation of the cultures. Following optimisation of culture growth, the next step was to optimise the concentration of imidazole used to elute the recombinant proteins off the affinity columns.

Optimising the expression and elution conditions for each of the recombinant proteins

A concentration range of between 150 to 250 mM imidazole is recommended for the elution of recombinant proteins off TALON[®] (Co²⁺) affinity resin. Based on the optimisation data using imidazole gradients, all of the recombinant proteins eluted between 25 to 100 mM imidazole. A similar trend was observed for the elution of the *E. coli* host cell proteins bound

to the columns as the peak eluents were between 50 to 100 mM imidazole. As a result a 10 mM imidazole concentration was used to “wash” the bound *E. coli* host proteins off the column, thus removing *E. coli* proteins bound with low affinity from the bound recombinant proteins which had higher affinity for the TALON[®] (Co²⁺) resin. A 250 mM imidazole concentration was then used to elute the bound recombinant proteins. The purity of the resulting purified recombinant proteins was satisfactory. The results for each of the recombinant proteins will now be discussed in turn.

LDH expression optimisation and confirming native conformation

Starting with rP_fLDH its monomeric form was close to that detected by Hurdayal *et al.* (2010) and Turgut-Balik *et al.* (2001), where the 145 kD tetramer in this study correlated with that obtained by Berwal *et al.* (2008). Dimeric forms of rP_fLDH after reducing SDS-PAGE were also detected by Hurdayal *et al.* (2010) and Krause *et al.* (2015). Dimer formation under reducing SDS-PAGE conditions is not uncommon as recombinant *P. falciparum* glutamate dehydrogenase was similarly detected as a dimer by Zocher *et al.* (2012). The lower molecular weight band detected in the rP_fLDH blot has been noted previously and is thought to be a truncated form of the protein due to an internal Shine Dalgarno sequence (GGAGGA) located between bases 46 to 51 in the coding sequence of the protein (Hurdayal *et al.*, 2010). Since two histidine tags were added to the coding sequence, the loss of one of these tags would still have allowed for the purification and subsequent detection of the recombinant protein on the anti-His tag blot. The rP_vLDH expressed here was close to that detected in the Hurdayal *et al.* (2010) and Turgut-Balik *et al.* (2004) studies who detected it at 34 kD. Although the native form eluted as a dimeric form and not the expected tetrameric form, the enzyme was still active. Both the recombinant *P. falciparum* and *P. vivax* LDH orthologs were therefore shown to be enzymatically active despite the presence of the additional His tags, which supported findings by Berwal *et al.* (2008) and Gomez *et al.* (1997). Yamamoto and Storey (1988) observed that human LDH tetramer and dimer formation were influenced by lactate or pyruvate concentrations respectively, where lactate promoted tetramer formation and pyruvate promoted dimer formation. Both forms were enzymatically active as well. With regard to the enzyme assay used here, since a low concentration of NAD was used (1 mM), this meant that the maximum absorbance of the reaction, if all NAD was reduced to NADH, would be approximately 0.16 at 340 nm (NADH $\epsilon = 6.22 \text{ mM}^{-1} \text{ cm}^{-1}$). The recombinant LDH enzymes therefore depleted all available NAD after ~140 seconds, hence the plateau of the A 340 nm readings after this point, with both

enzymes showing very similar activity curves. The rPyLDH protein detected here around 40 kD ran at a slightly larger size than the 39 kD band detected by Hurdayal *et al.* (2010). The addition of the His-tag from the pET-28(a) vector (36 amino acids approximately 3.7 kD) gives a calculated size of 37.7 kD from the native protein size. The 112 kD eluent from the MEC column suggests a trimeric form in solution.

GAPDH expression optimisation and confirming native conformation

The 38 kD monomer of rPfGAPDH was close to that purified by Satchell *et al.* (2005) and Daubenberger *et al.* (2003) who both recorded sizes of around 37 kD. The ~ 148 kD tetrameric form found here was larger than that obtained by Satchell *et al.* (2005) who isolated a ~130 kD form, but agreed with that of Sangolgi *et al.* (2016) and the predicted size from PlasmoDB. The size of the rPyGAPDH monomer of approximately 40 kD was close to the calculated size of ~ 40.7 kD resulting from the addition of the N-terminal His-tag (36 amino acids correlating to approximately 3.7 kD). This was close to the band detected by Sangolgi *et al.* (2016) in *P. yoelii* lysates. A trimeric form eluted from the MEC column, similar to the trimeric form of rPyLDH.

PMT expression optimisation and confirming native conformation

Finally the PMT species eluted from the MEC column showed that both the rPfPMT and rPyPMT proteins remained as monomers in solution which agreed with PlasmoDB (www.plasmodb.org) and previous expression data (Pessi *et al.*, 2004; Garg *et al.*, 2015).

These results are the first to our knowledge describing the expression of these proteins using auto-induction media. Interestingly the expression of rPfPMT was very low when grown in auto-inducing terrific broth, but was optimal for rPfGAPDH even though both were expressed from the same pET-15b plasmid vector. Overall the proteins expressed and purified in this chapter all correlated closely with their respective native sizes as well as their reduced monomeric forms. The results therefore support the further use of these recombinant forms of the *Plasmodium* target proteins for raising immune reagents in chapters 5 and 6 to follow.

Chapter 5

Assessment of polyclonal IgY raised against both the recombinant *Plasmodium* proteins and peptide targets of LDH, GAPDH and PMT

5.1 Introduction

The aim of the work described in this chapter was to raise polyclonal antibodies against the potential *Plasmodium* diagnostic target proteins and peptides identified in chapter 3. Two sets of antibodies were raised, the first against the peptide epitopes identified in chapter 3 which were synthesized and coupled to rabbit albumin as a carrier protein and the second against the whole recombinant proteins expressed and purified in chapter 4. The second aim was to assess all the antibodies and test if they cross-reacted with uninfected human red blood cell or *E. coli* BL21(DE3) expression host cell lysate proteins and to demonstrate their use in a double antibody sandwich ELISA assay mimicking a rapid diagnostic test system.

Antibodies are glycoproteins expressed by B-cells of the adaptive immune systems in all jawed vertebrates including fish, amphibians, reptiles, birds and mammals (Marchalonis *et al.*, 2006; Sun *et al.*, 2008). In mammals these proteins are divided into five classes IgG, IgD, IgE, IgA and IgM. In chickens only three classes are expressed where the equivalent of IgG is known as IgY and is found in serum as well as egg yolk and hence called yolk immunoglobulin (IgY) (Polson *et al.*, 1985). IgA and IgM form the two other classes of the chicken repertoire (Sun *et al.*, 2008). Since polyclonal IgY was raised in chickens against the targets in this study and monoclonal IgG is usually used in rapid diagnostic tests (Makler *et al.*, 1998; Murray *et al.*, 2008), only IgG and IgY will be discussed further. These two molecules are heterodimers comprising two heavy and two light chains. The light chains are separated into two domains in both cases, where the heavy chains of IgG and IgY consist of four domains, but IgY lacks a hinge region between the third and fourth domains unlike IgG (Sun *et al.*, 2008). The C-terminal domains of IgG and IgY are constant and the heavy chains form the Fc portion responsible for the effector functions of antibodies. The N-terminal domains, consisting of approximately 50 amino acids each, are variable and referred to as the variable heavy (V_H) and variable light (V_L) chains (van Regenmortel, 1993). It is these variable domains that are responsible for binding of antibodies to antigens. Both V_H and V_L form complementarity determining regions also known as the paratope which bind a 15 amino acid region known as an epitope on the antigen (Benjamin and Perdue, 1996).

Importantly the paratope allows an epitope with complementary characteristics including charge, shape and size resulting from its amino acid composition to bind to it. Of the 15 amino acids of the para- and epitope the main binding energy is between as few as five key residues of both sequences (Benjamin and Perdue, 1996; Dougan *et al.*, 1998).

A paratope may therefore bind a range of linear epitopes with varying affinities (Figure 5.1 (A)) as well as conformational epitopes formed by the specific quaternary folding of a protein antigen (Figure 5.1 (B)) (van Regenmortel, 1993). This means that antibodies may recognise unrelated antigens, which is commonly termed cross reactivity. Potential antibody cross reactivity based on linear epitopes can be predicted *in silico* to some extent using BLAST analyses as done in chapter 3, however cross reaction due to conformational epitopes needs to be assessed experimentally as was done here. An example of both types of cross reactivity was shown in Figure 5.1.

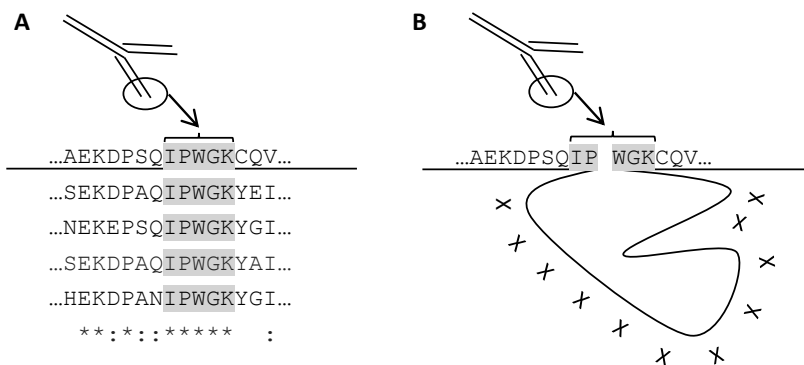


Figure 5.1 An illustration of potential cross reactivity caused by linear and conformational epitopes recognised by a hypothetical antibody

One of the specific peptide epitopes (WGK) chosen for *PfGAPDH* was used as an example, where (A) represents the linear epitopes within the five *Plasmodium* species infective to man (see Table 3.4) with the corresponding identities of each amino acid annotated as “*” being identical residues; “:” conserved and “.” semi-conserved residues and blank spaces noting no identity. In (B) an example of a conformational epitope was illustrated where “X” represents any amino acid residue within the hypothetical protein. The circled region of the “Y”-like structure above each amino acid sequence represents a hypothetical antibody binding region (paratope) where five conserved amino acid residues within the peptide epitopes are highlighted which may cause cross reactivity.

Initially antibodies were raised in chickens, which had several advantages. Since chickens package antibodies in egg yolk (IgY) to aid the development and immunity of the growing chick, this IgY can be purified from the yolk avoiding invasive bleeding (Polson *et al.*, 1985). Chickens are easily kept and eggs can be collected and stored for long periods at 4°C. Eggs collected and stored during weeks of peak antibody titres can then be used for IgY isolation which avoids isolating IgY from eggs each week, saving time and reagents. IgY yields from eggs in a single week are equivalent to weekly yields from much larger mammals such as horses or cattle, and chickens are easier and cheaper to keep (Li *et al.*, 2015a). Due to the evolutionary distance between humans and avian species, the Fc-domain of IgY is not

recognised by human Fc receptors, complement system or Rheumatoid factor which should avoid cross-reactivity in immunoassays (Delves *et al.*, 2006). Importantly false positive reactions can be a problem with some rapid diagnostic tests due to cross reactivity of IgG-Fc domains with Rheumatoid factor (Iqbal *et al.*, 2000) which would not be the case with IgY antibodies.

In order to refine the specificity of antibodies, chickens were immunised with the selected peptide epitopes coupled to rabbit albumin as a carrier protein (Hurdayal *et al.*, 2010; Tomar *et al.*, 2006). This was necessary since the peptides, which ranged from 11 to 17 amino acids in length, were too small to elicit an immune response by themselves (Borras-Cuesta *et al.*, 1987). The coupling chemistry involved a heterobifunctional cross linker, maleimidobenzoyl-N-hydroxysuccinimide ester (MBS) which coupled the peptide via the sulfhydryl of the added cysteine to an amine on the surface of rabbit albumin (Hurdayal *et al.*, 2010). This is an advantage of using peptides for antibody production, since there is no need to recombinantly express or purify the native target protein to produce antibodies. Using peptide epitopes, however, does not allow for production of potentially high avidity antibodies recognising specific conformational epitopes on the surface of a target antigen (Figure 5.1). The simplicity of using synthetic peptides for antibody production is appealing, but peptide solubility may be a concern in some instances. Poor solubility due to hydrophobic residues within peptides may result in these regions clumping together in an aqueous environment resulting in the precipitation of the peptides. Lateef *et al.* (2007) described an alternate method for the coupling of such “problematic” peptides and this was employed here for one of the GAPDH peptides (the CAD peptide).

Since LDH and GAPDH are both conserved metabolic proteins found in the *Plasmodium* and human genomes that share identity between these species’ orthologues (as argued in chapter 3), they potentially also share epitopes, both linear and conformational in nature. The concern with such targets is that antibodies raised against them may cross react with the human orthologues due to their similarity. With regard to PMT, a protein absent from the human genome, cross reactivity was not expected (Pessi *et al.*, 2004). Human antibodies may interfere with RDT detection as shown with HRP2 (Ho *et al.*, 2014). For this reason a human anti-malaria hyperimmune serum pool was assessed for the presence of antibodies against rPfLDH, rPfGAPDH and rPfPMT.

5.2 Results

5.2.1 Assessing the specificity of the IgY antibodies raised against rPfLDH and the selected LDH peptides

Polyclonal antibodies were raised against the whole recombinant *Plasmodium* target proteins or against their respective peptide targets. The antibodies were raised in chickens and isolated from egg yolk in the form of IgY. The data for antibody production and affinity purification of antibodies raised in this study were included here, where the data of antibodies raised previously can be found in the publications by Hurdayal *et al.* (2010) and Krause *et al.* (2015). All antibodies used in this study were assessed by western blot for 1) cross-reactivity against uninfected O⁺ red blood cell and *E. coli* BL21(DE3) expression host lysates and 2) specificity against the respective recombinant *Plasmodium* proteins expressed in chapter 4. Starting with the anti-*Plasmodium* LDH antibodies only the western blot results are shown in Figure 5.2.

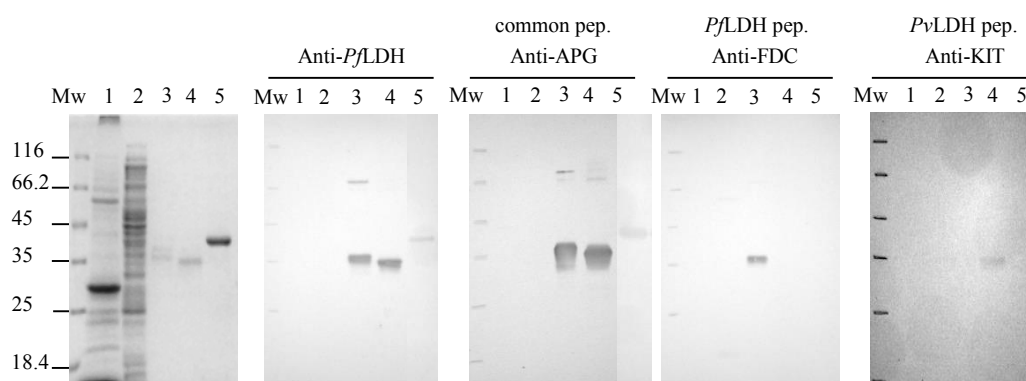


Figure 5.2 Panel of western blots showing specificity of the respective anti-LDH IgY antibodies

The affinity purified IgY against rPfLDH as well as the respective peptide epitopes were assessed for specificity by western blotting. The Coomassie stained reference gel in the far left panel was loaded as follows: Molecular weight marker (Mw); uninfected (O⁺) red blood cell lysate (lane 1); untransformed *E. coli* BL21(DE3) lysate (lane 2); purified rPfLDH (lane 3); purified rPvLDH (lane 4) and purified rPyLDH (lane 5). The blots were probed with the respective affinity purified IgY antibodies as labelled above the blots at 1 µg/ml and rabbit anti-chicken-HRPO at 1 in 12000.

The antibodies raised against recombinant PfLDH detected the *P. falciparum*, *P. vivax* and *P. yoelii* proteins (lanes 3 to 5 respectively). With respect to the antibodies against the common LDH peptide (APG peptide), all three *Plasmodium* proteins were also detected. The antibodies raised against the specific peptides (FDC – *P. falciparum* peptide and KIT – *P. vivax* peptide) only detected their respective recombinant proteins. Importantly none of the antibodies cross-reacted with either the uninfected red blood cell or *E. coli* host cell lysates (lanes 1 and 2 respectively).

5.2.2 Assessing the specificity of the IgY antibodies raised against r*Pf*GAPDH and the selected GAPDH peptides

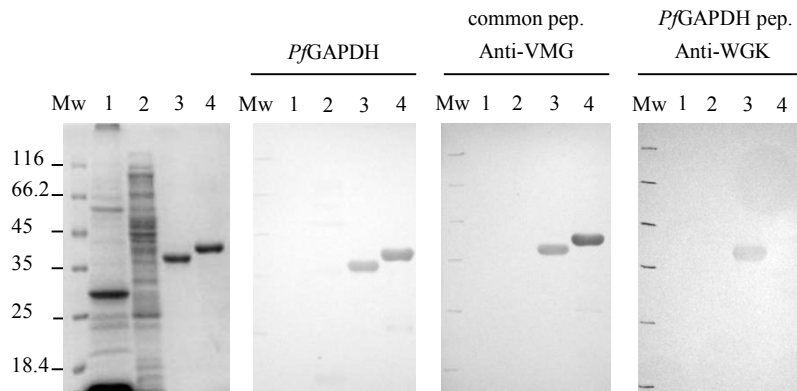


Figure 5.3 Panel of western blots showing specificity of the respective anti-GAPDH IgY antibodies. The affinity purified IgY against r*Pf*GAPDH as well as the respective peptide epitopes were assessed for specificity by western blotting. The Coomassie stained reference gel in the far left panel was loaded as follows: Molecular weight marker (Mw); uninfected (O^+) red blood cell lysate (lane 1); untransformed *E. coli* BL21(DE3) lysate (lane 2); purified r*Pf*GAPDH (lane 3) and purified r*Py*GAPDH (lane 4). The blots were probed with the respective affinity purified IgY antibodies as labelled above the blots at 1 μ g/ml and rabbit anti-chicken-HRPO at 1 in 12000.

The specificity assessment of the GAPDH antibodies was shown in Figure 5.3, whereas the results for the second *P. falciparum* specific peptide (CAD peptide) IgY are shown in Figure 5.4 as these antibodies were raised during this study. The IgY against the whole recombinant *P. falciparum* GAPDH detected both the *P. falciparum* and *P. yoelii* proteins (lanes 3 and 4 respectively) in Figure 5.3. The common peptide antibodies (VMG peptide) detected both protein orthologues as well, where the *P. falciparum* specific peptide (WGK – *P. falciparum* peptide) antibodies only detected the *P. falciparum* protein. None of the antibodies cross-reacted with any of the uninfected red blood cell or *E. coli* expression host proteins.

As for the second *P. falciparum* specific peptide (CAD – *P. falciparum* peptide), the antibody production results, cross-reactivity and specificity are shown together in Figure 5.4. The peptide had low solubility and precipitated as soon as it was diluted into buffer, which did not allow for the use of the Sephadex G-10 column during the coupling reactions with rabbit albumin. For this reason an alternate method described by Lateef *et al.* (2007) was used, which avoids the use of size exclusion chromatography. To assess the coupling success, the rabbit albumin-peptide coupled product was run in comparison to naïve rabbit albumin and the higher molecular weight products were evidence of successful coupling (panel A), where

a minimum of six and more than 24 peptides were coupled resulting in the three higher molecular weight bands highlighted by the arrows alongside the panel.

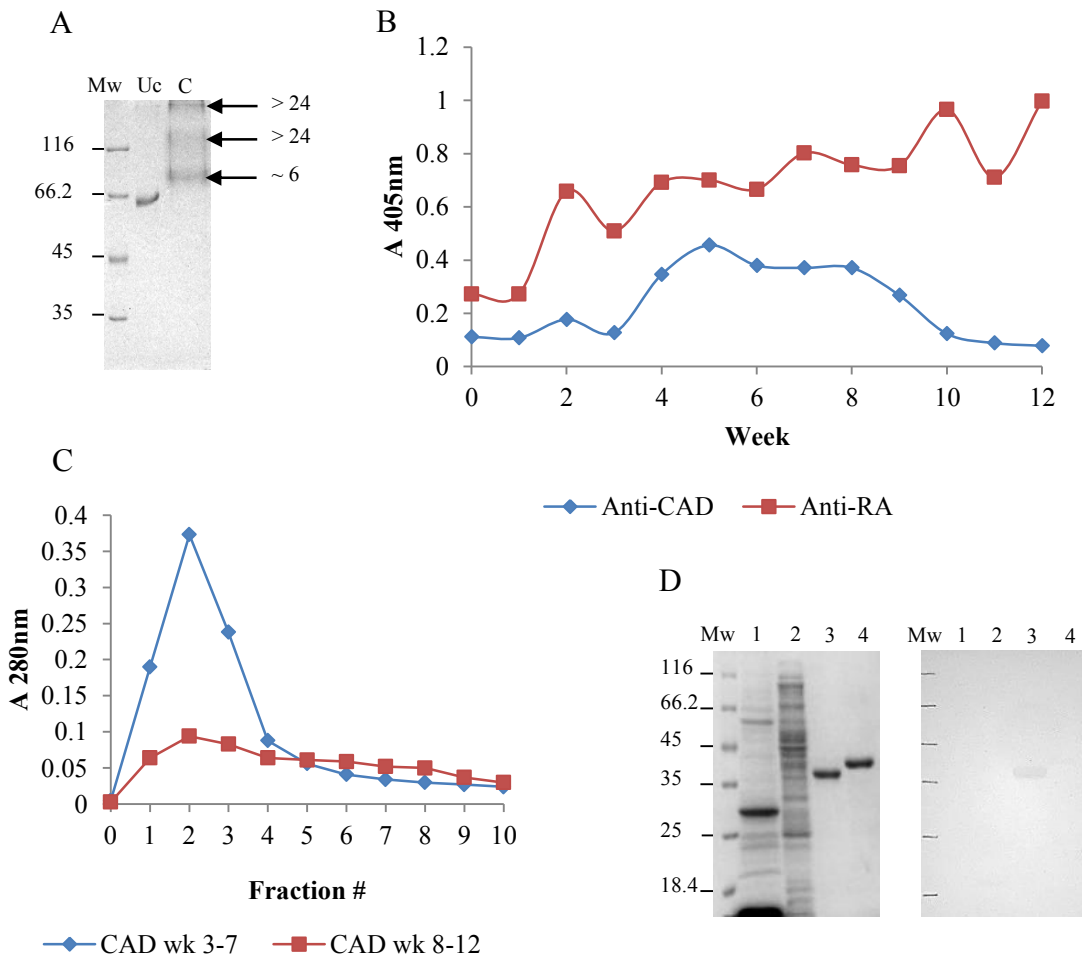


Figure 5.4 Raising and affinity purification of IgY against the *Pf*GAPDH specific peptide (CAD)
 The CAD (CADGFLDIGEKKVSVFA) peptide was coupled to rabbit albumin using the Lateef *et al.* (2007) protocol due to poor solubility of the peptide. The coupled rabbit albumin product was resolved on a 12.5% reducing SDS-PAGE gel, Coomassie stained and shown in (A). Uncoupled RA (lane Uc) was run in parallel to the coupled CAD-RA (lane C), with the molecular weight marker in lane (Mw). The increased MW products were highlighted alongside the gel with the estimated number of peptides coupled per RA molecule based on the size change of the RA bands. Egg antibody levels produced by each chicken were monitored by ELISA (the second chicken died) as shown in (B). Plates were coated with whole *rPf*GAPDH (1 µg/ml) due to the peptide solubility problem, or with RA (1 µg/ml) as a control. Crude IgY at 100 µg/ml and a rabbit anti-chicken-HRPO at 1 in 15000 were used. IgY isolated from weeks 3 to 7 and 8 to 12 were affinity purified over a *rPf*GAPDH AminoLink® column as shown in (C). The final affinity purified IgY was assessed for specificity by western blotting in (D). The Coomassie stained reference gel in the left panel was loaded as follows: Molecular weight marker (Mw); uninfected (O^+) red blood cell lysate (lane 1); untransformed *E. coli* BL21(DE3) lysate (lane 2); purified *rPf*GAPDH (lane 3) and purified *rPy*GAPDH (lane 4). The blot was probed with anti-CAD affinity purified IgY at 1 µg/ml and rabbit anti-chicken-HRPO at 1 in 12000.

Two chickens were immunised with the conjugated rabbit albumin, but unfortunately one of the chickens stopped laying eggs and died. The antibody production of the remaining chicken

was monitored by ELISA. Antibody levels detecting whole recombinant *Pf*GAPDH increased between weeks three and four, and started to decline between weeks nine and ten (panel B), although antibodies against rabbit albumin alone remained high until week 12. The resulting affinity purification data showed greatest yields from the week three to seven IgY pool, with very low yields from the week eight to 12 pool (panel C). For the affinity purification of the specific antibodies, a recombinant *Pf*GAPDH AminoLink[®] was used due to the low solubility of the peptide which did not allow for coupling to a SulfoLink[®] resin. A low overall yield of ~ 1.9 mg total IgY was attained, although the antibodies were specific to *Pf*GAPDH and did not cross react with uninfected red cell lysate or *E. coli* expression host lysate proteins (panel D).

5.2.3 Assessing the specificity of the IgY antibodies raised against rPfPMT, PvPMT and the selected PMT peptides

The next set of antibodies was raised against recombinant *Pf*PMT and *Pv*PMT as well as the respective PMT peptides selected in chapter 3. Recombinant *Pf*PMT as an immunogen generated IgY antibodies as early as week two in the one chicken and after week four in the second, which lasted between 13 to 14 weeks after the primary immunisation in both cases (Figure 5.5, panel A). In both chickens good signal was achieved with titres as low as 25 µg/ml still giving absorbance above 0.2 (all values were already corrected for background). The affinity purification profiles reflected the early antibody production in the first chicken as its yields were slightly greater than the specific IgY yield from the second chicken (panel B). The affinity purified IgY did not cross react with the uninfected red blood cell or *E. coli* host cell proteins, but did detect both recombinant *Pf*PMT and *Pv*PMT (panel C). Finally a ~ 29 kDa protein was detected using ECL in a *Pf*(D10) infected red blood cell culture lysate (panel D) corresponding to the predicted size of *Pf*PMT.

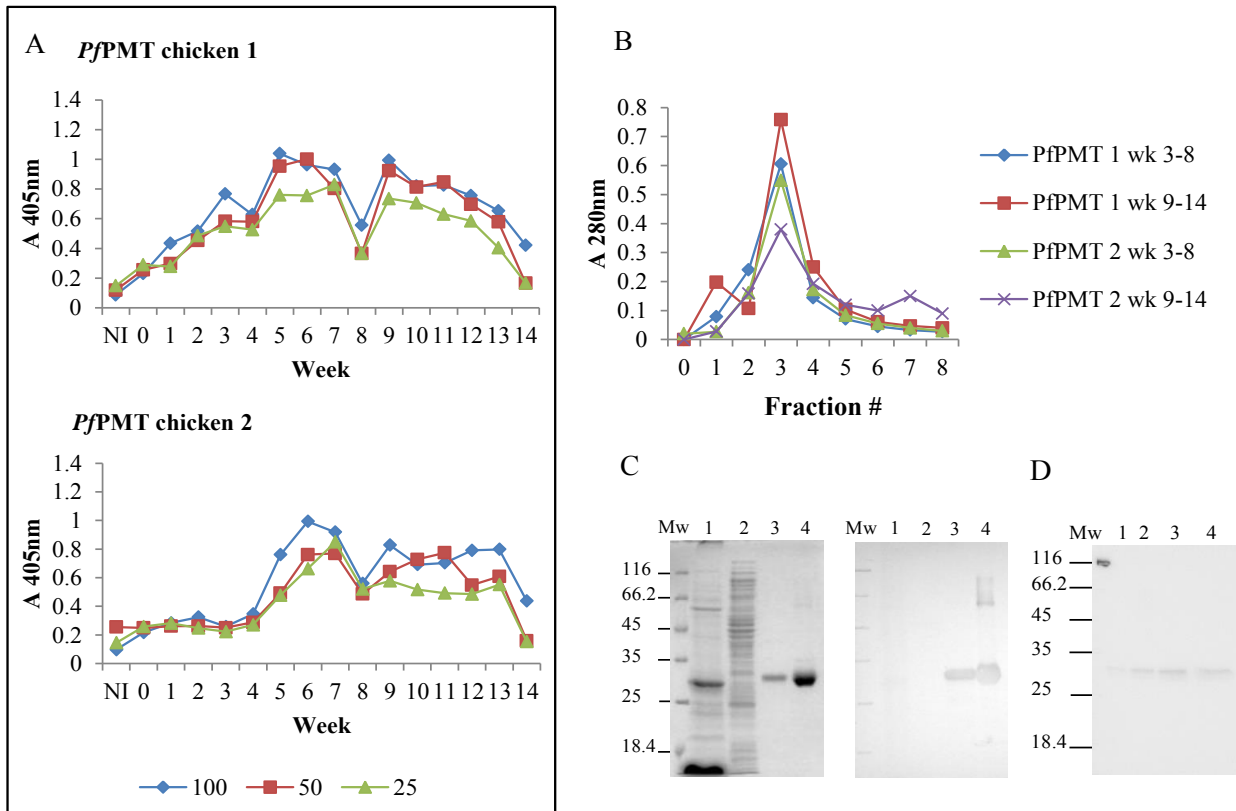


Figure 5.5 Raising and affinity purification of IgY against the whole rPfPMT protein

Egg antibody levels produced by each chicken were monitored by ELISA as shown in (A). Plates were coated with whole rPfPMT (1 µg/ml). Crude IgY was diluted to 100, 50 and 25 µg/ml and a rabbit anti-chicken-HRPO at 1 in 15000 were used. IgY isolated from weeks 3 to 8 and 9 to 14 were affinity purified over a rPfPMT AminoLink® column as shown in (B). The final affinity purified IgY was assessed for specificity by western blotting in (C). The Coomassie stained reference gel in the left panel was loaded as follows: Molecular weight marker (Mw); uninfected (*O*⁺) red blood cell lysate (lane 1); untransformed *E. coli* BL21(DE3) lysate (lane 2); purified rPfPMT (lane 3) and purified rPvPMT (lane 4). The blot shown in the right panel was detected with anti-rPfPMT affinity purified IgY at 1 µg/ml and rabbit anti-chicken-HRPO at 1 in 12000. The blot in (D) detected native PfPMT from Pf(D10) lysates at different concentrations: 2.5, 5, 7.5 and 10 µg (lanes 1 to 4), with the same IgY concentration but a 1 in 10000 secondary concentration instead and detected using ECL.

Similarly to recombinant PfPMT, chickens immunised with recombinant PvPMT elicited antibodies early from week two after the primary immunisation (Figure 5.6). Diluting the antibodies to 25 µg/ml had very little effect on the signal however (panel A) and this was reflected by greater yields off the affinity column (panel B) in comparison to the PfPMT antibody yields from Figure 5.5 (panel B). The affinity purified antibodies did not cross react with the uninfected red blood cell and *E. coli* host cell proteins (panel C) and detected both recombinant PfPMT and PvPMT proteins similarly to the anti-PfPMT antibodies. Due to the higher antibody yields and similar detection of both recombinant protein orthologues to the anti-PfPMT IgY, the anti-PvPMT IgY was coupled to HRPO for use as a detection antibody in a double antibody sandwich ELISA format for future work, as was done using LDH and GAPDH antibodies (Figures 5.11 and 5.12). After coupling, the anti-PvPMT IgY continued to detect both recombinant PfPMT and PvPMT as demonstrated in panel D of Figure 5.6.

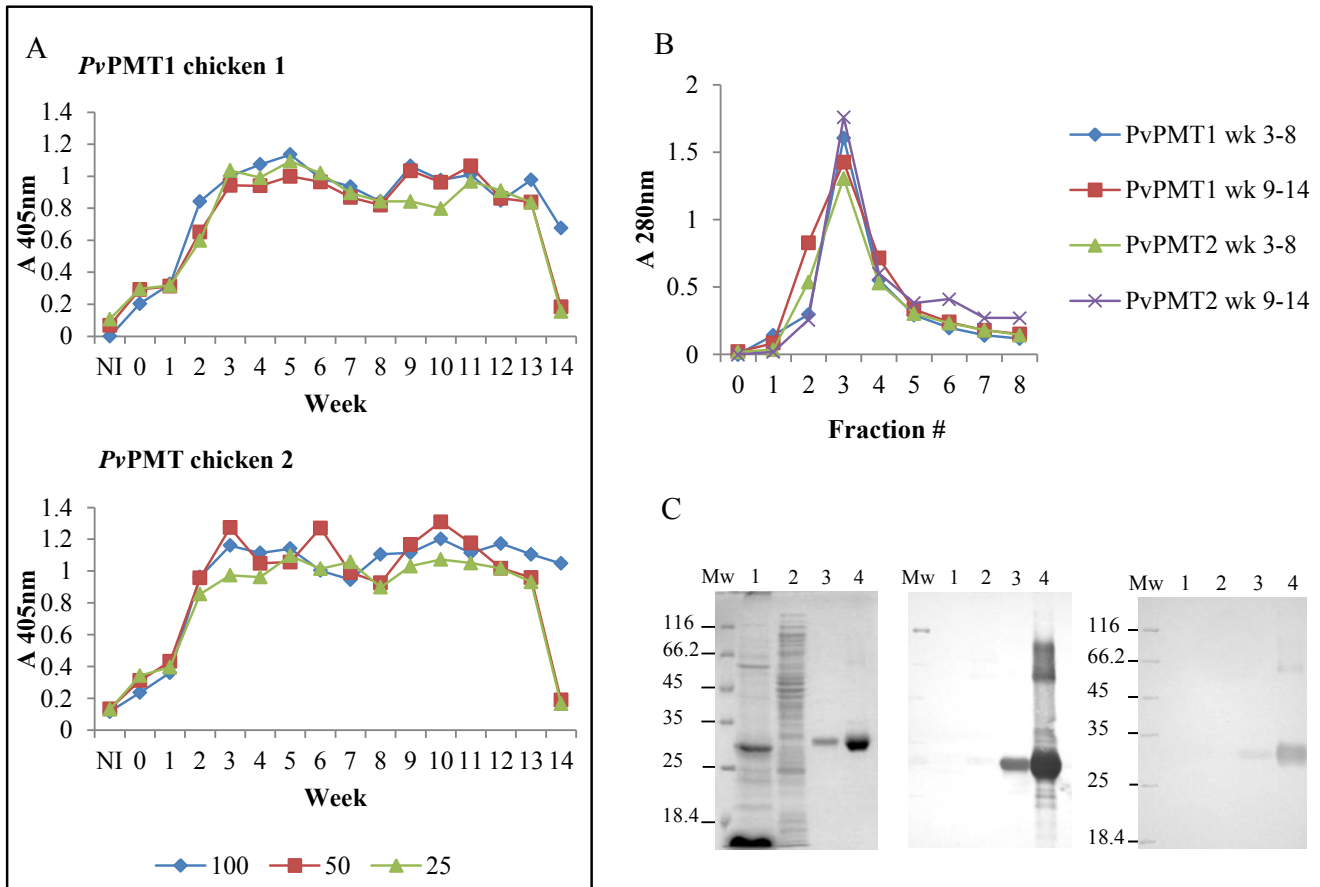


Figure 5.6 Raising and affinity purification of IgY against the whole rPvPMT protein

Egg antibody levels produced by each chicken were monitored by ELISA as shown in (A). Plates were coated with whole rPvPMT (1 µg/ml). Crude IgY was diluted to 100, 50 and 25 µg/ml and a rabbit anti-chicken-HRPO at 1 in 15000 were used. IgY isolated from weeks 3 to 8 and 9 to 14 were affinity purified over a rPvPMT AminoLink® column as shown in (B). The final affinity purified IgY was assessed for specificity by western blotting in (C). The Coomassie stained reference gel in the left panel was loaded as follows: Molecular weight marker (Mw); uninfected (O^+) red blood cell lysate (lane 1); untransformed *E. coli* BL21(DE3) lysate (lane 2); purified rPvPMT (lane 3) and purified rPvPMT (lane 4). The blot shown in the right panel was probed with anti-rPvPMT affinity purified IgY at 1 µg/ml and rabbit anti-chicken-HRPO at 1 in 12000. Anti-rPvPMT IgY was coupled to HRPO and used to detect both rPvPMT and rPvPMT in (D), where the reference gel was the same as in (C). The HRPO-coupled IgY was used at 1 in 200 dilution.

Interestingly all anti-PMT peptide antibodies had higher detection levels against their respective peptide targets than in the rabbit albumin control ELISAs (Figures 5.7 to 5.10 panel A) and all signals increased from as early as week two to three. The rabbit albumin ELISAs were included as controls of immunisation success, since rabbit albumin served as the carrier protein in each case. One chicken stopped laying for weeks three to five and eight to 12, hence the lack of data in Figure 5.7 (panel A). Poor yields of affinity purified antibodies were obtained for the common PMT peptide (DEG – common peptide) for chicken two weeks three to seven in Figure 5.7 panel B and the *P. knowlesi* PMT peptide (LYP – *P. knowlesi* peptide) for chicken 2 weeks eight to 12 in Figure 5.10 panel B.

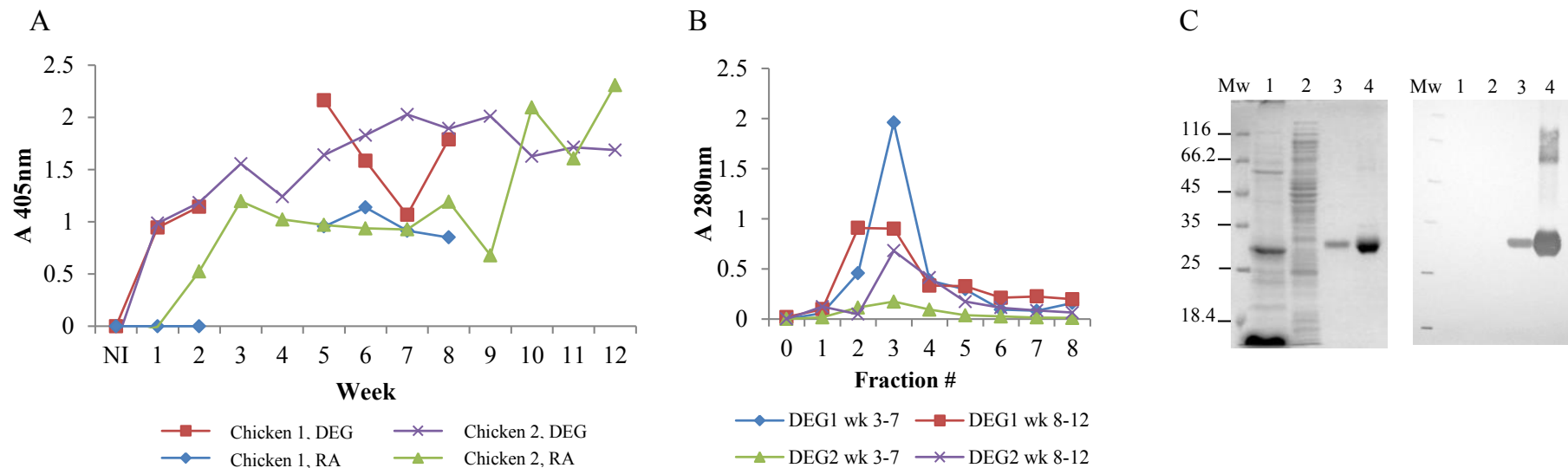


Figure 5.7 Raising and affinity purification of IgY against the common PMT peptide (DEG)

Egg antibody levels produced by each chicken were monitored by ELISA as shown in (A). Plates were coated at 1 $\mu\text{g/ml}$ with either the DEG (LENNQYTDEGVKC) peptide or Rabbit albumin (RA) as a control. Crude IgY at 100 $\mu\text{g/ml}$ and a rabbit anti-chicken-HRPO at 1 in 15000 were used. IgY isolated from weeks 3 to 7 and 9 to 12 were affinity purified over a DEG SulfoLink[®] column as shown in (B). The final affinity purified IgY was assessed for specificity by western blotting in (C). The Coomassie stained reference gel in the left panel was loaded as follows: Molecular weight marker (Mw); uninfected (O⁺) red blood cell lysate (lane 1); untransformed *E. coli* BL21(DE3) lysate (lane 2); purified rP/PMT (lane 3) and purified rPvPMT (lane 4). The blot shown in the right panel was probed with anti-DEG affinity purified IgY at 1 $\mu\text{g/ml}$ and rabbit anti-chicken-HRPO at 1 in 12000.

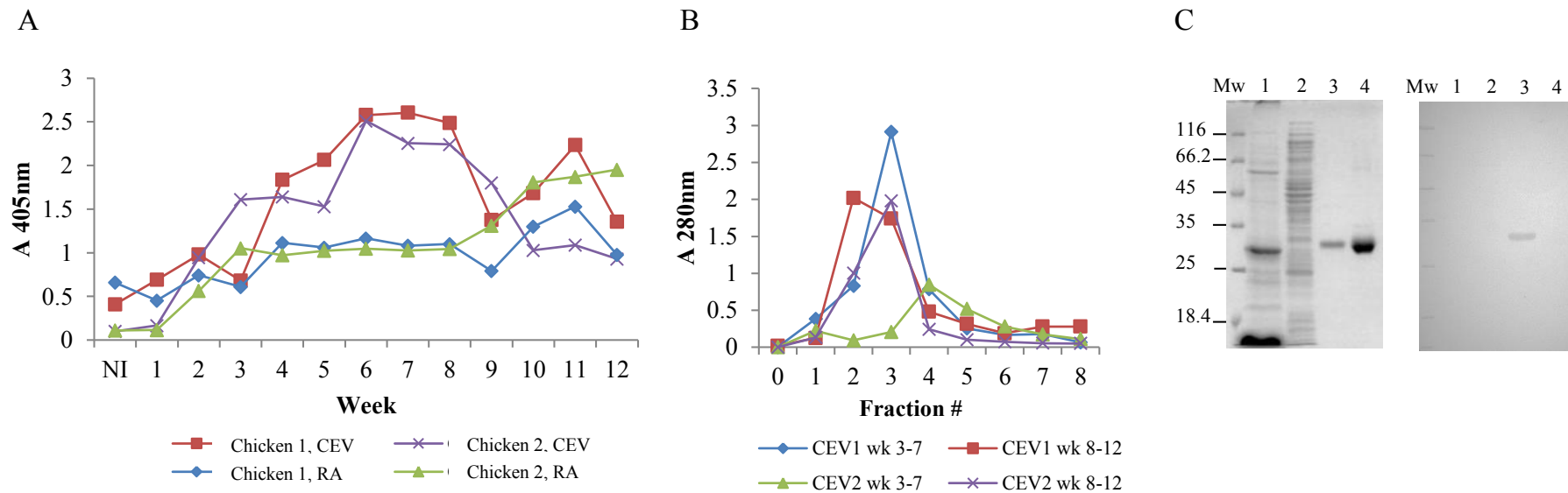


Figure 5.8 Raising and affinity purification of IgY against the *P. falciparum* specific PMT peptide (CEV)

Egg antibody levels produced by each chicken were monitored by ELISA as shown in (A). Plates were coated at 1 $\mu\text{g/ml}$ with either the CEV (CEVEHKYLHENKE) peptide or Rabbit albumin (RA) as a control. Crude IgY at 100 $\mu\text{g/ml}$ and a rabbit anti-chicken-HRPO at 1 in 15000 were used. IgY isolated from weeks 3 to 7 and 9 to 12 were affinity purified over a CEV SulfoLink[®] column as shown in (B). The final affinity purified IgY was assessed for specificity by western blotting in (C). The Coomassie stained reference gel in the left panel was loaded as follows: Molecular weight marker (Mw); uninfected (*O*⁺) red blood cell lysate (lane 1); untransformed *E. coli* BL21(DE3) lysate (lane 2); purified rPjPMT (lane 3) and purified rPvPMT (lane 4). The blot shown in the right panel was probed with anti-CEV affinity purified IgY at 1 $\mu\text{g/ml}$ and rabbit anti-chicken-HRPO at 1 in 12000.

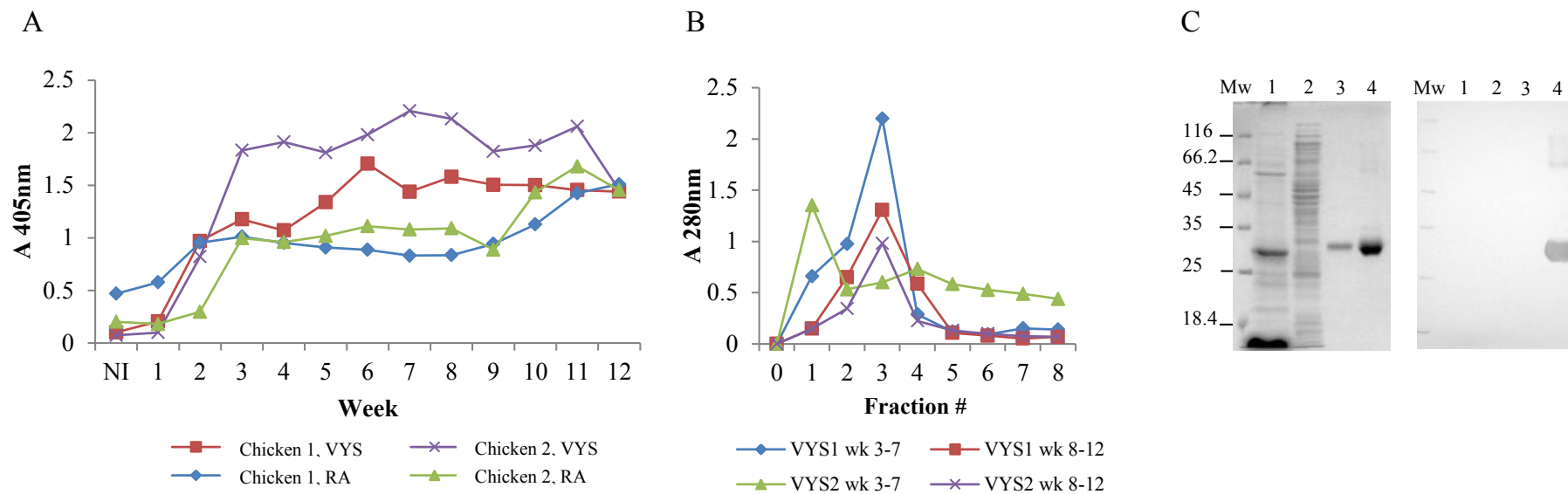


Figure 5.9 Raising and affinity purification of IgY against the *P. vivax* specific PMT peptide (VYS)

Egg antibody levels produced by each chicken were monitored by ELISA as shown in (A). Plates were coated at 1 $\mu\text{g/ml}$ with either the VYS (VYSIKEYNSLKDC) peptide or Rabbit albumin (RA) as a control. Crude IgY at 100 $\mu\text{g/ml}$ and a rabbit anti-chicken-HRPO at 1 in 15000 were used. IgY isolated from weeks 3 to 7 and 9 to 12 were affinity purified over a VYS SulfoLink[®] column as shown in (B). The final affinity purified IgY was assessed for specificity by western blotting in (C). The Coomassie stained reference gel in the left panel was loaded as follows: Molecular weight marker (Mw); uninfected (O^+) red blood cell lysate (lane 1); untransformed *E. coli* BL21(DE3) lysate (lane 2); purified rPvPMT (lane 3) and purified rPvPMT (lane 4). The blot shown in the right panel was probed with anti-VYS affinity purified IgY at 1 $\mu\text{g/ml}$ and rabbit anti-chicken-HRPO at 1 in 12000.

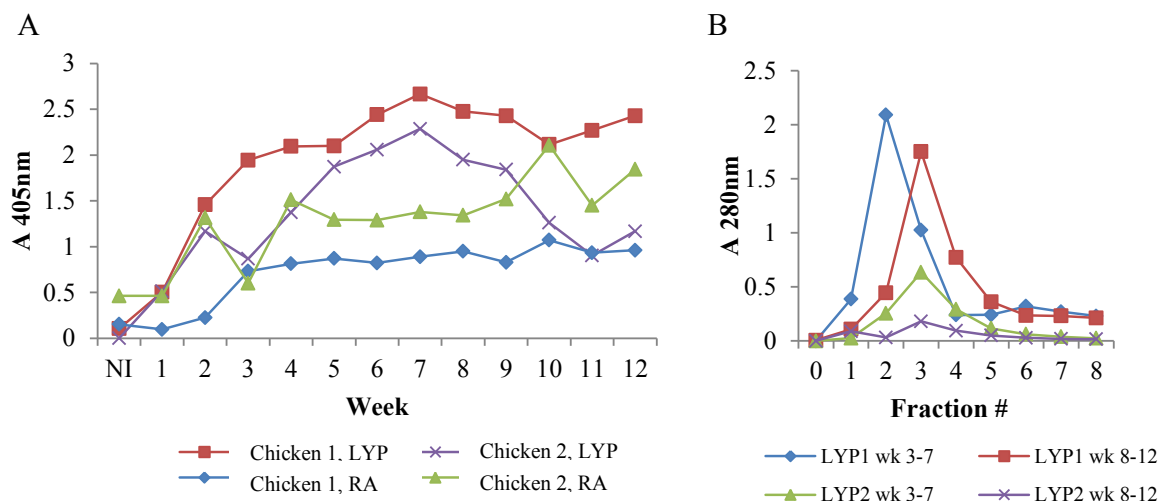


Figure 5.10 Raising and affinity purification of IgY against the *P. knowlesi* specific PMT peptide (LYP)

Egg antibody levels produced by each chicken were monitored by ELISA as shown in (A). Plates were coated at 1 µg/ml with either the LYP (LYPTDEYNSLKDC) peptide or Rabbit albumin (RA) as a control. Crude IgY at 100 µg/ml and a rabbit anti-chicken-HRPO at 1 in 15000 was used. IgY isolated from weeks 3 to 7 and 9 to 12 were affinity purified over a LYP SulfoLink® column as shown in (B).

None of the anti-PMT antibodies cross reacted with uninfected human red blood cell lysate or *E. coli* host cell proteins and detected their respective targets, with only the antibodies raised against the common peptide detecting both rPfPMT and rPvPMT as expected (panel C, Figures 5.7 to 5.9). Since there was no recombinant *P. knowlesi* PMT available, the *P. knowlesi* PMT peptide antibodies were not tested (Figure 5.10).

Interestingly when summarising the overall antibody yields (Table 5.1) and comparing the anti-peptide antibody yields to the anti-whole protein yields, better overall yields were observed for the peptides than the whole protein in the case of PfPMT, whereas the opposite was true for PvPMT. The anti-CAD (*PfGAPDH* specific peptide) and the anti-LYP (*PkPMT* specific peptide) data were included for completeness. The yields for the anti-CAD peptide were comparable to the yields for some of the individual chickens immunised with peptides (anti-DEG and anti-LYP chicken 2) as well as whole recombinant protein (anti-rPfPMT chicken 2). This was interesting since an alternative method was used to couple the CAD peptide to the rabbit albumin carrier protein.

Table 5.1 IgY yields per antigen used in this study

IgY sample	Chicken #	Yield (mg)	Total yield (mg)
Anti-CAD (<i>Pf</i> GAPDH pep.)	1*	1.9	1.9
Anti-r <i>Pf</i> PMT	1	5.9	8.6
	2	2.7	
Anti-r <i>Pv</i> PMT	1	51.9	117.7
	2	65.9	
Anti-DEG (common PMT pep.)	1	54.6	56.4
	2	1.7	
Anti-CEV (<i>Pf</i> PMT pep.)	1	70.0	123.1
	2	53.2	
Anti-VYS (<i>Pv</i> PMT pep.)	1	37.4	97.3
	2	59.9	
Anti-LYP (<i>Pk</i> PMT pep.)	1	105.7	108.5
	2	2.8	

*The anti-CAD data included only a single chicken, since the second chicken stopped laying eggs and died.

5.2.4 Double antibody sandwich ELISAs for the detection of the recombinant *Pf*LDH and *Pf*GAPDH proteins in solution

Finally the LDH and GAPDH antibodies mentioned earlier in Figures 5.2 and 5.3 were used to optimise double antibody sandwich ELISAs. This format of ELISA mimics the rapid diagnostic test format with a capture anti-peptide antibody to bind the specific antigen from solution and the secondary anti-recombinant antibody coupled to HRPO which recognises the bound antigen, producing the signal. Here the anti-peptide antibodies (capture step) were immobilised on the ELISA plate. With regard to the LDH ELISAs (Figure 5.11) capture with the common LDH peptide antibodies (anti-APG) at between 2 or 4 μg resulted in a more sensitive assay as this system reached an absorbance of around 1 in the presence of only 0.5 $\mu\text{g/ml}$ (equal to 0.05 μg total protein) and detected as little as 0.004 $\mu\text{g/ml}$ (0.0004 μg total protein) of recombinant *Pf*LDH.

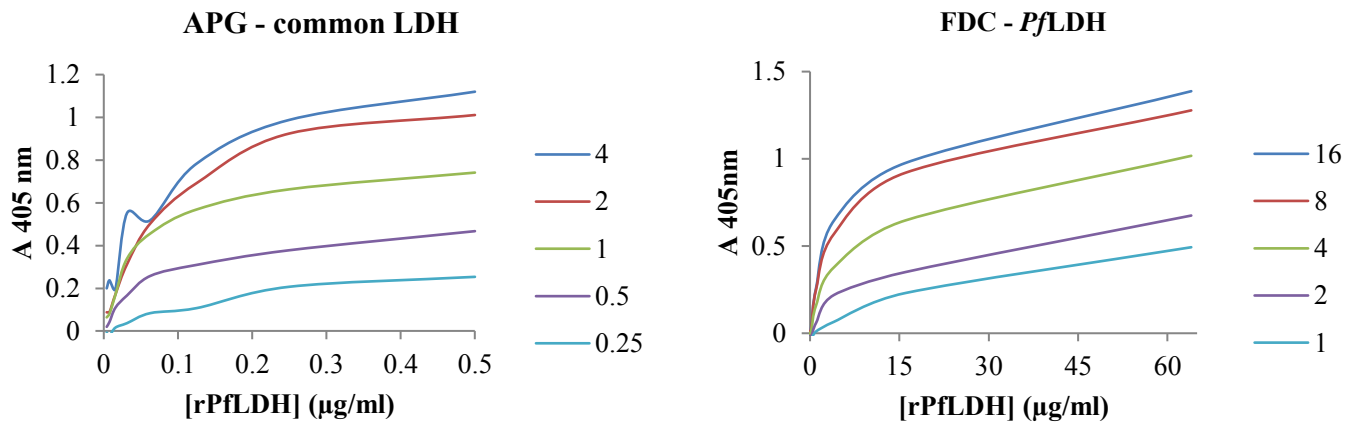


Figure 5.11 Double antibody-sandwich ELISAs to detect rPfLDH

Double antibody sandwich ELISAs were optimised for capturing and detecting rPfLDH. The LDH-common APG anti-peptide antibodies were used as capture antibody at 0.25 to 4 µg/ml to detect 0.5 to 0.004 µg/ml of protein. The PfLDH specific FDC anti-peptide antibodies were used as capture antibody at 1 to 16 µg/ml to detect 64 to 0.004 µg/ml of protein. The anti-rPfLDH IgY coupled to HRPO was used at 1 in 200 as the detection antibody in both assays.

In contrast the PfLDH peptide antibodies used as the capture antibody gave an absorbance of around 1 in the presence of 15 µg/ml (equal to 1.5 µg total protein) and detected as little as 0.004 µg/ml (0.0004 µg total protein) of recombinant PfLDH when captured with 8 to 16 µg of anti-FDC (PfLDH specific) IgY. Similar sensitivity to the anti-FDC (PfLDH specific) ELISA was achieved with both the GAPDH double antibody sandwich systems shown in Figure 5.12. Using either the common or the *P. falciparum* specific peptide IgY as the capture antibody, resulted in an absorbance of around 1 in the presence of 15 µg/ml (equal to 1.5 µg total protein) and as little as 0.004 µg/ml (0.0004 µg total protein) of recombinant PfGAPDH. Interestingly the change in absorbance between the different capture antibody concentrations used here was not as pronounced as in the LDH systems.

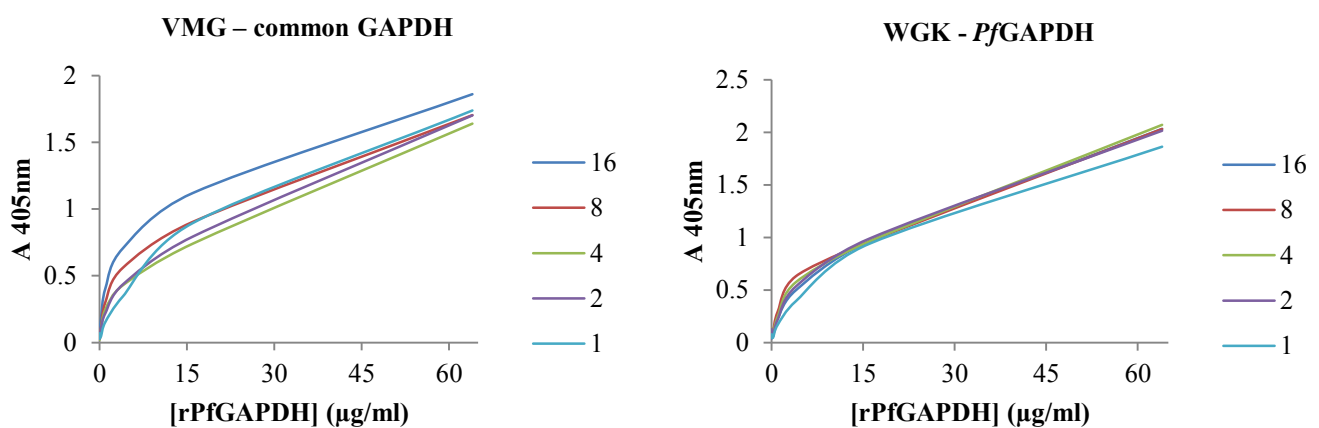


Figure 5.12 Double antibody-sandwich ELISAs to detect rPfGAPDH

Double antibody sandwich ELISAs were optimised for capturing and detecting rPfGAPDH. The GAPDH-common VMG and the PfGAPDH specific WGK anti-peptide antibodies were used as capture antibodies at 1 to 16 µg/ml to detect 64 to 0.004 µg/ml of protein. The anti-rPfGAPDH IgY coupled to HRPO was used at 1 in 200 as the detection antibody in both assays.

5.2.5 Human IgG pool affinity purified over the respective recombinant *P. falciparum* protein AminoLink[®] columns

A human anti-malaria hyperimmune serum pool (approximately 300 mg) was passed over five different recombinant *P. falciparum* protein AminoLink[®] affinity columns and the resulting yields of affinity purified antibodies were compared in Figure 5.13.

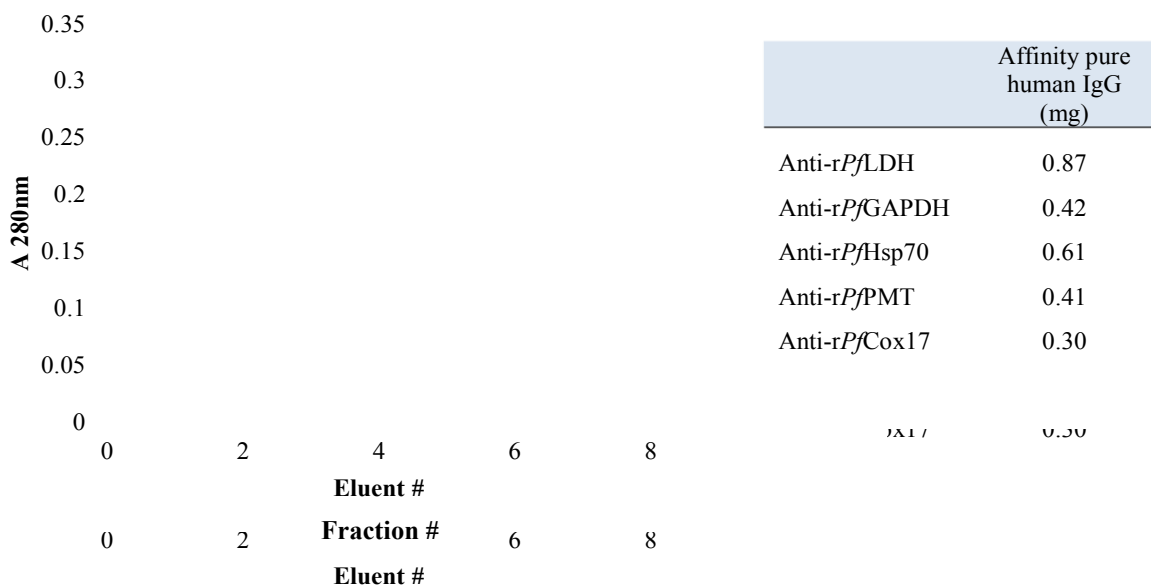


Figure 5.13 Affinity purified human IgG yields from an anti-malaria hyper immune serum pool against various recombinant *P. falciparum* proteins

Three hundred milligrams of a human anti-malaria hyperimmune serum pool was passed consecutively over a set of 5 recombinant *P. falciparum* AminoLink[®] affinity resins and the bound human IgG antibodies were eluted. Antibodies against rPfLDH; rPfGAPDH; rPfPMT; rPfHsp70 and rPfCox17 were affinity purified as indicated in the key alongside the figure. The resulting human IgG eluent absorbance at 280 nm were monitored and the respective yields calculated using the human IgG extinction coefficient ($\epsilon = 1.35$).

Since there is no human protein orthologue of PfPMT, it was expected that this protein may yield the greatest IgG response, however it was as immunogenic as PfGAPDH by comparison. PfLDH and its human orthologue share the lowest identity of the five proteins evaluated here (29% identity) and gave the highest yield of high affinity antibodies. This was followed by PfHsp70 which shared 31% identity, yielding the second most IgG. PfCox17, a copper chaperone, shares 44% homology however resulted in only 0.3 mg of affinity purified human IgG, although this protein is comparatively much smaller than the other proteins assessed here (Choveaux *et al.*, 2015). Finally PfGAPDH which shares 65% homology with its human orthologue, resulted in 0.42 mg of affinity purified human IgG, similar to the 0.41 mg from PfPMT.

5.3 Discussion

Polyclonal antibodies raised against a target protein potentially recognise epitopes both conformational and linear in nature. Since antibodies recognise approximately 15 amino acid regions, known as epitopes, a 30 kD protein has a minimum of 20 non-overlapping linear epitopes. Add to this the fact that epitopes may be overlapping and conformational in nature, formed by the specific quaternary fold of proteins, the amount of potential epitopes may exceed this number. The result is a broad spectrum of antibodies each targeting a separate epitope and each with its own specificity (Delves *et al.*, 2006). In this study two sets of polyclonal antibodies were raised against the chosen malaria proteins. These included antibodies raised against the whole recombinant proteins as well as antibodies raised against specific peptide epitopes. Linear epitopes can be used to produce “refined” polyclonal antibodies with specificity only to the chosen epitope (Hurdayal *et al.*, 2010; Tomar *et al.*, 2006). Both sets of antibodies were tested to see if they specifically detected their respective protein targets and did not cross-react with *E. coli* and uninfected human red blood cell proteins. If the collective pool of polyclonal antibodies specifically detects only the intended target protein, then this further validates the protein / peptide as a potential diagnostic target. Alternatively if the antibodies detect their intended target as well as multiple other related or unrelated targets, then the choice of protein / peptide target would have to be reconsidered. The *Plasmodium* proteins and epitopes chosen in this project were thus used to raise polyclonal antibodies in chickens and the resulting specificity of the purified antibodies was assessed. Each set of polyclonal antibodies raised here recognised their specific targets. Importantly none of the antibodies tested in this study cross-reacted with the uninfected human red blood cell or *E. coli* lysate proteins.

A general observation of the antibody production was that all antibody levels started increasing around week two after immunisation and maintained relatively high readings up to 12 weeks later. This is a typical response in chickens (Hurdayal *et al.*, 2010; Krause *et al.*, 2015). Importantly the rabbit albumin control included in the anti-peptide ELISA served as an indicator of immunisation success, rather than a comparative result, since rabbit albumin as a whole protein consists of multiple epitopes, thus potentially stimulating a broader immune response than the single peptide epitope attached to it.

Assessing anti-rPfLDH and anti-LDH peptide IgY specificity

Interestingly the anti-LDH antibodies raised against rPfLDH and the common peptide (APG) both detected the *P. falciparum*, *P. vivax* and *P. yoelii* orthologues. Similarly to the anti-His tag probed blots shown in chapter 4, a dimeric form of rPfLDH and rPvLDH was also detected. The species-specific peptide antibodies only detected their respective parent recombinant protein orthologues, which supported the specificity of the linear peptide epitopes selected in chapter 3 and was similar to the results observed by Hurdayal *et al.* (2010).

Assessing anti-rPfGAPDH and anti-GAPDH peptide IgY specificity

The poor solubility of the species specific PfGAPDH peptide CAD may have arisen due to interaction of hydrophobic residues within the linear epitope once it was dissolved in an aqueous solution, resulting in aggregation of the peptide (Malavolta *et al.*, 2006). This may have been due to the hydrophobic troughs on either side of the two lysine residues evident in the Predict7TM plot as shown in chapter 3 (Figure 3.4 (B) pg. 61). The alternative coupling method used here was described by Lateef *et al.* (2007) and circumvents solubility problems by performing the reaction in a polar solvent environment which was also suggested by Malavolta *et al.* (2006). The increased molecular weight rabbit albumin bands following the coupling reaction suggested the CAD peptide was successfully coupled to the carrier protein. Instead of using a peptide-coupled SulfoLink[®] resin for the affinity purification of the raised antibodies, the whole rPfGAPDH protein was coupled to an AminoLink[®] resin and used for the purification. The resulting yields were poor, yet comparable to the lower yields achieved in some of the chickens immunised with other peptides (the PMT common DEG and the *P. knowlesi* LYP peptides) as well as rPfPMT. The anti-CAD antibodies specifically detected rPfGAPDH despite these low yields. A possible alternative peptide which excludes one of the two hydrophobic troughs could improve the solubility whilst maintaining the desired specificity of the antibodies generated against it. This would mean shifting the selected amino acid residues comprising the peptide by four amino acids N- or C-terminally.

The remaining anti-GAPDH antibodies were specific, with the anti-rPfGAPDH and the antibodies against the common epitope detecting both the *P. falciparum* and *P. yoelii* orthologues. A similar result was obtained by Sangolgi *et al.* (2016), who used anti-rPfGAPDH mouse IgG antibodies for studies on *P. yoelii* GAPDH in a mouse model. Unlike LDH, the GAPDH sequences only shared 83% identity between the *P. falciparum* and

P. yoelii orthologues (Sangolgi *et al.*, 2016). The second species specific peptide antibodies (anti-WGK peptide) also detected only the parent recombinant *P. falciparum* GAPDH protein.

Assessing anti-rPfPMT, anti-rPvPMT and anti-PMT peptide IgY specificity

Antibodies against both recombinant PfPMT and PvPMT detected both orthologues on western blots, similarly to the antibodies raised against the common PMT peptide. The detection of faint bands in the uninfected red cell and *E. coli* lysate lanes in Figures 5.5 and 5.6 respectively are likely due to non-specific protein-protein interactions which may be resolved with more stringent washes and the addition of 0.1% (v/v) Tween 20 in the incubation buffers. The detection of higher and lower molecular weight bands in the western blots in Figures 5.5 to 5.9 may have been due to overloading the purified rPvPMT sample in those lanes. The species specific antibodies detected only their specific PMT targets, but the anti-*P. knowlesi* specific antibodies could not be tested since there was no rPkPMT available. The anti-rPfPMT antibodies detected a 29 kD band in a *P. falciparum* D(10) lysate, which is similar to the results reported by Pessi *et al.* (2004). Native *P. falciparum* LDH and GAPDH were detected with anti-rPfLDH and anti-rPfGAPDH antibodies in our previous work (Krause *et al.*, 2015). Therefore all three *P. falciparum* protein targets were detected in infected red blood cell lysates, and since none of the antibodies raised here detected any proteins in uninfected blood lysates, the potential use of these protein targets and the antibodies raised against them for malaria diagnosis looks promising.

Double antibody sandwich ELISA results

A series of double antibody sandwich assays were optimised to detect rPfLDH and PfGAPDH. This format mimics that of a rapid diagnostic test, where the only difference is the detection antibodies are usually labelled with colloidal gold, instead of HRPO (Makler *et al.*, 1998; Murray *et al.*, 2008). The detection range of the assays was from 0.05 µg to 0.0004 µg of rPfLDH (for the APG ELISA) and 0.0004 to 0.15 µg of recombinant protein for the remaining assays. These ranges are within physiological levels, at least in comparison to HRP2 in plasma, which ranges between 0.57 and 1.11 µg/ml (Dondorp *et al.*, 2005). HRP2 was present at approximately 6 times the concentration of PfLDH in a study by Martin *et al.* (2009), which would make LDH concentrations between 0.095 to 0.19 µg/ml in plasma and possibly higher levels in whole blood (Dondorp *et al.*, 2005). The assays developed here are thus predicted to be sensitive enough to detect the target antigens in infected blood samples.

Importantly the same AminoLink[®] affinity resins that were used for affinity purification of the human IgG antibodies were also used for the purification of the IgY antibodies earlier in this chapter and in our previous work (Krause *et al.*, 2015). The IgY antibodies eluted with higher 280 nm absorbance than the human antibodies, which suggests that the amount of protein present on the AminoLink[®] affinity resins was not limiting in this case. It can be assumed therefore, that the human IgG eluted off these columns presents the total IgG specific to the target antigens in this pool. Interestingly the final yields showed some correlation with the percentage identity shared between the human and *P. falciparum* orthologues. Interestingly, however, the *PfPMT* result was similar to that of *PfGAPDH*, even though *PfPMT* lacks any orthologues in the human proteome (Pessi *et al.*, 2004). These results may have implications in the performance of *Plasmodium* GAPDH and PMT targeting antibody based diagnostic tests in the field, as human IgG may compete for binding of the free antigens in patient blood as was the case with HRP2 based RDTs (Ho *et al.*, 2014). This has not been reported for LDH based tests to date and since the levels of specific human IgG against GAPDH and PMT purified here were lower than for LDH, these results were promising for these proposed targets.

Together the results in this chapter validated the use of the target antigens and polyclonal antibodies raised against both the whole recombinant proteins and their specific peptide epitopes in a malaria diagnostic format. Quantitative comparisons of LDH, GAPDH and PMT in infected blood lysates using the double antibody sandwich ELISA format would be essential data to further validate the chosen protein and peptide targets. The final chapter to follow focuses on raising monoclonal antibody reagents in the form of scFvs.

Chapter 6

Selection of monoclonal recombinant scFv antibodies from the *Nkuku*[®] library against the potential *Plasmodium* target proteins and their respective peptide epitopes

6.1 Introduction

Most malaria RDTs use monoclonal antibodies for the capture and detection of the malaria target antigens including HRP2, LDH and aldolase (Moody, 2002). Monoclonal antibodies have several advantages over polyclonal antibodies. Firstly their specificity can be well characterised, which can prove difficult with polyclonal antibodies due to multiple avidities. This is important for the consistent quality of RDTs. It is more difficult to standardise polyclonal antibody pools and this may result in variation of test performance between batches from different animals. Secondly, mass production of tests demands large quantities of antibodies. Raising polyclonal antibodies is very labour intensive and harmful to the animals used. Since monoclonal antibodies can be produced *in vitro* using hybridoma technology, this allows for expression of a potentially endless supply of identical antibodies. This characteristic is shared with recombinant scFv technology, however, the selection, recombinant expression and purification processes in the scFv system are less demanding than hybridoma technology (Baird *et al.*, 2009).

In this chapter, a naïve scFv library of chicken origin called the *Nkuku*[®] library was used to identify scFv clones that bound rPfLDH, rPfGAPDH and the specific peptides for each protein (chapter 3). The screening of scFv libraries is referred to as panning and is described in Figure 6.2. A simplified explanation of the *Nkuku*[®] library construction is presented below. The library was constructed from unimmunised chicken B-cell mRNA yielding a so-called naïve scFv library and was expanded with the addition of a synthetic variable heavy (V_H) coding region 3 (CDR3) repertoire. The library was formed by synthetically combining the coding regions for the variable light (V_L) and V_H chains of chicken antibodies, that is the V + J and V + J + D genes respectively. The end result was a large library of an estimated 5×10^{12} clones (van Wyngaardt *et al.*, 2004). The pHEN1 phagemid vector was used to construct the library (Hoogenboom *et al.*, 1991). The scFv coding genes were inserted between a pelB leader sequence and a cmc peptide tag in the pHEN1 vector (Figure 6.1). The cmc peptide

was followed by an amber (TAG) stop codon and phage coat protein III (pIII) coding regions. In amber suppressor *E. coli* host cells, like TG1 cells, the TAG stop codon is read through and codes for a Glutamate (E), hence the *supE* nomenclature for such strains. This results in expression of a scFv-pIII fusion protein of approximately 73 kD (Figure 6.1). In non-suppressor *E. coli* strains like the Top10 strain, expression stops at the amber codon resulting in a soluble scFv molecule of approximately 30 kD. During overexpression conditions, with the addition of the inducer IPTG, suppressor strains also express soluble scFv due to the slow read-through at the amber codon. The *pelB* leader locates the scFv to the periplasm and the *cmc* tag is used for detection of the soluble scFv proteins. The pHEN1 coding region is shown in Figure 6.1.

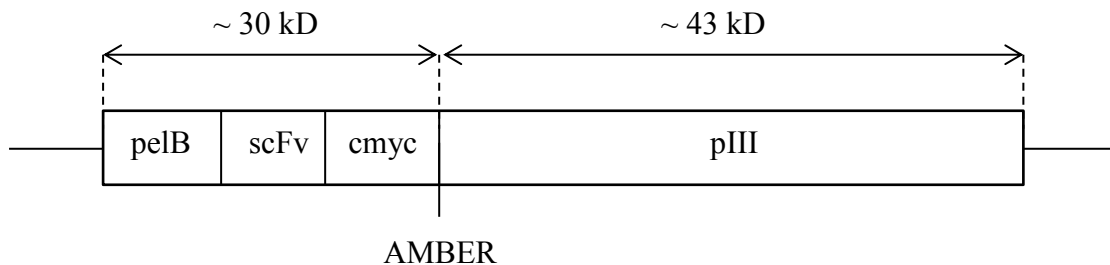


Figure 6.1 Representation of the pHEN1 coding region including the scFv and protein III regions
 The scFv coding sequences were inserted between a *pelB* leader and *cmc* peptide tag, resulting in an approximately 30 kD soluble scFv product in non-suppressor *E. coli*. Alternatively a scFv-pIII fusion protein is expressed in *supE* strains which read through the amber (TAG) codon, replacing it with Glutamate (E) and yielding a 73 kD protein.

Panning of the scFv library involved a combination of four steps, each with its own selective pressure (illustrated in *italics* in Figure 6.2). The steps will be explained briefly, starting with growing the library in the *E. coli* TG1 host cells. The *E. coli* host cells are grown in the presence of ampicillin containing media, as the pHEN1 vector codes for an ampicillin resistance gene (*Amp^r* cassette). Since pHEN1 codes only for the scFv-pIII fusion protein and no other phage coat proteins, a wild type phage (M13KO7), containing the kanamycin resistance marker is introduced to the culture. Subsequently kanamycin and ampicillin are added to the media to select for cells harbouring both the pHEN1 (*Amp^r*) and phage / M13KO7 (*Kan^r*) DNA. The incorporation of the M13KO7 DNA allows translation of the phage DNA into the coat proteins required for packaging new phage particles and the result is a mosaic bacteriophage population containing scFv-pIII and normal pIII on its surface. The phage particles are separated from the TG1 host cells by precipitating them from clarified media supernatant using the PEG/NaCl method (van Wyngaardt *et al.*, 2004). These phages

are then allowed to bind to the target antigen coated on the surface of immunotubes. Any unbound phages are washed off at this stage. The bound phages then infect fresh TG1 cells via the *E. coli* F-pili only if phages have normal pIII and / or the scFv-pIII (Noppe *et al.*, 2009). This step removes any non-infective clones and subsequent growth in ampicillin containing media removes any cells harbouring the M13KO7 (Kan^r) DNA instead of the pHEN1 vector. This completes one cycle of panning.

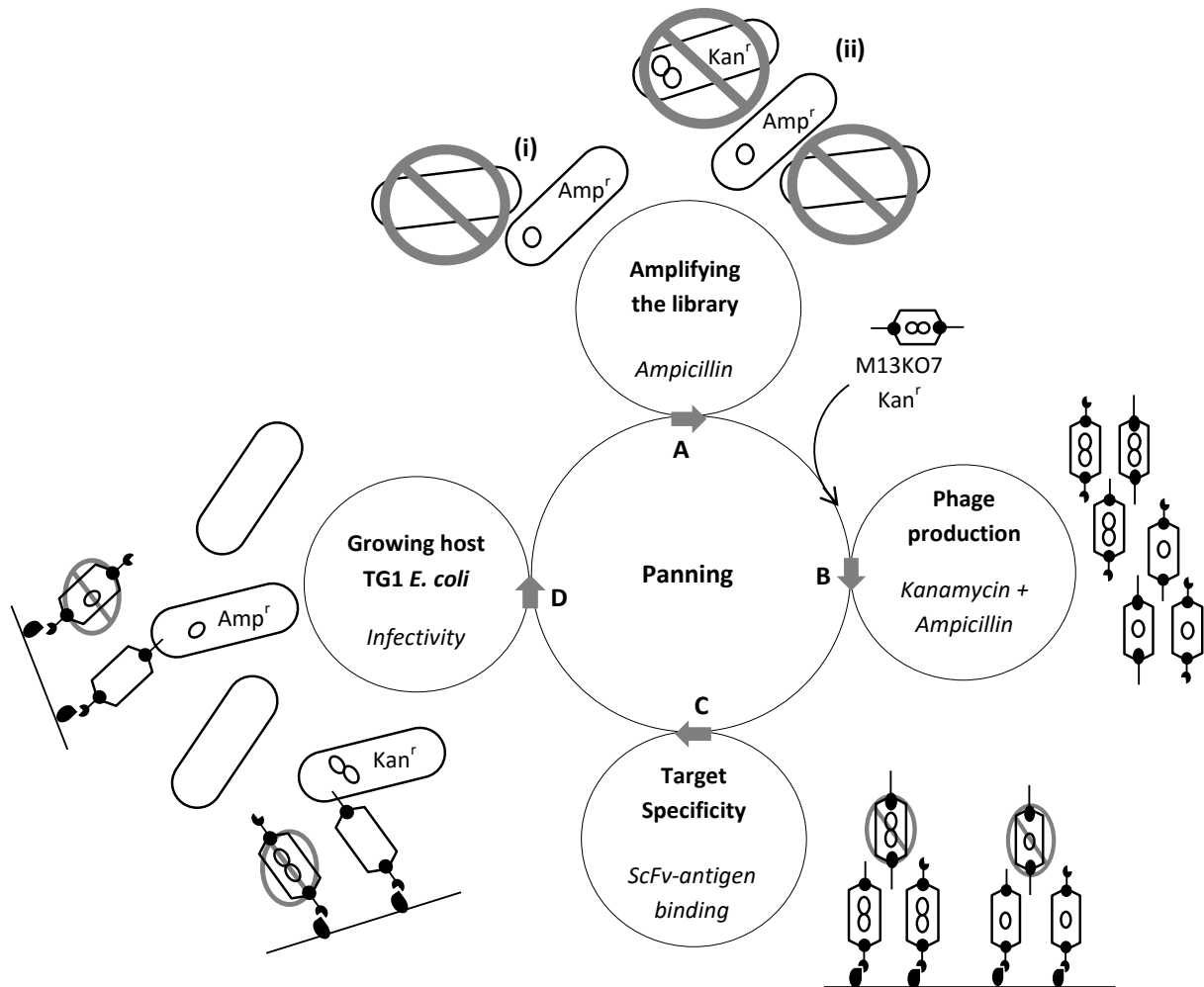


Figure 6.2 Schematic representation of one round of the panning procedure used to select for target antigen specific scFv-bearing phagemids from the *Nkuku*[®] library

The panning procedure combines four independent protocols A to D to select for scFv-bearing phagemids specific to a target antigen. The selective pressure at each step is in italics. To start the pHEN1 vector (○) harbouring the scFv coding sequences (also known as phagemid DNA) was transformed into *E. coli* TG1 cells. (A (i)) The infected *E. coli* population was propagated in ampicillin supplemented media, selecting against any uninfected cells. (B) The phagemid DNA was rescued by wild-type M13KO7 phage infection. This activates the M13 origin of replication and subsequent phage formation. Ampicillin and kanamycin pressure selected for cells containing both genomes. The resulting mosaic phage population contained either phagemid or phage DNA encapsulated with pIII-scFv (●●) which is coded by the phagemid DNA or normal pIII (●), coded by phage DNA. (C) Phages bearing antigen-specific pIII-scFv (●●●) on their surface bound the target antigen immobilised on a solid support and any unbound phages were removed by washing. (D) The antigen-bound phages were eluted by “on-column” infection of TG1 cells (Noppe *et al.*, 2009), removing any non-infective phages. Alternatively bound phages were eluted using a change in pH and then allowed to infect *E. coli* TG1 host cells. The TG1 cells that remained untransfected or contained the phage DNA (○○) were selected against using ampicillin (A (ii)). This completes one round of panning.

Phage technology has been used in malaria research, both for identification of peptide binders to parasite receptors as well as generating antibodies against certain parasite proteins (Chiliza *et al.*, 2008; Fu *et al.*, 1997; Lanzillotti and Coetzer, 2007; Lauterbach *et al.*, 2003; McIntosh *et al.*, 2007; Wajanarogana *et al.*, 2006).

6.2 Results

6.2.1 Raising and affinity purification of anti-cmyc IgY antibodies to detect soluble scFvs

ScFv antibodies are expressed as a soluble fusion protein containing the cmyc amino acid sequence. This can be detected by anti-cmyc antibodies. The commercial anti-cmyc 9E10 monoclonal antibody commonly used is expensive and since large quantities of this antibody would be required for routine detection and purification of scFvs, it was decided to raise anti-cmyc antibodies in chickens for this work (Figure 6.3).

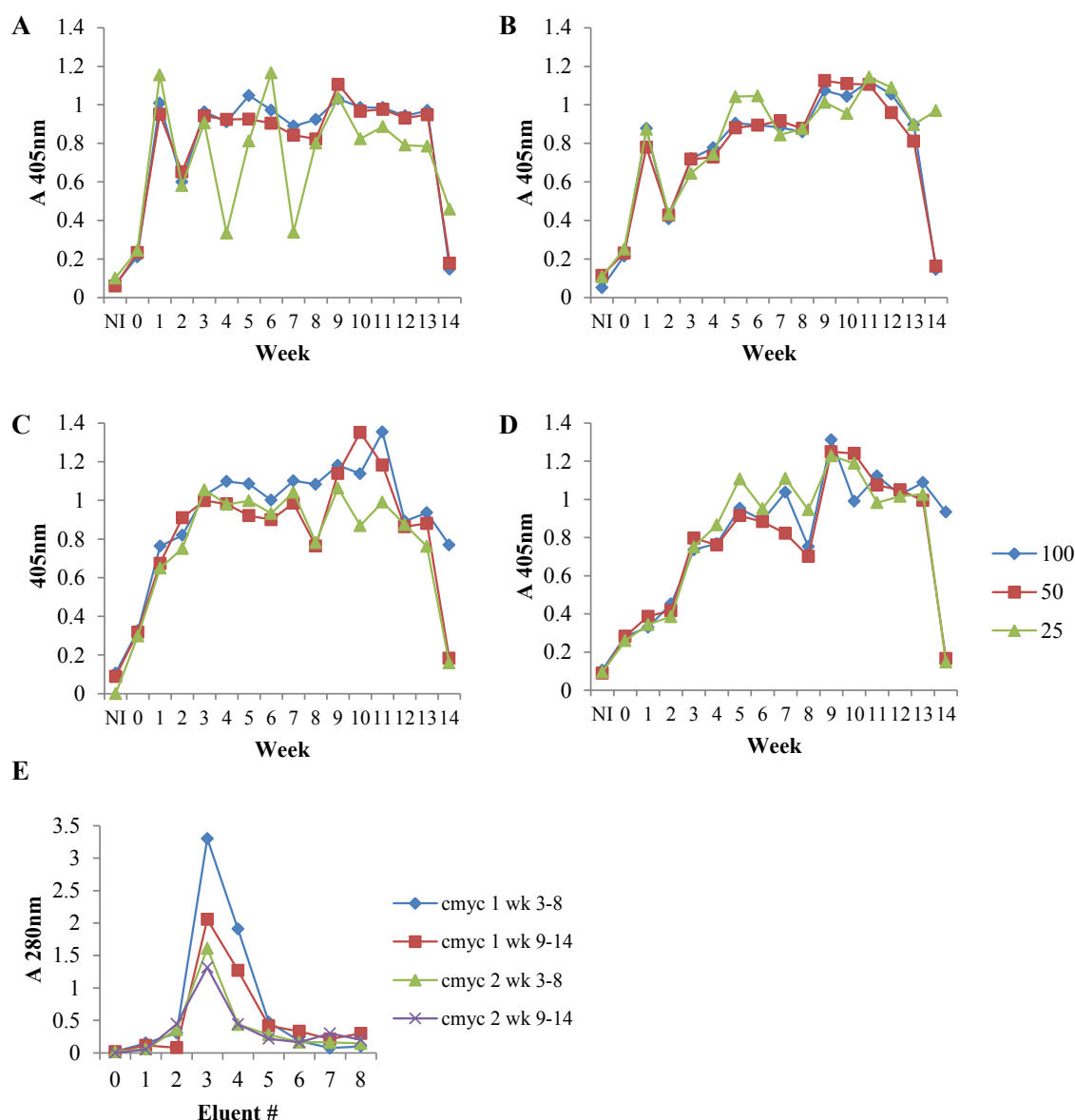


Figure 6.3 Titres and affinity purification of anti-cmyc antibodies from chicken eggs

Antibody production was monitored in the eggs from immunised chickens by ELISA (A to D). Plates were coated with cmyc peptide (1 $\mu\text{g}/\text{ml}$) in (A and C) or the carrier protein rabbit albumin as an immunisation control (B and D). Crude IgY was evaluated at 100, 50 and 25 $\mu\text{g}/\text{ml}$ (key shown alongside panel D) and detected with a rabbit anti-chicken-HRPO at 1 in 15000 dilution. IgY isolated from weeks 3 to 8 and 9 to 14 was affinity purified over a cmyc SulfoLink[®] affinity column as shown in (E).

The peptide tag, cmyc, which is of human origin, was coupled to rabbit albumin and immunised into chickens. Antibody production was monitored by ELISA and similar titres were obtained against cmyc as well as the carrier protein rabbit albumin (Figure 6.3 (A to D)). Antibodies were isolated from chicken eggs (Goldring and Coetzer, 2003). The subsequent elution profiles off the cmyc-SulfoLink[®] affinity column yielded 12.5 mg of affinity purified anti-cmyc IgY (Figure 6.3 (E)).

6.2.2 Panning the *Nkuku*[®] library

The *Nkuku*[®] library was panned using recombinant *Pf*LDH and *Pf*GAPDH. The peptide epitopes chosen for each of these proteins were also used to pan the library and a detailed list of the protein and peptide targets is shown in Table 6.1. The table includes details of the concentrations of the target antigens used for each round of panning.

Table 6.1 Malarial recombinant protein or peptide targets used to pan the *Nkuku*[®] library and the concentrations used per round

Protein target	Target species	Target description	Type	Panning concentrations used for rounds 1 to 4 (µg/ml)
LDH	<i>P. falciparum</i>	rPfLDH	protein	100, 50, 25, 10
	Common epitope	<u>APG</u> KSDKEWNRDDL-C	peptide	50, 25, 10, 1
	<i>P. falciparum</i> epitope	LISDAE <u>LEAIFD</u> -C	peptide	50, 25, 10, 1
	<i>P. vivax</i> epitope	<u>KITD</u> EEVEGIFD-C	peptide	50, 25, 10, 1
GAPDH	<i>P. falciparum</i>	rPfGAPDH	protein	100, 50, 25, 10
	Common epitope	C-KDDT <u>PIYVMGINH</u>	peptide	50, 25, 10, 1
	<i>P. falciparum</i> epitope	C-AEKDPSQIP <u>WGK</u> CQV	peptide	50, 25, 10, 1
	<i>P. falciparum</i> epitope	C- <u>ADG</u> FLLIGEKKVSVFA	peptide	50, 25, 10, 1
PMT	Common epitope	LENNQY <u>TDEGVK</u> -C	peptide	50, 25, 10, 1
	<i>P. falciparum</i> epitope	<u>C-EVE</u> HKYLHENKE	peptide	50, 25, 10, 1
	<i>P. vivax</i> epitope	<u>VYSI</u> KEYNSLKD-C	peptide	50, 25, 10, 1
	<i>P. knowlesi</i> epitope	<u>LYPT</u> DEYNSLKD-C	peptide	50, 25, 10, 1

The respective peptide names used in text and in the Figures to follow were underlined e.g. APG represents common peptide APGKSDKEWNRDDL-C and so on.

6.2.3 Polyclonal phagemid ELISA results after rounds one to four of panning

The polyclonal phagemid ELISA results after four rounds of panning are summarised in Figure 6.4. A common trend for most targets was an increase in signal in the ELISA from rounds one to four (FDC, rPfGAPDH, WGK, CEV, VYS and LYP). A few samples peaked in round three and then declined in round four (rPfLDH, KIT and DEG) and some peaked in the initial rounds and dropped with consecutive panning rounds (APG, VMG and ADG).

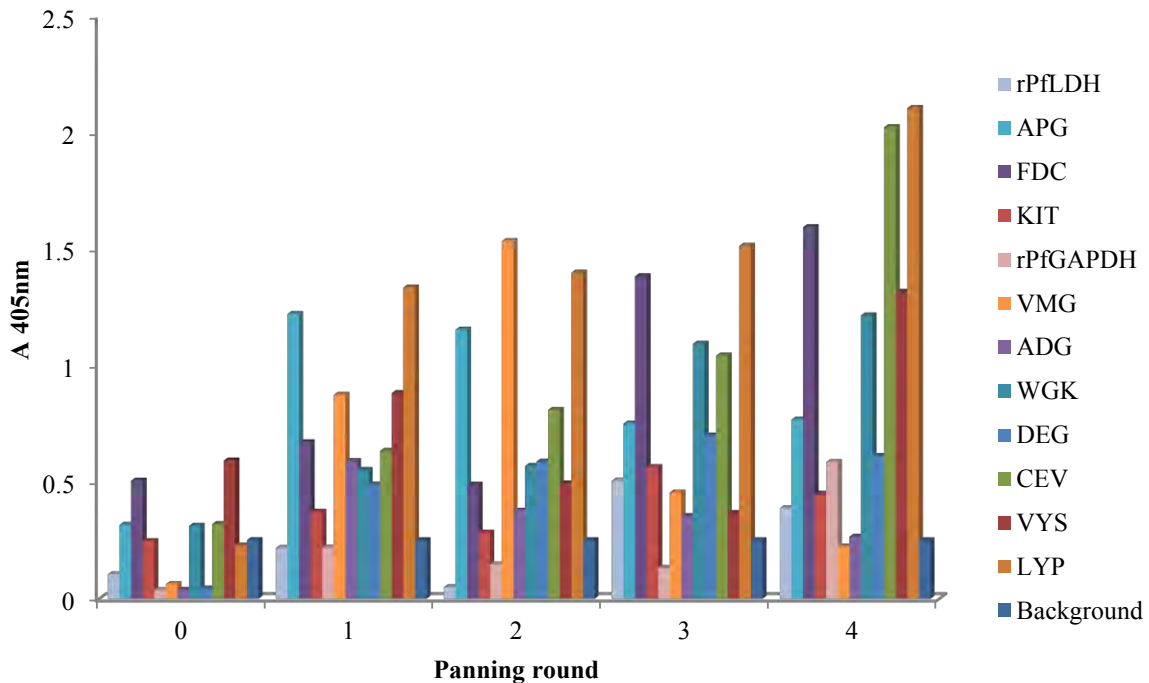


Figure 6.4 Polyclonal phagemid ELISA results for pans one to four of each of the respective target peptides and recombinant proteins

Polyclonal phagemid ELISAs were performed using the rescued phagemids at the end of each panning round as well as the original *Nkuku*[®] stock. The plates were coated with recombinant protein (100 µg/ml) or peptide (10 µg/ml) in PBS. Bound phagemids were detected using monoclonal mouse anti-M13 at 1 in 8000 dilution and a goat anti-mouse-IgG-HRPO at 1 in 1000. A background reading against the blocking agent was included for comparison.

6.2.4 Anti-LDH monoclonal phage selection

Due to the variation in signals between rounds one to four in the polyclonal ELISA, 48 colonies were selected from each panning round for all antigens giving a total of 192 clones per antigen. Initially the clones were screened for binding to the target antigen by a phagemid ELISA, after which the top six clones were screened further and subjected to background or cross-reactivity controls in both their phagemid as well as soluble expressed scFv forms (Figures 6.5 to 6.16 and 6.18). The results were presented in the same order as that used in Table 6.1 and Figure 6.4, starting with the LDH results.

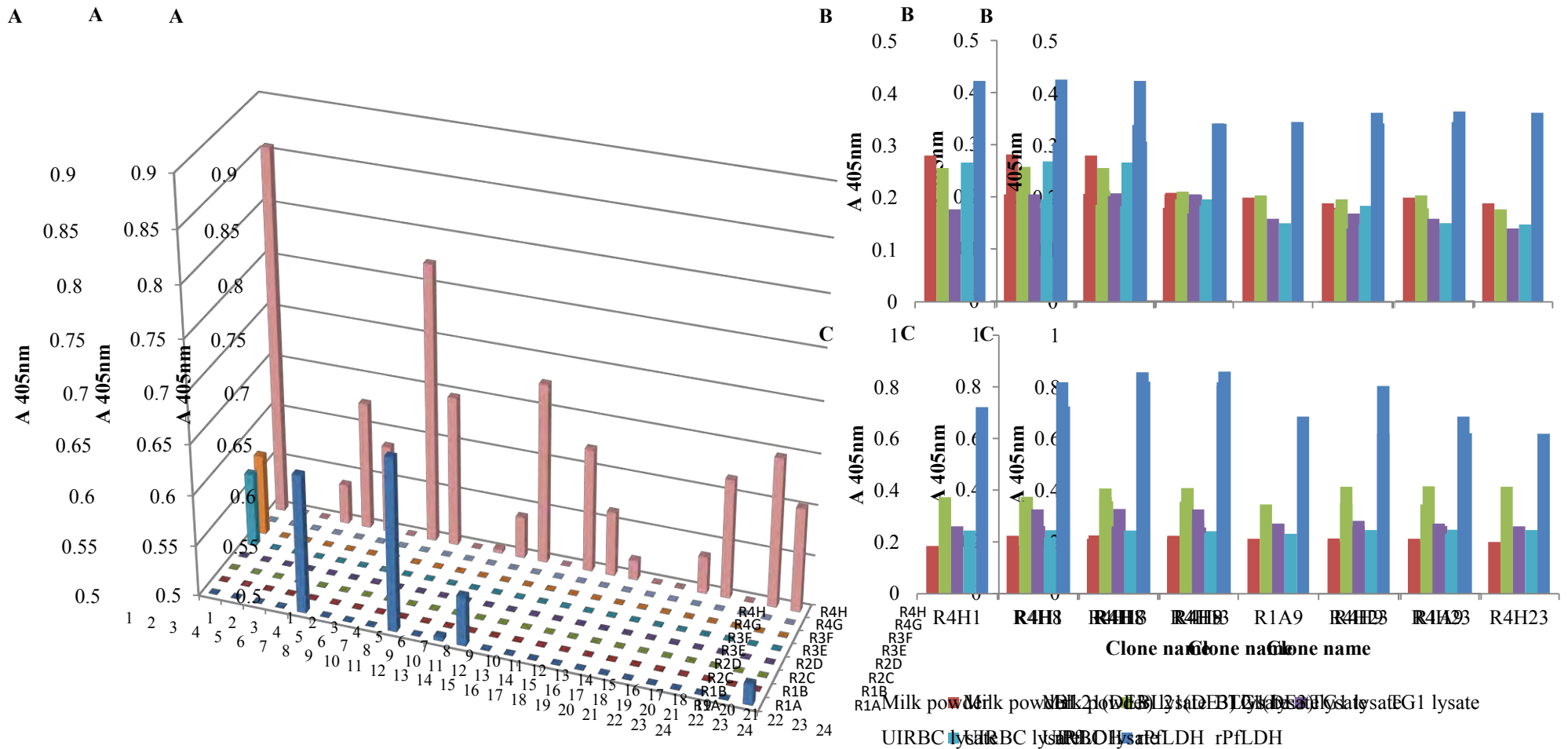


Figure 6.5 Monoclonal phage and soluble scFv ELISA results for the anti-rPflLDH clones

The initial phagemid ELISA to screen for monoclonal binders to rPflLDH were shown in (A) R1 to R4 denotes the panning round from which the clones were selected and A to H and 1 to 24 the specific 96-well culture well inoculated. Six clones with the highest absorbance readings from any round in (A) were characterised further in (B), where cross reactivity against milk powder; BL21(DE3) lysate; TG1 lysate and uninfected red blood cell lysate was assessed. All controls including rPflLDH were coated at 100 µg/ml (A and B). Phagemids were diluted 1:1 with MP-PBS-Tween and detected with a monoclonal mouse anti-M13 antibody at 1 in 8000 dilution and a goat-anti-mouse-IgG-HRPO at 1 in 1000 dilution. The same six clones were assessed as soluble expressed scFvs in (C). The soluble scFvs were similarly diluted 1:1 but were detected using anti-cmyc IgY at 10 µg/ml and a rabbit anti-chicken-HRPO antibody at 1 in 5000.

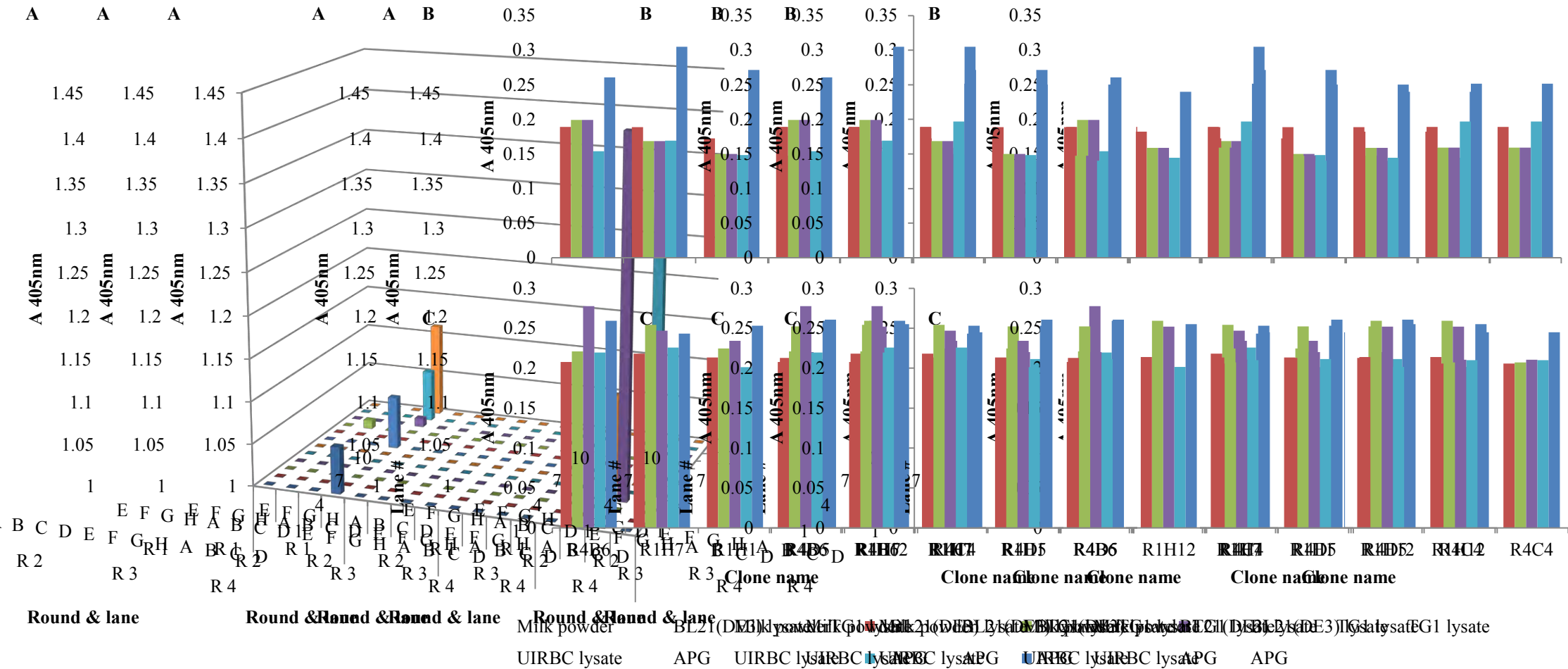


Figure 6.6 Monoclonal phage and soluble scFv ELISA results for the anti-APG (common LDH peptide) clones

The initial phagemid ELISA to screen for monoclonal binders to APG was shown in (A). R1 to R4 denotes the panning round from which the clones were selected and A to H and 1 to 12 the specific 96-well culture well inoculated. Six clones with the highest absorbance readings from any round in (A) were characterised further in (B), where cross reactivity against milk powder; BL21(DE3) lysate; TG1 lysate and uninfected red blood cell lysate was assessed. All controls including APG were coated at 100 µg/ml (A and B). Phagemids were diluted 1:1 with MP-PBS-Tween and detected with a monoclonal mouse anti-M13 antibody at 1 in 8000 dilution and a goat-anti-mouse-IgG-HRPO at 1 in 1000 dilution. The same six clones were assessed as soluble expressed scFvs in (C). The soluble scFvs were similarly diluted 1:1 but were detected using anti-myc IgY at 10 µg/ml and a rabbit anti-chicken-HRPO antibody at 1 in 5000.

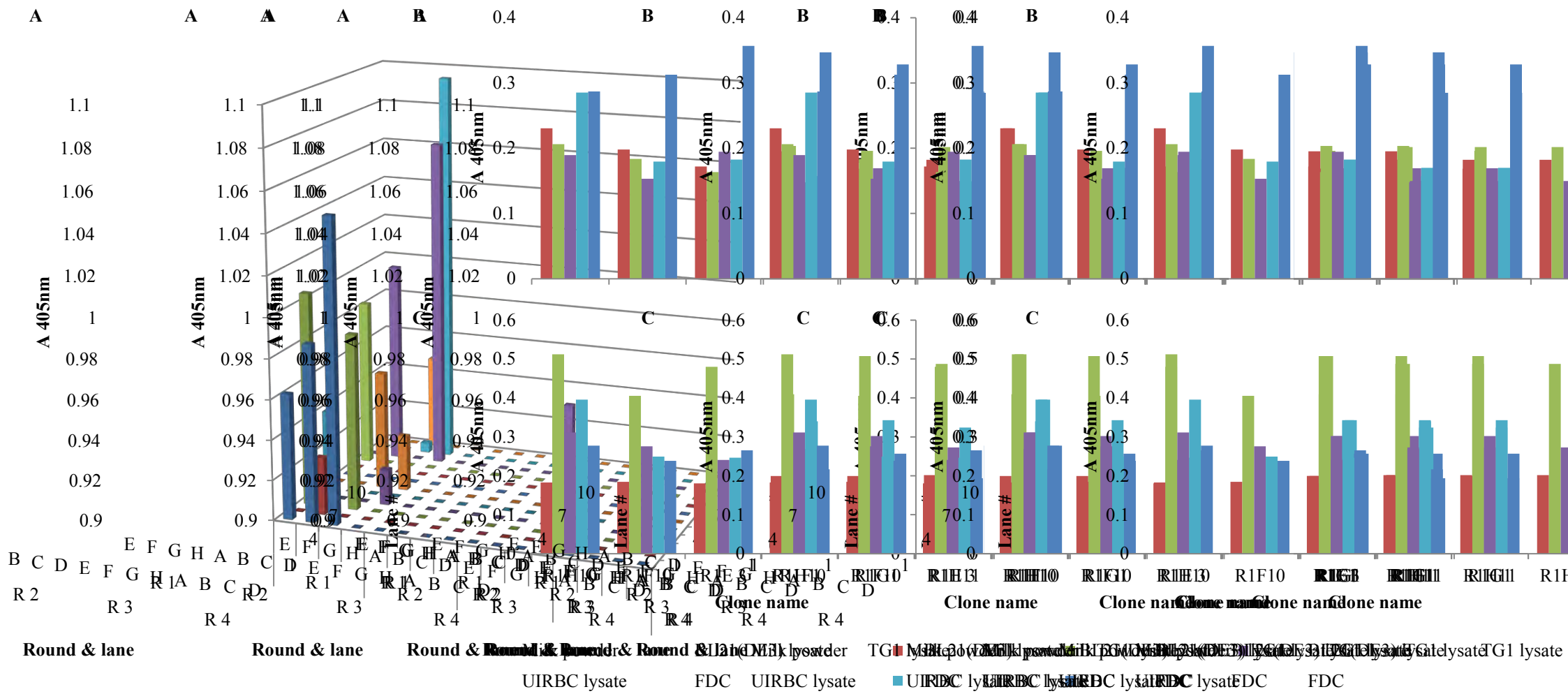


Figure 6.7 Monoclonal phage and soluble scFv ELISA results for the anti-FDC (*P. falciparum* LDH peptide) clones
 The initial phagemid ELISA to screen for monoclonal binders to FDC was shown in (A). R1 to R4 denotes the panning round from which the clones were selected and A to H and 1 to 12 the specific 96-well culture well inoculated. Six clones with the highest absorbance readings from any round in (A) were characterised further in (B), where cross reactivity against milk powder; BL21(DE3) lysate; TG1 lysate and uninfected red blood cell lysate was assessed. All controls including FDC were coated at 100 µg/ml (A and B). Phagemids were diluted 1:1 with MP-PBS-Tween and detected with a monoclonal mouse anti-M13 antibody at 1 in 8000 dilution and a goat-anti-mouse-IgG-HRPO at 1 in 1000 dilution. The same six clones were assessed as soluble expressed scFvs in (C). The soluble scFvs were similarly diluted 1:1 but were detected using anti-cmyc IgY at 10 µg/ml and a rabbit anti-chicken-HRPO antibody at 1 in 5000.

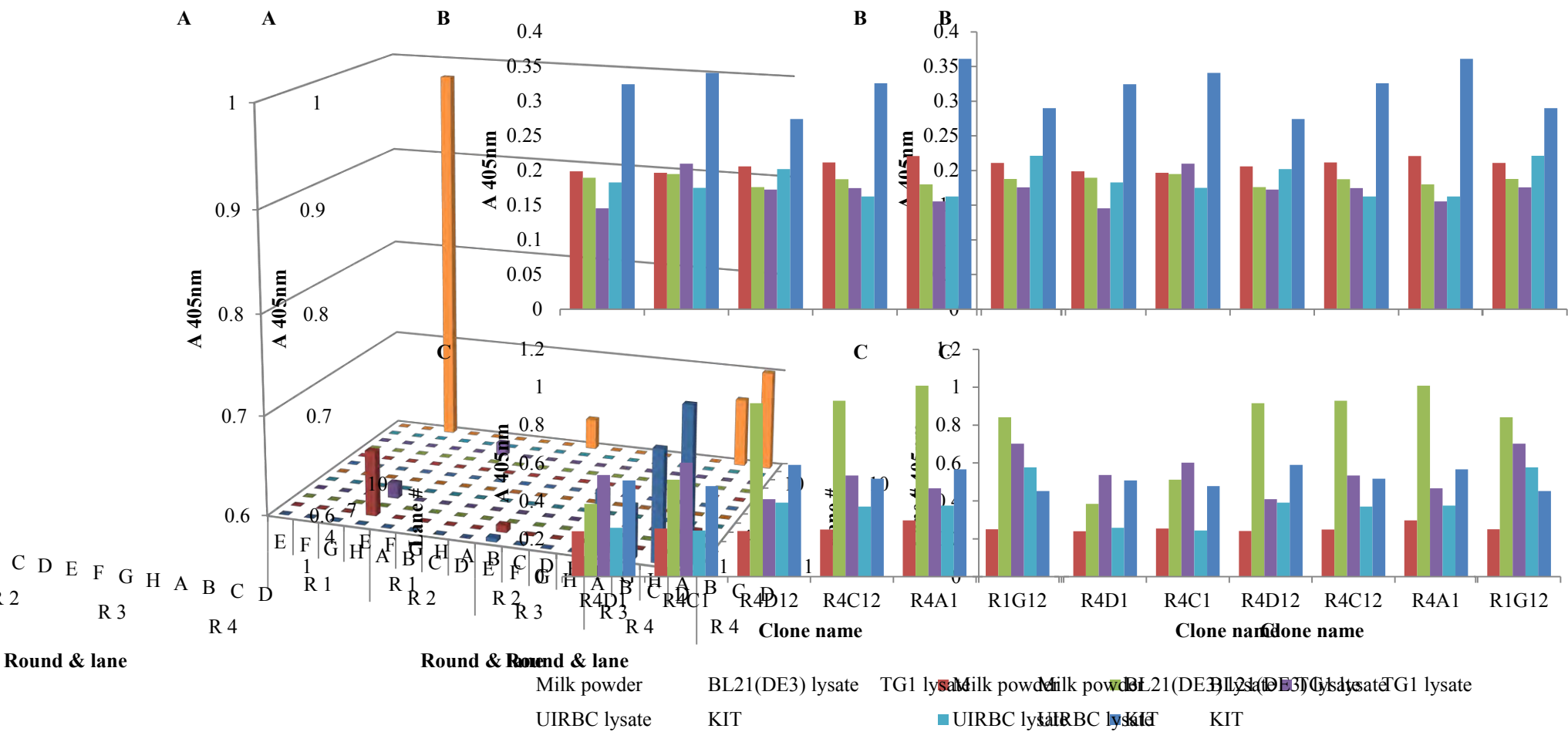


Figure 6.8 Monoclonal phage and scFv ELISA results for the anti-KIT (*P. vivax* LDH peptide) clones

The initial phagemid ELISA to screen for monoclonal binders to KIT was shown in (A). R1 to R4 denotes the panning round from which the clones were selected and A to H and 1 to 12 the specific 96-well culture well inoculated. Six clones with the highest absorbance readings from any round in (A) were characterised further in (B), where cross reactivity against milk powder; BL21(DE3) lysate; TG1 lysate and uninfected red blood cell lysate was assessed. All controls including KIT were coated at 100 µg/ml (A and B). Phagemids were diluted 1:1 with MP-PBS-Tween and detected with a monoclonal mouse anti-M13 antibody at 1 in 8000 dilution and a goat-anti-mouse-IgG-HRPO at 1 in 1000 dilution. The same six clones were assessed as soluble expressed scFvs in (C). The soluble scFvs were similarly diluted 1:1 but were detected using anti-cmyc IgY at 10 µg/ml and a rabbit anti-chicken-HRPO antibody at 1 in 5000.

Interestingly all clones with the highest signals in the preliminary ELISA (Figure 6.5 (A)) against *rPfLDH* were either from panning round one or four. The subsequent background or cross reactivity ELISA results showed specific detection of *rPfLDH* above background readings for all six selected clones (B and C). Five clones were selected from round four and one from round one. The signals against *rPfLDH* in the phagemid ELISA (B) increased to two fold over background in the soluble scFv format (C). Unfortunately none of the anti-peptide scFv clones performed as well in the soluble scFv ELISAs (Figures 6.6 to 6.8). The background phagemid ELISAs all showed positive signals above background levels for the specific antigens tested (B), however in the soluble scFv format none had signals above background (C). Based on these ELISA results, six anti-*rPfLDH* clones from Figure 6.5 were chosen for further analysis. These included clones R4H1, R4H8, R4H13, R1A9, R4H9 and R4H23.

6.2.5 Anti-GAPDH monoclonal phage selection

The next monoclonal results were for the antibodies detecting the GAPDH protein (Figures 6.9 to 6.12), starting with clones against whole *rPfGAPDH*. Like the *rPfLDH* results, clones with greatest signal were from round four, with single colonies from rounds one and two (Figure 6.9 (A)). Again the phagemid background ELISA results were complemented with the soluble scFv ELISA results, and the signal increased two-fold in each case (Figure 6.9 (B and C respectively)). The anti-peptide clones were disappointing as only a single clone against the *P. falciparum* ADG peptide gave a signal above background in the soluble scFv ELISA format (Figure 6.12 (C)). Again six clones against the whole *rPfGAPDH* (Figure 6.9) were chosen for further analysis. These were clones R1A11, R4H13, R4H15, R4H18, R4H20 and R4H23.

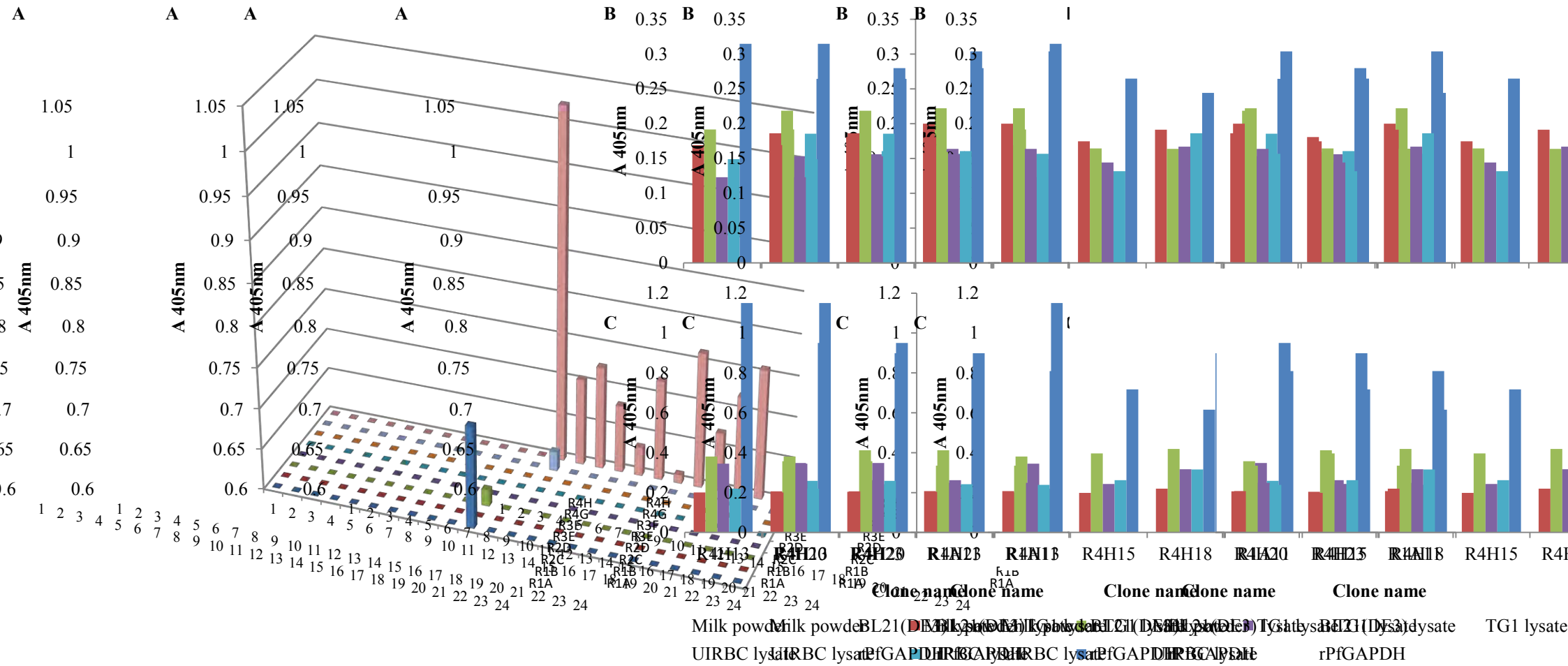
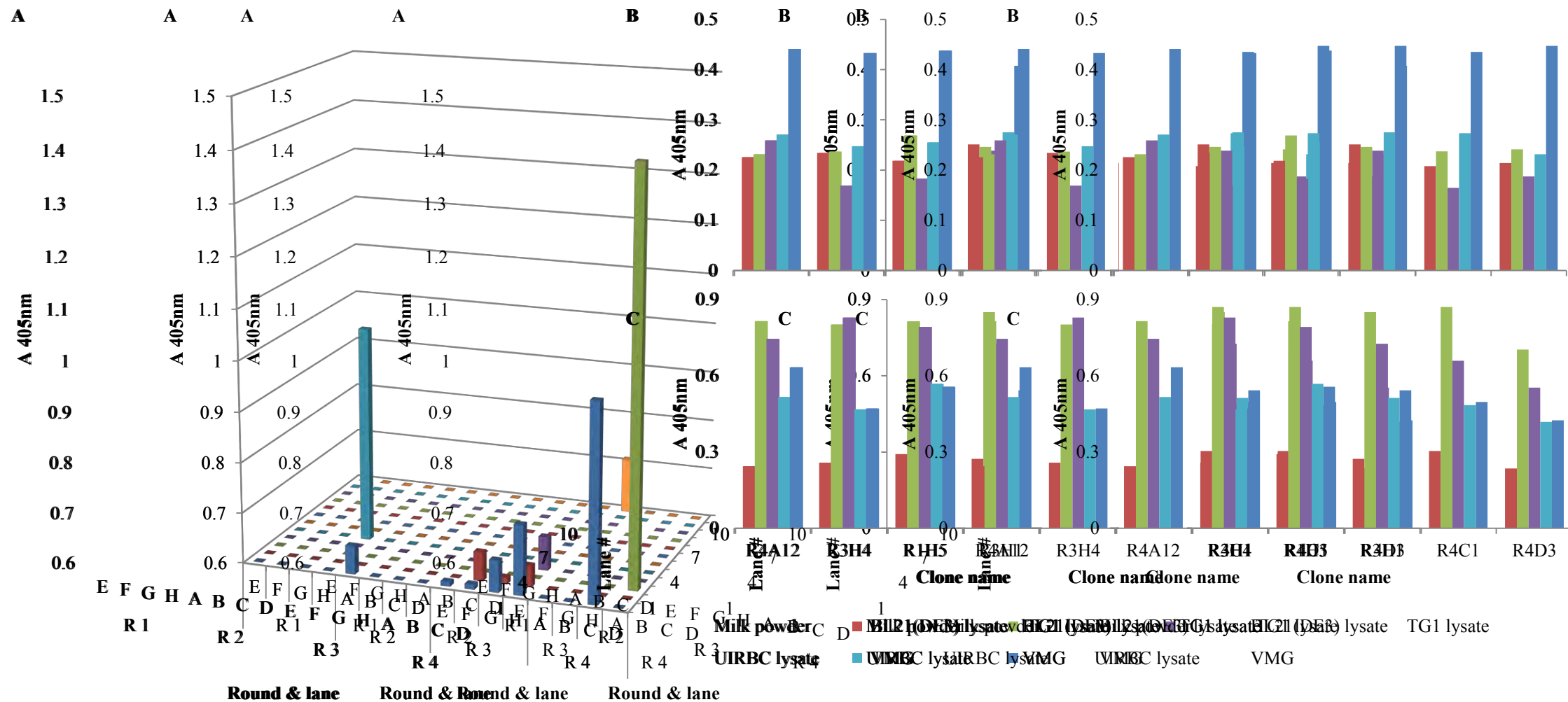


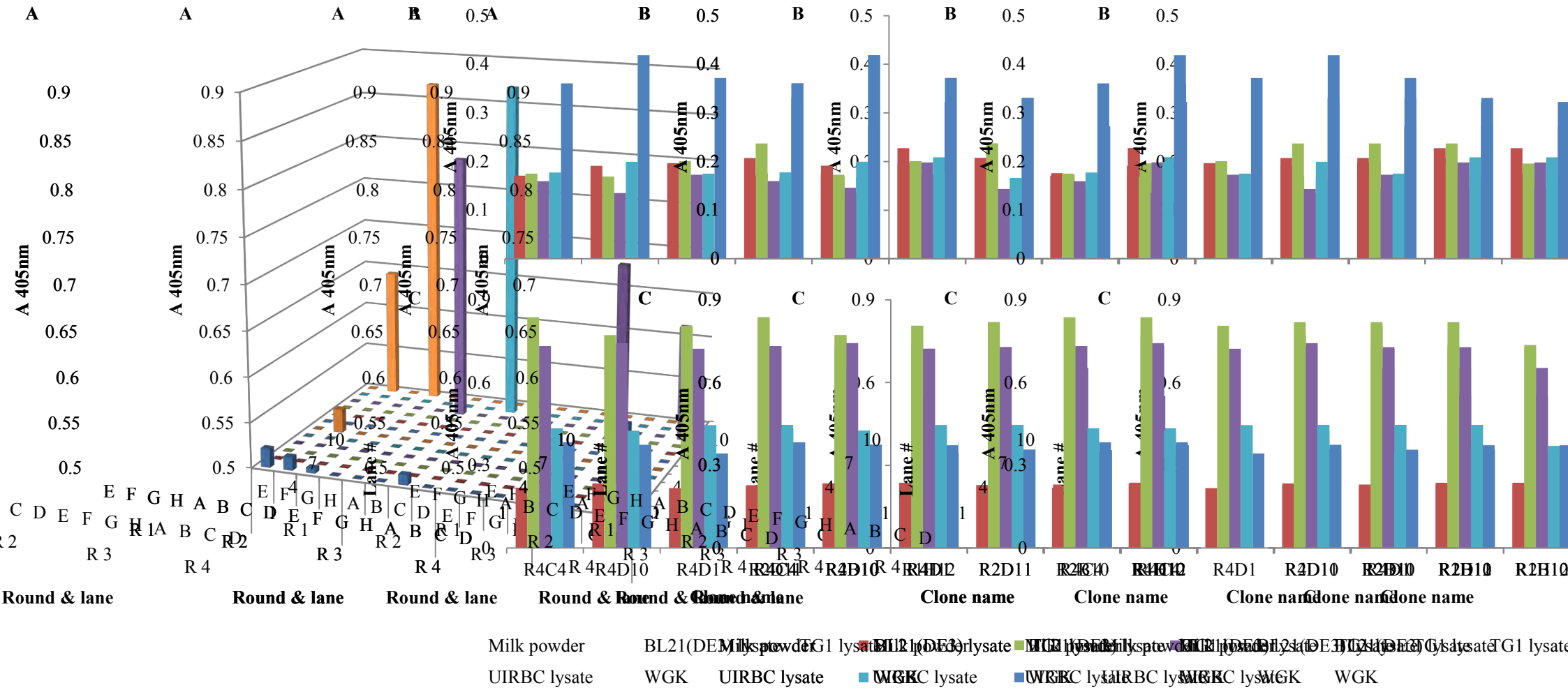
Figure 6.9 Monoclonal phage and soluble scFv ELISA results for the anti-*rPfGAPDH* clones

The initial phagemid ELISA to screen for monoclonal binders to *rPfGAPDH* was shown in (A). R1 to R4 denotes the panning round from which the clones were selected and A to H and 1 to 24 the specific 96-well culture well inoculated. Six clones with the highest absorbance readings from any round in (A) were characterised further in (B), where cross reactivity against milk powder; BL21(DE3) lysate; TG1 lysate and uninfected red blood cell lysate was assessed. All controls including *rPfGAPDH* were coated at 100 µg/ml (A and B). Phagemids were diluted 1:1 with MP-PBS-Tween and detected with a monoclonal mouse anti-M13 antibody at 1 in 8000 dilution and a goat-anti-mouse-IgG-HRPO at 1 in 1000 dilution. The same six clones were assessed as soluble expressed scFvs in (C). The soluble scFvs were similarly diluted 1:1 but were detected using anti-cmyc IgY at 10 µg/ml and a rabbit anti-chicken-HRPO antibody at 1 in 5000.



3 (common GAPDH peptide) clones

The initial phagemid ELISA to screen for monoclonal binders to VMG was shown in (A). R1 to R4 denotes the panning round from which the clones were selected and A to H and 1 to 12 the specific 96-well culture well inoculated. Six clones with the highest absorbance readings from any round in (A) were characterised further in (B), where cross reactivity against milk powder; BL21(DE3) lysate; TG1 lysate and uninfected red blood cell lysate was assessed. All controls including VMG were coated at 100 µg/ml (A and B). Phagemids were diluted 1:1 with MP-PBS-Tween and detected with a monoclonal mouse anti-M13 antibody at 1 in 8000 dilution and a goat-anti-mouse-IgG-HRPO at 1 in 1000 dilution. The same six clones were assessed as soluble expressed scFvs in (C). The soluble scFvs were similarly diluted 1:1 but were detected using anti-myc IgY at 10 µg/ml and a rabbit anti-chicken-HRPO antibody at 1 in 5000.



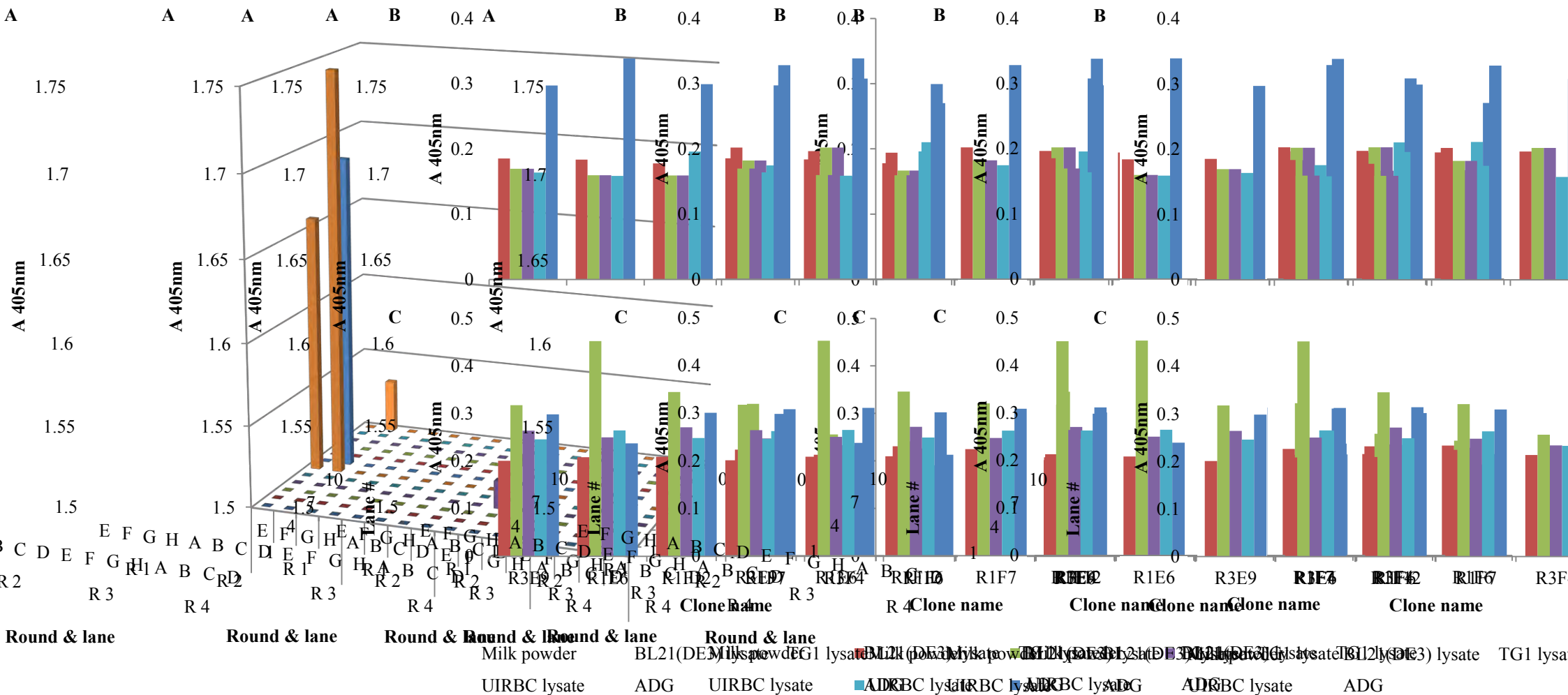


Figure 6.12 Monoclonal phage and soluble scFv ELISA results for the anti-ADG (*P. falciparum* GAPDH peptide) clones

The initial phagemid ELISA to screen for monoclonal binders to ADG was shown in (A). R1 to R4 denotes the panning round from which the clones were selected and A to H and 1 to 12 the specific 96-well culture well inoculated. Six clones with the highest absorbance readings from any round in (A) were characterised further in (B), where cross reactivity against milk powder; BL21(DE3) lysate; TG1 lysate and uninfected red blood cell lysate was assessed. All controls including ADG were coated at 100 µg/ml (A and B). Phagemids were diluted 1:1 with MP-PBS-Tween and detected with a monoclonal mouse anti-M13 antibody at 1 in 8000 dilution and a goat-anti-mouse-IgG-HRPO at 1 in 1000 dilution. The same six clones were assessed as soluble expressed scFvs in (C). The soluble scFvs were similarly diluted 1:1 but were detected using anti-myc IgY at 10 µg/ml and a rabbit anti-chicken-HRPO antibody at 1 in 5000.

6.2.6 Anti-PMT monoclonal phage selection

The largest number of positive clones was achieved with respect to the anti-PMT peptide clones. Positive clones from all except the *P. knowlesi* peptide were obtained. Starting with the common PMT peptide (DEG peptide), five clones were selected from round three and a single clone from round one (Figure 6.13 (A)). All six clones selected, had signals above background for both the phagemid (B) and soluble scFv ELISAs (C) and hence all of these were analysed further.

For the *P. falciparum* PMT peptide (CEV peptide) all clones were selected from round four (Figure 6.14 (A)). All six clones also resulted in signals above background for the phagemid (B) and soluble scFv ELISAs (C). As a result all six clones were analysed further.

The last of the positive scFv selections were for the *P. vivax* PMT peptide (VYS peptide). Four clones were selected from round one and single clones from rounds three and four (Figure 6.15 (A)). Each of the six selected clones detected the peptide in both the phagemid (B) and soluble scFv formats (C). Again all six clones were further analysed.

The clone selections against the *P. knowlesi* PMT peptide (LYP peptide) were not as promising. Of the six selected clones, five from round three and one from round one (Figure 6.16 (A)) only clones R1H1 and R3F2 gave specific signals above background in both the phagemid and soluble scFv formats (B and C respectively). The soluble ELISA results had very low absorbance values therefore none of these clones were further analysed.

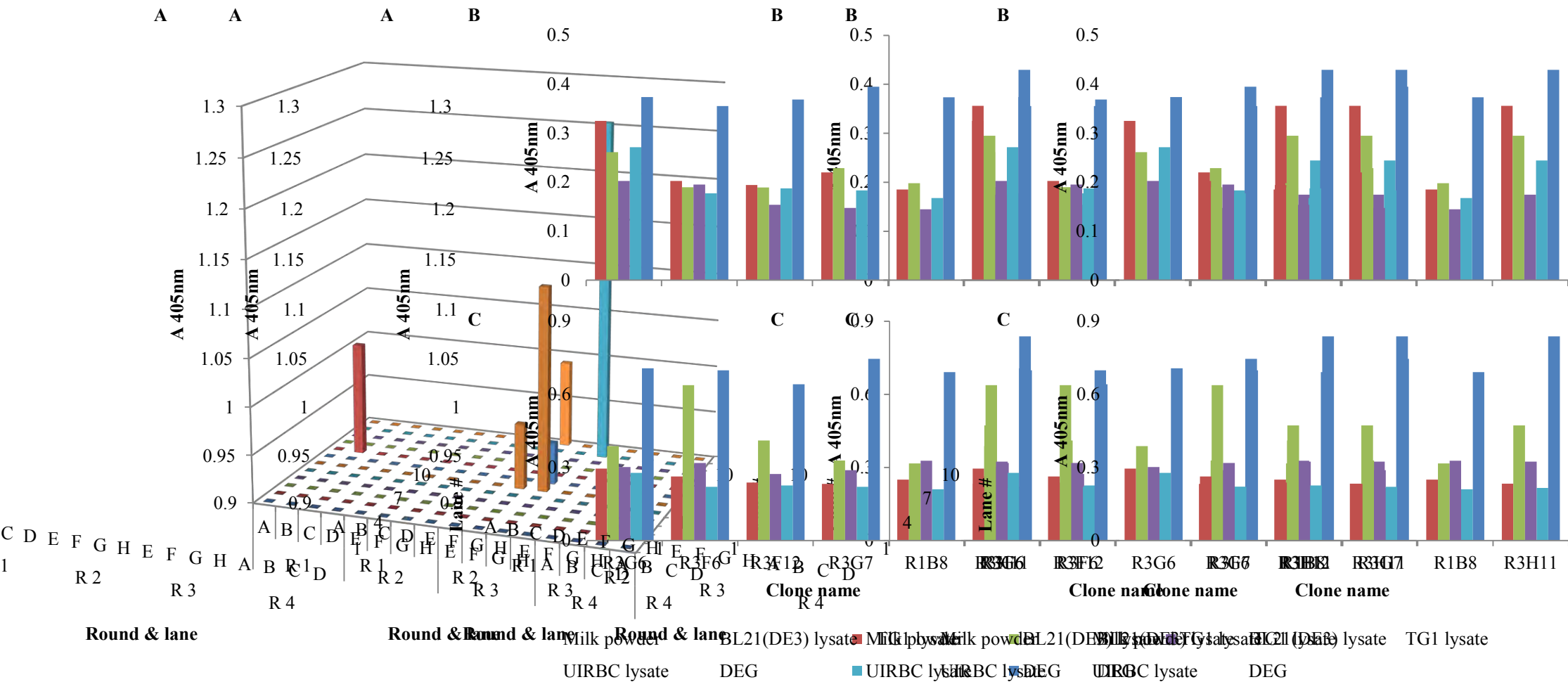


Figure 6.13 Monoclonal phage and soluble scFv ELISA results for the anti-DEG (common PMT peptide) clones

The initial phagemid ELISA to screen for monoclonal binders to DEG was shown in (A). R1 to R4 denotes the panning round from which the clones were selected and A to H and 1 to 12 the specific 96-well culture well inoculated. Six clones with the highest absorbance readings from any round in (A) were characterised further in (B), where cross reactivity against milk powder; BL21(DE3) lysate; TG1 lysate and uninfected red blood cell lysate was assessed. All controls including DEG were coated at 100 µg/ml (A and B). Phagemids were diluted 1:1 with MP-PBS-Tween and detected with a monoclonal mouse anti-M13 antibody at 1 in 8000 dilution and a goat-anti-mouse-IgG-HRPO at 1 in 1000 dilution. The same six clones were assessed as soluble expressed scFvs in (C). The soluble scFvs were similarly diluted 1:1 but were detected using anti-myc IgY at 10 µg/ml and a rabbit anti-chicken-HRPO antibody at 1 in 5000.

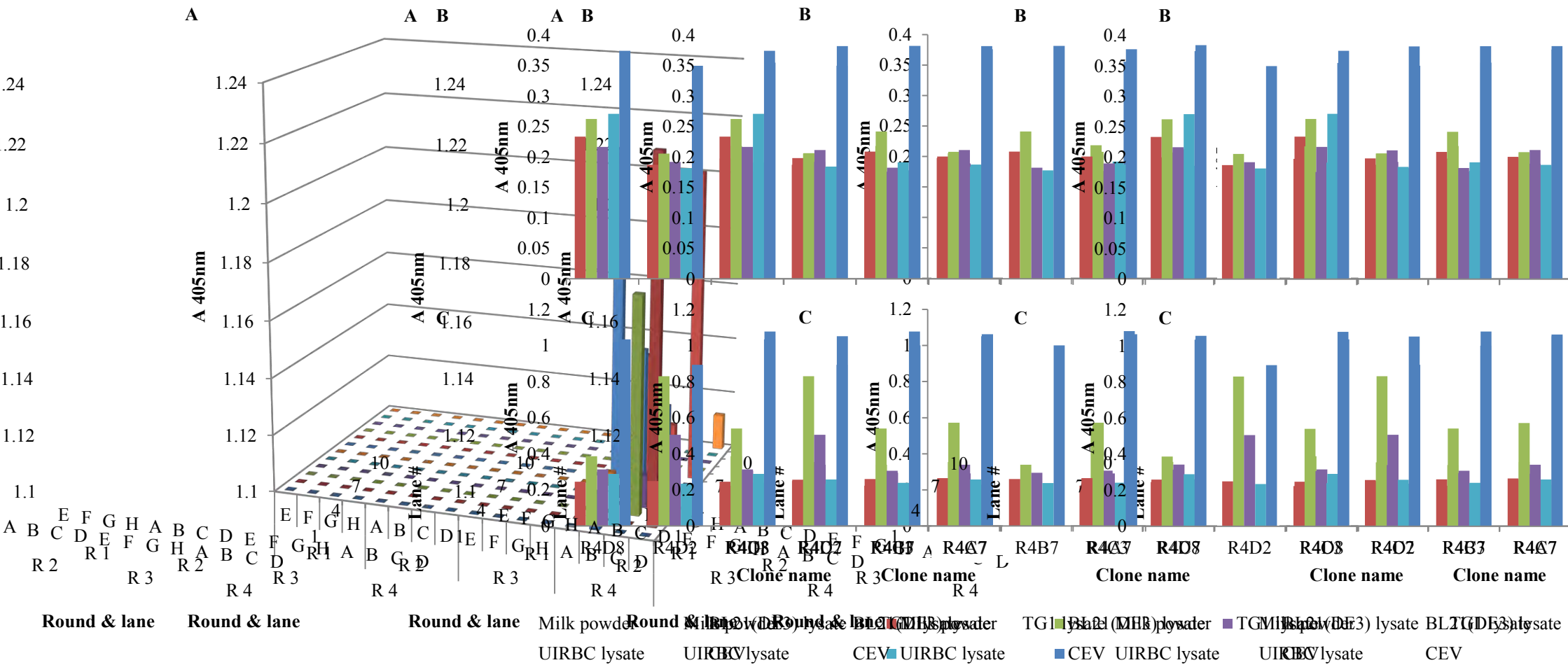


Figure 6.14 Monoclonal phage and soluble scFv ELISA results for the anti-CEV (*P. falciparum* PMT peptide) clones

The initial phagemid ELISA to screen for monoclonal binders to CEV was shown in (A). R1 to R4 denotes the panning round from which the clones were selected and A to H and 1 to 12 the specific 96-well culture well inoculated. Six clones with the highest absorbance readings from any round in (A) were characterised further in (B), where cross reactivity against milk powder; BL21(DE3) lysate; TG1 lysate and uninfected red blood cell lysate was assessed. All controls including CEV were coated at 100 µg/ml (A and B). Phagemids were diluted 1:1 with MP-PBS-Tween and detected with a monoclonal mouse anti-M13 antibody at 1 in 8000 dilution and a goat-anti-mouse-IgG-HRPO at 1 in 1000 dilution. The same six clones were assessed as soluble expressed scFvs in (C). The soluble scFvs were similarly diluted 1:1 but were detected using anti-myc IgY at 10 µg/ml and a rabbit anti-chicken-HRPO antibody at 1 in 5000.

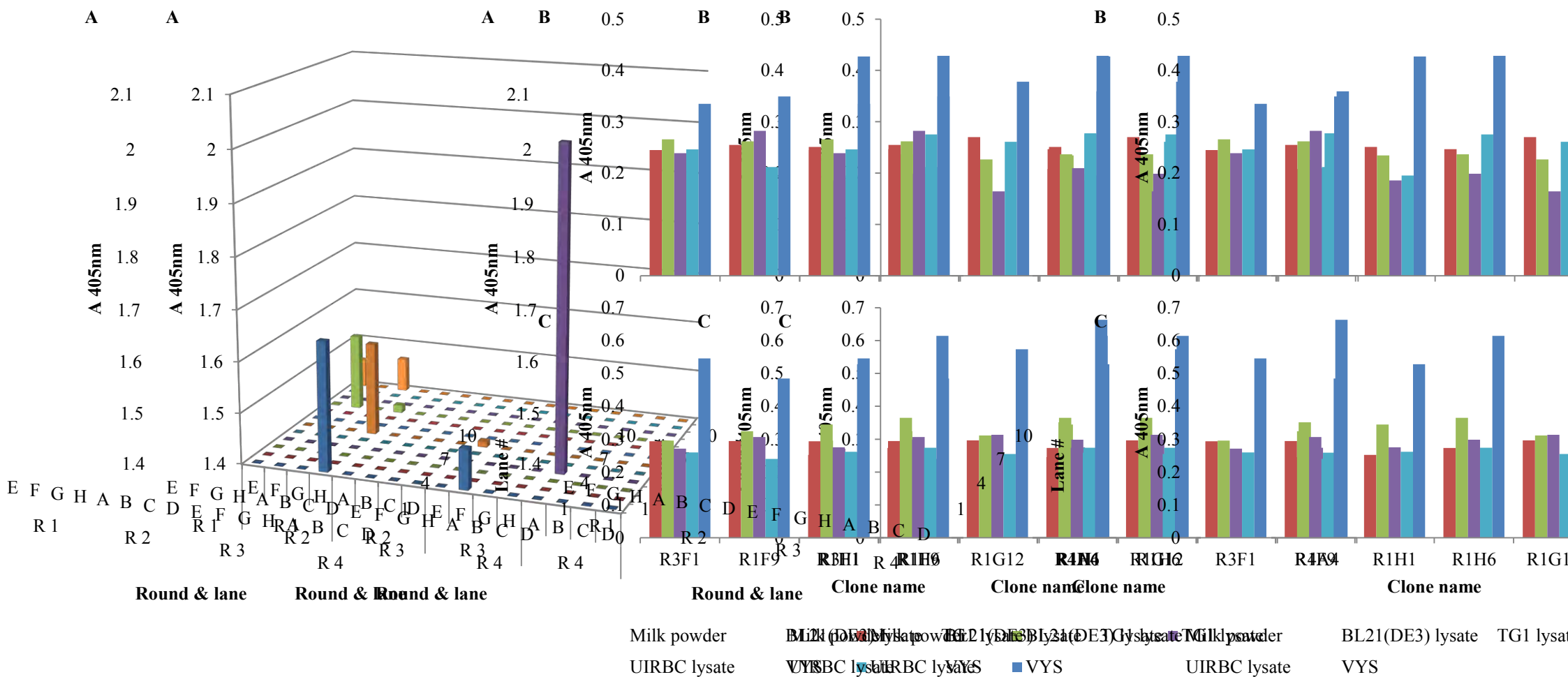


Figure 6.15 Monoclonal phage and soluble scFv ELISA results for the anti-VYS (*P. vivax* PMT peptide) clones

The initial phagemid ELISA to screen for monoclonal binders to VYS was shown in (A). R1 to R4 denotes the panning round from which the clones were selected and A to H and 1 to 12 the specific 96-well culture well inoculated. Six clones with the highest absorbance readings from any round in (A) were characterised further in (B), where cross reactivity against milk powder; BL21(DE3) lysate; TG1 lysate and uninfected red blood cell lysate was assessed. All controls including VYS were coated at 100 µg/ml (A and B). Phagemids were diluted 1:1 with MP-PBS-Tween and detected with a monoclonal mouse anti-M13 antibody at 1 in 8000 dilution and a goat-anti-mouse-IgG-HRPO at 1 in 1000 dilution. The same six clones were assessed as soluble expressed scFvs in (C). The soluble scFvs were similarly diluted 1:1 but were detected using anti-myc IgY at 10 µg/ml and a rabbit anti-chicken-HRPO antibody at 1 in 5000.

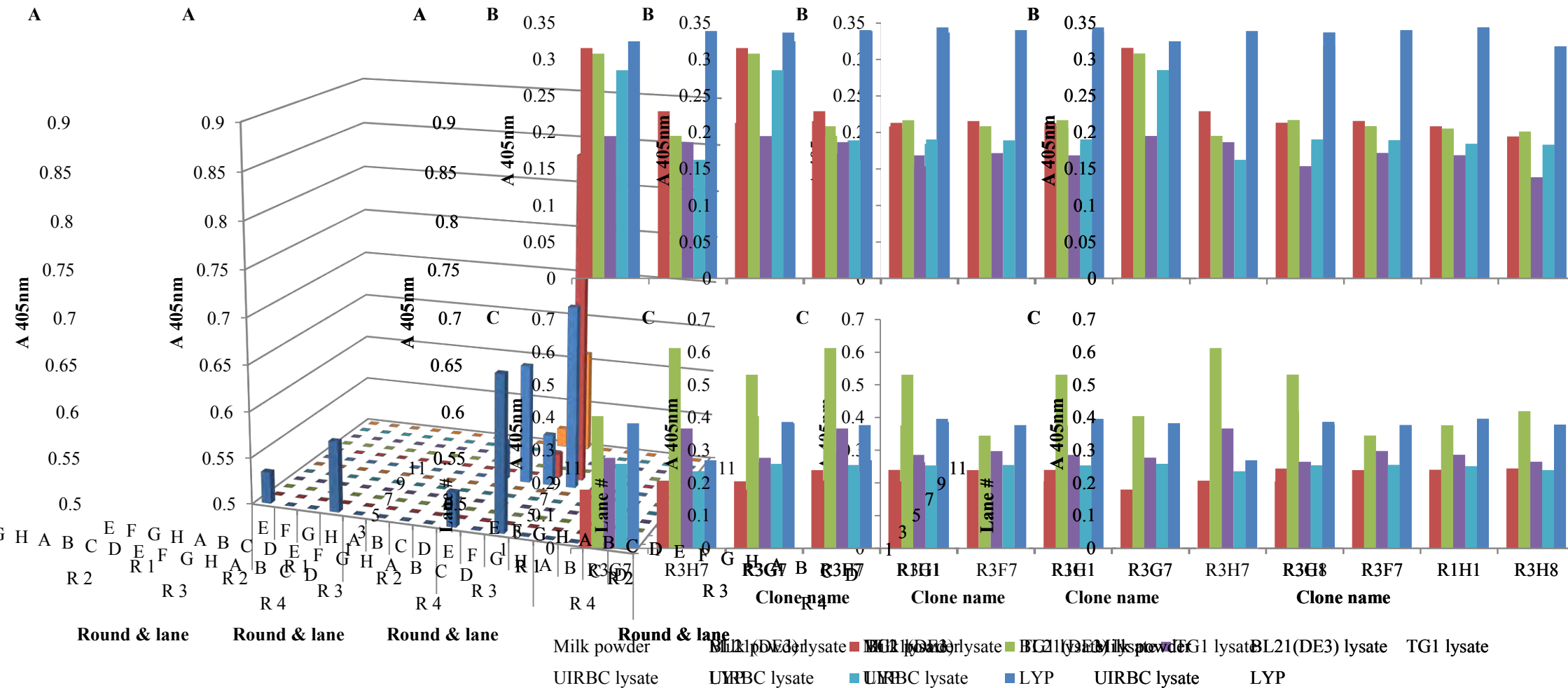


Figure 6.16 Monoclonal phage and soluble scFv ELISA results for the anti-LYP (*P. knowlesi* PMT peptide) clones

The initial phagemid ELISA to screen for monoclonal binders to LYP was shown in (A). R1 to R4 denotes the panning round from which the clones were selected and A to H and 1 to 12 the specific 96-well culture well inoculated. Six clones with the highest absorbance readings from any round in (A) were characterised further in (B), where cross reactivity against milk powder; BL21(DE3) lysate; TG1 lysate and uninfected red blood cell lysate was assessed. All controls including LYP were coated at 100 µg/ml (A and B). Phagemids were diluted 1:1 with MP-PBS-Tween and detected with a monoclonal mouse anti-M13 antibody at 1 in 8000 dilution and a goat-anti-mouse-IgG-HRPO at 1 in 1000 dilution. The same six clones were assessed as soluble expressed scFvs in (C). The soluble scFvs were similarly diluted 1:1 but were detected using anti-cmyc IgY at 10 µg/ml and a rabbit anti-chicken-HRPO antibody at 1 in 5000.

6.2.7 Detection of soluble scFv fragments using the anti-cmyc IgY

The presence of an amber stop codon (TAG) between the cmyc and protein III sequences (Figure 6.1) meant that if the scFvs were expressed from *E. coli* suppressor strains a ~ 30 kD pelB-scFv-cmyc protein was expected. The anti-rPflDH clones selected in Figure 6.4 were used to assess this and were transfected into *E. coli* Top 10 cells. The resulting expression was assessed by SDS-PAGE and western blot in Figure 6.17.

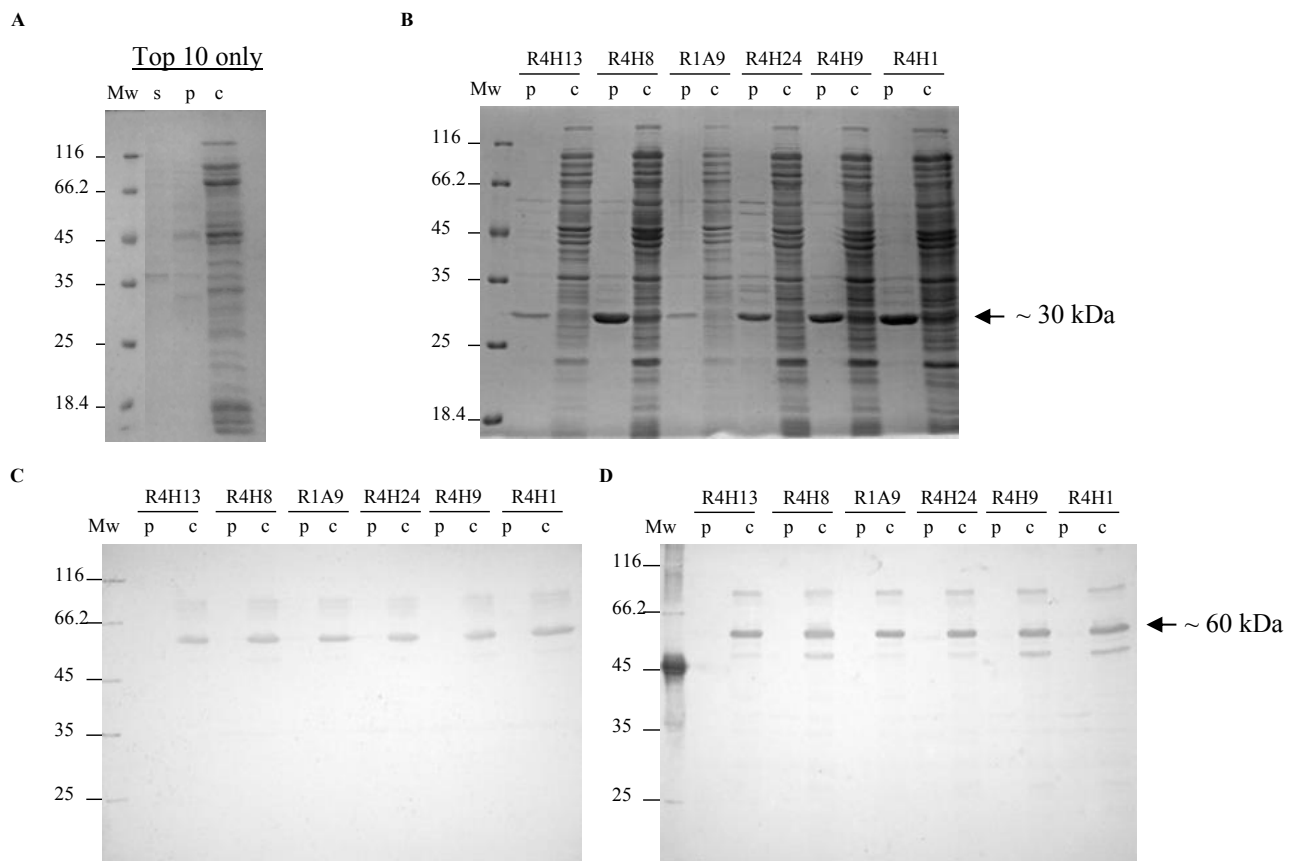


Figure 6.17 Expression of the top six anti-rPflDH scFvs analysed by SDS-PAGE and western blot
 The culture media, periplasm and cytoplasm fractions of an untransformed Top 10 *E. coli* culture were analysed on 12.5% reducing SDS-PAGE gel stained with Coomassie blue (A). The periplasm and cytoplasm of the top six scFv clones expressed from infected *E. coli* Top 10 cells using Terrific broth were similarly assessed in (B). The cmyc-tagged scFvs were subsequently detected with anti-cmyc-IgY at 1 µg/ml and a rabbit anti-chicken-IgY-HRPO at 1 in 10000 (C) or anti-cmyc-rabbit-IgG at 1 in 80 and a goat anti-rabbit-IgG-HRPO at 1 in 2500 (D). Lanes were labelled as (Mw) molecular weight marker; (s) supernatant / culture media; (p) periplasm; (c) cytoplasm fractions and the respective clones were labelled above the lanes in the panels (B to D).

Due to the PelB leader peptide, the scFv fragments are reported to reside in the periplasm after expression. For this reason the periplasmic fractions and cytoplasmic fractions were separately analysed on SDS-PAGE gels. A prominent band approximately 31 kD in size was produced in the periplasm of transfected *E. coli* cells (B), which was absent from the control (A). However when probed with the anti-cmyc IgY (C), as well as rabbit anti-cmyc crude

serum (D), a band around 60 kD was present in the cytoplasmic fraction. The anti-r*Pf*LDH clone R4H1 was assessed further by passing both the cytoplasmic as well as periplasmic fractions over an anti-cmyc-IgY Hydrazide[®] column. Only the cytoplasmic fraction contained protein that bound the column and was eluted as an approximately 68 kD band as shown in Figure 6.18.

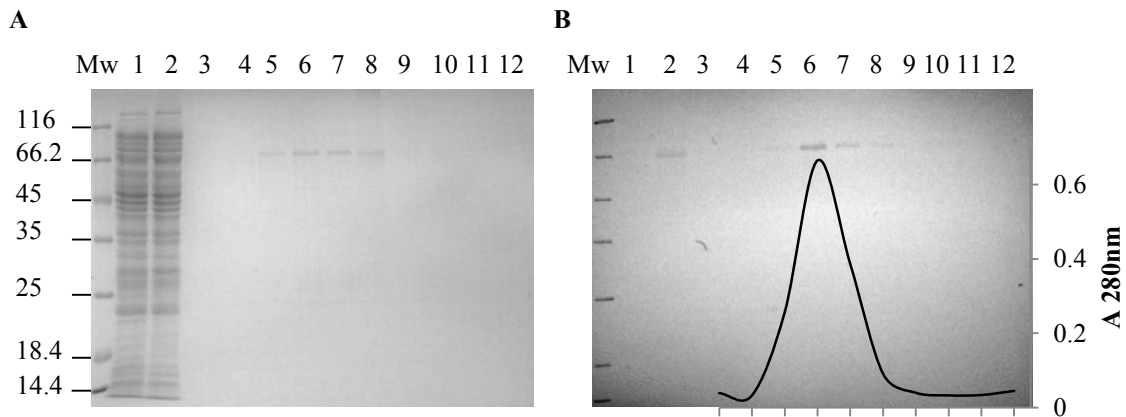


Figure 6.18 Expression and affinity purification of the anti-r*Pf*LDH scFv clone R4H1 analysed by SDS-PAGE and western blot

The anti-r*Pf*LDH scFv clone R4H1 was expressed in *E. coli* Top 10 cells using Terrific broth. The cmyc-tagged scFvs were affinity purified using an anti-cmyc-IgY Hydrazide[®] resin and the purification steps were analysed on a 12.5% reducing SDS-PAGE gel (A) and probed with the anti-cmyc tag IgY at 1 µg/ml and a secondary rabbit anti-chicken-IgY-HRP0 antibody at 1/10000 dilution (B). The elution profile measuring absorbance at 280 nm was shown as an insert on the western blot. The lanes were loaded with molecular weight marker (Mw); Top 10 unbound cell lysate (lane 1); supernatant sample loaded onto the Hydrazide[®] column (lane 2); eluents 1 to 10 (lanes 3 to 12).

6.2.8 Sequencing results of the scFv clones

The 30 clones selected for further analysis from the ELISA results were first assessed by colony and nested PCR and AluI restriction endonuclease digest before sequencing. Only 13 of the 30 scFv clones were sent for sequencing and were selected based on the following results. First colony PCR was performed on all 30 clones using the OP52 forward and M13 reverse primers to amplify the expected ~1000 bp scFv coding regions (van Wyngaardt *et al.*, 2004). The resulting positive clones which gave ~1000 bp amplicons included five LDH clones (clone R4H13 was excluded); six GPADH clones, where clone R4H20 amplified an ~800 bp sequence; two anti-DEG (common PMT peptide) clones R3F12 and R3G7 and three clones against the *Pv*PMT peptide (VYS peptide) R1F9, R1H1 and R1G12 (Figure 6.19).

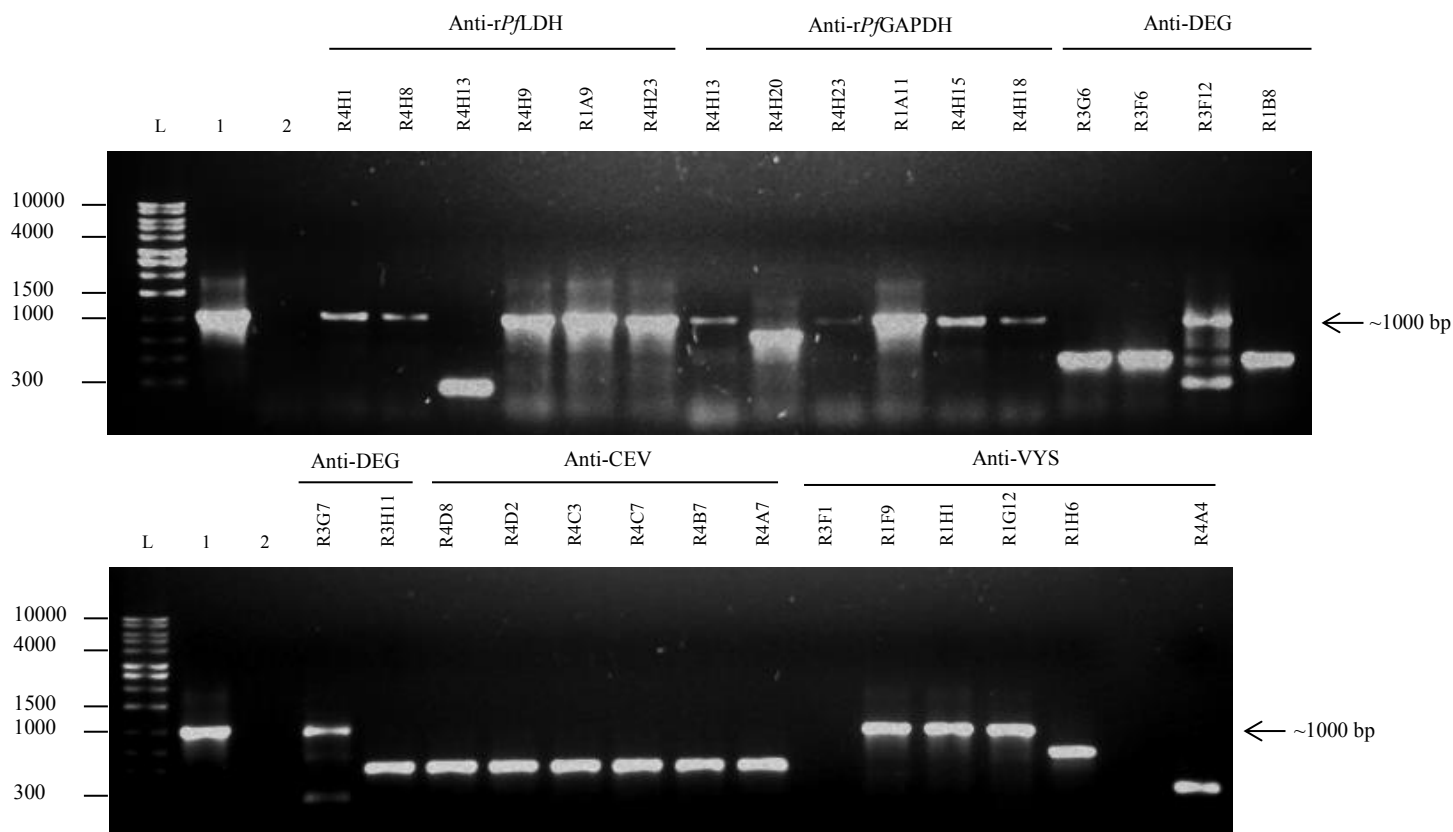


Figure 6.19 Colony PCR of the selected clones against *rPfl*LDH, *rPfg*GAPDH and the PMT peptides
 Colony PCR was performed on the selected scFv clones against *rPfl*LDH, *rPfg*GAPDH and the PMT peptides (DEG, CEV and VYS) and assessed on a 1% agarose gel visualised with EtBr. An unrelated clone was picked and used as a positive control in lane 1, where lane 2 was an uninfected *E. coli* TG1 colony used as a negative control. The DNA ladder was loaded in the lane marked L. All other lanes were labelled with the respective clone abbreviation loaded in that lane.

Following successful colony PCR amplification of the scFv coding regions (~1000 bp amplicons), nested PCR was performed using a primer specific to the (GGGGG)₃ linker coding sequence.

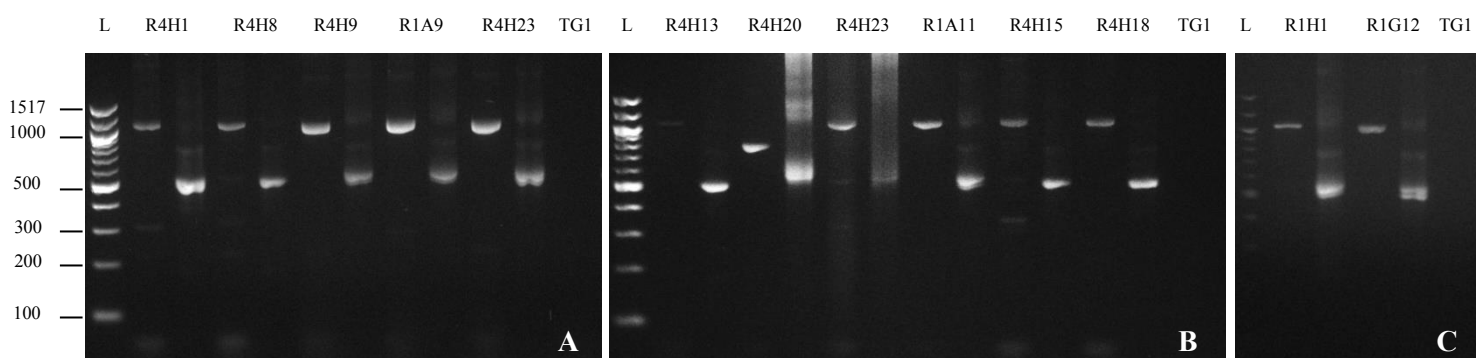


Figure 6.20 Nested PCR of the selected clones against *rPfl*LDH, *rPfg*GAPDH and the *Pv*PMT peptide (VYS)
 Nested PCR was performed on the selected scFv clones against *rPfl*LDH (A), *rPfg*GAPDH (B) and the *Pv*PMT peptide (VYS) in (C) and assessed on a 3% agarose gel visualised with EtBr. An uninfected *E. coli* TG1 colony used as a negative control and the sample loaded in the TG1 lane. The DNA ladder was loaded in the lane marked L. All other lanes were labelled with the respective clone abbreviation loaded in that lane.

Successful amplification should result in amplicons around 500 bp in size as seen in Figure 6.20. This narrowed the number of clones to 13 of the original 30. Only the GAPDH clone R4H20 once again ran at ~800 bp for the colony PCR amplicon, but a nested PCR amplicon of approximately 500 bp was observed. To assess the identity of the 13 clones, the colony PCR amplicons were digested with the restriction endonuclease AluI (Finlay *et al.*, 2006). Depending on the number of AluI sites within each clone's coding sequence, a unique "fingerprint" or pattern may be observed when resolved on agarose as shown in Figure 6.21. The resulting digest patterns suggested clones R4H1 and R4H8 to be similar; R4H9 and R4H23 and the two anti-*Pv*PMT peptide clones R1H1 and R1G12. All 13 clones shown in Figure 6.21 were sent for sequencing using the colony PCR primer sets from Figure 6.19. The results for the LDH clones were presented first in Figure 6.22.

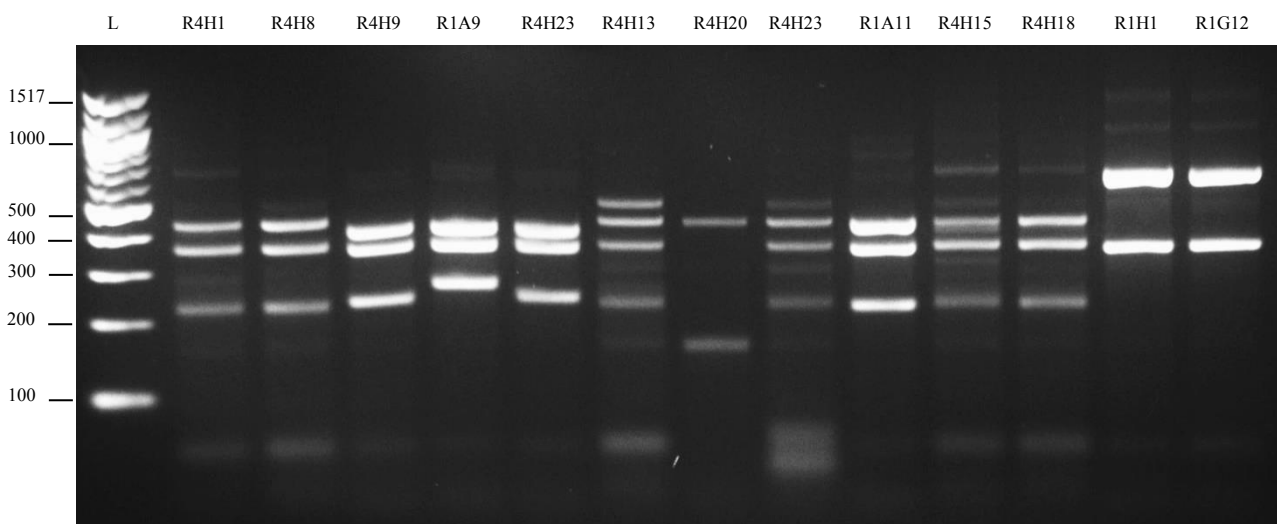


Figure 6.21 AluI digest of the selected clones against *rPfl*LDH, *rPfl*GAPDH and the *Pv*PMT peptide (VYS)

AluI digest was performed on the colony PCR products of the selected scFv clones against *rPfl*LDH, *rPfl*GAPDH and the *Pv*PMT peptide (VYS) and assessed on a 3% agarose gel visualised with EtBr. The DNA ladder was loaded in the lane marked L. All other lanes were labelled with the respective clone abbreviation loaded in that lane.

To link the sequencing results with the AluI digest results in Figure 6.21, the number of AluI restriction sites (AG[^]CT) within each of the anti-*rPfl*LDH scFv coding regions was determined. The R4H1 clone coding sequence harboured two sites, which resulted in fragments of around 428, 368 and 233 bp which were visible in Figure 6.21. Clone R4H8's coding sequence contained four sites, resulting in fragments of 428, 376, 259, 22 and 21 bp. The three larger fragments were visible on the agarose gel, whilst the smaller fragments were too small to be observed. The R4H9 clone coding sequence contained two restriction sites resulting in three fragments of 404, 360 and 230 bp which were visible (Figure 6.21).

The R1A9 clone had two restriction sites within its coding sequence and resulted in three fragments of around 359, 261 and 257 bp respectively. The only aberration in the AluI results was the larger band within the R1A9 sample, which may have been as a result of incomplete digestion that may result in a band of approximately 518 bp (261+257 bp). The size difference between the 261 and 257 bp fragments is unlikely to be visible and the band at around 260 bp on the gel most likely includes both fragments. Finally the R4H23 clone against rPfLDH had two restriction sites within its coding sequence, resulting in three bands of around 402, 358 and 234 bp respectively, which also correlated with the results of the restriction digest shown in Figure 6.21.

The heavy and light chains in scFv coding sequences each code for a set of four framework regions (FR1 to 4) and three complementarity determining regions (CDR1 to 3) as indicated in Figure 6.22 (A). Most conservation between sequences is expected for the framework regions, which held true for most clones except the R4H23 clone which contained unique FR1 to three regions for its heavy chain. Most amino acid variations amongst all five clones were within the CDRs and in particular the CDR2 and 3 of both the light and heavy chains. The least variation was within the CDR1 of the light chain in all cases. Interestingly only clones R4H1 and R4H8 had identical CDRs and only varied within their heavy chain CDR1 and 2 respectively. None of the clones resembled those isolated from an immune chicken library screened with rPfLDH by Chiliza *et al.* (2008) as shown in the alignment in Figure 6.22 (B) though there were a few conserved amino acids within the respective CDRs.

Analysis of the anti-rPfGAPDH scFv clones was done next. Based on the sequencing results, clone R4H20 had three AluI restriction sites which should have resulted in four fragments of 434, 172, 153 and 23 bp respectively. From Figure 6.21 only two of these bands were visible, namely the 434 bp and 172 bp fragments. The R1A11 clone contained two restriction sites resulting in three fragments of 428, 398 and 240 bp respectively, which were all visible on the agarose gel. The individual sequences are shown in Figure 6.23. The R4H18 clone was only successfully sequenced in the reverse direction, hence an incomplete sequence was shown in Figure 6.23. A high degree of similarity between it and the R1A11 clone was observed, however, and the CDR1 to 3 of the heavy chain were almost identical to those of the R1A11 clone. What was more interesting was that clone R1A11 and clone R4H1 against rPfLDH (Figure 6.22) shared 85% identity, with identical CDRs throughout.

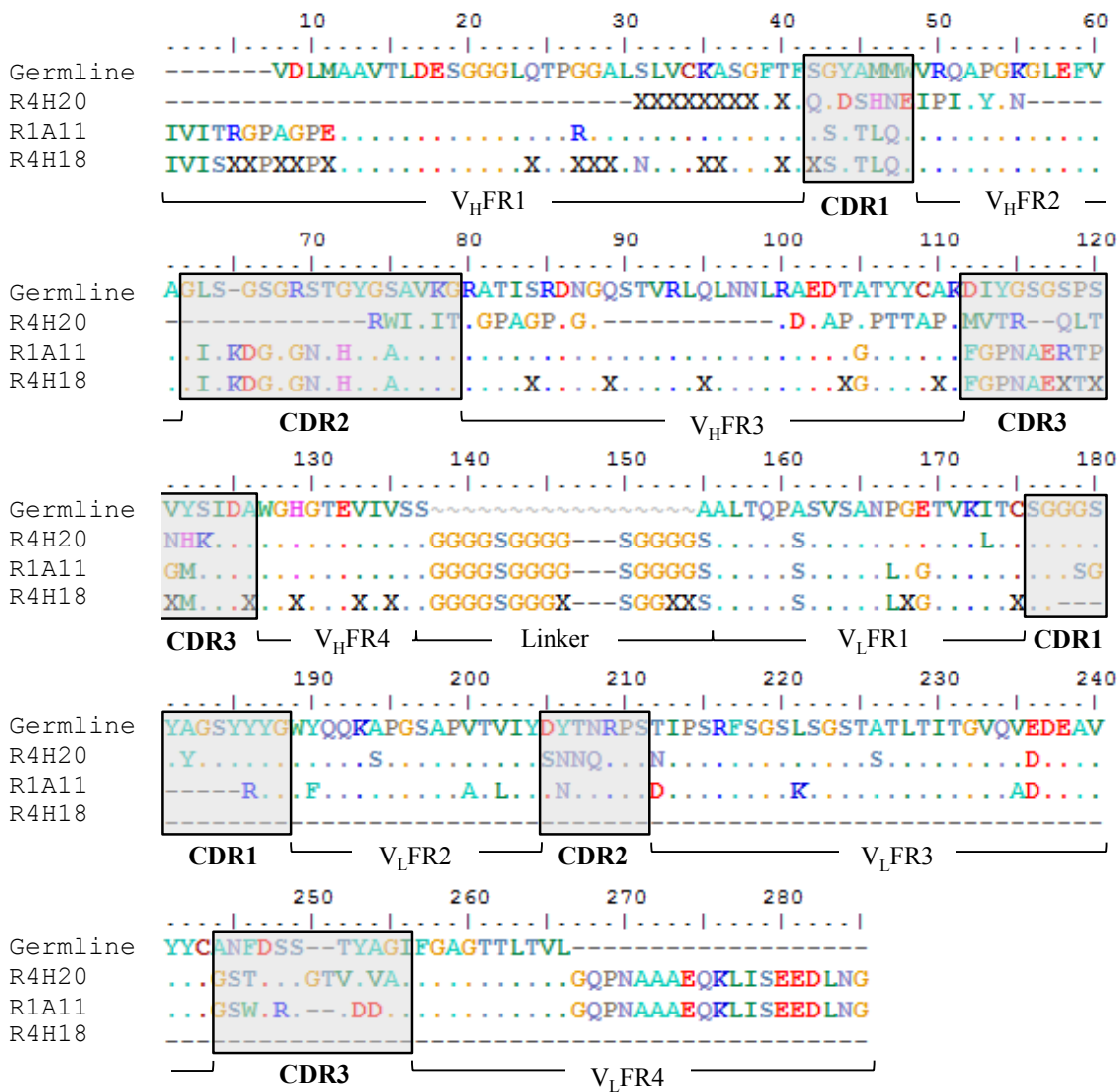


Figure 6.23 Alignment of the anti-rPfGAPDH scFv clones' translated sequences with a chicken germline immunoglobulin sequence

The translated amino acid sequence for the anti-rPfGAPDH clones were aligned with a chicken IgG germline amino acid sequence. The linker region (G₄S)₃ and the framework regions 1 to 4 were underlined, with V_H and V_L for heavy and light chains respectively. The complementarity determining regions (CDR) 1 to 3 for both the V_H and V_L chains were box-shaded and in bold. In the alignments "." represent identical residues to the germline sequence, letters represent an amino acid substitution, "-" represent gaps in the alignment and "X" represent an undetermined amino acid codon from the sequencing results.

Finally the anti-PvPMT peptide scFv clones were assessed as shown in Figure 6.24. Both clones harboured only single Alu1 restriction sites. This was predicted to result in 648 and 393 bp fragments for clone R1H1 and 644 and 397 bp fragments for clone R1G12 which correlated with the bands detected on the agarose gel in Figure 6.21.

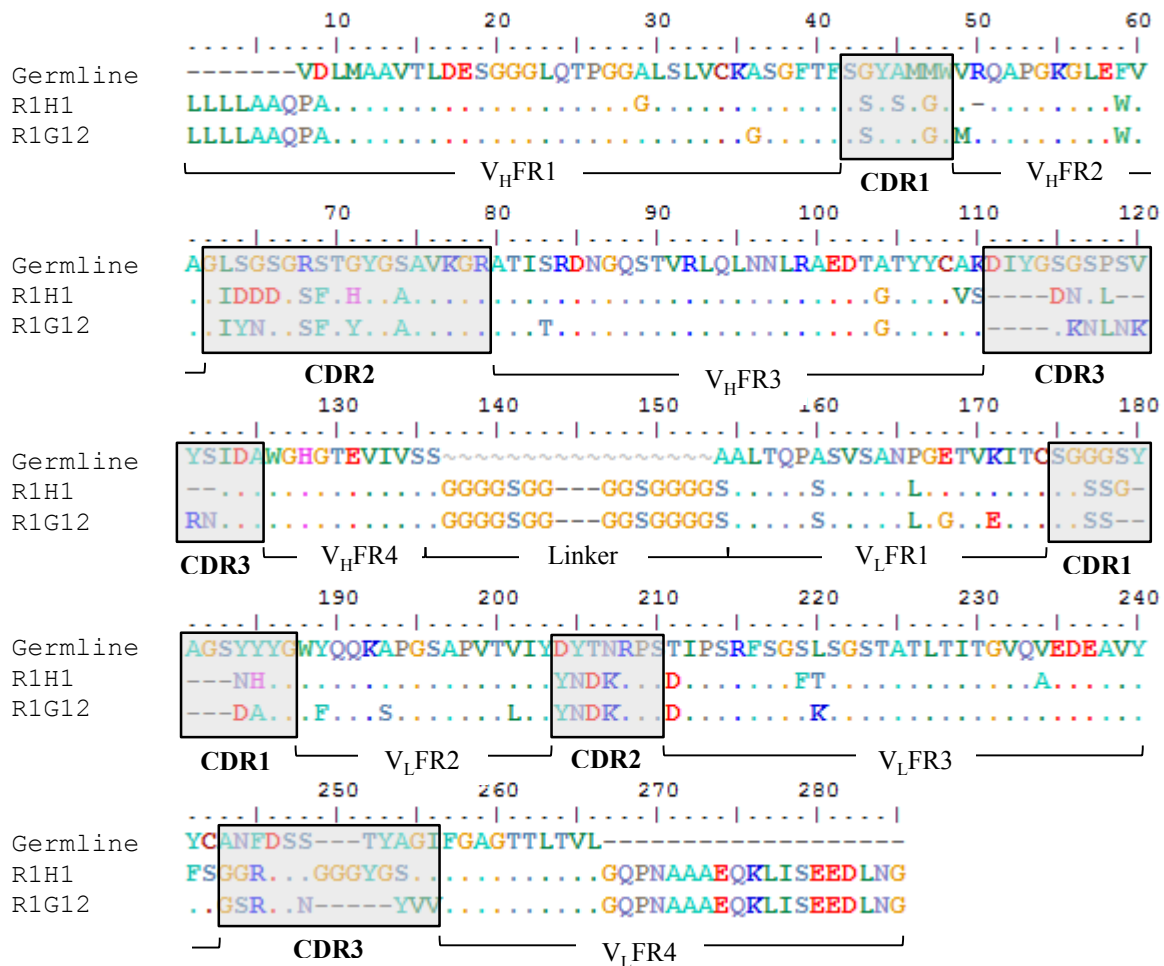


Figure 6.24 Alignment of the anti-PvPMT peptide (VYS) scFv clones' translated sequences with a chicken germline immunoglobulin sequence

The translated amino acid sequence for the anti-PvPMT peptide (VYS) scFv clones were aligned with a chicken IgG germline amino acid sequence. The linker region (G₄S)₃ and the framework regions 1 to 4 were underlined, with V_H and V_L for heavy and light chains respectively. The complementarity determining regions (CDR) 1 to 3 for both the V_H and V_L chains were box-shaded and in bold. In the alignments “.” represent identical residues to the germline sequence, letters represent an amino acid substitution, “-” represent gaps in the alignment and “X” represent an undetermined amino acid codon from the sequencing results.

The two clones share an identical CDR2 region in their light chains, with several amino acid differences in their remaining CDRs. Importantly these were the only two scFv sequences which were in frame for both the vector encoded N-terminal (LLLLAAQPA) and C-terminal myc sequence (EQKLISEEDLN).

6.3 Discussion

The initial results from panning the scFv library against *rPfl*LDH, *rPfg*GAPDH and the peptides against *Plasmodium* LDH, GAPDH and PMT, showed increasing signals from rounds one to four for the polyclonal ELISA. Some clones showed higher signals in earlier rounds, however, and as a result single colonies were selected for further analysis from all four rounds for all targets. The initial monoclonal ELISA screen of the selected clones was promising. Six clones with the highest signals were selected for each target and these were assessed for background reactions with *E. coli* and uninfected red blood cell lysates as well as the blocking reagent. Colony PCR was performed on promising clones from the ELISA assays and if the expected 1000 bp amplicon for the scFv sequence was amplified, then the clone was assessed further. A similar strategy was employed by Leow *et al.* (2014) whilst screening a scFv library for binders against *Plasmodium falciparum* Histidine rich protein 2. Sizes of the PCR amplicons may vary slightly due to different CDRs however the presence of the framework regions within the sequences should allow for selection of such clones by PCR (van Wyngaardt *et al.*, 2004). There was one exception to this pattern in the study and that was clone R4H20 isolated against *rPfg*GAPDH which was sequenced before adopting this strategy. This clone encodes for a shortened heavy chain region, lacking a portion of the first framework region and hence an 800 bp amplicon was observed after colony PCR.

In addition to the colony PCR, samples were assessed by nested PCR. A nested primer was designed that anneals to the coding region for the (GGGGS)₃ linker region common to all the scFv clones as this links the heavy and light chains (van Wyngaardt *et al.*, 2004). In doing so an amplicon of approximately 500 bp was expected and this would exclude any clones lacking the linker region. Prior to sequencing, the PCR amplicons of all clones were digested with Alu1 which recognises an AG[^]CT restriction site. This was used by Finlay *et al.* (2006) to assess clone population homology. Initially a few clones seemed identical based on this analysis, however sequencing revealed substituted amino acids at various positions within CDRs of the clones. This method could be used as a crude measure of clonal diversity and is perhaps only useful in cases where high numbers of positive clones are identified in an initial screen.

Most of the variation in the CDRs for the clones selected here fell within the heavy chain regions, especially CDR2 and 3. This was expected since the CDR3 VH coding region is the main source of antibody variation as it plays a major role in antibody binding (Marks *et al.*, 1991; Nissim *et al.*, 1994; Sheets *et al.*, 1998; van Wyngaardt *et al.*, 2004). Interestingly the

clones raised against rPfLDH showed little homology within their CDRs with clones against the same protein isolated from an immune chicken scFv library (Chiliza *et al.*, 2008). This could be explained by the different libraries used in the two studies, since scFv libraries are constructed from variable gene mRNA of B-cells. The *Nkuku*[®] library is a naïve library, whereas Chiliza *et al.* (2008) used an immune library. Immune libraries are constructed from mRNA of B-cells which have undergone immune maturation in the host's immune system, as opposed to the whole naïve repertoire (Clackson *et al.*, 1991). AbD Serotec[®] supply a commercial scFv monoclonal antibody for the detection of *Plasmodium falciparum* and *Plasmodium vivax* LDH. It was selected from the HuCAL[®] library and is a synthetic human antibody gene-based library expressed on phages by bacteria, but no sequence information was available, so no sequence comparison can be made here.

The most costly steps in the selection of scFv antibodies from libraries are the monoclonal antibodies required for detection of the phage and scFv particles in the ELISAs, as well as the sequencing reactions to identify the selected clones (Rahim *et al.*, 2003; van Wyngaardt *et al.*, 2004). In this work it was decided to produce our own polyclonal chicken antibodies against the cmc peptide tag used in the pHEN1 vector (Hoogenboom *et al.*, 1991). The antibodies were successfully used in the soluble scFv ELISA format; however initial purification of scFv from periplasmic isolations did not purify the expected 30 kD protein. Instead a protein around 70 kD in size was purified from cytoplasmic fractions of *E. coli* used to express the scFvs. This was close to an expected size of approximately 73 kD for scFv-pIII fusion proteins.

An explanation for the lack of detection of soluble scFvs (not linked to proteinIII) on western blots using the anti-cmyc antibodies raised here may be due to conformational orientation of the cmc tag which may prevent binding of the antibodies. Perhaps extending the peptide to include the GAA(E) at the C-terminus which would mimic the extended cmc coded for in the pHEN1 vector, where (E) is coded for by the amber codon would improve detection (Hoogenboom *et al.*, 1991). The addition of GAA may not affect the antibody binding due to the small side chain groups of these amino acids. Depending on the expression host (*supE*^{+/-}) the final E may be added, however and its polar side chain may well affect the affinity of antibodies. The two clones specific for the PvPMT peptide mentioned in Figure 6.24 should be expressed in *E. coli* Top10 cells and purified using the anti-cmyc antibody column. Since the sequencing data suggests that the clones are in-frame with the vector coding sequence (LLLLAAQPA) as well as a full cmc tag (EQKLISEEDLN), these scFvs should purify

effectively as the expected 30 kD proteins. An *E. coli* Top10 lysate should also be included as a control in western blots to ensure that the ~70 kD protein is not of *E. coli* origin.

There have been cases where stop codons can be read through, which could also explain the detection of the larger ~70 kD scFv-proteinIII fusion even though a non-suppressor *E. coli* Top10 strain was used. MacBeath *et al.* (1998) reported that the stop codon UGA may regularly be read through in protein overexpression systems and substituted with a tryptophan (T) or selenocysteine instead (Major *et al.*, 1996). This was similarly suggested by Carcamo *et al.* (1998) for the UAA codon. The ability of ribosomes to change open reading frames by -1; +1; +6 has been documented and in some cases ribosomal hopping and the ability to read through certain stop codons has also been reported (Weiss *et al.*, 1991). Importantly the UAG (amber stop codon) is also read through in suppressor *E. coli* strains such as TG1 used during panning and use of non-suppressor strains such as Top10 is meant to increase soluble scFv fragments (not linked to proteinIII). This may alter the binding properties of scFvs as a result and should be assessed.

There were multiple cases of scFv clones isolated here that did not amplify the expected ~1000 bp coding regions even though they seemed to be good binders based on ELISA results. A few authors reported cases in which the final sequencing results after panning rounds have revealed frameshift mutations and stop codons within sequences (Carcamo *et al.*, 1998; Jacobsson and Frykberg, 1996). In the Carcamo *et al.* (1998) study the frequency of frameshift mutations or the presence of stop codons (UAA and UGA) was as high as 56% of clones (a total of 133 clones selected), where those lacking an open reading frame (either a -1 or +1 frameshift mutation) gave ELISA signals equal to or greater than those with open reading frames. High guanine (G) and thymine (T) content in scFv DNA could potentially result in secondary mRNA structures caused by G:U (uracil) pairing in turn affecting translation. The authors suggest that regular clones with open reading frames are preferentially selected during panning, however if such clones are not selected then enrichment of rare binding clones may occur, such as those lacking open reading frames. Jacobsson and Frykberg (1996) also observed a high frequency of frameshift mutants in genomic libraries of *Staphylococcus aureus* origin cloned into a M13 based phagemid system. They suggested ribosomal “slippage” as a mechanism of translation in such cases.

We decided to exclude such clones from this study by using colony and nested PCR, which resulted in a total of ten clones which will be characterised further in future studies. The high

homology between the R4H1 anti-r*Pf*LDH and R1A11 anti-r*Pf*GAPDH clones was interesting and should be characterised further. This homology may have resulted from the clones detecting the same region on the recombinant proteins such as the histidine-tag or alternatively conformational epitopes on the common Rossman fold motif shared between the two dehydrogenases is also possible. To conclude in this chapter monoclonal antibody reagents against all three target proteins were isolated, including scFv's against whole recombinant proteins as well as a linear peptide epitope target. The preliminary screens showed that the clones detected their targets but further characterisation of binding affinities and specificity are required.

Chapter 7

General discussion and future work

7.1 *Brief overview*

An effective diagnostic test should ideally conform to the ASSURED criteria: **A**ffordable, **S**ensitive, **S**pecific, **U**ser-friendly, **R**apid and robust, **E**quipment-free and **D**eliverable to end-users (Peeling *et al.*, 2006). Of all the malaria diagnostic tests on the market thus far, RDTs best match these criteria, although some new methods such as haemozoin and LAMP based methods show promise for point-of-care diagnosis (Lukianova-Hleb *et al.*, 2015; Orban *et al.*, 2016; Pirstill and Cote, 2015; Polley *et al.*, 2010; Yongkiettrakul *et al.*, 2014). The introduction of RDTs in malaria control programmes has reduced the cost of malaria drug therapy due to a reduction in over-diagnosis and treatment (Harchut *et al.*, 2013). The reduced cost of treatment has offset the additional cost of RDTs and in most cases the overall cost per patient has remained the same. An important additional benefit of the use of RDTs is improved case management and a less “liberal” use of anti-malarial drugs (Yukich *et al.*, 2010). Paper based test formats have also been used to allow for simple quality control checks for antimalarial drugs (Weaver and Lieberman, 2015) and a test for G6PD deficiency prior to primaquine treatment has been developed (Bancone *et al.*, 2015).

Of concern is the lack of quality RDTs on the market. According to the WHO only 10% of tests were capable of detecting malaria parasitemia at 200 parasites per microliter in 2011 (Davis *et al.*, 2014). This has since been addressed by the implementation of quality control screens for RDTs by the WHO, the results of which are published as recommendations for use in malaria control programmes (WHO Malaria rapid diagnostic test performance, 2013). RDTs can effectively be used as a source of DNA for further molecular analysis such as the presence of drug resistance markers (Morris *et al.*, 2013). Subsequent PCR analysis can also be used for quality control of RDTs. This places RDTs at a pivotal point in the patient treatment time line. RDTs have the advantage of already being in the field and familiar to users. Implementing any improvements and innovations to these tests therefore has important practical advantages in comparison to introducing a new type of test. The findings presented here could aid in improving current tests without having major implications for end user implementation. The major findings are summarised and discussed.

Novel diagnostic reagents and targets identified in this study included the following: two potential diagnostic proteins, glyceraldehyde-3-phosphate dehydrogenase (GAPDH) and phosphoethanolamine-N-methyltransferase (PMT); five peptide epitopes allowing pan-malarial and species-specific detection of GAPDH and PMT, where the other peptides against LDH formed part of earlier work (data not shown, Hurdayal *et al.* 2010); polyclonal chicken antibodies against all five novel peptides, rPfPMT and rPvPMT were produced; anti-myc peptide chicken antibodies for the detection and affinity purification of soluble scFvs; human antibodies against the *P. falciparum* protein orthologs, including LDH, GAPDH and PMT; monoclonal scFv clones against all three targets, including whole rPfLDH and rPfGAPDH proteins as well as the *P. vivax* PMT peptide epitope. To discuss these findings, the general discussion will be separated into findings from each of the chapter 3 to 6 and future work pertaining to each chapter included.

7.2 Identification of new malaria diagnostic candidates (chapter 3)

The aim was to identify new protein targets for diagnosis (chapter 3). The approach was to compile a list of potential targets using specific criteria, from which GAPDH and PMT were chosen. These two proteins were chosen based on the following: (1) both proteins are present throughout the parasite life cycle; (2) both proteins were predicted to be expressed at higher levels than the current target LDH; (3) slight amino acid sequence variations allowed for selection of species-specific and common peptides similar to the approach taken by Hurdayal *et al.* (2010) and Tomar *et al.* (2006); (4) the proteins have been expressed previously and importantly the crystal structures were available to verify the location of potential peptide epitopes on the surface of the proteins. Importantly the peptides selected here were specific to the parasite proteins and were not found to be part of the human orthologs. This was important for the GAPDH peptides. PMT is a protein that is unique to the parasite and not found in humans (Pessi *et al.*, 2004). As *P. knowlesi* is becoming a more prominent infection in humans (Cox-Singh *et al.*, 2008; Lee *et al.*, 2009), specific peptides for this species from both LDH and GAPDH should be evaluated in future, as well as the *P. knowlesi* specific PMT peptide identified here.

7.3 Recombinant expression of the target proteins (chapter 4)

The selected protein targets were recombinantly expressed, including: the *P. falciparum*, *P. vivax* and *P. yoelii* orthologs of LDH; the *P. falciparum* and *P. yoelii* orthologs of GAPDH and the *P. falciparum* and *P. vivax* orthologs of PMT. This was the first description, to our knowledge, of expressing these proteins using auto induction media. High yields (> 5 mg)

from 50 ml cultures were obtained in most cases. These recombinant proteins formed the basis of testing the specificity of the selected anti-peptide polyclonal chicken antibodies. Recombinant LDH and GAPDH were also used to screen the *Nkuku*[®] scFv library (van Wyngaardt *et al.*, 2004). An additional use of the recombinant antigens expressed here could be for RDT quality controls as demonstrated by Lon *et al.* (2005). The heat stability of the antigens should be assessed for this purpose. A heat stable target protein may also have implications for sample preparation methods, similar to the CSP ELISA protocol described in the introduction. The heat stability of CSP is exploited and samples are briefly heated to remove contaminating proteins which reduces cross-reactivity and false positive reactions within the assay (Bashar *et al.*, 2013; Durnez *et al.*, 2011). Importantly for future analysis, *P. vivax* GAPDH needs to be recombinantly expressed and purified to assess the specificity of the antibodies produced here, or alternatively *P. vivax* field samples could be used.

7.4 Producing polyclonal IgY against the selected peptide and protein targets (chapter 5)

Novel polyclonal chicken anti-peptide, anti-rPfPMT and anti-rPvPMT antibodies (IgY) that showed specificity to their respective recombinant protein targets were produced. This validated the bioinformatics approach used to identify the peptide epitopes described in chapter 3. Since a polyclonal response against the respective whole recombinant malaria proteins (GAPDH and PMT) showed no cross-reactivity with human red blood cell or *E. coli* proteins, the use of the target proteins for diagnosis of malaria was explored. Although the DAS ELISA format used in chapter 5 demonstrated the use of the anti-peptide capture and anti-recombinant protein detection antibodies, there are important differences to the RDT format. Firstly RDTs are paper or nitrocellulose based and the antibodies may perform differently when bound to this as opposed to an ELISA well (Shields *et al.*, 1991). Secondly the detection antibodies in RDTs are often conjugated to gold nanoparticles as opposed to HRPO (Moody, 2002). The advantage of an enzyme-linked signal enhancement is therefore lost in an RDT format and the sensitivity of the tests may be lower than demonstrated here. These DAS-ELISAs still need to be optimised for PMT. Piper *et al.* (2011) demonstrated the importance of optimising capture and detection antibodies used in RDTs and the implication on RDT sensitivity. Similarly, the antibody combinations tested here detected LDH with different sensitivities dependent on whether they were used as the capture or detection reagent and tests can be improved by assessing which antibody combinations work best together. In previous work we have shown there to be approximately four to eight fold higher levels of *P. falciparum* GAPDH to LDH in a *P. falciparum* (D10) laboratory strain. This

places *P. falciparum* GAPDH in competitive concentrations with Hrp2, which is estimated to be present at six times the concentration of LDH (Marquart *et al.*, 2012; Miller *et al.*, 1994). PMT levels still need to be quantified using a DAS-ELISA approach and immunoprecipitation studies. PMT was detected in western blots of parasite lysate samples in this study. Ultimately all new diagnostic target proteins will be compared to the current target Hrp2, which is being expressed in our laboratory.

7.5 *Assessing the relative levels of human antibodies against each target from a human anti-malaria hyperimmune antibody pool (chapter 5)*

Experiments designed to determine the concentrations of specific antibodies against particular *P. falciparum* proteins in a human anti-malaria hyperimmune antibody pool revealed important information regarding the suitability of the chosen targets. Since RDTs are antibody based tests, high antigenicity of the target protein, although ideal for raising antibodies in animals, may not be an ideal characteristic for diagnostic tests. High levels of host antibodies against the diagnostic target protein may compete with test antibodies for binding to the target molecule resulting in reduced test signal and false negative results as reported for Hrp2 based tests (Ho *et al.*, 2014). The same pool of human antibodies was sequentially passed over *P. falciparum* LDH, GAPDH and PMT recombinant protein affinity columns. Using rPfLDH as the reference, approximately half the affinity purified yield of human antibodies were attained off the rPfGAPDH and rPfPMT affinity columns. These human affinity purified antibodies could also be used in competition ELISAs to assess the extent to which they might interfere with target protein detection in the DAS-ELISA formats.

7.6 *ScFv clones against all peptides, rPfLDH and rPfGAPDH from the Nkuku[®] library (chapter 6)*

Five novel scFv clones were identified against rPfLDH, which were unique and differed from those identified and isolated from an immune chicken scFv library by Chiliza *et al.* (2008). The different sequences obtained here could be explained by the type of libraries used in both studies. The naïve library used here (van Wyngaardt *et al.*, 2004), as opposed to an immune library used in the study by Chiliza *et al.* (2008), meant that the cloned V-genes of the immune library would have undergone affinity-maturation in the host animal prior to construction of the library, where naïve library V-genes would not (van Wyngaardt *et al.*, 2004; Yamanaka *et al.*, 1996). Three novel scFv clones against rPfGAPDH were identified and sequenced. The R4H1 anti-rPfLDH and R1A11 anti-rPfGAPDH clones should be

evaluated further to assess whether they potentially react with the His-tag present on both recombinant *Pf*GAPDH and *Pf*LDH proteins.

A novel clone was identified against the *P. vivax* PMT peptide (VYSIKEYNSLKD). This demonstrates the possibility of using peptides to screen the library. It would be interesting to assess whether peptides coupled to rabbit albumin, as was done for raising anti-peptide antibodies in chickens (chapter 5), would improve the success rate of the panning procedure against peptide targets as opposed to direct coating of immunotubes with the peptides as was done here. This may present the peptides in a more native conformation than when they are directly coated onto immunotubes. The Nkuku[®] library was panned again, but phagemids were eluted off the immunotubes prior to infecting the log-phase *E. coli* TG1 cells (van Wyngaardt *et al.*, 2004), as opposed to using the on-column infection for all targets described here (Noppe *et al.*, 2009). The polyclonal scFv results look promising (data not shown) and the monoclonal scFv results of this screen will be compared to the success of the on-column TG1 infection method used here.

7.7 *Future studies involving the scFv clones identified here*

The affinity of the scFv clones, identified in this study, for their respective targets could be improved. One such method known as *in vitro* affinity-maturation uses error-prone PCR and chain shuffling methods to introduce variation in the initial V-gene region of the selected scFv in the hopes of improving its affinity (Hoogenboom *et al.*, 1998). This may also be a method of deriving antibodies of varying affinities, which may have use in the development of semi-quantitative RDTs (discussed later, see Figure 7.1). Tests with certain parasitemia cut-offs could be developed which could allow clinicians to test for severe and hyperparasitemic malaria infections for example and potentially track treatment success. In addition a unique method of detection of target proteins, namely immune-PCR is possible. The scFv portion on the surface of the phagemid binds its target antigen and the phagemid DNA is subsequently amplified using PCR. This method therefore combines PCR with scFv technology and reduces limits of detection of protein targets dramatically as was done with Hrp2 (Abkallo *et al.*, 2014).

The expression and purification of the scFvs selected here needs to be optimised. We produced our own polyclonal chicken antibodies against the cmc peptide tag used in the scFv vector, which allowed for detection and affinity purification of expressed scFv antibodies. Further work in optimising the expression and improving the soluble scFv yields

from bacterial cultures is required. Alternate His-tag vectors such as the pET plasmids may also be assessed for this purpose and auto-induction versus IPTG induction as well as alternate expression host bacteria should be evaluated. An improved yield of scFv antibodies would potentially lower the cost of RDT production. Further work mimicking the RDT format, such as DAS ELISAs need to be done using the scFv's in this case, as well as immunoprecipitation analyses. The sensitivity of scFv's in detecting recombinant versus native protein targets needs to be tested.

7.8 Comparative characterisation of the scFv and polyclonal IgY reagents

All of the scFv and IgY reagents need to be assessed further in terms of their affinity for their respective targets. This would require surface plasmon resonance analysis, a technique not available in this laboratory at present, as well as competition or inhibition ELISAs with the IgY parent antibodies and the specific peptides (van Wyngaardt *et al.*, 2004). This would present an ideal platform to compare the scFv antibodies to their parent polyclonal IgY molecules. In addition, the heat stability of the antibodies needs to be assessed as this pertains to potential long term storage conditions for these reagents in an RDT format (Chiodini *et al.*, 2007). This would require circular dichroism and additional functional ELISA assays (Chiliza *et al.*, 2008). Temperatures in the tropics often exceed 40°C and in poorly ventilated storage containers they may be even higher (Jorgensen *et al.*, 2006). If the need for a cold chain can be avoided then the cost and logistics of distributing tests in the field would be reduced / simplified. The scFv antibodies may be more heat labile than their IgY parent molecules although this was not tested here. A novel panning protocol was used to identify thermo-stable anti-Hrp2 antibodies for use in RDTs (Leow *et al.*, 2014). This method could also be assessed and compared to the scFv clones and IgY antibodies produced here.

7.9 The possibility of capturing the native target proteins using IgY and scFv antibodies and exploiting their native enzymatic activity for detection

The effect of the anti-LDH IgY and scFv antibodies on the LDH enzyme activity should be assessed. If the antibodies have no effect, then they could be used for capturing LDH from samples, where LDH activity is then used as the detection step, similar to the tests developed by Makler *et al.* (1993) and Piper *et al.* (1999). This could also be useful for drug screening studies. Unfortunately the poor stability of the GAPDH substrate does not currently allow for its use in detection steps. The PMT enzymatic activity relies on detection of phospholipids using TLC plates (Pessi *et al.*, 2004), which makes it a difficult assay to perform and not suited to routine diagnosis in this format.

7.10 Retrospective analysis of the peptide targets with respect to post-translational modifications

Since all three proteins (LDH, GAPDH and PMT) are targets for post translational modification by acetylation and phosphorylation, these changes in charge on the proteins and more importantly on peptide epitopes could affect the ability of antibodies to bind to them. The peptides selected in this study were therefore analysed for the presence of acetylation and phosphorylation sites.

The acetylation of the selected peptides was based on the Miao *et al.* (2013) data. According to the Miao *et al.* (2013) data both the common peptides chosen in LDH and GAPDH in this study are acetylated (only one lysine residue in the case of the LDH peptide). The *P. falciparum* specific PMT peptide is also acetylated (only the one lysine (225) residue). The glutamate (236) in the *P. vivax* and *P. knowlesi* peptides corresponds to an acetylated lysine in the *P. falciparum* amino acid sequence which may actually improve the specificity of the antibodies against these two peptides. A possible approach to assess the effect of acetylation on antibody-based detection would be to raise antibodies against the acetylated peptides. Alternatively the antibodies raised here could be characterised by comparing their affinity for the acetylated and non-acetylated peptide targets using a direct ELISA approach.

The kinase specific phosphorylation predictions were done online (NetPhos 2.0 (<http://www.cbs.dtu.dk/services/NetPhos/>)). The common LDH peptide and the *P. falciparum* specific peptide are predicted to be phosphorylated (at their respective serine residues). The common GAPDH peptide was predicted to be phosphorylated at both its threonine and tyrosine residues, where the *P. falciparum* specific peptide (ADG) was only predicted to be phosphorylated once at its internal serine residue. Finally the common PMT peptide was predicted to be phosphorylated only once in the *P. falciparum* sequence (tyrosine) with a possible additional site in both the *P. vivax* and *P. knowlesi* proteins (substituted serine residue). The *P. falciparum* specific peptide is potentially phosphorylated only once (tyrosine residue), where both serine residues in the *P. vivax* peptide are predicted to be phosphorylated. In the case of the *P. knowlesi* peptide the tyrosine and serine residues are predicted to be phosphorylated.

Ideally selected peptides without any post-translational modification sites, would be used, however this would narrow the possible peptides even further. Importantly the phosphorylation sites are predicted sites and not necessarily true sites on the native proteins

within the parasite. This highlights the importance of assessing the detection of the targets from parasite lysate samples and field isolates. It is also important to remember that not all proteins undergo post-translational modification and that acetylation and phosphorylation events will occur to a selected pool of native proteins with a regulatory purpose. Therefore a pool of unmodified native proteins will remain allowing detection on diagnostic tests. It should also be remembered that of the 15 amino acids of the para- and epitope, the main binding energy is between as few as five key residues of both the antibody and antigen sequences (Benjamin and Perdue., 1996; Dougan *et al.*, 1998). Therefore the post-translational modifications identified here may not necessarily have an effect on antibody affinity, especially if the residues fall outside of the five key residues comprising the para- and epitope.

7.11 Retrospective analysis of the peptide targets with respect to single point mutations

The *P. falciparum* LDH protein primary amino acid sequences shared between 98.1 to 100% identity (NCBI and PlasmoDB accessed 8.4.2016). One of the 16 LDH protein sequence entries had a G87R mutation and two had a D96L mutation. Both fall within the common peptide selected here. The G87R mutation is a change from a hydrophobic to a charged residue, and the D96L is a charged to hydrophobic residue mutation. Both may potentially alter the binding affinities of antibodies at this epitope. The *P. vivax* LDH primary amino acid sequence entries shared between 97.7 to 100% identity. The following mutations fell within the common epitope: S89G; D90V and D90N. The D90V mutation may have the most significant effect on the antibody binding affinity as this is the substitution of a charged for hydrophobic residue, which was found in two of the 33 samples aligned. An E212G mutation fell within the *P. vivax* peptide region and may affect antibody binding since it is a charged to hydrophobic residue mutation.

The *P. falciparum* GAPDH sequences shared between 99.1 to 100% identity, where the single amino acid mutations Q140K and L272P did not fall within any of the chosen peptide regions. The *P. vivax* sequences were 100% identical. Finally of the PMT sequences only one of 20 *P. falciparum* isolates had a 99.6% identity, where all others were 100% identical. This was for an I192T mutation which falls outside of any of the chosen peptide sequences. All *P. vivax* and *P. knowlesi* isolates were identical although there were only two entries in the NCBI database for *P. knowlesi* at the time.

These slight amino acid variations may have implications for antibody affinity for LDH and will have to be assessed with parasite culture lysates and patient samples in future work. Thus far no mutations with implications for the anti-peptide antibodies against both PMT and GAPDH have been identified, which again support their potential for diagnosis.

7.12 *Comparing the half-lives of the target proteins*

The estimated half-lives of *P. falciparum* aldolase, LDH, Hrp2, GAPDH and PMT are all around 30 hours in mammalian reticulocytes. This was predicted using the ExPASy ProtParam tool (<http://web.expasy.org/protparam/>) which bases its calculation on the N-terminal amino acid of the protein, which is a methionine in all five cases here (Varshavsky, 1997). *In vivo* half-lives for aldolase and LDH were found to be approximately seven days (Ashley *et al.*, 2009; Aydin-Schmidt *et al.*, 2013) and seven to 28 days for Hrp2 (Aydin-Schmidt *et al.*, 2013; Marquart *et al.*, 2012). The half-life in serum of GAPDH and PMT will have to be determined. GAPDH and LDH could be compared in a mouse model to assess their relation to parasitemia and to assess the possibility of using GAPDH as a target for tracking treatment. This cannot be done with PMT as it is absent in mouse malaria parasites (Dechamps *et al.*, 2010).

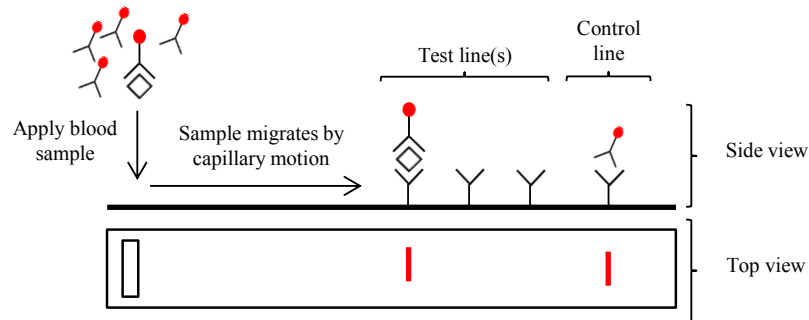
7.13 *Essential field testing of the antibodies in an RDT format*

Concerns with RDTs themselves include interference or competition of circulating antibodies with detection antibodies in tests (Ho *et al.*, 2014). For this reason it is essential to assess RDT performance of any new targets with clinical samples. Cross-reactivity with alternate pathogens and Rheumatoid factor are also a concern and need to be assessed (Gillet *et al.*, 2013). The choice of using chicken antibodies in this work was deliberate. Since IgY and scFv's lack an Fc portion, tests using these reagents should not react with human Rheumatoid factor (Delves *et al.*, 2006; Hoogenboom *et al.*, 1991; Iqbal *et al.*, 2000).

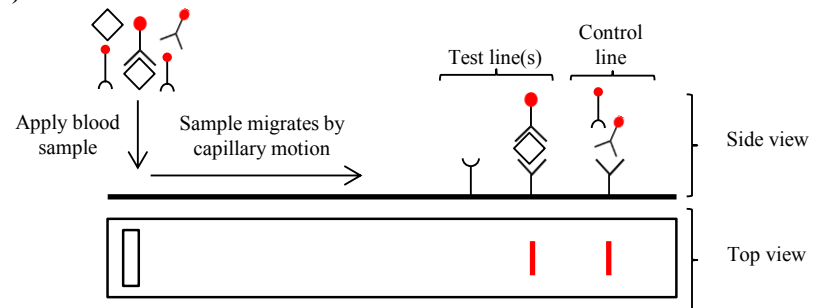
7.14 *A proposed semi-quantitative test for malaria*

In order to address the need for semi-quantitative detection of severe malaria infections as expressed by Barnes *et al.* (2015) and White *et al.* (2009), we propose multiple-test line detection systems (Figure 7.1). Quantifying the parasitemia is important as it has an effect on the dose and duration of treatment of malaria infections. Suboptimal dosing is also suggested to be an important driving factor for the spread of drug resistance in malaria parasites (Barnes *et al.*, 2015; White *et al.*, 2009).

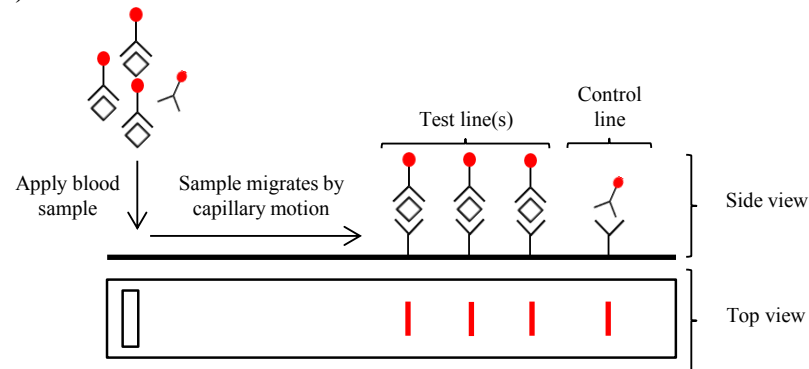
A i) mild malaria



B i) mild malaria



A ii) severe malaria



B ii) severe malaria

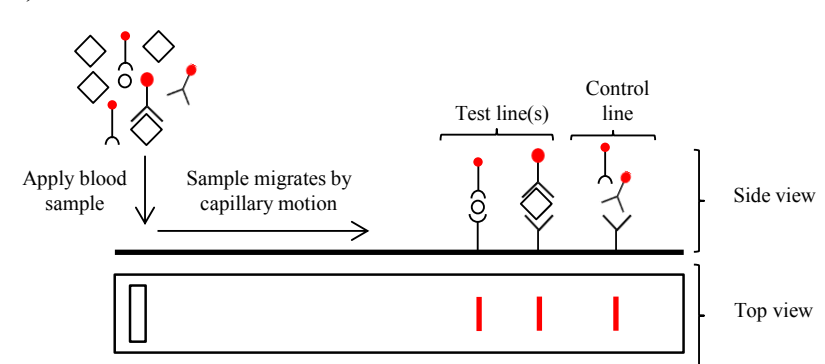


Figure 7.1 Proposed multi-test line semi-quantitative detection of malaria

Scheme (A) presents the multiple test line approach in which a single target antigen (\diamond) is detected by multiple capture antibody test lines. In a mild case a single band appears, but as the parasitemia increases, a corresponding increase in the target antigen allows for multiple test lines to be detected, indicating severe malaria. Alternatively separate proteins present at different concentrations within the parasite are targeted in (B), such as Hrp2 (\diamond) and Cox17 (\circ) for example. A mild malaria infections allows detection of Hrp2, however Cox17 is present at too low a concentration to be detected. As parasitemia increases to severe malaria, the Cox17 concentration increases to detectable levels, resulting in a second test line indicative of a severe malaria infection. Detection antibodies are usually labelled with a visible marker such as colloidal gold for example (\bullet).

The multiple test lines would effectively “mop up” the antibody-antigen complexes resulting in multiple test lines. The severity of infection would correlate to the number of test lines that develop. Four lines could be used to detect severe malaria and one line would present mild malaria, for example. Such a system could be optimised based on the known quantity of detection antibody added to the sample buffer used in the sample preparation. The more target antigen present in the sample (diamonds in Figure 7.1 (A)), the more antibody-antigen complexes form and are captured on the test strip forming test lines. Another possibility is that multiple antigen detection could be used; targeting proteins such as Cox17 (circle in Figure 7.1 (B)) for example (Choveaux *et al.*, 2015). A protein present at lower concentrations than the current targets would require a higher parasitemia to be detected in a diagnostic test, which could be indicative of severe or hyperparasitemic infections. This could be exploited to allow for semi-quantitative diagnosis. Screening the scFv library for less sensitive clones would allow for concentration dependent detection of protein targets as well.

Further innovations in RDT technology involve the development of novel reagents such as aptamers (Godonoga *et al.*, 2016; Lee *et al.*, 2014). A collaboration with Rhodes University in developing aptamers for the detection of *P. falciparum* and *P. vivax* LDH using the recombinant proteins raised here as targets, as well as the *P. falciparum* specific peptide epitope has been submitted to PLoS ONE (Frith *et al.*, submitted 2016). The beauty of these methods is the robust nature of DNA aptamers and their stability which could allow for reusable tests as demonstrated by Dirkzwager *et al.* (2015). Inertial microfluidics has also been used to concentrate parasitized red blood cells and remove white blood cells from samples (Warkiani *et al.*, 2015). Sample processing using Nickel coated magnetic beads improved the limit of detection of Hrp2 based tests by eightfold. This meant that the test was able to detect parasitemia as low as three parasites per microliter (Davis *et al.*, 2014). Similar methods could be applied to other RDT targets in order to improve their sensitivity. A simple paper-based concentration method was employed by Pereira *et al.* (2015) which improved an LDH based RDTs limit of detection tenfold and only added an additional 5 minutes to the test time. Some groups have suggested alternate antigens for RDTs including glutamate dehydrogenase and thioredoxin peroxidase I (de Dominguez and Rodriguez-Acosta, 1996, 2000; Hakimi *et al.*, 2015) and three uncharacterised malaria proteins from saliva (Huang *et al.*, 2012).

7.15 Conclusions

This study further validated the Hurdayal *et al.* (2010) and Tomar *et al.* (2006) approaches to the identification and use of peptide epitopes on the surface of target proteins for specific antibody-based detection of these targets up to a species level. Two malaria metabolic proteins, GAPDH and PMT were identified which allowed the use of this approach and development of specific antibodies. These targets show potential for use in malaria diagnosis as they are suggested to be present at higher concentrations than LDH, where PMT is unique to *Plasmodium* (*P. falciparum*, *P. vivax* and *P. knowlesi*) and not found in humans. The immunoreagents raised here and the targets identified in this study show potential of improving the current malaria RDT platform. Additional data regarding temperature stability and performance of these reagents in an RDT format will be invaluable. These novel targets show potential for the improvement of the RDT platform, but could also be used in alternate detection systems such as the DNA aptamer and immune-PCR assays for example.

Bibliography

- Abkallo, H. M., W. Liu, S. Hokama, P. E. Ferreira, S. Nakazawa, Y. Maeno, N. T. Quang, N. Kobayashi, O. Kaneko, M. A. Huffman, S. Kawai, R. P. Marchand, R. Carter, B. H. Hahn and R. Culleton. (2014) DNA from pre-erythrocytic stage malaria parasites is detectable by PCR in the faeces and blood of hosts. *Int J Parasitol*, **44** (7), 467-73.
- Adams, M. J., Buehner, M., Chandrasekhar, K., Ford, G.C., Hackert, M.L., Liljas, A., Rossman, M.G., Smiley, I.E., Allison, W.S., Everse, J., Kaplan, N.O., Taylor, S.S. (1973) Structure-Function Relationships in Lactate Dehydrogenase. *Proc Natl Acad Sci USA*, **70** (7), 1968-1972.
- Adeoye, G. O. and I. C. Nga. (2007) Comparison of Quantitative Buffy Coat technique (QBC) with Giemsa-stained Thick Film (GTF) for diagnosis of malaria. *Parasitol Int*, **56** (4), 308-12.
- Akinyi, S., J. Gaona, E. V. Meyer, J. W. Barnwell, M. R. Galinski and V. Corredor. (2008) Phylogenetic and structural information on glyceraldehyde-3-phosphate dehydrogenase (G3PDH) in *Plasmodium* provides functional insights. *Infect Genet Evol*, **8** (2), 205-12.
- Akler, A. P., Lim, P., Sem, R., Shah, N.K., Yi, P., Bouth, D.M., Tsuyuoka, R., Maguire, J.D., Fandeur, T., Ariey, F., Wongsrichanalai, C., Meshnick, S.R. (2007) Pfmdr1 and in vivo resistance to Artesunate-Mefloquine in *Falciparum* malaria on the Cambodian-Thai border. *Am J Trop Med Hyg*, **76** (4), 641-647.
- Alam, A., M. K. Neyaz and S.I. Hasan. (2014) Exploiting unique structural and functional properties of malarial glycolytic enzymes for antimalarial drug development. *Malar Res Treat*, doi: 10.1155/2014/451065
- Alves, F. P., L. H. Gil, M. T. Marrelli, P. E. Ribolla, E. P. Camargo and L. H. Da Silva. (2005) Asymptomatic carriers of *Plasmodium spp.* as infection source for malaria vector mosquitoes in the Brazilian Amazon. *J Med Entomol*, **42** (5), 777-9.
- Anderios, N., NoorRain A., Vythilingam, L. (2009) *In vivo* study of human *Plasmodium knowlesi* in Macaca fascicularis. *Exp Parasitol*, **124**, 181-189.
- Antia, R., A. Yates and J. C. de Roode (2008) The dynamics of acute malaria infections. I. Effect of the parasite's red blood cell preference. *Proc Biol Sci*, **275** (1641), 1449-58.
- Araújo, M. S., Messias, M.R., Figueiró, M.R., Gil, L.H.S., Probst, C.M., and N. M. Vidal, Katsuragawa, T.H., Krieger, M.A., Pereira da Silva, L.H., Ozaki, L.S. (2013) Natural *Plasmodium* infection in monkeys in the state of Rondônia (Brazilian Western Amazon). *Malaria Journal*, **12** (180), doi:10.1186/1475-2875-12-180.

Ashley, E. A., Touabi, M., Ahrer, M., Hutagalung, R., Htun, K., Luchavez, J., Dureza, C., Proux, S., Leimanis, M., Min Lwin, M., Koscalova, A., Comte, E., Hamade, P., Page, A., Nosten, F., Guerin, P.J. (2009) Evaluation of three parasite lactate dehydrogenase-based rapid diagnostic tests for the diagnosis of *falciparum* and *vivax* malaria. *Malaria Journal*, **8** (241), doi: 10.1186/1475-2875-8-241.

Aydin-Schmidt, B., Mubi, M., Morris, U., Petzold, M., Ngasala, B.E., Premji, Z., Björkman, A., Mårtensson, A. (2013) Usefulness of *Plasmodium falciparum*-specific rapid diagnostic tests for assessment of parasite clearance and detection of recurrent infections after artemisinin-based combination therapy. *Malaria Journal*, **12** (349), doi:10.1186/1475-2875-12-349.

Bachmann, J., F. Burte, S. Pramana, I. Conte, B. J. Brown, A. E. Orimadegun, W. A. Ajetunmobi, N. K. Afolabi, F. Akinkunmi, S. Omokhodion, F. O. Akinbami, W. A. Shokunbi, C. Kampf, Y. Pawitan, M. Uhlen, O. Sodeinde, J. M. Schwenk, M. Wahlgren, D. Fernandez-Reyes and P. Nilsson. (2014) Affinity proteomics reveals elevated muscle proteins in plasma of children with cerebral malaria. *PLoS Pathog*, **10** (4), e1004038. Doi: 10.1371/journal.ppat.1004038

Baird, C.L., Fischer, C.J., Pefaur, N.B., Miller, K.D., Kagan, J., Srivastava, S., Rodland, K.D. (2009) Developing Recombinant Antibodies for Biomarker Detection. *Cancer Biomarkers* **6**, 271-79.

Baird, J. K., Purnomo, J.T. R. (1992) Diagnosis of malaria in the field by fluorescence microscopy of QBC capillary tubes. *Trans R Soc Trop Med Hyg*, **86** (1), 3-5.

Baker, J., McCarthy, J., Gatton, M., Kyle, D.E., Belizario, V., Luchavez, J., Bell, D., Cheng, Q. (2005) Genetic Diversity of *Plasmodium falciparum* Histidine-Rich Protein 2 (PfHRP2) and Its Effect on the Performance of PfHRP2-Based Rapid Diagnostic Tests. *J Inf Dis*, **192**, 870-877.

Baldacci, P. and R. Menard. (2004) The elusive malaria sporozoite in the mammalian host. *Mol Microbiol*, **54** (2), 298-306.

Bancone, G., C. S. Chu, N. Chowwiwat, R. Somsakchaicharoen, P. Wilaisrisak, P. Charunwatthana, P. Bansil, S. McGray, G. J. Domingo and F. H. Nosten. (2015) Suitability of capillary blood for quantitative assessment of G6PD activity and performances of G6PD point-of-care tests. *Am J Trop Med Hyg*, **92** (4), 818-24.

Bannister, L. H., Hopkins, J.M., Fowler, R.E., Krishna, S., Mitchell, G.H. (2000) A brief illustrated guide to the ultrastructure of *Plasmodium falciparum* asexual blood stages. *Parasitol Today*, **16** (10), 427-433.

Barnes, K. I., WorldWide Antimalarial Resistance Network (WWARN) Lumefantrine PK/PD Study Group. (2015) Artemether-lumefantrine treatment of uncomplicated *Plasmodium falciparum* malaria: a systematic review and meta-analysis of day 7 lumefantrine concentrations and therapeutic response using individual patient data. *BMC Medicine*, **13** (227), doi: 10.1186/s12916-015-0456-7.

Bashar, K., Tuno, N., Ahmed, T.U., Howladera, A.J. (2013) False positivity of circumsporozoite protein (CSP)–ELISA in zoophilic *anophelines* in Bangladesh. *Acta Tropica*, **125**, 220-225.

Bass, C., Nikou, D., Blagborough, A.M., Vontas, J., Sinden, R.E., Williamson, M.S., Field, L.M. (2008) PCR-based detection of *Plasmodium* in *Anopheles* mosquitoes: a comparison of a new high-throughput assay with existing methods. *Malaria Journal*, **7** (177), doi:10.1186/1475-2875-7-177.

Beeching, N. J., D. G. Laloo and B. A. Bannister. (2007) Management of *vivax* malaria with primaquine. *J Infect*, **55** (3), 282.

Benjamin, D. C. and S. S. Perdue. (1996) Site-Directed Mutagenesis in Epitope Mapping. *Methods*, **9** (3), 508-15.

Berwal, R., N. Gopalan, K. Chandel, G. B. Prasad and S. Prakash. (2008) *Plasmodium falciparum*: enhanced soluble expression, purification and biochemical characterization of lactate dehydrogenase. *Exp Parasitol*, **120** (2), 135-41.

Beshir, K. B., Hallett, R.L., Eziefula, A.C., Bailey, R., Watson, J., Wright, S.G., Chiodini, P.L., Polley, S.D., Sutherland, C.J. (2010) Measuring the efficacy of anti-malarial drugs in vivo: quantitative PCR measurement of parasite clearance. *Malaria Journal*, **9** (312), doi:10.1186/1475-2875-9-312.

Betson, M., M. Jawara and T. S. Awolola. (2009) Status of insecticide susceptibility in *Anopheles gambiae* s.l. from malaria surveillance sites in The Gambia. *Malaria Journal*, **8**, 187.

Bilal, M., M. Saleem, S. T. Amanat, H. A. Shakoor, R. Rashid, A. Mahmood and M. Ahmed. (2015) Optical diagnosis of malaria infection in human plasma using Raman spectroscopy. *J Biomed Opt*, **20** (1), 017002. Doi: 10.1117/1.JBO.20.1.017002

Bisoffi, Z., F. Gobbi, A. Angheben and J. Van den Ende. (2009) The role of rapid diagnostic tests in managing malaria. *PLoS Med*, **6** (4), e1000063. Doi: 10.1371/journal.pmed.1000063

Blanford, S., W. Shi, R. Christian, J. H. Marden, L. L. Koekemoer, B. D. Brooke, M. Coetzee, A. F. Read and M. B. Thomas. (2011) Lethal and pre-lethal effects of a fungal biopesticide contribute to substantial and rapid control of malaria vectors. *PLoS One*, **6** (8), e23591. doi: 10.1371/journal.pone.0023591

- Blommel, P. G., K. J. Becker, P. Duvnjak and B. G. Fox.** (2007) Enhanced bacterial protein expression during auto-induction obtained by alteration of lac repressor dosage and medium composition. *Biotechnol Prog*, **23** (3), 585-98.
- Bobenchik, A. M., Y. Augagneur, B. Hao, J. C. Hoch and C. Ben Mamoun.** (2011) Phosphoethanolamine methyltransferases in phosphocholine biosynthesis: functions and potential for antiparasite therapy. *FEMS Microbiology Reviews*, **35** (4), 609-619.
- Bobenchik, A. M., W. H. Witola, Y. Augagneur, L. N. Lochlainn, A. Garg, N. Pachikara, J. Y. Choi, Y. O. Zhao, S. Usmani-Brown, A. Lee, S. H. Adjalley, S. Samanta, D. A. Fidock, D. R. Voelker, E. Fikrig and C. Ben Mamoun.** (2013) *Plasmodium falciparum* phosphoethanolamine methyltransferase is essential for malaria transmission. *Proc Natl Acad Sci USA*, **110** (45), 18262-18267.
- Borras-Cuesta, F., A. Petit-Camurdan and Y. Fedon.** (1987) Engineering of immunogenic peptides by co-linear synthesis of determinants recognized by B and T cells. *Eur J Immunol*, **17** (8), 1213-5.
- Bozdech, Z., M. Llinas, B. L. Pulliam, E. D. Wong, J. Zhu and J. L. DeRisi.** (2003) The transcriptome of the intraerythrocytic developmental cycle of *Plasmodium falciparum*. *PLoS Biol*, **1** (1), e5.doi: 10.1371/journal.pbio.0000005.
- Bradford, M. M.** (1976) A Rapid and Sensitive Method for the Quantification of Microgram Quantities of Protein Utilizing the Principle of Protein-Dye Binding. *Anal Biochem*, **72**, 248-254.
- Brown, W. M., Yowell, A.C., Hoard, A., Vander Jagt, T.A., Hunsaker, L.A., Deck, L.M., Royer, R.E., Piper, R.C., Dame, J.B., Makler, M.T., Vander Jagt, D.L.** (2004) Comparative Structural Analysis and Kinetic Properties of Lactate Dehydrogenases from the Four Species of Human Malarial Parasites. *Biochemistry*, **43**, 6219-6229.
- Buehner, M., G. C. Ford, D. Moras, K. W. Olsen and M. G. Rossman.** (1973) D-glyceraldehyde-3-phosphate dehydrogenase: three-dimensional structure and evolutionary significance. *Proc Natl Acad Sci USA*, **70** (11), 3052-4.
- Busso, D., M. Stierle, J. C. Thierry and D. Moras.** (2008) A comparison of inoculation methods to simplify recombinant protein expression screening in *Escherichia coli*. *Biotechniques*, **44** (1), 101-6.
- Butykai, A., A. Orban, V. Kocsis, D. Szaller, S. Bordacs, E. Tatrai-Szekeres, L. F. Kiss, A. Bota, B. G. Vertessy, T. Zelles and I. Kezsmarki.** (2013) Malaria pigment crystals as magnetic micro-rotors: key for high-sensitivity diagnosis. *Sci Rep*, **3**, 1431.doi: 10.1038/srep01431

- Carcamo, J., M. W. Ravera, R. Brissette, O. Dedova, J. R. Beasley, A. Alam-Moghe, C. Wan, A. Blume and W. Mandecki.** (1998) Unexpected frameshifts from gene to expressed protein in a phage-displayed peptide library. *Proc Natl Acad Sci USA*, **95** (19), 11146-51.
- Carmenes, R. S., J. P. Freije, M. M. Molina and J. M. Martin.** (1989) Predict7, a Program for Protein-Structure Prediction. *Biochem Biophys Res Comm*, **159** (2), 687-693.
- Carnevale, E. P., Kouri, D., DaRe, J.T., McNamara, D.T., Mueller, I., Zimmerman, P.A.** (2007) A Multiplex Ligase Detection Reaction-Fluorescent Microsphere Assay for Simultaneous Detection of Single Nucleotide Polymorphisms Associated with *Plasmodium falciparum* Drug Resistance. *J Clin Microbiol*, **45** (3), 752-761.
- Carter, R., Voller, A.** (1973) Enzyme Typing of Malaria Parasites. *Brit Med J* **1**: 149-50.
- Casali, N.** (2003) *Escherichia coli* host strains. *Methods Mol Biol*, **235**, 27-48.
- Cha S., Park K., Srinivasan P., Schindler C.W., van Rooijen N., Stins M., Jacobs-Lorena M.** (2015) CD68 acts as a major gateway for malaria sporozoite liver infection. *J Exp Med*, **212** (9), 1391-1403.
- Chen, K., Yuen, C., Aniweh, Y., Preiser, P., Liu, Q.** (2016) Towards ultrasensitive malaria diagnosis using surface enhanced Raman spectroscopy. *Scientific Reports*, **6** (20177), DOI: 10.1038/srep20177.
- Chevallet, M., Luche, S., Rabilloud, T.** (2006) Silver staining of proteins in polyacrylamide gels. *Nat Protoc*, **1** (4), 1852-1858
- Chew, C. H., Lim, Y.A.L., Lee, P.C., Mahmud, R., Chua, K.H.** (2012) Hexaplex PCR Detection System for Identification of Five Human *Plasmodium* Species with an Internal Control. *J Clin Microbiol*, **50** (12), 4012-4019.
- Chiliza, T. E., W. Van Wyngaardt and D. H. Du Plessis.** (2008) Single-chain antibody fragments from a display library derived from chickens immunized with a mixture of parasite and viral antigens. *Hybridoma (Larchmt)*, **27** (6), 413-21.
- Chin, W., P. G. Contacos, G. R. Coatney and H. R. Kimball.** (1965) A Naturally Acquired Quotidian-Type Malaria in Man Transferable to Monkeys. *Science*, **149** (3686), 865.
- Chiodini, P.L., Bowers, K., Jorgensen, P., Barnwell, J.W., Grady, K.K., Luchavez, J., Moody, A.H., Cenizal, A., Bell, D.** (2007) The Heat Stability of Plasmodium Lactate Dehydrogenase-Based and Histidine-Rich Protein 2-Based Malaria Rapid Diagnostic Tests. *Trans Roy Soc Trop Med Hyg* **101**, 331-37.

- Cho, C. H., M. H. Nam, J. S. Kim, E. T. Han, W. J. Lee, J. S. Oh, S. S. An and C. S. Lim.** (2011) Genetic variability in *Plasmodium vivax* aldolase gene in Korean isolates and the sensitivity of the Binax Now malaria test. *Trop Med Int Health*, **16** (2), 223-6.
- Chou, P. Y. and G. D. Fasman.** (1979) Prediction of beta-turns. *Biophys J*, **26** (3), 367-83.
- Choveaux, D. L., R. G. Krause, J. M. Przyborski and J. P. Goldring.** (2015) Identification and initial characterisation of a *Plasmodium falciparum* Cox17 copper metallochaperone. *Exp Parasitol*, **148**, 30-9.
- Choveaux, D. L., J. M. Przyborski and J. P. Goldring.** (2012) A *Plasmodium falciparum* copper-binding membrane protein with copper transport motifs. *Malaria Journal*, **11**, 397.doi: 10.1186/1475-2875-11-397
- Chuangchaiya, S., K. Jangpatarapongsa, P. Chootong, J. Sirichaisinthop, J. Sattabongkot, K. Pattanapanyasat, K. Chotivanich, M. Troye-Blomberg, L. Cui and R. Udomsangpetch.** (2010) Immune response to *Plasmodium vivax* has a potential to reduce malaria severity. *Clin Exp Immunol*, **160** (2), 233-9.
- Chung, D. W., N. Ponts, S. Cervantes and K. G. Le Roch.** (2009) Post-translational modifications in *Plasmodium*: more than you think! *Mol Biochem Parasitol*, **168** (2), 123-34.
- Clackson, T., Hoogenboom, H.R., Griffiths, A.D., Winter, G.** (1991) Making Antibody Fragments Using Phage Display Libraries. *Nature* **352**, 624-28.
- Collins, W. E. and G. M. Jeffery.** (2007) *Plasmodium malariae*: parasite and disease. *Clin Microbiol Rev*, **20** (4), 579-92.
- Cox-Singh, J., T. M. Davis, K. S. Lee, S. S. Shamsul, A. Matusop, S. Ratnam, H. A. Rahman, D. J. Conway and B. Singh.** (2008) *Plasmodium knowlesi* malaria in humans is widely distributed and potentially life threatening. *Clin Infect Dis*, **46** (2), 165-71.
- Dakic, Z., V. Iovic, M. Pavlovic, L. Lavadinovic, M. Markovic and O. Djurkovic-Djakovic.** (2014) Clinical significance of molecular methods in the diagnosis of imported malaria in returning travelers in Serbia. *Int J Infect Dis*, **29**, 24-30.
- Daneshvar, C., Davis, T.M., Cox-Singh, J., Rafa'ee, M.Z., Zakaria, S.K., Divis, P.C., Singh, B.** (2009) Clinical and laboratory features of human *Plasmodium knowlesi* infection. *Clin Infect Dis*, **49** (6), 852-860.
- Daubenberger, C. A., F. Poltl-Frank, G. Jiang, J. Lipp, U. Certa and G. Pluschke.** (2000) Identification and recombinant expression of glyceraldehyde-3-phosphate dehydrogenase of *Plasmodium falciparum*. *Gene*, **246** (1-2), 255-64.

- Daubenberger, C. A., E. J. Tisdale, M. Curcic, D. Diaz, O. Silvie, D. Mazier, W. Eling, B. Bohrmann, H. Matile and G. Pluschke.** (2003) The N'-terminal domain of glyceraldehyde-3-phosphate dehydrogenase of the apicomplexan *Plasmodium falciparum* mediates GTPase Rab2-dependent recruitment to membranes. *Biol Chem*, **384** (8), 1227-37.
- David, P. H., M. Hommel, L. H. Miller, I. J. Udeinya and L. D. Oligino.** (1983) Parasite sequestration in *Plasmodium falciparum* malaria: spleen and antibody modulation of cytoadherence of infected erythrocytes. *Proc Natl Acad Sci USA*, **80** (16), 5075-9.
- Davis, K. M., L. E. Gibson, F. R. Haselton and D. W. Wright.** (2014) Simple sample processing enhances malaria rapid diagnostic test performance. *Analyst*, **139** (12), 3026-31.
- Day, N. P., T. D. Pham, T. L. Phan, X. S. Dinh, P. L. Pham, V. C. Ly, T. H. Tran, T. H. Nguyen, D. B. Bethell, H. P. Nguyen and N. J. White.** (1996) Clearance kinetics of parasites and pigment-containing leukocytes in severe malaria. *Blood*, **88** (12), 4694-700.
- de Boer, H. A., Comstock, L.J., Vasser, M.** (1983) The tac promoter: a functional hybrid derived from the trp and lac promoters. *Proc Natl Acad Sci USA*, **80** (1), 21-25.
- de Dominguez, N. and A. Rodriguez-Acosta.** (1996) Glutamate dehydrogenase antigen detection in *Plasmodium falciparum* infections. *Korean J Parasitol*, **34** (4), 239-46.
- de Dominguez, N. & A. Rodriguez-Acosta** (2000) A 33-35 kDa circulating antigen from *Plasmodium falciparum*. *Folia Parasitol (Praha)*, **47** (4), 267-72.
- Dechamps, S., M. Maynadier, S. Wein, L. Gannoun-Zaki, E. Marechal and H. J. Vial.** (2010) Rodent and nonrodent malaria parasites differ in their phospholipid metabolic pathways. *J Lipid Res*, **51** (1), 81-96.
- Delahunt, C., Horning, M.P., Wilson, B.K., Proctor, J.L., Hegg, M.C.** (2014) Limitations of haemozoin-based diagnosis of *Plasmodium falciparum* using dark-field microscopy. *Malaria Journal*, **13** (147), doi:10.1186/1475-2875-13-147.
- Delves, P. J., Martin, S.J., Burton, D.R., Riott, I.M.** (2006). *Roitt's Essential immunology*. Blackwell Publishing Ltd., London, 37-38; 57; 112; 221-223.
- Demarse, N. A., S. Ponnusamy, E. K. Spicer, E. Apohan, J. E. Baatz, B. Ogretmen and C. Davies.** (2009) Direct binding of glyceraldehyde 3-phosphate dehydrogenase to telomeric DNA protects telomeres against chemotherapy-induced rapid degradation. *J Mol Biol*, **394** (4), 789-803.

Demas, A., J. Oberstaller, J. DeBarry, N. W. Lucchi, G. Srinivasamoorthy, D. Sumari, A. M. Kabanywany, L. Villegas, A. A. Escalante, S. P. Kachur, J. W. Barnwell, D. S. Peterson, V. Udhayakumar and J. C. Kissinger. (2011) Applied genomics: data mining reveals species-specific malaria diagnostic targets more sensitive than 18S rRNA. *J Clin Microbiol*, **49** (7), 2411-8.

Deme, A. B., Park, D.J., Bei, A.K., Sarr, O., Badiane, A.S., Gueye, P.E.H.O., Ahouidi, A., Ndir, O., Mboup, S., Wirth, D.F., Ndiaye, D., Volkman, S.K. (2014) Analysis of pfhrp2 genetic diversity in Senegal and implications for use of rapid diagnostic tests. *Malaria Journal*, **13** (34), doi:10.1186/1475-2875-13-34.

Demirev, P. A., A. B. Feldman, D. Kongkasuriyachai, P. Scholl, D. Sullivan, Jr. and N. Kumar. (2002) Detection of malaria parasites in blood by laser desorption mass spectrometry. *Anal Chem*, **74** (14), 3262-6.

Dinko, B., Oguike, M.C., Larbi, J.A., Bousema, T., Sutherland, C.J. (2013) Persistent detection of *Plasmodium falciparum*, *P. malariae*, *P. ovale curtisi* and *P. ovale wallikeri* after ACT treatment of asymptomatic Ghanaian school-children. *Int J Parasitol: Drugs and Drug Resistance*, **3**, 45-50.

Dirkzwager, R. M., A. B. Kinghorn, J. S. Richards and J. A. Tanner. (2015) APTEC: aptamer-tethered enzyme capture as a novel rapid diagnostic test for malaria. *Chem Commun (Camb)*, **51** (22), 4697-700.

Dondorp, A. M., Desakorn, V., Pongtavornpinyo, W., Sahassananda, D., Silamut, K., Chotivanich, K., Newton, P.N., Pitisuttithum, P., Smithyman, A.M., White, N.J., Day, N.P.J. (2005) Estimation of the Total Parasite Biomass in Acute *Falciparum* Malaria from Plasma PfHRP2. *PLOS Medicine*, **2** (8), doi:10.1371/journal.pmed.0020204.

Dondorp, A. M., F. Nosten, P. Yi, D. Das, A. P. Phy, J. Tarning, K. M. Lwin, F. Ariey, W. Hanpithakpong, S. J. Lee, P. Ringwald, K. Silamut, M. Imwong, K. Chotivanich, P. Lim, T. Herdman, S. S. An, S. Yeung, P. Singhasivanon, N. P. Day, N. Lindegardh, D. Socheat and N. J. White. (2009) Artemisinin resistance in *Plasmodium falciparum* malaria. *N Engl J Med*, **361** (5), 455-67.

Dostert, C., Guarda, G., Romero, J.F., Menu, P., Gross, O., Tardivel, A., Suva, M.L., Stehle, J.C., Kopf, M., Stamenkovic, I., Corradin, G., Tschopp, J. (2009) Malarial hemozoin is a Nalp3 inflammasome activating danger signal. *PLoS One*, **4** (8), e6510. doi: 10.1371/journal.pone.0006510.

- Dougan, D. A., Malby, R.L., Gruen, L.C., Kortt, A.A., Hudson, P.J.** (1998) Effects of substitutions in the binding surface of an antibody on antigen affinity. *Prot Eng*, **11** (1), 65-74.
- Duraisingh, M. T., Curtis, J., Warhurst, D.C.** (1998) *Plasmodium falciparum*: Detection of Polymorphisms in the Dihydrofolate Reductase and Dihydropteroate Synthetase Genes by PCR and Restriction Digestion. *Exp Parasitol*, **89**, 1-8.
- Durnez, L., Van Bortel, W., Denis, L., Roelants, P., Veracx, A., Trung, H.D., Sochantha, T., and M. Coosemans.** (2011) False positive circumsporozoite protein ELISA: a challenge for the estimation of the entomological inoculation rate of malaria and for vector incrimination. *Malaria Journal*, **10** (195), doi:10.1186/1475-2875-10-195.
- Echeverry, D. F., N. A. Deason, J. Davidson, V. Makuru, H. Xiao, J. Niedbalski, M. Kern, T. L. Russell, T. R. Burkot, F. H. Collins and N. F. Lobo.** (2016) Human malaria diagnosis using a single-step direct-PCR based on the *Plasmodium* cytochrome oxidase III gene. *Malaria Journal*, **15** (1), 128. doi: 10.1186/s12936-016-1185-x
- Egan, T. J., J. M. Combrinck, J. Egan, G. R. Hearne, H. M. Marques, S. Ntenti, B. T. Sewell, P. J. Smith, D. Taylor, D. A. van Schalkwyk and J. C. Walden.** (2002) Fate of haem iron in the malaria parasite *Plasmodium falciparum*. *Biochem J*, **365** (2), 343-7.
- Emini, E. A., J. V. Hughes, D. S. Perlow and J. Boger.** (1985) Induction of hepatitis A virus-neutralizing antibody by a virus-specific synthetic peptide. *J Virol*, **55** (3), 836-9.
- Fast, N. M., J. C. Kissinger, D. S. Roos and P. J. Keeling.** (2001) Nuclear-encoded, plastid-targeted genes suggest a single common origin for apicomplexan and dinoflagellate plastids. *Mol Biol Evol*, **18** (3), 418-26.
- Fatih, F. A., A. Siner, A. Ahmed, L. C. Woon, A. G. Craig, B. Singh, S. Krishna and J. Cox-Singh.** (2012) Cytoadherence and virulence - the case of *Plasmodium knowlesi* malaria. *Malaria Journal*, **11**, 33. doi: 10.1186/1475-2875-11-33
- Feachem, R. G. A., Phillips, A.A., Hwang, J., Cotter, C., Wielgosz, B., Greenwood, B.M., Sabot, O., Rodriguez, M.H., Abeyasinghe, R.R., Ghebreyesus, T.A., Snow, R.W.** (2010) Shrinking the malaria map: progress and prospects. *Lancet*, **376** (9752), 1566-1578.
- Finlay, W. J., I. Shaw, J. P. Reilly and M. Kane.** (2006) Generation of high-affinity chicken single-chain Fv antibody fragments for measurement of the *Pseudonitzschia pungens* toxin domoic acid. *Appl Environ Microbiol*, **72** (5), 3343-9.
- Foth, B. J., S. A. Ralph, C. J. Tonkin, N. S. Struck, M. Fraunholz, D. S. Roos, A. F. Cowman and G. I. McFadden.** (2003) Dissecting apicoplast targeting in the malaria parasite *Plasmodium falciparum*. *Science*, **299** (5607), 705-8.

- Foth, B. J., N. Zhang, B. K. Chaal, S. K. Sze, P. R. Preiser and Z. Bozdech.** (2011) Quantitative time-course profiling of parasite and host cell proteins in the human malaria parasite *Plasmodium falciparum*. *Mol Cell Proteomics*, **10** (8), M110 006411.doi: 10.1074/mcp.M110.006411.
- Frita, R., Carapau, D., Mota, M.M., Hänscheid, T.** (2012) In Vivo Hemozoin Kinetics after Clearance of *Plasmodium berghei* Infection in Mice. *Mal Res Treat*, doi:10.1155/2012/373086.
- Fu, Y., L. N. Shearing, S. Haynes, P. Crewther, L. Tilley, R. F. Anders and M. Foley.** (1997) Isolation from phage display libraries of single chain variable fragment antibodies that recognize conformational epitopes in the malaria vaccine candidate, apical membrane antigen-1. *J Biol Chem*, **272** (41), 25678-84.
- Fujioka, H. and M. Aikawa.** (2002) Structure and life cycle. *Chem Immunol*, **80**, 1-26.
- Fung, A. O., R. Damoiseaux, S. Grundeen, J. L. Panes, D. H. Horton, J. W. Judy and T. B. Moore.** (2012) Quantitative detection of PfHRP2 in saliva of malaria patients in the Philippines. *Malaria Journal*, **11**, 175. 10.1186/1475-2875-11-175
- Gamboa, D., M. F. Ho, J. Bendezu, K. Torres, P. L. Chiodini, J. W. Barnwell, S. Incardona, M. Perkins, D. Bell, J. McCarthy and Q. Cheng.** (2010) A large proportion of *P. falciparum* isolates in the Amazon region of Peru lack pfhrr2 and pfhrr3: implications for malaria rapid diagnostic tests. *PLoS One*, **5** (1), e8091. 10.1371/journal.pone.0008091
- Garg, A., T. Lukk, V. Kumar, J. Y. Choi, Y. Augagneur, D. R. Voelker, S. Nair and C. Ben Mamoun.** (2015) Structure, function and inhibition of the phosphoethanolamine methyltransferases of the human malaria parasites *Plasmodium vivax* and *Plasmodium knowlesi*. *Sci Rep*, **5**, 9064.doi:10.1038/srep09064
- Gillet, P., D. Mumba Ngoyi, A. Lukuka, V. Kande, B. Atua, J. van Griensven, J. J. Muyembe, J. Jacobs and V. Lejon.** (2013) False positivity of non-targeted infections in malaria rapid diagnostic tests: the case of human african trypanosomiasis. *PLoS Negl Trop Dis*, **7** (4), e2180.doi: 10.1371/journal.pntd.0002180
- Gilson, P. R. and B. S. Crabb.** (2009) Morphology and kinetics of the three distinct phases of red blood cell invasion by *Plasmodium falciparum* merozoites. *Int J Parasitol*, **39** (1), 91-6.
- Gkrania-Klotsas, E., Lever, A.M.L.** (2007) An update on malaria prevention, diagnosis and treatment for the returning traveller. *Blood Reviews*, **21**, 73-87.
- Glavan, A. C., Christodouleas, D.C., Mosadegh, B., Yu, H.D., Smith, B.S., Lessing, J., Fernández-Abedul, M.T., Whitesides, G.M.** (2014) Folding Analytical Devices for Electrochemical ELISA in Hydrophobic RH Paper. *Anal Chem*, **86**, 11999-12007.

- Godonoga, M., T. Y. Lin, A. Oshima, K. Sumitomo, M. S. Tang, Y. W. Cheung, A. B. Kinghorn, R. M. Dirkzwager, C. Zhou, A. Kuzuya, J. A. Tanner and J. G. Heddle.** (2016) A DNA aptamer recognising a malaria protein biomarker can function as part of a DNA origami assembly. *Sci Rep*, **6**, 21266.doi: 10.1038/srep21266
- Goldberg, D. E., A. F. Slater, R. Beavis, B. Chait, A. Cerami and G. B. Henderson.** (1991) Hemoglobin degradation in the human malaria pathogen *Plasmodium falciparum*: a catabolic pathway initiated by a specific aspartic protease. *J Exp Med*, **173** (4), 961-9.
- Goldring, J. P. D., Coetzer, T.H.T.** (2003) Isolation of Chicken Immunoglobulins (IgY) from Egg Yolk. *Biochem Mol Biol Ed*, **31** (3), 185-187.
- Golgi, C.** (1886) Sull'infezione malarica. *Arch Sci Med*, **10**, 109-135.
- Gomez-Arreaza, A., H. Acosta, W. Quinones, J. L. Concepcion, P. A. Michels and L. Avilan.** (2014) Extracellular functions of glycolytic enzymes of parasites: unpredicted use of ancient proteins. *Mol Biochem Parasitol*, **193** (2), 75-81.
- Gomez, M. S., R. C. Piper, L. A. Hunsaker, R. E. Royer, L. M. Deck, M. T. Makler and D. L. Vander Jagt.** (1997) Substrate and cofactor specificity and selective inhibition of lactate dehydrogenase from the malarial parasite *P. falciparum*. *Mol Biochem Parasitol*, **90** (1), 235-46.
- Gove, S., J. Tulloch, J. Cattani and A. Schapira.** (1993) Usefulness of clinical case-definitions in treatment of childhood malaria or pneumonia. *Lancet*, **341** (8840),304-5.
- Granchi, C., S. Bertini, M. Macchia and F. Minutolo.** (2010) Inhibitors of lactate dehydrogenase isoforms and their therapeutic potentials. *Curr Med Chem*, **17** (7), 672-97.
- Grant, B. D., C. A. Smith, K. Karvonen and R. Richards-Kortum.** (2016) Highly Sensitive Two-Dimensional Paper Network Incorporating Biotin-Streptavidin for the Detection of Malaria. *Anal Chem*, **88** (5), 2553-7.
- Grassi, B., Feletti, R.** (1890) Parasites malariques chez les oiseaux. *Arch. Ital. de Biologie*, **13**, 297-300.
- Grimberg, B. T.** (2011) Methodology and application of flow cytometry for investigation of human malaria parasites. *J Immunol Methods*, **367** (1-2), 1-16.
- Guarente, L.** (2011) The logic linking protein acetylation and metabolism. *Cell Metab*, **14** (2), 151-3.
- Guerra, C. A., S. I. Hay, L. S. Lucioparedes, P. W. Gikandi, A. J. Tatem, A. M. Noor and R. W. Snow.** (2007) Assembling a global database of malaria parasite prevalence for the Malaria Atlas Project. *Malaria Journal*, **6**, 17. Doi: 10.1186/1475-2875-6-17

- Gulka, C. P., J. D. Swartz and D. W. Wright.** (2015) Ni(II)NTA AuNPs as a low-resource malarial diagnostic platform for the rapid colorimetric detection of *Plasmodium falciparum* Histidine-Rich Protein-2. *Talanta*, **135**, 94-101.
- Gwer, S., C. R. Newton and J. A. Berkley.** (2007) Over-diagnosis and co-morbidity of severe malaria in African children: a guide for clinicians. *Am J Trop Med Hyg*, **77** (6), 6-13.
- Hafalla, J. C., O. Silvie and K. Matuschewski.** (2011) Cell biology and immunology of malaria. *Immunol Rev*, **240** (1), 297-316.
- Hakimi, H., Y. Goto, K. Suganuma, J. M. Angeles, S. Kawai, N. Inoue and S. Kawazu.** (2015) Development of monoclonal antibodies against *Plasmodium falciparum* thioredoxin peroxidase 1 and its possible application for malaria diagnosis. *Exp Parasitol*, **154**, 62-6.
- Hanscheid, T.** (1999) Diagnosis of malaria: a review of alternatives to conventional microscopy. *Clin Lab Haematol*, **21** (4), 235-45.
- Harchut, K., C. Standley, A. Dobson, B. Klaassen, C. Rambaud-Althaus, F. Althaus and K. Nowak.** (2013) Over-diagnosis of malaria by microscopy in the Kilombero Valley, Southern Tanzania: an evaluation of the utility and cost-effectiveness of rapid diagnostic tests. *Malaria Journal*, **12**, doi: 10.1186/1475-2875-12-159
- Harlow, E., Lane, D.** (1988) *Antibodies a laboratory manual*. Cold Spring Harbor Laboratory Press
- Hay, S. I., C. A. Guerra, P. W. Gething, A. P. Patil, A. J. Tatem, A. M. Noor, C. W. Kabaria, B. H. Manh, I. R. Elyazar, S. Brooker, D. L. Smith, R. A. Moyeed and R. W. Snow.** (2009) A world malaria map: *Plasmodium falciparum* endemicity in 2007. *PLoS Med*, **6** (3), e1000048. doi: 10.1371/journal.pmed.1000048
- Hay, S. I., C. A. Guerra, A. J. Tatem, A. M. Noor and R. W. Snow.** (2004) The global distribution and population at risk of malaria: past, present, and future. *Lancet Infect Dis*, **4** (6), 327-336.
- Heard, K. S., M. Diguette, A. C. Heard and A. Carruthers.** (1998) Membrane-bound glyceraldehyde-3-phosphate dehydrogenase and multiphasic erythrocyte sugar transport. *Exp Physiol*, **83** (2), 195-202.
- Hill, F., Gemünd, C., Benes, V., Ansorge, W., Gibson, J.** (2000) An estimate of large-scale sequencing accuracy. *EMBO Reports*, **1**, 29-31.
- Ho, M. F., J. Baker, N. Lee, J. Luchavez, F. Ariey, S. Nhem, W. Oyibo, D. Bell, I. Gonzalez, P. Chiodini, M. L. Gatton, Q. Cheng and J. S. McCarthy.** (2014) Circulating antibodies against *Plasmodium falciparum* histidine-rich proteins 2 interfere with antigen detection by rapid diagnostic tests. *Malaria Journal*, **13**, doi: 10.1186/1475-2875-13-480

- Hobro, A. J., A. Konishi, C. Coban and N. I. Smith.** (2013) Raman spectroscopic analysis of malaria disease progression via blood and plasma samples. *Analyst*, **138** (14), 3927-33.
- Hofmann, N., Mwingira, F., Shekalaghe, S., Robinson, L.J., Mueller, I., Felger, I.** (2015) Ultra-Sensitive Detection of *Plasmodium falciparum* by Amplification of Multi-Copy Subtelomeric Targets. *PLOS Medicine*, **12** (3), DOI:10.1371/journal.pmed.1001788.
- Hoogenboom, H.R., de Bruine, A.P., Hufton, S.E., Hoet, R.M., Arends, J., Roovers, R.C.** (1998) Antibody Phage Display Technology and Its Applications. *Immunotechnology* **4** (1), 1-20.
- Hoogenboom, H. R., A. D. Griffiths, K. S. Johnson, D. J. Chiswell, P. Hudson and G. Winter.** (1991) Multi-subunit proteins on the surface of filamentous phage: methodologies for displaying antibody (Fab) heavy and light chains. *Nucleic Acids Res*, **19** (15), 4133-7.
- Hopp, T. P. and K. R. Woods.** (1981) Prediction of protein antigenic determinants from amino acid sequences. *Proc Natl Acad Sci USA*, **78** (6), 3824-8.
- Horton, J. R., K. Sawada, M. Nishibori, X. Zhang and X. Cheng.** (2001) Two polymorphic forms of human histamine methyltransferase: structural, thermal, and kinetic comparisons. *Structure*, **9** (9), 837-49.
- Houze, S., V. Hubert, G. Le Pessec, J. Le Bras and J. Clain.** (2011) Combined deletions of *pfhrp2* and *pfhrp3* genes result in *Plasmodium falciparum* malaria false-negative rapid diagnostic test. *J Clin Microbiol*, **49** (7), 2694-6.
- Huang, H., M. M. Mackeen, M. Cook, E. Oriero, E. Locke, M. L. Thezenas, B. M. Kessler, D. Nwakanma and C. Casals-Pascual.** (2012) Proteomic identification of host and parasite biomarkers in saliva from patients with uncomplicated *Plasmodium falciparum* malaria. *Malaria Journal*, **11**, doi: 10.1186/1475-2875-11-178.
- Hurdayal, R., Achilonu, I., Choveaux, D., Coetzer, T.H.T., Goldring, J.P.D.** (2010) Anti-peptide antibodies differentiate between *plasmodial* lactate dehydrogenases. *Peptides*, **31**, 525-532.
- Iqbal, J., Sher, A., Rab, A.** (2000) Plasmodium falciparum Histidine-Rich Protein 2-Based Immunocapture Diagnostic Assay for Malaria: Cross-Reactivity with Rheumatoid Factors. *J Clin Microbiol*, **38** (3), 1184-1186.
- Iqbal, J., Siddique, A., Jameel, M., Hira, P.R.** (2004) Persistent histidine-rich protein 2, parasite lactate dehydrogenase, and panmalarial antigen reactivity after clearance of *Plasmodium falciparum* mono-infection. *J Clin Microbiol*, **42** (9), 4237.

- Ishengoma, D. S., S. Lwitiho, R. A. Madebe, N. Nyagonde, O. Persson, L. S. Vestergaard, I. C. Bygbjerg, M. M. Lemnge and M. Alifrangis.** (2011) Using rapid diagnostic tests as source of malaria parasite DNA for molecular analyses in the era of declining malaria prevalence. *Malaria Journal*, **10**, doi: 10.1186/1475-2875-10-6
- Jacobsson, K. and L. Frykberg.** (1996) Phage display shot-gun cloning of ligand-binding domains of prokaryotic receptors approaches 100% correct clones. *Biotechniques*, **20** (6), 1070-6, 1078, 1080-1.
- Jameson, B. A. and H. Wolf.** (1988) The antigenic index: a novel algorithm for predicting antigenic determinants. *Comput Appl Biosci*, **4** (1), 181-6.
- Jarra, W., Snounou, G.** (1998) Only Viable Parasites Are Detected by PCR following Clearance of Rodent Malarial Infections by Drug Treatment or Immune Responses. *Infect Imm*, **66** (8), 3783-3787.
- Jirků, M., Pomajbíková, K., Petrželková, K.J., Hůzová, Z., Modrý, D., Lukeš, J.** (2012) Detection of *Plasmodium spp.* in Human Feces. *Emerging Infectious Diseases*, **18** (4), 634-636.
- Jorgensen, P., Chanthap, L., Rebuena, A., Tsuyuoka, R., Bell, D.** (2006) Malaria Rapid Diagnostic Tests in Tropical Climates: The Need for a Cool Chain. *Am J Trop Med Hyg* **74** (5), 750-54.
- Kallander, K., J. Nsungwa-Sabiiti and S. Peterson.** (2004) Symptom overlap for malaria and pneumonia-policy implications for home management strategies. *Acta Trop*, **90** (2), 211-4.
- Kamau, E., S. Alemayehu, K. C. Feghali, D. Saunders and C. F. Ockenhouse.** (2013) Multiplex qPCR for detection and absolute quantification of malaria. *PLoS One*, **8**, e71539.doi: 10.1371/journal.pone.0071539
- Kaneda, M., K. Takeuchi, K. Inoue and M. Umeda.** (1997) Localization of the phosphatidylserine-binding site of glyceraldehyde-3-phosphate dehydrogenase responsible for membrane fusion. *J Biochem*, **122** (6), 1233-40.
- Kappe, S. H., A. M. Vaughan, J. A. Boddey and A. F. Cowman.** (2010) That was then but this is now: malaria research in the time of an eradication agenda. *Science*, **328** (5980), 862-6.
- Kattenberg, J. H., E. A. Ochodo, K. R. Boer, H. D. Schallig, P. F. Mens and M. M. Leeflang.** (2011) Systematic review and meta-analysis: rapid diagnostic tests versus placental histology, microscopy and PCR for malaria in pregnant women. *Malaria Journal*, **10**, doi: 10.1186/1475-2875-10-321
- Kawai, S., M. Hirai, K. Haruki, K. Tanabe and Y. Chigusa.** (2009) Cross-reactivity in rapid diagnostic tests between human malaria and zoonotic simian malaria parasite *Plasmodium knowlesi* infections. *Parasitol Int*, **58** (3), 300-2.

- Kebaier, C., Voza, T., Vanderberg, J.** (2009) Kinetics of Mosquito-Injected *Plasmodium* Sporozoites in Mice: Fewer Sporozoites Are Injected into Sporozoite-Immunized Mice. *PLOS Pathogens*, **5**, e1000399. doi: 10.1371/journal.ppat.1000399
- Kermekchiev, M. B., L. I. Kirilova, E. E. Vail and W. M. Barnes.** (2009) Mutants of Taq DNA polymerase resistant to PCR inhibitors allow DNA amplification from whole blood and crude soil samples. *Nucleic Acids Res*, **37** (5), e40. doi: 10.1093/nar/gkn1055
- Kersting, S., Rausch, V., Bier, F.F., von Nickisch-Rosenegk, M.** (2014) Rapid detection of *Plasmodium falciparum* with isothermal recombinase polymerase amplification and lateral flow analysis. *Malaria Journal*, **13** (99), doi:10.1186/1475-2875-13-99.
- Khoshmanesh, A., M. W. Dixon, S. Kenny, L. Tilley, D. McNaughton and B. R. Wood.** (2014) Detection and quantification of early-stage malaria parasites in laboratory infected erythrocytes by attenuated total reflectance infrared spectroscopy and multivariate analysis. *Anal Chem*, **86** (9), 4379-86.
- Kidane, G. and R. H. Morrow.** (2000) Teaching mothers to provide home treatment of malaria in Tigray, Ethiopia: a randomised trial. *Lancet*, **356** (9229), 550-5.
- Kim, J. W., Dang, C.V.** (2005) Multifaceted roles of glycolytic enzymes. *Tr Biochem Sci*, **30** (3), 142-150.
- Kiszewski, A., A. Mellinger, A. Spielman, P. Malaney, S. E. Sachs and J. Sachs.** (2004) A global index representing the stability of malaria transmission. *Am J Trop Med Hyg*, **70** (5), 486-98.
- Kochar, D. K., V. Saxena, N. Singh, S. K. Kochar, S. V. Kumar and A. Das.** (2005) *Plasmodium vivax* malaria. *Emerg Infect Dis*, **11** (1), 132-4.
- Koekemoer, L. L., E. M. Rankoe, J. P. la Grange, J. Govere and M. Coetzee.** (2001) False detection of *Plasmodium falciparum* sporozoites in *Anopheles marshallii* group mosquitoes. *J Am Mosq Control Assoc*, **17** (3), 160-5.
- Koenderink, J. B., R. A. Kavishe, S. R. Rijpma and F. G. Russel.** (2010) The ABCs of multidrug resistance in malaria. *Trends Parasitol*, **26** (9), 440-6.
- Krause, R. G. E., Grobler, A.F., Goldring, J.P.D.** (2015) Comparing Antibody Responses in Chickens Against *Plasmodium falciparum* Lactate Dehydrogenase and Glyceraldehyde-3-phosphate Dehydrogenase with Freund's and Pheroid® Adjuvants. *Immunol Inv*, **44** (7), 627-642.
- Kristensen, T., R. Lopez and H. Prydz.** (1992) An estimate of the sequencing error frequency in the DNA sequence databases. *DNA Seq*, **2** (6), 343-6.

Kumar, N., V. Pande, R. M. Bhatt, N. K. Shah, N. Mishra, B. Srivastava, N. Valecha and A. R. Anvikar. (2013) Genetic deletion of HRP2 and HRP3 in Indian *Plasmodium falciparum* population and false negative malaria rapid diagnostic test. *Acta Trop*, **125** (1), 119-21.

Kumar, N., J. P. Singh, V. Pande, N. Mishra, B. Srivastava, R. Kapoor, N. Valecha and A. R. Anvikar. (2012) Genetic variation in histidine rich proteins among Indian *Plasmodium falciparum* population: possible cause of variable sensitivity of malaria rapid diagnostic tests. *Malaria Journal*, **11**, doi: 10.1186/1475-2875-11-298

Kumar, R. K., Xiavour, S., Latha, S., Kumar, V., Sukamaran. (2014) Anti-Human IgG-Horseradish Peroxidase and its use in ELISA and Western Blotting Experiments. *J Chromatograph Separat Techniq*, **5** (211), doi:10.4172/2157-7064.1000211

Kyte, J. and R. F. Doolittle. (1982) A simple method for displaying the hydropathic character of a protein. *J Mol Biol*, **157** (1), 105-32.

Laemmli, U. K. (1970) Cleavage of structural proteins during the assembly of the head of bacteriophage T4. *Nature*, **227**, 680-685.

Lalremruata, A., M. Magris, S. Vivas-Martinez, M. Koehler, M. Esen, P. Kempaiah, S. Jeyaraj, D. J. Perkins, B. Mordmuller and W. G. Metzger. (2015) Natural infection of *Plasmodium brasilianum* in humans: Man and monkey share quartan malaria parasites in the Venezuelan Amazon. *EBioMedicine*, **2** (9), 1186-92.

Lamperti, E. D., J. M. Kittelberger, T. F. Smith and L. Villa-Komaroff. (1992) Corruption of genomic databases with anomalous sequence. *Nucleic Acids Res*, **20** (11), 2741-7.

Lanzillotti, R. and T. L. Coetzer. (2008) Phage display: a useful tool for malaria research? *Trends Parasitol*, **24** (1), 18-23.

Larentis, A. L., J. F. Nicolau, S. Esteves Gdos, D. T. Vareschini, F. V. de Almeida, M. G. dos Reis, R. Galler and M. A. Medeiros. (2014) Evaluation of pre-induction temperature, cell growth at induction and IPTG concentration on the expression of a leptospiral protein in *E. coli* using shaking flasks and microbioreactor. *BMC Res Notes*, **7**, doi: 10.1186/1756-0500-7-671.

Lasonder, E., Y. Ishihama, J. S. Andersen, A. M. Vermunt, A. Pain, R. W. Sauerwein, W. M. Eling, N. Hall, A. P. Waters, H. G. Stunnenberg and M. Mann. (2002) Analysis of the *Plasmodium falciparum* proteome by high-accuracy mass spectrometry. *Nature*, **419** (6906), 537-42.

Lateef, S. S., S. Gupta, L. P. Jayathilaka, S. Krishnanchettiar, J. S. Huang and B. S. Lee. (2007) An improved protocol for coupling synthetic peptides to carrier proteins for antibody production using DMF to solubilize peptides. *J Biomol Tech*, **18** (3), 173-6.

- Lau, Y., Fong, M., Mahmud, R., Chang, P., Palaeya, V., Cheong, F., Chin, L., Anthony, C.N., Al-Mekhlafi, M., Chen, Y.** (2011) Specific, sensitive and rapid detection of human *Plasmodium knowlesi* infection by loop-mediated isothermal amplification (LAMP) in blood samples. *Malaria Journal*, **10** (197), doi:10.1186/1475-2875-10-197.
- Lauterbach, S. B., Lanzillotti, R., Coetzer, T.L.** (2003) Construction and use of *Plasmodium falciparum* phage display libraries to identify host parasite interactions. *Malaria Journal*, **2**, DOI: 10.1186/1475-2875-2-47.
- Laveran, A.** (1880) Note sur un nouveau parasite trouve dans le sang de plusieurs maladies attients de fièvre palustre. *Bull Acad Med*, **9**, 1235-1236.
- LeClair, N. P., Conrad, M.D., Baliraine, F.N., Nsanzabana, C., Nsohya, S.L., Rosenthala, P.J.** (2013) Optimization of a Ligase Detection Reaction-Fluorescent Microsphere Assay for Characterization of Resistance-Mediating Polymorphisms in African Samples of *Plasmodium falciparum*. *J Clin Microbiol*, **51** (8), 2564-2570.
- LeRoch, K. G., Zhou, Y., Blair, P.L., Grainger, M., Moch, J.K., Haynes, J.D., De La Vega, P., Holder, A.A., Batalov, S., Carucci, D.J., Winzeler, E.A.** (2003) Discovery of gene function by expression profiling of the malaria parasite life cycle. *Science*, **301** (5639), 1503-1508.
- Lee, K. S., Divis, P.C.S., Zakaria, S.K., Matusop, A., Julin, R.A., Conway, D.J., Cox-Singh, J., Singh, B.** (2011) *Plasmodium knowlesi*: Reservoir Hosts and Tracking the Emergence in Humans and Macaques. *PLOS Pathogens*, **7** (4), e1002015.
- Lee, N., J. Baker, D. Bell, J. McCarthy and Q. Cheng.** (2006) Assessing the genetic diversity of the aldolase genes of *Plasmodium falciparum* and *Plasmodium vivax* and its potential effect on performance of aldolase-detecting rapid diagnostic tests. *J Clin Microbiol*, **44** (12), 4547-9.
- Lee, P. C., E. T. Chong, F. Anderios, Y. Al Lim, C. H. Chew and K. H. Chua.** (2015) Molecular detection of human *Plasmodium* species in Sabah using PlasmoNex multiplex PCR and hydrolysis probes real-time PCR. *Malaria Journal*, **14**, doi: 10.1186/s12936-015-0542-5.
- Lee, S., D. H. Manjunatha, W. Jeon and C. Ban.** (2014) Cationic surfactant-based colorimetric detection of *Plasmodium* lactate dehydrogenase, a biomarker for malaria, using the specific DNA aptamer. *PLoS One*, **9**, e100847. doi: 10.1371/journal.pone.0100847.
- Leitgeb, A. M., Blomqvist, K., Cho-Ngwa, F., Samje, M., Nde, P., Titanji, V., Wahlgren, M.** (2011) Low anticoagulant heparin disrupts *Plasmodium falciparum* rosettes in fresh clinical isolates. *Am J Trop Med Hyg*, **84** (3), 390-396.

- Leow, C. H., M. Jones, Q. Cheng, S. Mahler and J. McCarthy.** (2014) Production and characterization of specific monoclonal antibodies binding the *Plasmodium falciparum* diagnostic biomarker, histidine-rich protein 2. *Malaria Journal*, **13**, doi: 10.1186/1475-2875-13-277
- Li, X., L. Wang, Y. Zhen, S. Li and Y. Xu.** (2015a) Chicken egg yolk antibodies (IgY) as non-antibiotic production enhancers for use in swine production: a review. *J Anim Sci Biotechnol*, **6** (1), 40.
- Li, Y. C., G. Z. Wang, F. Meng, W. Zeng, C. H. He, X. M. Hu and S. Q. Wang.** (2015b) Genetic diversity of *Plasmodium vivax* population before elimination of malaria in Hainan Province, China. *Malaria Journal*, **14**, doi: 10.1186/s12936-015-0545-2.
- Lon, C. T., S. Alcantara, J. Luchavez, R. Tsuyuoka and D. Bell.** (2005) Positive control wells: a potential answer to remote-area quality assurance of malaria rapid diagnostic tests. *Trans R Soc Trop Med Hyg*, **99** (7), 493-8.
- Lucchi, N. W., M. A. Karell, I. Journal, E. Rogier, I. Goldman, D. Ljolje, C. Huber, K. E. Mace, S. E. Jean, E. E. Akom, R. Oscar, J. Buteau, J. Boncy, J. W. Barnwell and V. Udhayakumar.** (2014) PET-PCR method for the molecular detection of malaria parasites in a national malaria surveillance study in Haiti, 2011. *Malaria Journal*, **13**, doi: 10.1186/1475-2875-13-462.
- Lucchi, N. W., J. Narayanan, M. A. Karell, M. Xayavong, S. Kariuki, A. J. DaSilva, V. Hill and V. Udhayakumar.** (2013) Molecular diagnosis of malaria by photo-induced electron transfer fluorogenic primers: PET-PCR. *PLoS One*, **8** (2), e56677. doi: 10.1371/journal.pone.0056677.
- Lukianova-Hleb, E., Bezek, S., Szigeti, R., Khodarev, A., Kelley, T., Hurrell, A., Berba, M., Kumar, N., D'Alessandro, U., Lapotko, D.** (2015) Transdermal Diagnosis of Malaria Using Vapor Nanobubbles. *Emerging Infectious Diseases*, **21** (7), 1122-1127.
- MacBeath, G. and P. Kast.** (1998) UGA read-through artifacts-when popular gene expression systems need a patch. *Biotechniques*, **24** (5), 789-94.
- Major, L. L., E. S. Poole, M. E. Dalphin, S. A. Mannering and W. P. Tate.** (1996) Is the in-frame termination signal of the *Escherichia coli* release factor-2 frameshift site weakened by a particularly poor context? *Nucleic Acids Res*, **24** (14), 2673-8.
- Makler, M. T., C. J. Palmer and A. L. Ager.** (1998) A review of practical techniques for the diagnosis of malaria. *Ann Trop Med Parasitol*, **92** (4), 419-33.
- Makler, M.T., Hinrichs, D.J.** (1993a) Measurement of the Lactate Dehydrogenase Activity of Plasmodium Falciparum as an Assessment of Parasitemia. *Am J Trop Med Hyg* **48** (2), 205-10.

- Makler, M. T., Ries, J.M., Williams, J.A., Bancroft, J.E., Piper, R.C., Gibbins, B.L., Hinrichs, D.J.** (1993b) Parasite Lactate Dehydrogenase as an assay for *Plasmodium falciparum* drug sensitivity *Am J Trop Med Hyg*, **48** (6), 739-741.
- Malavolta, L., M. R. Pinto, J. H. Cuvero and C. R. Nakaie.** (2006) Interpretation of the dissolution of insoluble peptide sequences based on the acid-base properties of the solvent. *Protein Sci*, **15** (6), 1476-88.
- Maltha, J., D. Gamboa, J. Bendezu, L. Sanchez, L. Cnops, P. Gillet and J. Jacobs.** (2012) Rapid diagnostic tests for malaria diagnosis in the Peruvian Amazon: impact of pfhpr2 gene deletions and cross-reactions. *PLoS One*, **7** (8), e43094.doi: 10.1371/journal.pone.0043094.
- Maltha, J., P. Gillet, L. Cnops, J. van den Ende, M. van Esbroeck and J. Jacobs.** (2010) Malaria rapid diagnostic tests: *Plasmodium falciparum* infections with high parasite densities may generate false positive *Plasmodium vivax* pLDH lines. *Malaria Journal*, **9**, doi: 10.1186/1475-2875-9-198.
- Marchalonis, J. J., M. K. Adelman, S. F. Schluter and P. A. Ramsland.** (2006) The antibody repertoire in evolution: chance, selection, and continuity. *Dev Comp Immunol*, **30** (1-2), 223-47.
- Marks, J. D., H. R. Hoogenboom, T. P. Bonnert, J. McCafferty, A. D. Griffiths and G. Winter.** (1991) By-passing immunization. Human antibodies from V-gene libraries displayed on phage. *J Mol Biol*, **222** (3), 581-97.
- Markwalter, C. F., Davis, K.M., Wright, D.W.** (2016) Immunomagnetic capture and colorimetric detection of malarial biomarker *Plasmodium falciparum* lactate dehydrogenase. *Anal Biochem*, **493**, 30-34.
- Marquart, L., A. Butterworth, J. S. McCarthy and M. L. Gatton.** (2012) Modelling the dynamics of *Plasmodium falciparum* histidine-rich protein 2 in human malaria to better understand malaria rapid diagnostic test performance. *Malaria Journal*, **11**, doi: 10.1186/1475-2875-11-74.
- Martin, S. K., Rajasekariah, G., Awinda, G., Waitumbi, J., Kifude, C.** (2009) Unified Parasite Lactate Dehydrogenase and Histidine-Rich Protein ELISA for Quantification of *Plasmodium falciparum*. *Am J Trop Med Hyg*, **80** (4), 516-522.
- Martinez-Torres, D., F. Chandre, M. S. Williamson, F. Darriet, J. B. Berge, A. L. Devonshire, P. Guillet, N. Pasteur and D. Pauron.** (1998) Molecular characterization of pyrethroid knockdown resistance (kdr) in the major malaria vector *Anopheles gambiae* s.s. *Insect Mol Biol*, **7** (2), 179-84.

- Masilamani, V., S. Devanesan, M. Ravikumar, K. Perinbam, M. S. AlSalhi, S. Prasad, S. Palled, K. M. Ganesh and A. H. Alsaeed.** (2014) Fluorescence spectral diagnosis of malaria: a preliminary study. *Diagn Pathol*, **9**, doi: 10.1186/s13000-014-0182-z.
- McCutchan, T. F., Piper, R.C., Makler, M.T.** (2008) Use of malaria rapid diagnostic test to identify *Plasmodium knowlesi* infection. *Emerging Inf Dis*, **14** (11), 1750-1752.
- McIntosh, R. S., Shi, J., Jennings, R.M., Chappel, J.C., de Koning-Ward, T.F., Smith, T., Green, J., van Egmond, M., Leusen, J.H.W., Lazarou, M., van de Winkel, J., Jones, T.S., Crabb, B.S., Holder, A.A., Pleass, R.J.** (2007) The Importance of Human FcγRI in Mediating Protection to Malaria. *PLOS Pathogens*, **3** (5), e72. doi:10.1371/journal.ppat.0030072.
- Mehta, M., Sonawat, H.M., Sharma, S.** (2006) Glycolysis in *Plasmodium falciparum* results in modulation of host enzyme activities. *J Vec Bor Dis*, **43**, 95-103.
- Mens, P. F., Moers, A.P.H.A., de Bes, L.M., Flint, J., Sak, J.R.S., Keerecharoen, L., van Overmeir, C., Verweij, J.J., Hallett, R.L., Wihokhoen, B., Proux, S., Schallig, H.D.F.H., van Amerongen, A.** (2012) Development, validation and evaluation of a rapid PCR-nucleic acid lateral flow immuno-assay for the detection of *Plasmodium* and the differentiation between *Plasmodium falciparum* and *Plasmodium vivax*. *Malaria Journal*, **11**, doi:10.1186/1475-2875-11-279.
- Miao, J., M. Lawrence, V. Jeffers, F. Zhao, D. Parker, Y. Ge, W. J. Sullivan, Jr. and L. Cui.** (2013) Extensive lysine acetylation occurs in evolutionarily conserved metabolic pathways and parasite-specific functions during *Plasmodium falciparum* intraerythrocytic development. *Mol Microbiol*, **89** (4), 660-75.
- Mikita, K., K. Thakur, N. M. Anstey, K. A. Piera, C. A. Pardo, J. B. Weinberg, J. Mukemba, S. Florence, E. D. Mwaikambo, D. L. Granger and D. J. Sullivan.** (2014) Quantification of *Plasmodium falciparum* histidine-rich protein-2 in cerebrospinal spinal fluid from cerebral malaria patients. *Am J Trop Med Hyg*, **91** (3), 486-92.
- Miller, L. H., M. F. Good and G. Milon.** (1994) Malaria pathogenesis. *Science*, **264** (5167), 1878-83.
- Mohanty, S. K., A. Uppal and P. K. Gupta.** (2004) Self-rotation of red blood cells in optical tweezers: prospects for high throughput malaria diagnosis. *Biotechnol Lett*, **26** (12), 971-4.
- Mohon, A. N., R. Elahi, W. A. Khan, R. Haque, D. J. Sullivan, Jr. and M. S. Alam.** (2014) A new visually improved and sensitive loop mediated isothermal amplification (LAMP) for diagnosis of symptomatic *falciparum* malaria. *Acta Trop*, **134**, 52-7.
- Moody, A.** (2002) Rapid diagnostic tests for malaria parasites. *Clin Microbiol Rev*, **15** (1), 66-78.

- Morris, U., B. Aydin-Schmidt, D. Shakely, A. Martensson, L. Jornhagen, A. S. Ali, M. I. Msellem, M. Petzold, J. P. Gil, P. E. Ferreira and A. Bjorkman.** (2013) Rapid diagnostic tests for molecular surveillance of *Plasmodium falciparum* malaria -assessment of DNA extraction methods and field applicability. *Malaria Journal*, **12**, doi: 10.1186/1475-2875-12-106.
- Mouatcho, J. C. and J. P. Goldring.** (2013) Malaria rapid diagnostic tests: challenges and prospects. *J Med Microbiol*, **62** (10), 1491-505.
- Mouatcho, J. C., Hargreaves, K., Koekemoer, L.L., Brooke, B.D., Oliver, S.V., Hunt, R.H., Coetzee, M.** (2007) Indoor collections of the *Anopheles funestus* group (Diptera: Culicidae) in sprayed houses in northern KwaZulu-Natal, South Africa. *Malaria Journal*, **6** (30), doi:10.1186/1475-2875-6-30.
- Moyes, C. L., Henry, A.J., Golding, N., Huang, Z., Singh, B., Baird, J.K., P. N. Newton, Huffman, M., Duda, K.A., Drakeley, C.J., Elyazar, I.R.F., and N. M. Anstey, Chen, Q., Zommers, Z., Bhatt, S., Gething, P.W., Hay, S.I.** (2014) Defining the Geographical Range of the *Plasmodium knowlesi* Reservoir. *PLOS Neglected Tropical Diseases*, **8** (3), e2780. doi:10.1371/journal.pntd.0002780.
- Mruk, D.D., Yan Chen, C.** (2011) Enhanced chemiluminescence (ECL) for routine immunoblotting. *Spermatogenesis*, **1** (2), 121-122
- Murray, C. J., K. F. Ortblad, C. Guinovart, S. S. Lim, T. M. Wolock, D. A. Roberts, E. A. Dansereau, N. Graetz, R. M. Barber, J. C. Brown, H. Wang, H. C. Duber, M. Naghavi, D. Dicker, L. Dandona, J. A. Salomon, K. R. Heuton, K. Foreman, D. E. Phillips, T. D. Fleming, A. D. Flaxman, B. K. Phillips, E. K. Johnson, M. S. Coggeshall, F. Abd-Allah, S. F. Abera, J. P. Abraham, I. Abubakar, L. J. Abu-Raddad, N. M. Abu-Rmeileh, T. Achoki, A. O. Adeyemo, A. K. Adou, J. C. Adsuar, E. E. Agardh, D. Akena, M. J. Al Kahbouri, D. Alasfoor, M. I. Albittar, G. Alcalá-Cerra, M. A. Alegretti, Z. A. Alemu, R. Alfonso-Cristancho, S. Alhabib, R. Ali, F. Alla, P. J. Allen, U. Alsharif, E. Alvarez, N. Alvis-Guzman, A. A. Amankwaa, A. T. Amare, H. Amini, W. Ammar, B. O. Anderson, C. A. Antonio, P. Anwari, J. Arnlov, V. S. Arsenijevic, A. Artaman, R. J. Asghar, R. Assadi, L. S. Atkins, A. Badawi, K. Balakrishnan, A. Banerjee, S. Basu, J. Beardsley, T. Bekele, M. L. Bell, E. Bernabe, T. J. Beyene, N. Bhala, A. Bhalla, Z. A. Bhutta, A. B. Abdulhak, A. Binagwah, J. D. Blore, B. B. Basara, D. Bose, M. Brainin, N. Breitborde, C. A. Castaneda-Orjuela, F. Catala-Lopez, V. K. Chadha, J. C. Chang, P. P. Chiang, T. W. Chuang, M. Colomar, L. T. Cooper, C. Cooper, K. J. Courville, B. C. Cowie, M. H. Criqui, R. Dandona, A. Dayama, D. De Leo, L. Degenhardt, B. Del Pozo-Cruz, K. Deribe, *et al.* (2014) Global, regional, and national incidence and mortality for HIV, tuberculosis, and malaria during 1990-2013: a systematic analysis for the Global Burden of Disease Study 2013. *Lancet*, **384** (9947), 1005-70.**

- Murray, C. K., Bennett, J.W.** (2009) Rapid Diagnosis of Malaria. *Interdisc Perspec Inf Dis*, **1**, 1-7.
- Murray, C. K., R. A. Gasser, Jr., A. J. Magill and R. S. Miller.** (2008) Update on rapid diagnostic testing for malaria. *Clin Microbiol Rev*, **21** (1), 97-110.
- Najafabadi, Z. G., Oormazdi, H., Akhlaghi, L., Meamar, A.R., Nateghpour, M., Farivar, L., Razmjou, E.** (2014) Detection of *Plasmodium vivax* and *Plasmodium falciparum* DNA in human saliva and urine: Loop-mediated isothermal amplification for malaria diagnosis. *Acta Tropica*, **136**, 44-49.
- Nankoberanyi, S., Mbogo, G.W., LeClair, N.P., Conrad, M.D., Tumwebaze, P., Tukwasibwe, S., Kanya, M.R., Tappero, J., Nsohya, S.L., Rosenthal, P.J.** (2014) Validation of the ligase detection reaction fluorescent microsphere assay for the detection of *Plasmodium falciparum* resistance mediating polymorphisms in Uganda. *Malaria Journal*, **13** (95), doi:10.1186/1475-2875-13-95.
- Ng, O. T., Ooi, E.E., Lee, C.C., Lee, P.J., Ng, L.C., Pei, S.W., Tu, T.M., Loh, J.P., Leo, Y.S.** (2008) Naturally Acquired Human *Plasmodium knowlesi* Infection, Singapore. *Emerging Inf Dis*, **15** (5), 814-816.
- Nirmalan, N., P. F. Sims and J. E. Hyde.** (2004) Quantitative proteomics of the human malaria parasite *Plasmodium falciparum* and its application to studies of development and inhibition. *Mol Microbiol*, **52** (4), 1187-99.
- Nissim, A., H. R. Hoogenboom, I. M. Tomlinson, G. Flynn, C. Midgley, D. Lane and G. Winter.** (1994) Antibody fragments from a 'single pot' phage display library as immunochemical reagents. *EMBO J*, **13** (3), 692-8.
- Noedl, H., K. Yingyuen, A. Laoboonchai, M. Fukuda, J. Sirichaisinthop and R. S. Miller.** (2006) Sensitivity and specificity of an antigen detection ELISA for malaria diagnosis. *Am J Trop Med Hyg*, **75** (6), 1205-8.
- Noppe, W., Plieva, F., Galaev, I.Y., Pottel, H., Deckmyn, H., Mattiasson, B.** (2009) Chromato-Panning: An Efficient New Mode of Identifying Suitable Ligands from Phage Display Libraries. *BMC Biotechnology* **9** (21), doi:10.1186/472-6750-9-21.
- Ogonu, T., E. Shu, B. U. Ezeonwu, B. Lige, A. Derrick, R. E. Umeh and E. Agbo.** (2014) The performance evaluation of a urine malaria test (UMT) kit for the diagnosis of malaria in individuals with fever in south-east Nigeria: cross-sectional analytical study. *Malaria Journal*, **13**, doi: 10.1186/1475-2875-13-403.

Okoth, S. A., Abdallah, J.F., Ceron, N., Adhin, M.R., Chandrabose, J., Krishnalall, K., Huber, C.S., Goldman, I.F., de Oliveira, A.M., Barnwell, J.W., Udhayakumar, V. (2015) Variation in *Plasmodium falciparum* Histidine-Rich Protein 2 (Pfhrp2) and *Plasmodium falciparum* Histidine-Rich Protein 3 (Pfhrp3) Gene Deletions in Guyana and Suriname. *PLOS One*, **10** (5), e0126805. doi:10.1371/journal.pone.0126805.

Olesen, C. H., Brahim, K., Vandahl, B., Lousada-Dietrich, S., Jogdand, P.S., Vestergaard, L.S., Dodoo, D., Højrup, P., Christiansen, M., Larsen, S.O., Singh, S., Theisen, M. (2010) Distinct patterns of blood-stage parasite antigens detected by plasma IgG subclasses from individuals with different level of exposure to *Plasmodium falciparum* infections. *Malaria Journal*, **9** (296), doi:10.1186/1475-2875-9-296.

Olszewski, K. L., Llinás, M. (2011) Central carbon metabolism of *Plasmodium* parasites. *Mol Biochem Parasitol*, **175**, 95-103.

Orban, A., M. Rebelo, P. Molnar, I. S. Albuquerque, A. Butykai and I. Kezsmarki. (2016) Efficient monitoring of the blood-stage infection in a malaria rodent model by the rotating-crystal magneto-optical method. *Sci Rep*, **6**, doi: 10.1038/srep23218.

Peeling, R. W., K. K. Holmes, D. Mabey and A. Ronald. (2006) Rapid tests for sexually transmitted infections (STIs): the way forward. *Sex Transm Infect*, **82** (Suppl 5), doi: 10.1136/sti.2006.024265.

Pereira, D. Y., R. Y. Chiu, S. C. Zhang, B. M. Wu and D. T. Kamei. (2015) Single-step, paper-based concentration and detection of a malaria biomarker. *Anal Chim Acta*, **882**, 83-9.

Perkins, M. D. and D. R. Bell. (2008) Working without a blindfold: the critical role of diagnostics in malaria control. *Malaria Journal*, **7** (Suppl 1-S5). Doi: 10.1186/1475-2875-7-S1-S5.

Pessi, G., J. Y. Choi, J. M. Reynolds, D. R. Voelker and C. B. Mamoun. (2005) In vivo evidence for the specificity of *Plasmodium falciparum* phosphoethanolamine methyltransferase and its coupling to the Kennedy pathway. *J Biol Chem*, **280** (13), 12461-6.

Pessi, G., G. Kociubinski and C. B. Mamoun. (2004) A pathway for phosphatidylcholine biosynthesis in *Plasmodium falciparum* involving phosphoethanolamine methylation. *Proc Natl Acad Sci USA*, **101** (16), 6206-11.

Piper, R., J. Lebras, L. Wentworth, A. Hunt-Cooke, S. Houze, P. Chiodini and M. Makler. (1999) Immunocapture diagnostic assays for malaria using *Plasmodium* lactate dehydrogenase (pLDH). *Am J Trop Med Hyg*, **60** (1), 109-18.

Piper, R. C., I. Buchanan, Y. H. Choi and M. T. Makler. (2011) Opportunities for improving pLDH-based malaria diagnostic tests. *Malaria Journal*, **10**, doi: 10.1186/1475-2875-10-213.

- Pirnstill, C. W. and G. L. Cote.** (2015) Malaria Diagnosis Using a Mobile Phone Polarized Microscope. *Sci Rep*, **5**, doi: 10.1038/srep13368.
- Polley, S. D., Y. Mori, J. Watson, M. D. Perkins, I. J. Gonzalez, T. Notomi, P. L. Chiodini and C. J. Sutherland.** (2010) Mitochondrial DNA targets increase sensitivity of malaria detection using loop-mediated isothermal amplification. *J Clin Microbiol*, **48** (8), 2866-71.
- Polson, A., Coetzer, T.H.T., Kruger, J., von Maltzahn, E., van der Merwe, K.J.** (1985) Improvements in the isolation of IgY from the yolks of eggs laid by immunized hens. *Immunol Inves*, **14**, 323-327.
- Port, J. R., Nguetse, C., Adukpo, S., Velavan, T.P.** (2014) A reliable and rapid method for molecular detection of malarial parasites using microwave irradiation and loop mediated isothermal amplification. *Malaria Journal*, **13**, doi:10.1186/1475-2875-13-454.
- Prescott, W. R., R. G. Jordan, M. P. Grobusch, V. M. Chinchilli, I. Kleinschmidt, J. Borovsky, M. Plaskow, M. Torrez, M. Mico and C. Schwabe.** (2012) Performance of a malaria microscopy image analysis slide reading device. *Malaria Journal*, **11**, doi: 10.1186/1475-2875-11-155.
- Prugnolle, F., P. Durand, C. Neel, B. Ollomo, F. J. Ayala, C. Arnathau, L. Etienne, E. Mpoudi-Ngole, D. Nkoghe, E. Leroy, E. Delaporte, M. Peeters and F. Renaud.** (2010) African great apes are natural hosts of multiple related malaria species, including *Plasmodium falciparum*. *Proc Natl Acad Sci USA*, **107** (4), 1458-63.
- Rahim, A., C. Coutelle and R. Harbottle.** (2003) High-throughput Pyrosequencing of a phage display library for the identification of enriched target-specific peptides. *Biotechniques*, **35** (2), 317-20, 322, 324.
- Rao, M. R., R. N. Padhy and M. K. Das.** (2015) Prevalence of dengue viral and malaria parasitic co-infections in an epidemic district, Angul of Odisha, India: An eco-epidemiological and cross-sectional study for the prospective aspects of public health. *J Infect Public Health*. Doi: 10.1016/j.jiph.2015.10.019.
- Rebelo, M., Sousa, C., Shapiro, H.M., Mota, M.M., Grobusch, M.P., Hänscheid, T.** (2013) A Novel Flow Cytometric Hemozoin Detection Assay for Real-Time Sensitivity Testing of *Plasmodium falciparum*. *PLOS ONE*, **8** (4), e61606. doi:10.1371/journal.pone.0061606.
- Rosano, G. L. and E. A. Ceccarelli.** (2014) Recombinant protein expression in *Escherichia coli*: advances and challenges. *Front Microbiol*, **5**, doi: 10.3389/fmicb.2014.00172
- Ross, R.** (1897) Observations on a Condition Necessary to the Transformation of the Malaria Crescent. *Br Med J*, **1** (1883), 251-5.

- Rougemont, M., Van Saanen, M., Sahli, R., Hinrikson, H.P., Bille, J., Jatton, K.** (2004) Detection of Four *Plasmodium* Species in Blood from Humans by 18S rRNA Gene Subunit-Based and Species-Specific Real-Time PCR Assays. *J Clin Microbiol*, **42** (12), 5636-5643.
- Sabbatani, S., S. Fiorino and R. Manfredi.** (2010) The emerging of the fifth malaria parasite (*Plasmodium knowlesi*): a public health concern? *Braz J Infect Dis*, **14** (3), 299-309.
- Sambrook, J., Fritsch, E.F., Maniatis, T.** (1989) *Molecular Cloning: A Laboratory Manual*. 2nd Edition. Cold Spring Harbor Laboratory Press
- Sangolgi, P. B., C. Balaji, S. Dutta, N. Jindal and G. K. Jarori.** (2016) Cloning, expression, purification and characterization of *Plasmodium* spp. glyceraldehyde-3-phosphate dehydrogenase. *Protein Expr Purif*, **117**, 17-25.
- Saravanan, P., Kumar, S.** (2009) Diagnostic and immunoprophylactic applications of synthetic peptides in veterinary microbiology. *Microbiol Res*, **1** (1), doi:10.4081/mr.2010.el.
- Satchell, J. F., R. L. Malby, C. S. Luo, A. Adisa, A. E. Alpyurek, N. Klonis, B. J. Smith, L. Tilley and P. M. Colman.** (2005) Structure of glyceraldehyde-3-phosphate dehydrogenase from *Plasmodium falciparum*. *Acta Crystallogr D Biol Crystallogr*, **61** (9), 1213-21.
- Sathpathi, S., A. K. Mohanty, P. Satpathi, S. K. Mishra, P. K. Behera, G. Patel and A. M. Dondorp.** (2014) Comparing Leishman and Giemsa staining for the assessment of peripheral blood smear preparations in a malaria-endemic region in India. *Malaria Journal*, **13**, doi: 10.1186/1475-2875-13-512.
- Schneider, P., Reece, S.E., van Schaijk, B.C.L., Bousema, T., Lanke, K.H.W., Meaden, C.S.J., Gadalla, A., Ranford-Cartwright, L.C., Babiker, H.A.** (2015) Quantification of female and male *Plasmodium falciparum* gametocytes by reverse transcriptase quantitative PCR. *Mol Biochem Parasitol*, **199** (1-2), 29-33.
- Schneider, P., Wolters, L., Schoone, G., Schallig, H., Sillekens, P., Hermsen, R., Sauerwein, R.** (2005) Real-Time Nucleic Acid Sequence-Based Amplification Is More Convenient than Real-Time PCR for Quantification of *Plasmodium falciparum*. *J Clin Microbiol*, **43** (1), 402-405.
- Scholl, P. F., D. Kongkasuriyachai, P. A. Demirev, A. B. Feldman, J. S. Lin, D. J. Sullivan, Jr. and N. Kumar.** (2004) Rapid detection of malaria infection *in vivo* by laser desorption mass spectrometry. *Am J Trop Med Hyg*, **71** (5), 546-51.
- Schumann, W., Ferreira, C.S.** (2004) Production of recombinant proteins in *Escherichia coli*. *Gen Mol Biol*, **27** (3), 442-453.

Semenova, V.A., Steward-Clark, E., Stamey, K.L., Taylor, T.H., Schmidt, D.S., Martin, S.K., Marano, N., Quinn, C.P. (2004) Mass Value Assignment of Total and Subclass Immunoglobulin G in a Human Standard Anthrax Reference Serum. *Clin Diag Lab Immunol*: 919-23.

Shaikh, S., H. Memon, B. Iohano, A. Shaikh, I. Ahmed and J. K. Baird. (2012) Severe disease in children hospitalized with a diagnosis of *Plasmodium vivax* in south-eastern Pakistan. *Malaria Journal*, **11**, doi: 10.1186/1475-2875-11-144.

Sharma, M. K., Agarwal, G.S., Rao, V.K., Upadhyay, S., Merwyn, S., Gopalan, N., Rai, G.P., Vijayaraghavan, R., Prakash, S. (2010) Amperometric immunosensor based on gold nanoparticles/alumina sol-gel modified screen-printed electrodes for antibodies to *Plasmodium falciparum* histidine rich protein-2. *Analyst*, **135**, 608-614.

She, R. C., M. L. Rawlins, R. Mohl, S. L. Perkins, H. R. Hill and C. M. Litwin. (2007) Comparison of immunofluorescence antibody testing and two enzyme immunoassays in the serologic diagnosis of malaria. *J Travel Med*, **14** (2), 105-11.

Sheets, M. D., P. Amersdorfer, R. Finnern, P. Sargent, E. Lindquist, R. Schier, G. Hemingsen, C. Wong, J. C. Gerhart and J. D. Marks. (1998) Efficient construction of a large nonimmune phage antibody library: the production of high-affinity human single-chain antibodies to protein antigens. *Proc Natl Acad Sci USA*, **95** (11), 6157-62.

Shields, M.J., Siegel, J.N., Clark, C.R., Hines, K.K., Potempa, L.A., Gewurz, H., Anderson, B. (1991) An Appraisal of Polystyrene-(Elisa) and Nitrocellulose-Based (Elifa) Enzyme Immunoassay Systems Using Monoclonal Antibodies Reactive toward Antigenically Distinct Forms of Human C-Reactive Protein. *J Immunol Meth* **141** (2), 253-61.

Shin, H., Kim, J., Lee, W., Sohn, Y., Lee, S., Kang, Y., Lee, H. (2013) Polymorphism of the parasite lactate dehydrogenase gene from *Plasmodium vivax* Korean isolates. *Malaria Journal*, **12**, doi:10.1186/1475-2875-12-166.

Shortt, H. E. and P. C. Garnham. (1948) Pre-erythrocytic stage in mammalian malaria parasites. *Nature*, **161**, 126.

Singh, B., A. Bobogare, J. Cox-Singh, G. Snounou, M. S. Abdullah and H. A. Rahman. (1999) A genus- and species-specific nested polymerase chain reaction malaria detection assay for epidemiologic studies. *Am J Trop Med Hyg*, **60** (4), 687-92.

Singh, B., Daneshvar, C. (2013) Human Infections and Detection of *Plasmodium knowlesi*. *Clin Microbiol Rev*, **26** (2), 165-184.

Sinha, S., B. Medhi and R. Sehgal. (2014) Challenges of drug-resistant malaria. *Parasite*, **21**, 61.

- Siraj, A. S., M. Santos-Vega, M. J. Bouma, D. Yadeta, D. Ruiz Carrascal and M. Pascual.** (2014) Altitudinal changes in malaria incidence in highlands of Ethiopia and Colombia. *Science*, **343** (6175), 1154-8.
- Sirima, S. B., A. Konate, A. B. Tiono, N. Convelbo, S. Cousens and F. Pagnoni.** (2003) Early treatment of childhood fevers with pre-packaged antimalarial drugs in the home reduces severe malaria morbidity in Burkina Faso. *Trop Med Int Health*, **8** (2), 133-9.
- Sirover, M. A.** (1999) New insights into an old protein: the functional diversity of mammalian glyceraldehyde-3-phosphate dehydrogenase. *Biochim Biophys Acta*, **1432** (2), 159-84.
- Sirover, M. A.** (2005) New nuclear functions of the glycolytic protein, glyceraldehyde-3-phosphate dehydrogenase, in mammalian cells. *J Cell Biochem*, **95** (1), 45-52.
- Sirover, M. A.** (2012) Subcellular dynamics of multifunctional protein regulation: mechanisms of GAPDH intracellular translocation. *J Cell Biochem*, **113** (7), 2193-200.
- Sivashanmugam, A., V. Murray, C. Cui, Y. Zhang, J. Wang and Q. Li.** (2009) Practical protocols for production of very high yields of recombinant proteins using *Escherichia coli*. *Protein Sci*, **18** (5), 936-48.
- Smit, S., S. Stoychev, A. I. Louw and L. M. Birkholtz.** (2010) Proteomic profiling of *Plasmodium falciparum* through improved, semiquantitative two-dimensional gel electrophoresis. *J Proteome Res*, **9** (5), 2170-81.
- Smith, J. D. and A. G. Craig.** (2005) The surface of the *Plasmodium falciparum*-infected erythrocyte. *Curr Issues Mol Biol*, **7** (1), 81-93.
- Snounou, G., S. Viriyakosol, X. P. Zhu, W. Jarra, L. Pinheiro, V. E. do Rosario, S. Thaithong and K. N. Brown.** (1993) High sensitivity of detection of human malaria parasites by the use of nested polymerase chain reaction. *Mol Biochem Parasitol*, **61** (2), 315-20.
- Snow, R. W., E. Eckert and A. Teklehaimanot.** (2003) Estimating the needs for artesunate-based combination therapy for malaria case-management in Africa. *Trends Parasitol*, **19** (8), 363-9.
- Solano, C. M., Okoth, S.A., Abdallah, J.F., Pava, Z., Dorado, E., Incardona, S., Huber, C.S., de Oliveira, A.M., Bell, D., Udhayakumar, V., Barnwell, J.W.** (2015) Deletion of *Plasmodium falciparum* Histidine- Rich Protein 2 (pfhrp2) and Histidine-Rich Protein 3 (pfhrp3) Genes in Colombian Parasites. *PLOS One*, **10** (7), e0131576. doi:10.1371/journal.pone.0131576.
- Sorensen, H. P. and K. K. Mortensen.** (2005) Soluble expression of recombinant proteins in the cytoplasm of *Escherichia coli*. *Microb Cell Fact*, **4** (1), 1.

- Sousa-Figueiredo, J. C., Oguttu, D., Adriko, M., Besigye, F., Nankasi, A., Arinaitwe, M., Namukuta, A., Betson, M., Kabatereine, N.B., Stothard, J.R.** (2010) Investigating portable fluorescence microscopy (CyScope®) as an alternative rapid diagnostic test for malaria in children and women of child-bearing age. *Malaria Journal*, **9**, DOI: 10.1186/1475-2875-9-245.
- Sousa, L. P., Mariuba, L.A.M., Holanda, R.J., Pimentel, J.P., Almeida, M.E.M. Chaves, Y.O., Borges, D., Lima, E., Crainey, J.L., Orlandi, P.P., Lacerda, M.V., Nogueira, P.A.** (2014) A novel polyclonal antibody-based sandwich ELISA for detection of *Plasmodium vivax* developed from two lactate dehydrogenase protein segments. *BMC Infectious Diseases*, **14** (49), doi:10.1186/1471-2334-14-49.
- Stone, W., B. P. Goncalves, T. Bousema and C. Drakeley.** (2015) Assessing the infectious reservoir of *falciparum* malaria: past and future. *Trends Parasitol*, **31** (7), 287-96.
- Studier, F. W.** (2005) Protein production by auto-induction in high density shaking cultures. *Protein Expr Purif*, **41** (1), 207-34.
- Suh, K. N., K. C. Kain and J. S. Keystone.** (2004) Malaria. *CMAJ*, **170** (11), 1693-702.
- Sun, J., Jiang, Z., Hu, S.** (2008) Effect of four adjuvants on immune response to F4 fimbriae in chickens. *Vet Immunol Immunopathol*, **121**, 107-112.
- Syed, S. N., H. Schulze, D. Macdonald, J. Crain, A. R. Mount and T. T. Bachmann.** (2013) Cyclic denaturation and renaturation of double-stranded DNA by redox-state switching of DNA intercalators. *J Am Chem Soc*, **135** (14), 5399-407.
- Ta, T. H., Hisam, S., Lanza, M., Jiram, A.I., Ismail, N., Rubio, J.M.** (2014) First case of a naturally acquired human infection with *Plasmodium cynomolgi*. *Malaria Journal*, **13**, doi:10.1186/1475-2875-13-68.
- Teng, R., Lehane, A.M., Winterberg, M., Shafik, S.H., Summers, R.L., Martin, R.E., van Schalkwyk, D.A., Junankar, P.R., Kirk, K.** (2014) 1H-NMR metabolite profiles of different strains of *Plasmodium falciparum*. *Bioscience Reports*, **34** (6), 685-699.
- Tomar, D., Biswas, S., Tripathi, V., Rao, D.N.** (2006) Development of diagnostic reagents: Raising antibodies against synthetic peptides of PfHRP-2 and LDH using micosphere delivery. *Immunobiology*, **211**, 797-805.
- Tonnang, H. E., R. Y. Kangalawe and P. Z. Yanda.** (2010) Predicting and mapping malaria under climate change scenarios: the potential redistribution of malaria vectors in Africa. *Malaria Journal*, **9**, doi: 10.1186/1475-2875-9-111.
- Towbin, H., Staehelin, T., Gordon, J.** (1979) Electrophoretic transfer of proteins from polyacrylamide gels to nitrocellulose sheets: procedure and some applications. *Proc Natl Acad Sci USA*, **76** (9), 4350-4354

- Tristan, C., N. Shahani, T. W. Sedlak and A. Sawa.** (2011) The diverse functions of GAPDH: views from different subcellular compartments. *Cell Signal*, **23** (2), 317-23.
- Turgut-Balik, D., E. Akbulut, D. K. Shoemark, V. Celik, K. M. Moreton, R. B. Sessions, J. J. Holbrook and R. L. Brady.** (2004) Cloning, sequence and expression of the lactate dehydrogenase gene from the human malaria parasite, *Plasmodium vivax*. *Biotechnol Lett*, **26** (13), 1051-5.
- Turgut-Balik, D., Shoemark, D.K., Sessions, R.B., Moreton, K.M., Holbrook, J.J.** (2001) Mutagenic exploration of the active site of lactate dehydrogenase from *Plasmodium falciparum*. *Biotechnology Letters*, **23**, 923-927.
- van Hellemond, J. J., M. Rutten, R. Koelewijn, A. M. Zeeman, J. J. Verweij, P. J. Wismans, C. H. Kocken and P. J. van Genderen.** (2009) Human *Plasmodium knowlesi* infection detected by rapid diagnostic tests for malaria. *Emerg Infect Dis*, **15** (9), 1478-80.
- van Regenmortel, M. H. V.** (1993) Eggs as protein and antibody factories. *Proc Eur Sym Qual Poult Meat*, 257-263.
- van Wyngaardt, W., Malatji, T., Mashau, C., Fehrsen, J., Jordaan, F., Miltiadou, D., du and D. H. Plessis.** (2004) A large semi-synthetic single-chain Fv phage display library based on chicken immunoglobulin genes. *BMC Biotechnology*, **4** (6), doi:10.1186/1472-6750-4-6.
- Vander Jagt, D. L., Intress, C., Heidrich, J.E., Mrema, J.E.K., Rieckmann, K.H., Heidrich, H.G.** (1982) Marker Enzymes of *Plasmodium falciparum* and Human Erythrocytes as Indicators of Parasite Purity. *J Parasitol* **68** (6), 1068-71.
- Varshavsky, A.** (1997) The N-End Rule Pathway of Protein Degradation. *Genes to Cells* **2**, 13-28.
- Veigas, B., P. Pedrosa, F. F. Carlos, L. Mancio-Silva, A. R. Grosso, E. Fortunato, M. M. Mota and P. V. Baptista.** (2015) One nanoprobe, two pathogens: gold nanoprobe multiplexing for point-of-care. *J Nanobiotechnology*, **13**, 48.
- Verma, R., N. S. Jayaprakash, M. A. Vijayalakshmi and K. Venkataraman.** (2015) Novel monoclonal antibody against truncated C terminal region of Histidine Rich Protein2 (PfHRP2) and its utility for the specific diagnosis of malaria caused by *Plasmodium falciparum*. *Exp Parasitol*, **150**, 56-66.
- Veron, V. and B. Carme.** (2006) Recovery and use of *Plasmodium* DNA from malaria rapid diagnostic tests. *Am J Trop Med Hyg*, **74** (6), 941-3.
- Voet, D., Voet, J.G.** (2004). *Biochemistry*. John Wiley and sons, inc., 70; 131; 503; 604-607.

- Wajanarogana, S., Prasomrothanakul, T., Udomsangpetch, R., Tungpradabkul, S.** (2006) Construction of a human functional single-chain variable fragment (scFv) antibody recognizing the malaria parasite *Plasmodium falciparum*. *Biotechnol Appl Biochem*, **44**, 55-61.
- Warkiani, M. E., A. K. Tay, B. L. Khoo, X. Xiaofeng, J. Han and C. T. Lim.** (2015) Malaria detection using inertial microfluidics. *Lab Chip*, **15** (4), 1101-9.
- Weaver, A. A. and M. Lieberman.** (2015) Paper test cards for presumptive testing of very low quality antimalarial medications. *Am J Trop Med Hyg*, **92** (6), 17-23.
- Weiss, R. B.** (1991) Ribosomal frameshifting, jumping and readthrough. *Curr Opin Cell Biol*, **3** (6), 1051-5.
- Welch, W.H.** (1897). *Malaria: Definition, Synonyms, History, and Parasitology. System of Practical Medicine.* Lea Brothers & Co., 1
- White, N. J., Pongtavornpinyo, W., Maude, R.J., S. Saralamba, Aguas, R., Stepniewska, K., Lee, S.J., and A. M. Dondorp, White, L.J., Day, N.P.J.** (2009) Hyperparasitaemia and low dosing are an important source of anti-malarial drug resistance. *Malaria Journal*, **8**, doi:10.1186/1475-2875-8-253.
- WHO.** (2015a). Guidelines for the treatment of malaria. *WHO Press*. Available at: http://apps.who.int/iris/bitstream/10665/162441/1/9789241549127_eng.pdf
- WHO.** (2015b). World malaria Report 2015. *WHO Press*. Available at: http://apps.who.int/iris/bitstream/10665/200018/1/9789241565158_eng.pdf
- Wihokhoen, B., Dondorp, A.M., Turner, P., Woodrow, C.J., Imwong, M.** (2016) Use of Blood Smears and Dried Blood Spots for Polymerase Chain Reaction–Based Detection and Quantification of Bacterial Infection and *Plasmodium falciparum* in Severely Ill Febrile African Children. *Am J Trop Med Hyg*, **94** (2), 322-326.
- Witola, W. H., G. Pessi, K. El Bissati, J. M. Reynolds and C. B. Mamoun.** (2006) Localization of the phosphoethanolamine methyltransferase of the human malaria parasite *Plasmodium falciparum* to the Golgi apparatus. *J Biol Chem*, **281** (30), 21305-11.
- Wurtz, N., B. Fall, K. Bui, A. Pascual, M. Fall, C. Camara, B. Diatta, K. B. Fall, P. S. Mbaye, Y. Dieme, R. Bercion, B. Wade, S. Briolant and B. Pradines.** (2013) Pfhrrp2 and pfhrrp3 polymorphisms in *Plasmodium falciparum* isolates from Dakar, Senegal: impact on rapid malaria diagnostic tests. *Malaria Journal*, **12**, doi: 10.1186/1475-2875-12-34.
- Yamamoto, S. and K. B. Storey.** (1988) Dissociation-association of lactate dehydrogenase isozymes: influences on the formation of tetramers versus dimers of M4-LDH and H4-LDH. *Int J Biochem*, **20** (11), 1261-5.

Yamanaka, H.I., Inoue, T., Ikeda-Tanaka, O. (1996) Chicken Monoclonal Antibody Isolated by a Phage Display System. *J Immunol* **157**, 1156-62.

Yongkiettrakul, S., Jaroenram, W., Arunrut, N., Chareanchim, W., Pannengpetch, S., Suebsing, R., Kiatpathomchai, W., Pornthanakasem, W., Yuthavong, Y., Kongkasuriyachai, D. (2014) Application of loop-mediated isothermal amplification assay combined with lateral flow dipstick for detection of *Plasmodium falciparum* and *Plasmodium vivax*. *Parasitol Int*, **63** (6), 777-784.

Yuen, C. and Q. Liu. (2012) Magnetic field enriched surface enhanced resonance Raman spectroscopy for early malaria diagnosis. *J Biomed Opt*, **17** (1), 017005.

Yukich, J., V. D'Acremont, J. Kahama, N. Swai and C. Lengeler. (2010) Cost savings with rapid diagnostic tests for malaria in low-transmission areas: evidence from Dar es Salaam, Tanzania. *Am J Trop Med Hyg*, **83** (1), 61-8.

Yusof, R., Y. L. Lau, R. Mahmud, M. Y. Fong, J. Jelip, H. U. Ngian, S. Mustakim, H. M. Hussin, N. Marzuki and M. Mohd Ali. (2014) High proportion of *knowlesi* malaria in recent malaria cases in Malaysia. *Malaria Journal*, **13**, doi: 10.1186/1475-2875-13-168.

Zimmerman, P. A., Howes, R.E. (2015) Malaria diagnosis for malaria elimination. *Current Opinion Inf Dis*, **28** (5), 446-454.

Zocher, K., K. Fritz-Wolf, S. Kehr, M. Fischer, S. Rahlfs and K. Becker. (2012) Biochemical and structural characterization of *Plasmodium falciparum* glutamate dehydrogenase 2. *Mol Biochem Parasitol*, **183** (1), 52-62.